Testing the TT-OSL Single-Aliquot Protocol for Quartz Sediment Dating

Jillian Elizabeth Moffatt
School of Chemistry and Physics; Physics
The University of Adelaide

Submitted for the degree of Master of Philosophy

June 2014

CONTENTS

ABSTRACT

Thermally-transferred optically stimulated luminescence (TT-OSL) is a form of optically stimulated luminescence that saturates at much higher doses than conventional OSL (Wang et al, 2006b). Luminescence sediment dating is a technique whereby the natural radiation dose given to a sample is measured. This is divided by the environmental radiation rate of the sample site to give the sample's age. As TT-OSL is able to measure higher doses than conventional OSL, it has been considered a candidate for long range luminescence sediment dating, beyond one million years. In this thesis, TT-OSL single-aliquot sediment dating protocols were tested on selected samples from the south-east of South Australia (SESA) stranded dune sequence, a sequence of ancient dunes ranging from 0 to 900 thousand years of age that have previously been independently dated using luminescence and non-luminescence dating methods. A young sample with a high natural dose from Baldina Creek, Burra, South Australia was also dated. Measurements of the thermal depletion of the TT-OSL signal were also made.

It was found that, for the SESA samples, TT-OSL dating results do not agree with previous independent measurements above 200 ka. The results for the young Baldina Creek sample were within the expected range.

DECLARATION

I certify that this work contains no material which has been accepted for the award of any other degree or diploma in any university or other tertiary institution and, to the best of my knowledge and belief, contains no material previously published or written by another person, except where due reference has been made in the text. In addition, I certify that no part of this work will, in the future, be used in a submission for any other degree or diploma in any university or other tertiary institution without the prior approval of the University of Adelaide.

I give consent to this copy of my thesis, when deposited in the University Library, being made available for loan and photocopying, subject to the provisions of the Copyright Act 1968.

I also give permission for the digital version of my thesis to be made available on the web, via the University's digital research repository, the Library catalogue, and also through web search engines, unless permission has been granted by the University to restrict access for a period of time.

Signed

Jillian Moffatt
June, 2014

ACKNOWLEDGEMENTS

I wish to thank my supervisors, Nigel Spooner and Barnaby Smith, for all their information and advice while I was doing my project and writing my thesis.

Most of the south-east of South Australia samples used in this thesis were sampled by J R Prescott and D J Huntley. The samples I used were owned by J R Prescott, who kindly allowed me access to them and his sampling notes. After J R Prescott sadly passed away, D J Huntley was kind enough to fill in gaps in my knowledge of the samples, and allowed me access to his sampling notes.

Samples were prepared in the main by Rochelle Dumaua.

Fourier Transform Spectrometer measurements were supervised by Don Creighton.

Soil analysis of the samples was done by "Genalysis Laboratory Services Pty Ltd", and the gamma spectrometry measurements of the Baldina Creek sample were analysed by "Minty Geophysics".

In this thesis I benefited from access to the Cosmic Ray Spreadsheet created by J. R. Prescott and J. T. Hutton, the "AGE99" program by R. Grün, and the "fmix" and "cdose-prf" programs by R. Galbraith.

I wish to thank the Environmental Luminescence group for all their help during my thesis. Rochelle Dumaua, Frances Williams, Nigel Spooner and Don Creighton taught me how to work the various instruments used in this thesis. Owen Williams taught me how to use the pulsed OSL module. Nigel Spooner, Daniele Questiaux, John Prescott and Chris Kalnins taught me much about data analysis. Nigel Spooner, Peter Hunter, and Don Creighton worked hard to ensure that the instruments were always running their best, and without their work this would be a much shorter thesis.

I wish to thank David Huntley for his many useful comments on my thesis.

I benefited much from helpful conversations with Tilanka Munasinghe on Matlab coding.

Finally, I wish to thank Sheila and Bruce Moffatt, and Andrew Cunningham for supporting me during my studies.

01-INTRODUCTION

Thermally transferred optically stimulated luminescence (TT-OSL) is a relatively new quartz luminescence dating technique which has the potential to date sediments exposed to higher doses than can be dated by optically stimulated luminescence (OSL) (Wang et al, 2006a). OSL is the standard luminescence dating method for buried sediments of late Quaternary age, but cannot date quartz that has been exposed to a greater dose of ionising radiation than around 150 Gy. This translates to an upper limit for using optical dating of around half a million years. TT-OSL has the potential to be useful for dating older sediments, and sediments in areas with high environmental radiation dose rates.

In their review of TT-OSL, Duller and Wintle (2011) noted that TT-OSL needs to be tested with an independently dated control sequence in order to review its usefulness for dating. The stranded dunes of the south-east of South Australia (SESA) provide such a sequence, suitable for testing quartz and other luminescence dating protocols (Huntley et al, 1985). It provides samples with ages from 0 to 950,000 years. While the sequence does not provide environmental doses at the limit of what TT-OSL has been shown to be able to measure (thousands of Gy), it does provide samples that are unable to be dated using OSL due to their large natural doses.

In this thesis the published research is assimilated into a general single-aliquot dating protocol for TT-OSL, which is applied to selected SESA samples. The results are discussed, and further research has been undertaken to attempt to resolve some of the issues found in the protocol. An improved protocol for the SESA samples was devised and tested. Kinetic measurements were done to assess the thermal stability of the TT-OSL signal, and simple models were made to try to explain the behaviour of the SESA TT-OSL results.

From these results I hope to obtain the answers to a number of questions, namely:

-Is TT-OSL suitable for dating buried sediments at natural doses where optical dating fails?

-Is TT-OSL suitable for dating buried sediments older than can be dated using conventional OSL (more than half a million years)?

-Is TT-OSL more suitable for dating older sediments than other luminescence methods, such as thermoluminescence (TL)?

-How precise are TT-OSL measurements, and how much time and sample is needed to obtain a result?

A summary of my findings is found in the conclusions section.

02-BACKGROUND

PROJECT AIM

Thermally transferred optically stimulated luminescence (TT-OSL) is a new luminescence dating technique first proposed in 2006 (Wang et al, 2006b). Optically stimulated luminescence (OSL), currently the most common luminescence dating technique for buried sediment layers, can typically only date samples with an accumulated dose of around 150 Gy or less, leading to an age limit of dateable samples between 200 and 500 ka. In contrast, TT-OSL signal-to-dose relationships have been shown not to saturate after thousands of Grays of laboratory dose (Burbidge et al, 2009). This means that TT-OSL techniques could potentially be used to date older sediment layers than can be currently dated with conventional optical dating techniques.

Previous tests of the TT-OSL luminescence dating technique have either looked at the TT-OSL dose response to laboratory-given doses, or compared TT-OSL results to those of other luminescence methods or newer dating techniques (see p. 41 for a review on current literature). This does not give information about TT-OSL's reliability at measuring large natural doses, which are deposited in sediments over a long period of time. It also does not give information about the reliability of TT-OSL dating when other luminescence dating methods fail. In their review of TT-OSL protocols, Duller and Wintle stated that TT-OSL "still needs to be demonstrated by analysis of samples with good independent age control" (Duller and Wintle, 2012).

The south-east of South Australia (SESA) stranded dune sequence is a series of stranded dunes (beach ridges) situated in approximately parallel lines inland from the coast from Robe to Naracoorte, South Australia. They were caused by a combination of sea level fluctuations and land which is slowly rising. Previous doses measured using thermoluminescence (TL) in this sequence range from approximately 0 to 500 Gy. Sample ages range from 0 to 900

thousand years (ka). The dunes have been dated via TL, modelling, and oxygen-isotope analysis. Younger dunes have also been dated using optical dating, and the dunes at Naracoorte have been dated via palaeomagnetic reversal.

Due to its independent age controls and varied sample ages, the south-east of South Australia stranded dune sequence provides a low-to-medium natural dose-rate quartz test sequence for luminescence protocols (Huntley et al, 1985). In this thesis I will use TT-OSL to calculate ages for selected well-dated dunes of this sequence, and compare these to independent, and OSL and TL ages.

After its proposal in 2006, much research has been done on developing a single-aliquot dating protocol using TT-OSL. In this thesis I have assimilated the published research into a general dating protocol which has been applied to the well-dated SESA samples. The results are discussed, and improvements suggested and tested to attempt to resolve some of the issues found in acquiring ages for the samples. In addition, experiments to find information on the kinetic properties of the TT-OSL signal were also undertaken in order to determine the trapping lifetime of the TT-OSL under ambient conditions, and the protocol was tested on a young sample with a high dose.

LUMINESCENCE SEDIMENT DATING

-Luminescence, thermoluminescence, and optically stimulated luminescence-

Luminescence is the emission of light from a non-metallic object at a temperature lower than the corresponding emission of that wavelength by incandescence. While luminescence behaviour had been studied extensively beforehand, it was only in 1888 that an umbrella term for all luminescence phenomena was proposed (Wiedemann, 1888). It is caused by the excitation of electrons or holes in a material, which when returning to a ground state lose energy in the form of photons. Luminescence phenomena include fluorescence and phosphorescence, among others.

While most forms of luminescence occur within a few seconds of the initial electron ionisation event, delayed forms of luminescence exist, including thermoluminescence (TL). Thermoluminescence occurs in regular or amorphous substances with a similar unexcited energy level for electrons throughout the material. In the energy band theory of solids, this is called the ground state of the material (McKeever, 1985).

When there are breaks in the structure of the material, due to irregularities such as crystal defects or ion substitution, the unexcited energy level for electrons differs at that point. This can form a metastable state (also called a trap) within the material, between the ground state and the conduction band (McKeever, 1985). While electrons can exist in these states, they can spontaneously exit them under ambient temperatures, with a frequency much higher than an electron in a truly stable state. For a simple, first-order material, the average time an electron will spend in a particular metastable state (also called the lifetime of the trap) is

$$\tau = s^{-1}e^{\frac{E}{kT}}$$ (McKeever, 1985)

Where E is the energy difference between the trap and the conduction band, T is the temperature of the material, and k is Boltzmann's constant. s is the frequency factor (units of time^-1), which represents the amount of chances per unit of time the electron has of escaping the trap. Looking at the trap as a potential well, the frequency factor, s is equal to n*R; where n is the number of times the electron hits the wall of the potential well, and R is the wall reflection coefficient (Furetta, 2008). At ambient temperatures, the lifetime of the trap can range from seconds to millions of years, depending on E and s.

As the lifetime is inversely proportional to temperature, applying heat to the material greatly decreases the lifetime, and the right temperature range for each trap can induce a large exodus of electrons from the metastable state to the conduction band. From the conduction band these electrons can travel to recombination centres, emitting photons in the process of recombination (see fig. 2.1).

Thermoluminescence is therefore a two-step process: first electrons are excited into the conduction band by an ionising force, and some of these electrons subsequently populate a

proportion of the metastable states of the material. Secondly, after an indeterminate period of time (shorter than the time taken for the electron to spontaneously exit the trap at ambient temperatures), the material is heated, stimulating electrons out of the traps, into the conduction band and then into light-emitting recombination centres.

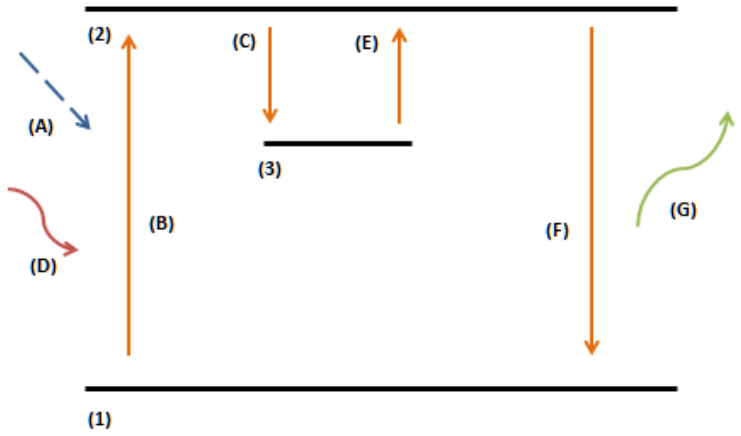

Figure 2.1: A band-structure diagram of the simple thermoluminescence model.
1) The ground state of the material
2) The excited state of the material
3) A metastable state
A) An ionising force affects the material
B) An electron or hole is excited from the ground state of the material
C) An electron or hole falls from the excited state to a metastable state
D) The material is exposed to heat
E) The electron or hole is excited from the metastable state to the excited state
F) The electron or hole falls from the excited state to a recombination centre
G) The process in (F) releases energy in the form of a photon.

[A note on terminology: while the words 'stimulation' and 'excitation' can be used in both steps of the TL process, to prevent confusion in this thesis I will use 'excitation' or 'ionisation', and 'trapping' for stages in the first process,

and 'stimulation' or 'de-trapping', and 'light emission' for stages in the second process.]

The link between the two stages of TL production is non-obvious to an observer. While a series of experiments and observations on a diamond with known TL properties was conducted by Robert Boyle (1663), it was only in the 1700's that the regeneration of TL after heating was discovered (Du Fay, 1738). The discovery of X-rays and radioactive elements provided experimentalists strong artificial ionisation sources to provide the initial population of TL traps, and it was only after these discoveries that TL was studied in any great detail.

TL measurements are usually done by heating a sample by increasing the temperature at a continuous rate, and measuring the subsequent light emission via a photomultiplier. This linear modulation (LM) of temperature creates a distinctive glow curve shape (see fig. 2.2). The production of the rising edge is dominated by the progressively increasing likelihood of an electron escaping its trap, and the production of the falling edge is dominated by the decreasing size of the population of occupied traps. For first-order kinetics and a LM temperature rise, the shape of the light emission is

$$I(T) = \frac{s'}{\beta} n e^{-\frac{E}{kT}} \qquad \text{(McKeever, 1985)}$$

Where I is the number of photons emitted, s'=s/N (N is the concentration of available traps), n is the number of filled traps, and β is the heating rate. Using this linear temperature modulation has a number of advantages. The LM effect is easy to create, and produces distinctive curves at positions dependent on the trap kinetics and the heating rate. This is particularly useful in materials with a number of different trap types, as the different s and E values of the traps will mean that their glow curves will be positioned in different temperature ranges. This allows identification and separate analysis of traps with differing properties (providing they differ sufficiently and the heating rate is slow enough).

Another form of delayed luminescence is optically stimulated luminescence (OSL). As its name suggests, OSL is stimulated by light rather than (or as well as) heat (Huntley et al, 1985); otherwise it behaves in much the same way as TL, and

is produced by charge released from metastable states that can often also be measured using TL. The rate of optical depletion of an OSL trap (or the inverse of the lifetime of the trap, not taking into account thermal depletion) is

$$\lambda = \theta P \qquad \text{(Bailey, 2001)}$$

Where θ is the photo-ionisation cross-section (the cross-section for the movement of electrons from the trap to the conduction band), and P is the photon flux of the optical stimulation. The photo-ionisation cross-section is

$$\theta(\hbar, \omega) = \frac{1}{\mathrm{n}}\left(\frac{E_{eff}}{E_o}\right)^2 \frac{16\pi e^2 \hbar}{3m^* c} \frac{(E_i)^{0.5}(\hbar\omega - E_i)^{1.5}}{(\hbar\omega)^3} \qquad \text{(Lucovsky, 1965)}$$

where n is the refractive index of the material, E_{eff}/E_o is the ratio between the electric field of the stimulating photon and the electric field of the material, E_i is the observed binding energy, ω is the frequency of the stimulating photon, and m* is the effective mass of the electron.

While from 1996 OSL has sometimes been measured while using a linearly modulated signal (Bulur, 1996), producing peaks equivalent in shape to those gained from TL, OSL is often stimulated by an unmodulated, or continuous wave (CW) signal (see fig. 2.2). This produces (in the case of a material containing only one type of optically stimulated trap) an exponentially decaying signal (Aitken, 1998), due to the population of occupied traps able to be stimulated at a particular optical power decreasing over stimulation time. CW-OSL has a number of advantages over LM-OSL for simple luminescence intensity measurements. It is easier to produce, simply by switching on a light source such as a laser or light emitting diode. The signal produced also has a sharper peak than that gained by LM-OSL, and so gives better counting statistics and therefore smaller errors to the integral of the light emission. However, using CW stimulation can make it difficult to separate signals from different trap types, and so for complicated materials with a variety of optically stimulated traps, and for kinetic analysis, LM stimulation can be preferable.

Example one:

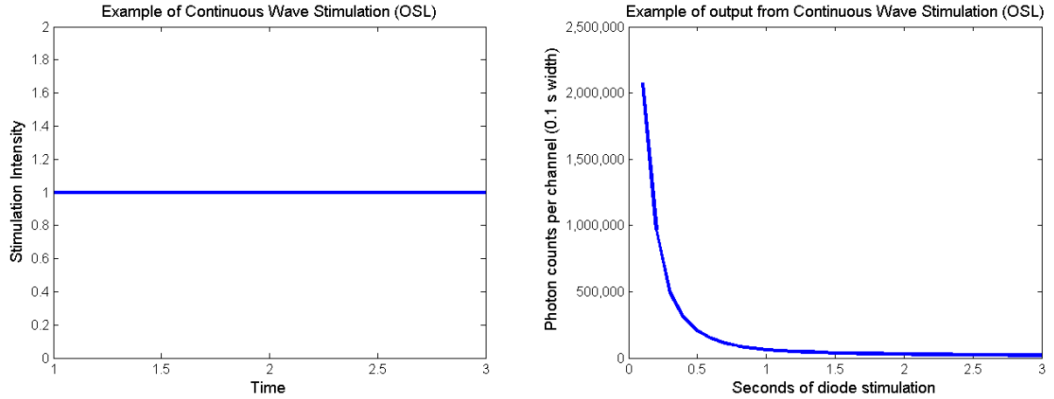

Example Two:

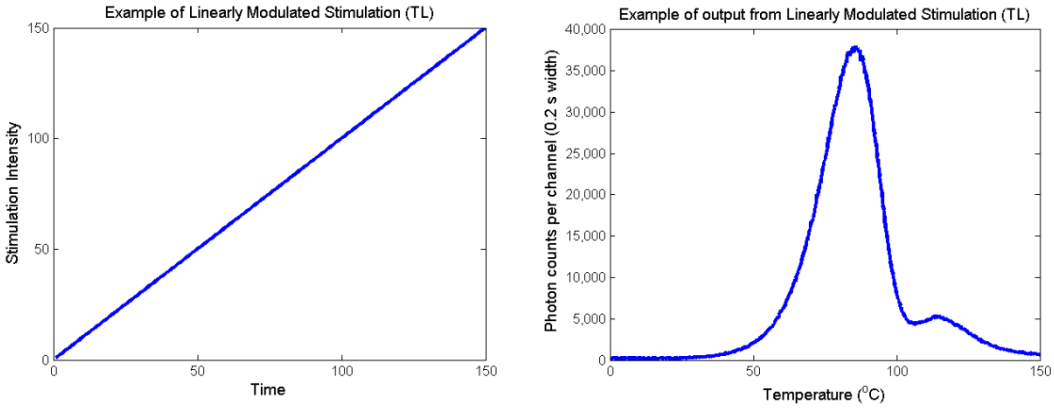

Figure 2.2: Examples of linearly modulated and continuous wave stimulation. Example 1, for CW-stimulation is of the OSL of a quartz sample stimulated with diodes at 90% power. Example 2, of LM-stimulation is of the TL of a recently irradiated quartz sample from 0 to 150 °C. Peaks from two different trap populations are visible.

In addition to CW-OSL and LM-OSL, measuring the luminescence produced from a pulsed stimulation is also possible. Pulsed OSL (POSL) is created by switching a LED on and off in pulses. The luminescence produced is usually characterised by a build-up of luminescence while the stimulation is on, and a decay when it is turned off. POSL is a useful tool for analysing the behaviour of traps and recombination centres, and charge movement between them. It can be used to reduce noise (especially fluorescence) from stimulation light, by only recording light from when the stimulation source is turned off (Bøtter-Jensen et al, 2003). POSL can also be used for separating luminescence components made up of different traps (e.g. Denby et al, 2006 and Ankjaergaard et al, 2010), which may come from different minerals, in a mixed-mineral sample.

-TL and OSL Dosimetry-

As the proportion of filled traps in a material is a function of the amount of ionising radiation the material has been exposed to (providing that the lifetime of the trap is much larger than the time between excitation and stimulation), TL and OSL materials can be used as radiation dosimeters. The proportion of traps filled by ionising radiation depends on the flux of the ionising radiation, the energy of the radiation, the type of radiation (e.g. UV or gamma photons, or α or β particles) and the amount of traps already filled. The dose response curve in the simplest case is a saturating exponential with the dependence almost linear when the proportion of traps already filled is near zero, and creating an asymptote when the proportion of traps already filled is near 100% (see fig 2.3). In some materials, traps can be created by radiation, modifying the trap population as the material is dosed, and giving a saturating exponential plus linear dose response curve (Aitken, 1998).

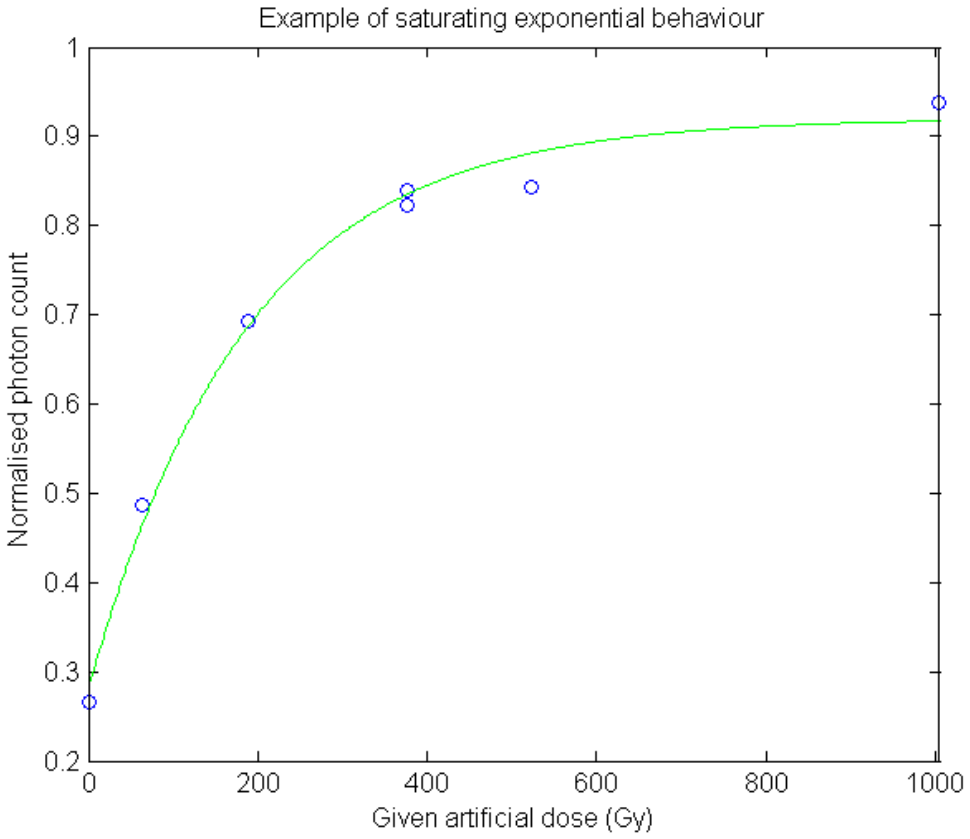

Figure 2.3: An example of saturating exponential behaviour, taken from a Naracoorte East sample's DI-TT-OSL results using the TT-OSL response to a test dose for normalisation. The saturating exponential fit to the data points (shown as a green line) was created using Matlab's Curve Fitting Toolbox.

Finding the dose a material has been given has two stages. The first is the measurement of the natural luminescence emission of the sample; the second is matching this emission to a dose response curve. As the formation of defects creating metastable states is a complex and non-uniform process, each sample has a unique dose response curve and must be calibrated separately. There are a number of frequently used calibration protocols:

-MAAD

The multiple-aliquot additive dose (MAAD) method involves preparing a number of aliquots of a sample, and then irradiating a number of them with a series of different known doses. Each aliquot then has a dose equal to the unknown natural dose (ND) plus a known artificial dose (Di). A graph of (ND + Di) vs signal is plotted, and a curve fitted to the

plot. It is assumed that there is no residual luminescence, so there is no signal at zero dose. The natural dose is then extrapolated from the fit (Aitken, 1985).

-MAR

In the multiple aliquot regenerated dose (MAR) method a number of aliquots are prepared as in the MAAD method, and some are bleached by natural or artificial light or heat sources. These bleached aliquots are given a range of large and small doses. A graph of dose vs signal is plotted, and a curve fitted to the plot. The dose corresponding to the natural signal is interpolated from this fit (Aitken, 1985).

-Australian Slide

The Australian slide method combines both the MAAD and MAR methods together. Some aliquots are given an additional dose, forming an additive dose curve, while others are bleached and then dosed, forming a regenerated dose curve. The additive dose curve is interposed onto the regenerated dose curve, and shifted until the curve shapes match (scaling is possible to correct for sensitivity changes, but is not "good practice"), thus finding the relationship between ND+Di and Di. In this method the type of fit used does not matter, as only the shape of the curves creates the final result (Prescott et al, 1993).

-SAR

The single-aliquot regenerative dose protocol is mainly used in OSL measurements. The natural dose is measured, and the stimulation time is chosen so that the luminescence signal from the aliquot reaches zero or a residual level by its end. The aliquot is then irradiated with a known dose, and the subsequent OSL signal is measured. A succession of known doses is given to the aliquot. As the sensitivity of a material to a known dose changes with repeated dosing and bleaching cycles, a small test dose is given to the aliquot between each major dose cycle, to monitor the aliquot's change of signal output from the same dose (Murray and Wintle, 2000).

While TL and OSL dosimetry is a useful tool, not all TL or OSL materials are suitable for dosimetry, or useful in all scenarios. Whether a TL or OSL material is suitable for dosimetry in a particular scenario depends on a number of the material's TL and OSL properties, including:

-Sensitivity and resolvability
The material must have a sensitivity to dose suitable for its potential purpose. The dose dependence in the dose range to be measured must be linear or follow a saturating exponential curve. In general, materials with interfering luminescence properties (such as phosphorescence or fluorescence) with high photon counts, or large residual luminescence signals are not suitable for measuring small doses, as an increased background luminescence level can overwhelm small signals.

-Saturation points
The material must saturate at doses much larger than the dose range being measured. Doses measured near the saturation point of the material can be very imprecise, and doses that exceed the saturation point can only be measured to a lower limit.

-Lifetimes
The luminescence signal being measured must have a lifetime much longer than the time between the start of dose deposition and the measurement. A lifetime shorter than or near this dose-to-measurement time will mean that the signal will have begun to fade naturally in ambient temperatures, and the dose calculated will be an underestimate. In cases where artificially stimulating the material to empty the trap population is not possible and very short-term dosimetry is used, a lifetime around an order of magnitude larger than the dose-to-measurement time, but not above is preferable, as build of signal due to background radiation will be minimised while still ensuring that the signal will not fade.

-Anomalous fading
Electrons or holes usually escape from metastable states at a rate dictated by the metastable state's thermal stability (lifetime). In some materials, the electrons escape from the metastable state population at a rate faster than would be expected, a phenomenon called anomalous fading. Anomalous fading has been attributed to quantum tunnelling (Wintle, 1973; Visocekas et al, 1976), and is found in materials such as ZnS, CaF_2, and feldspars (McKeever, 1985). If not accounted for in a measurement, a material that is subject to anomalous fading will give an underestimation of the dose received.

-Quenching
Quenching is a process in which a proportion of the electrons or holes stimulated from metastable states travel to the

ground state via non-radiative processes. While not usually affecting measurements of the dose received, quenching can lower the total luminescence measured and so increase counting errors. There are three main types of quenching:

-Impurity quenching: Impurity quenching occurs when impurities in a crystal form non-radiative centres, which then compete with radiative centres as pathways for electrons moving to the ground state. Heavy metals are especially affective at forming non-radiative paths (McKeever, 1985).

-Concentration quenching: In some cases, luminescence is quenched by an overabundance of luminescence centres. This is thought to be due to luminescence centres in close proximity reacting to one another to become non-luminescent (Curie, 1963). This effect can be seen when materials with luminescence centres caused by dopants (deliberate impurities) are created. Increasing the proportion of the dopant in the material for a time results in an increase of total luminescence output. After a certain proportion, however, the luminescence output of the material begins to slowly decline (McKeever, 1985).

-Thermal quenching: Thermal quenching is a type of quenching wherein the proportion of electrons travelling to the ground state by non-radiative processes is dependent on temperature. The luminescence efficiency of a material subject to thermal quenching is:

$$\eta(T) = (1-Ke^{-\frac{W}{kT}})^{-1} \qquad \text{(Wintle, 1975)}$$

Where K is a constant, k is Boltzmann's constant, T is the temperature, and W is the energy depth of the non-radiative process. Wintle (1975) found that W can be found experimentally by subtracting the value of E of the metastable state in question gained by the initial rise method (which is affected by thermal quenching) from the true value of E, found by a procedure not affected by thermal quenching (such as peak shift, or Hoogenstraaten's method). While thermal quenching does not affect OSL measurements taken at a constant temperature, care must be taken when doing TL measurements, to ensure that each measurement is reading the same proportion of the excited electrons. Samples must be of the same thickness, as must their holders, to ensure the thermal lag remains the same for all measurements. In addition, the temperature the samples are held at must be increased at a slow rate, to minimise the effect of temperature errors. The quartz 325 °C peak in quartz is particularly susceptible to thermal quenching (Wintle, 1974 and Spooner, 1994).

The advantage of using TL or OSL for dosimetry is that the thermoluminescence material stores the information on doses it receives for a length of time dictated by the material's charge trapping lifetime, which could be between milliseconds to millions of years. While immediate radiation measurements are more useful in some cases, TL and OSL are ideal for integrated-over-time dose accumulation measurements. Examples of uses of TL and OSL include medium to long-term measurements of radiation exposure in medical, research and mining environments; forensic dosimetry; and luminescence dating.

-TL and optical dating-

TL and OSL can be used to date geological and archaeological items such as burnt flints (Valladas, 1985), pottery (Fleming, 1972), teeth and shells (Kiyotaka, 1987), and buried sediment layers (Huntley et al, 1985). This is done by measuring via TL or OSL the dose the archaeological item or sediment layer has received. This dose is then divided by the background radiation dose rate for the site. This gives a value for the amount of time the trap population of the measured material has been filling. It should be noted that this means TL and optical dating gives a value for the age of the resetting event experienced by the dated item, rather than a set age.

There are a number of requirements that need to be met before an archaeological or geological item can be dated by TL or OSL. The first is, as one would expect, the item contains thermoluminescent or OSL materials. In addition to the issues mentioned for dosimetry measurements above, in order to date an item one also needs:

-A zero age to date from:
While biogenic calcites can be dated from their formation (Duller et al, 2009), other minerals were formed well before their reworking into the state which is to be dated. These materials therefore need to be exposed to a resetting event which lowers the number of filled traps in the material to a residual level. It is from this event that the material will be dated. For burnt flints and pottery, the resetting mechanism is the act of firing or burning the object; for sediments, it is exposure to sunlight before burial. While for pottery one can be confident that the item has been heated to a high enough temperature to empty the traps used for dating, if a flint has not been heated to a sufficient

temperature, or a sediment deposit has not been exposed to enough light to fully reset its trap population, an accurate age cannot be derived from the object.

-An accurate calculation for the background radiation dose per unit time:
For dating an item using TL or OSL, it is equally important to get accurate results for both the total dose absorbed by the material over time (called 'equivalent dose') and the dose rate the material has been exposed to. Background dose can come from a number of sources, including cosmic rays, radiation from the surrounding material, and radioactive inclusions inside the material itself. Each source has its own dependencies and complications, as listed below:

-Cosmic rays: the dose from cosmic rays depends on the geographic location of the material, its position from sea level, and the depth of burial. While depth of burial can change over time (due to new layers of deposition, or weathering), and some archaeological objects can change location (for example a high-value pot being exported to a different city), most changes are either very gradual (and so a reasonably accurate average can be calculated), or occur at short periods at the start of the material's dateable life, rendering their effect negligible for sufficiently old materials.

-Surrounding material: dose from the surrounding material is subject to the same location and burial dependencies as cosmic rays—an unburied material will have much less surrounding material to administer a dose than a buried one. For a sediment layer, dose can come from within the layer itself. If the layer is sufficiently thin or a sample is from near a sediment layer boundary, dose can also come from the layers surrounding it. For an archaeological object, dose to any one point can come from the surrounding sediment and from other parts of the object. Dose from the material's surroundings can change due to changes in average moisture content, as water is a passive absorber of radiation. Some radioactive daughter products are water soluble, and in wet environments can be moved out of the surrounding sediment. This reduces the total radioactivity of the sediment, as it means any radioactive products further down in the parent-daughter chain are not present in the soil. Average moisture content can change for long stretches of time in old material, due to climate changes. If moisture contents have changed over time, a study of the radioactive elements in the sediment will show a disequilibrium of parent to daughter products in the soil from that expected in the

modern environment (radon escape increases with increasing water content). If sufficient information is known to estimate the timeframes of each climate condition, calculations can potentially be modified to take this change in radioactivity into account (Prescott and Hutton, 1995).

-Radioactive inclusions: not all of the parts that make up an archaeological material can be dated, due to a lack of TL or OSL properties, short lifetimes, or other reasons. Usually a material is dated via small grains of TL or OSL material within the material's structure (often feldspars or quartz). These grains can contain inclusions, some of which may be radioactive. Radioactivity inside the grains causes α radiation to become a significant part of the total dose. As α radiation does not travel far through any material, external α radiation only affects a small layer around the outside of each grain. This layer is usually stripped from the grain during sample preparation, and so dose due to α radiation is usually considered negligible. If the radiation comes from within the grain, there is a significant α radiation component that must be accounted for in dose calculations. Grains with inclusions often have much higher dose exposure rates than grains without. Even in single grain analysis, calculating a separate dose rate for each grain is not usually possible. Unless the inclusions themselves are to be dated (such as in zircon dating), grains with inclusions are usually avoided where possible.

-Sediment dating-

There are two main luminescence minerals commonly found in sediment layers: quartz and feldspar. Quartz has a number of relatively distinct TL peaks, one of which (peaking at 325 °C when increasing the temperature at 5 K/s) is highly bleachable by visible and UV light, and is the main source of the quartz OSL signal (Smith et al, 1986 and Spooner, 1988). This peak has a lifetime of approximately 20 million years at 20 °C (Spooner and Questiaux, 2000). Its bleachability and large lifetime makes it ideal for sediment dating. However, this peak saturates at around 150 Gy, translating to an upper dateable age limit of approximately half a million years.

Feldspar, another common thermoluminescent mineral, saturates at much higher doses than quartz, and so can in principle be used to date older samples. However, it is susceptible to anomalous fading, a phenomena in which electrons or holes exit traps at a rate higher than suggested by the kinetically-derived lifetime of the trap (McKeever, 1985). It

is thought that this is due to quantum mechanical tunnelling, in which an electron in a trap can escape without the energy needed to raise it to another energy level. This means that a normal feldspar measurement will underestimate the dose received, and therefore the age of the sample. Feldspar signals can be stimulated by visible, UV and infrared light. Methods to obtain accurate results from faded feldspar have been developed and tested.

Other luminescence sediment dating methods include zircon dating, in which small zircon crystals are dated (Sutton and Zimmerman, 1979; Templer, 1985), and dating by inclusions, in which zircon, quartz, or feldspar inclusions in larger grains are dated (Templer, 1986; Huntley et al, 1993b). Which mineral to date is chosen after considering a number of factors, including the approximate guessed age of the sample, the minerals present in the sediment, the geological history of the sediment, and the purpose behind dating the sediment.

The resetting event used in sediment dating is the layer's last exposure to sunlight (see fig 2.4). For this reason, OSL measurements are preferred over TL, as OSL traps are more readily reset by light. Determining whether a sediment layer was exposed to enough sunlight for all the sediment measured to have had a zero-dose measurement at the time of the resetting event is assessed from a number of factors. These include the type of mineral used for dating, the method of sediment deposition, and laboratory tests.

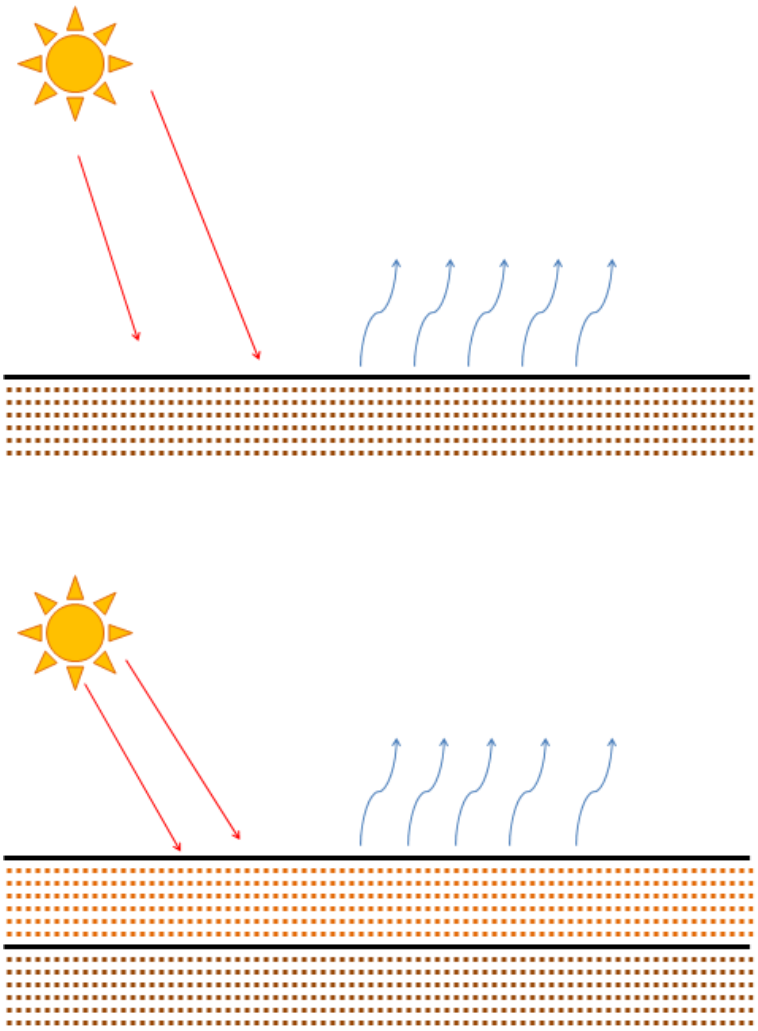

Figure 2.4: A diagram of a sediment layer a) exposed to light and being 'reset', and b) being buried, which allows charge from dose to remain in metastable states.

The mineral used for sediment dating can be used to estimate the likelihood of the sediment deposit being reset before burial. Feldspar OSL and infrared stimulated luminescence (IRSL) can be reset quickly, in low light conditions or by long wavelengths. The 325 °C quartz trap (the quartz OSL trap) can be reset by visible and UV light exposure, but not long-wavelength light. Other quartz TL traps can only be reset quickly by UV light, and cannot be reset by long wavelengths.

The history and method of deposition of the sediment determines the intensity and spectrum of light it has been

exposed to, and the length of time it was exposed. Wind-blown sands are exposed to direct sunlight, often for days or more before deposition. Glacially deposited sediment may be exposed only to dim light, and only for a short period of time. Water-borne sediment, even if exposed to sunlight in shallow water, will be exposed to a shortened wavelength spectrum of light due to the attenuation of UV light in water. From these facts, judgements about the likelihood of adequate resetting can be made. For instance: aeolian, or wind-blown sediment make up the deposits most likely to be totally bleached for both quartz OSL and TL trap populations. In addition, when exposed to a limited amount of light, OSL and IRSL feldspar trap populations are more likely to be bleached than OSL quartz trap populations, due to the feldspar's broader bleaching spectrum.

Along with estimates of light exposure due to knowledge of the sediment's origins, experiments using the TL or OSL signal have also been developed to review the likelihood of incomplete bleaching at burial. A common experiment for TL is the plateau test, used to calculate whether signals have thermally decayed over time (Aitken, 1985). Quartz TL is made up of a number of peaks, each with different bleaching characteristics and lifetimes. Quartz OSL, while dominated by one trap population, also includes harder-to-bleach components. If the sample has been fully bleached at deposition, all trap populations of sufficient lifetime will give similar equivalent dose results. If the sample has not been fully bleached, harder-to-bleach trap populations will give larger equivalent dose results than easily-bleached populations. A similar test is used for continuous-wave OSL measurements. While one trap is usually dominant in OSL measurements of feldspar and quartz, there can be smaller, harder-to-bleach components that may become dominant after the main OSL signal has been bleached out. Comparing the equivalent dose gained from the initial OSL signal (in the first second) and the dose measurement gained after the first second can give the similar information as a TL plateau test. However, as the smaller components of OSL signal are in general harder-to-bleach, the traps populations responsible may not be at residual levels at the 'zero age'. This, in addition to the fact that traps contributing to smaller OSL components may have shorter lifetimes than the dominant component, mean that the OSL plateau test is not as reliable as the TL plateau test.

Other concerns in sediment dating are generally to do with the unadulterated state of the sediment layer. Bioturbation, the turbation of sediment by living creatures such as plants, animals, and insects can mix grains from different sediment layers together, creating a mixture of grains of two or more ages. Solution pipes and other water drainage processes can also mix layers together. Weathering and geological movement can expose a layer to sunlight, rendering it unsuitable for dating. While some laboratory tests can be used to determine the suitability of a sample for dating, studying the geological history of the sediment layer and the careful selection of the sampling site is just as important.

The problems stated above can often lead to each grain in a sample having a different proportion of filled traps. In this case single grain dating is used. In this method, each sediment grain is measured separately. A large number of grains are measured, creating a distribution of ages. If the sample contains grains from more than one sediment layer, peaks will form in the distribution, corresponding to the different sediment ages. If some grains were only partially bleached before deposition, the sample distribution will have a peak at or near the age of the sediment layer, with a large tail of higher ages indicating the unbleached or partially bleached grains. If weathering or some other phenomenon partially exposed some but not all of the grains to light, there will be a peak in the distribution at the age of the sediment layer, with a large tail of smaller ages indicating the partially bleached grains exposed after deposition. Single grains can tell one more information about the history of the sample, but a lot of grains must be measured in order to retrieve this information. There are other disadvantages to the single-grain method: not all grains give off luminescence, meaning that not all grains measured will give a result, and single grains give off comparably little light, which means that counting errors will be large. Due to these disadvantages, single grain dating is in general only used when a sample's history indicates that the acquired dose of each grain in the sample may not be homogenous, or if the history of the sample is unknown.

When all grains in a sample are thought to have approximately the same acquired dose, dating is done using aliquots, a number of grains collected together. Assuming the number of grains is high enough, aliquots will average out any non-systematic variation in the acquired dose and in the "micro-dosimetry" experienced by each grain, and each aliquot dated

of a particular sample will give a similar dose. Aliquots often contain hundreds or thousands of grains, and give off a large amount of light when stimulated, resulting in smaller counting errors. Less aliquots are needed, therefore, to confirm a result for an age.

QUARTZ SEDIMENT DATING

Quartz grains found in sediment have properties dependent on their origin and history. While all natural quartz has shared luminescence properties, each quartz grain and grain population is distinct, and analysis of its unique properties must be made before the sample's suitability for sediment dating can be determined.

-Quartz thermoluminescence-

Thermoluminescence emission depends on two types of defects: metastable states (traps) and recombination centres. Metastable states trap and store electrons before stimulated emission, and their properties determine the stability of emissions and the intensity of stimulation needed to acquire a signal. Heating quartz at a constant temperature rate gives rise to a number of peaks, consistent with different trap populations. At 5 K/s, the most common peaks in quartz grains are situated at 95-110, 150-180, 200-220, 260-280, 305-325, and 375 °C (Scholefield, 1994a). These peaks are commonly referred to the 110, 180, 220, 280, 325 and 375 °C peaks. In addition, higher temperature peaks such as the 480 °C peak exist (Spooner, 1987). The position of the peaks may shift a little, depending on the origin of the quartz (de Brito Farias and Wantanabe, 2012). Unless otherwise stated, throughout the rest of this section I will refer to peaks by their position when heated at 5 K/s.

Quartz traps at 220 and 325 °C are caused by oxygen vacancies, created by heat or radiation (de Brito Farias and Wantanabe, 2012). It has been shown in laboratory tests that cycles of radiation and heating or exposure to light will progressively sensitise traps with peaks below 350 °C (Spooner, 1987). This indicates that the history of a sample can indicate its propensity for intense emissions: old, extensively reworked quartz grains may be in general brighter than younger, un-reworked grains recently derived from bedrock from a similar origin.

After being stimulated from a trap to the conduction band, an electron will only emit light if it travels down to a light-emitting recombination centre. The energy level difference between the conduction band and the recombination centre is the upper energy limit in determining the wavelength of the emitted light. In addition, competition for recombination centres can change the shape of TL curves. The 110, 160, 220, and 325 degree peaks have been said to use the same recombination centres (Scholefield, 1994b and Franklin et al, 1995).

Quartz thermoluminescence is often divided into red thermoluminescence (RTL), blue thermoluminescence (BTL), and UV thermoluminescence, so named due to the wavelength of the emission. BTL is often found in quartz samples with relatively small amounts of impurities (Westaway, 2009). It is found in quartz of hydrothermal, slow-cooling plutonic, and synthetic origins (Hashimoto et al, 2007). Near-UV emissions can be seen for the 110, 160, 220, and 325 °C peaks, while lower-wavelength blue emissions can be seen at 260-280, 375, and above 450 °C (Krbetschek et al, 1997). Intense red signals are found in volcanic quartz, as well as granitic and pegmatic quartz (Westaway, 2009), and quartz extracted from burnt archaeological materials (Hashimoto et al, 2007). While red TL may be created by a variety of different recombination centres, blue TL is thought to be created by aluminium and germanium impurities, and UV TL by titanium and lithium impurities, oxygen vacancies, and H_3O_4 hole centres (Krbetschek et al, 1997). Hashimoto et al (2007) found that while Al^-H^+ centres are light-emitting recombination centres, Al-OH centres are not, and provide a quenching effect. The fact that different aluminium sites both promote and quench BTL centres sheds some light on the fact that, as Subedi et al (2012) state, most quartz samples are affected by thermal quenching.

-Quartz optically stimulated luminescence-

Quartz OSL signals are usually dominated by one source, shown to be the 325 °C peak (Smith et al, 1986). This is known as the 'fast component' of OSL, as the trap empties very quickly under visible light stimulation. Other components have been identified under blue stimulation, which appear in different strengths and numbers in each sample. Jain et al (2003) analysed 12 samples of quartz of various origin, and identified seven components of the OSL signal, up to six of them present in the same sample. These components included an

'ultra fast', a 'medium', and four 'slow' components. These do not include the 110 °C peak, which bleaches under visible stimulation (Wintle and Murray, 1997). The middle component and one slow component appear to correlate with higher temperatures, only being completely thermally removed by heating above 400 °C. Another slow component appears to originate lower than the 325 °C peak (Jain et al, 2003).

The 325 °C peak is ideal for sediment dating, as it bleaches very quickly under ambient light conditions, yet in lightless conditions has a lifetime at 20 °C of approximately 20 million years (Spooner and Questiaux, 2000). Other components of OSL, however, are not as ideal, due to being less thermally stable, and therefore fading over time, or being more optically stable, and therefore likely to not be completely bleached at burial. A number of techniques exist to exclude the effects of less ideal OSL components from the overall signal. One is to mathematically isolate the fast component by fitting various decaying exponential curves to the signal. Another is to only use the first part of the OSL curve (usually less than the first second), where the fast component is dominant. In conjunction with this, subtracting a background signal from near the used integral of the signal curve rather than the end can subtract out proportions of the slower components.

The most significant thermally unstable trap is the 110 °C peak, which is found in almost all quartz samples (Pagonis et al, 2002), and has a lifetime of less than two hours at 20 °C. Other shallow traps include the 160, 180, 220, and 280 degree peaks, with lifetimes in the order of months, years, thousands of years, and hundreds of thousands of years respectively (Spooner and Questiaux, 2000). Due to its short lifetime, at natural background radiation rates any electrons temporarily trapped in the 110 °C peak spontaneously escape and return to the ground state or get trapped by more thermally stable traps before there is any significant charge build-up in the 110 °C peak population. The 110 °C peak's properties are so significant that most TL and OSL quartz protocols take it into account, by using it to monitor sensitivity changes or changing protocols to ensure it does not affect results from other peaks.

-Quartz protocols-

Protocols for measuring the TL or OSL of materials must take into account the material's properties, including the peaks

most likely to be useful for dosimetry, the emission spectra of the peaks, and the potential for interference by other peaks. Thus TL and OSL protocols for quartz are more specialised than the general protocols stated above for dose reconstruction. Details of these modifications can be found below.

For quartz TL dating:

-Spectra: quartz TL emissions are at a variety of wavelengths, and specific peaks can be almost isolated from other very close peaks by choosing a suitable filter set. For instance, the 325 °C peak, which peaks at 440 nm (Scholefield et al, 1994b), and the 375 °C peak, which peaks at 482 nm (Scholefield et al, 1994b), are similar in temperature of emission, and have wavelengths of emission that overlap. However, the 325 °C peak can be almost completely isolated from the 375 °C peak by using a Schott UG11 filter (Spooner et al, 1988), and vice-versa by a Schott GG-475 filter (Prescott and Fox, 1990).

-Incandescence: The two main quartz TL peaks used for sediment dating, the 325 and the 375 °C peaks (Smith, 1983), are found at temperatures at which incandescence begins to dominate the observed photon signals. Filters that block low-wavelength photons can minimise the effect of incandescence on the observed signal. However, a background run (reheat) is still needed to take into account this effect. After the first increase in temperature to read the TL signal, the sample is cooled, then heated to the same temperature as before, at the same rate. This second run is subtracted from the first, to take away incandescence and other background effects such as photomultiplier dark count.

-Normalisation: in order to compare different aliquots to each other, the signals being compared must be normalised. This is sometimes done by the weight of each aliquot. However, as some quartz grains are much brighter than others, in a typical ~10 mg aliquot only a few grains may contribute to the majority of the signal. This allows for large variability between aliquots, and so the mass normalising method is not always useful. Another way to normalise TL signals is the 'pre-dose method' (Aitken, 1985) which uses the 110 °C peak to normalise the signal of the higher peaks. In natural samples, the 110 °C peak is not evident, as it has a very short lifetime in ambient temperatures. In this method, artificially-dosed aliquots are left for a number of hours before use, to ensure that they too do not have charge trapped in the 110 °C peak. Immediately before TL measurement, a small test dose is given to the measured

aliquot. The 110 °C peak signal from this test dose is used to normalise the signal from the higher temperature TL peaks. This normalising method depends on the time between the test dose and 110 °C TL reading to be constant for all aliquots (a reasonable assumption when using automated TL readers), and that the 110 °C peak has the same sensitivity proportional to higher temperature peaks for all aliquots.

-Preheat: the 280 °C trap has a lifetime at 20 °C of around 80-100 thousand years, which is unsatisfactory for dating Quaternary samples. Due to its proximity to the 325 °C peak, measurements of the 325 °C peak without taking into account the 280 °C peak will include significant amounts of a partially faded signal. In 2001, Huntley and Prescott successfully isolated the 325 and 280 °C peaks by preheating the samples at 160 °C for 33 hours, and by preheating at 220 °C for five minutes.

For quartz optical dating:

-Spectra: filters are essential when measuring OSL signals, as the stimulation intensity (typically in the order of mW) is much larger than that of the signal (typically fW). The 325 °C peak has a strong UV emission, and so a 7 mm U340 filter is often used to conveniently and effectively separate this signal from blue or green stimulation sources.

-Backgrounds: OSL is usually measured using continuous wave (CW) modulation, and so the background stays approximately the same throughout the entire process. OSL stimulation is usually maintained until the signal reaches a residual level. A proportion of the residual signal is averaged and used as the background signal to subtract from the initial OSL.

-Normalisation: OSL normalisation is usually done via a test dose measurement after each OSL stimulation. This test dose is usually very small, especially when using single aliquot procedures. In light of this, preheats given to the test dose are usually smaller than the one given before reading the signal, to minimise the thermal erosion of useful signal. However, this means that the proportion of OSL components in the initial OSL signal may not be identical to the proportion of OSL components in the test signal. It has been shown that OSL components do not always sensitise at the same rate (Jain et al, 2003). This indicates that not treating the initial signal and test signal identically may not be suitable for all samples.

-Temperature of stimulation: the 110 °C peak population, when empty, can trap electrons stimulated in OSL experiments,

reducing the OSL signal. OSL measurements are usually done at 125 °C, to prevent this phenomenon.

-Dose deposition: natural background dose deposition is at a rate slow enough that the 110 °C peak is virtually always empty. Charge trapped in this peak population escapes in ambient conditions, and is redistributed into recombination centres and other traps. This creates problems when comparing natural doses to laboratory doses, which by necessity must be deposited at much higher dose rates than the natural signal. To try to recreate the right charge distribution over the shallow 110 to 325 °C traps, three different solutions are used. One is to irradiate samples at an elevated temperature, in an attempt to recreate the dose rate to kinetic activity ratio of the natural dose. Another is to irradiate the samples for small intervals, with pauses in between partial doses to allow the 110 peak charges to dissipate (called dose fractionation). The third is to give the sample a preheat (Smith et al, 1986) (usually at 220 °C (Smith et al, 1986), 260 °C (Li et al, 1999), or 280 °C (Murray and Roberts, 1998)) after irradiation, to stimulate the electron populations of the shallow traps and redistribute them to the ground state or to more stable traps. Since the first method needs specialised equipment, and the second increases the time taken for irradiations significantly, the third is the preferred method in most protocols. Even when one of the other methods are used, a preheat is often still done to ensure the more stable 160, 180 and 220 °C traps are empty, to allow for elevated temperature OSL measurements.

THERMALLY TRANSFERED OPTICALLY STIMULATED LUMINESCENCE

Thermal transfer is a phenomenon in which charge is transferred from one trap to another at an elevated temperature. This is a disadvantage for the preheat technique mentioned above, as the elevated temperature transfers charge into the 325 °C trap population, among others. This can be shown as after a preheat and illumination to empty all shallow traps, a preheat will still transfer charge into the principle OSL trap population (see figure 2.5). This extra signal is called thermally transferred optically stimulated luminescence, or TT-OSL. As the TT-OSL signal is quite small, methods of correcting for the signal are usually not carried out unless the sample is very young (Wintle and Murray, 2000). For young samples, various correcting techniques have been developed (Rhodes and Bailey, 1997; Li and Li, 2006).

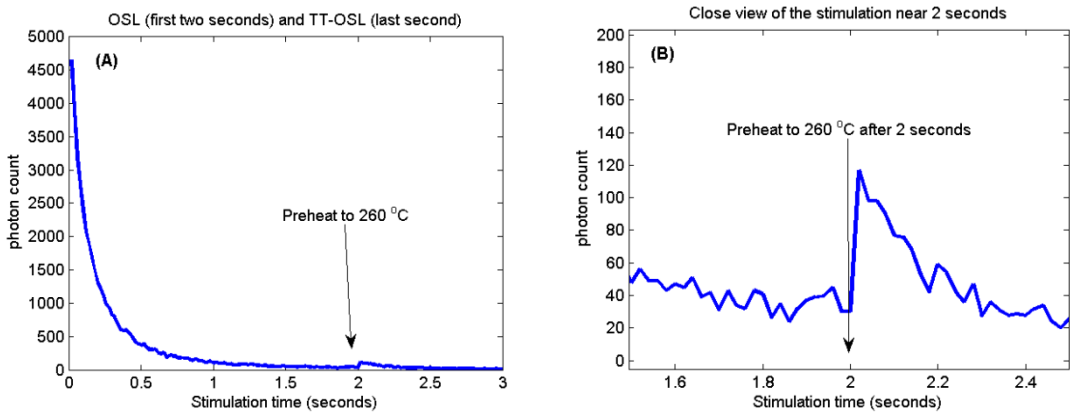

Figure 2.5: A) An example of two OSL stimulations of the same sample, with a 260 °C preheat in between. B) A closer view of the difference between the result before and after the preheat. After the preheat more signal is seen than directly before.

Wang et al (2006b) found that TT-OSL has a dose dependence, and saturates at much higher doses than OSL. TT-OSL was therefore suggested as a potential dating signal for use in sediments older than can be dated by OSL.

-TT-OSL origins and use for dating-

The thermally-transferred signal can be said to consist of two components, a highly dose dependent component (called ReOSL), and a less dose dependent signal (called BT-OSL). BT-OSL was originally thought to be dose independent, but subsequent experiments indicated it has a dose dependence (Porat et al, 2009 and Kim et al, 2009).

A note on terminology: although the terms "ReOSL" and "BT-OSL" assume that the signals are caused by the double and single transfer mechanisms (see below) respectively, they are still used in the literature to refer to the two TT-OSL signals despite changes in thought about the signals' origin. A more general set of terms for the signals would be "dose dependent" (DD) and "dose independent" (DI), and it is these I will be using for the remainder of this thesis. ("Less dose dependent" may be a more accurate description than "dose independent", but I have chosen "dose independent" for the sake of brevity.)

The dose dependent component of the thermally-transferred signal was originally thought to be caused by recuperation of the original signal (Wang et al, 2006b). Once stimulated by

light, the electrons can either fall back down to the ground state, down to a recombination centre, or down to its own or another type of trap. Recuperation is a phenomenon in which excited electrons fall back into another trap population, and are then transferred back into their original metastable state by thermal stimulation (Aitken and Smith, 1988). This was called the double transfer mechanism, as the charge was moved two times: once from the OSL trap population to a separate trap population, and then back again.

It was thought that the OSL signal in quartz was not being saturated by a lack of metastable electron trapping states, but rather by a lack of recombination centres. TT-OSL signals are much smaller than the original OSL signals. In the double transfer case, this means it is only a small proportion of the original OSL trap charge, and due to the smaller amount of charge, saturation by lack of recombination centres would not take place.

The dose independent signal, by contrast, was thought to come from unbleachable traps. As this signal came directly from a deeper trap, this process was called the basic transfer or single transfer mechanism.

After further study, it was thought that the dose dependent signal is also produced by a single transfer mechanism (Li & Li, 2006). Experiments and simulations have suggested that the DD component and DI component are related to the traps that peak at 290 and 325 °C respectively when viewed via TL at 0.2 degrees per second (Adamiec et al, 2010). It was suggested in 2011 that the highly dose dependent part of the TT-OSL signal is produced by both the single and double transfer mechanisms, the double transfer mechanism ("recuperation") making up around 10% of the TT-OSL signal (Shen et al, 2011).

The origin of the TT-OSL signal dictates its suitability for luminescence dating, and changes in thought about its origin must necessitate a re-evaluation of its usefulness for dating. In the first case, the dose dependent TT-OSL (DD-TT-OSL) originated from the same trap as the OSL signal, and thus had the same bleachability and stability. New thoughts on the origin of the TT-OSL consider that the DD-TT-OSL signal may come instead from the less bleachable TL traps, thus limiting the cases in which the procedure is applicable to dating. This also raises the question as to whether TT-OSL, if only originating from metastable states easily

measured in TL, is any more accurate as a dating technique than measuring the TL directly. While TT-OSL measures signals sampled from a selection of two, three or more traps, TL is able to resolve each trap emission separately, and can select the best peak or peaks to use considering the bleaching scenario and saturation prospects of each individual sample. Whether TT-OSL dating has any advantages over TL for dating very old sediments is not immediately clear. This question is one I hope to answer in this project.

-Reading TT-OSL signals and comparisons with OSL signals-

As the TT-OSL signal is much smaller than the OSL signal, to measure TT-OSL the OSL signal must first be removed, usually by the same optical stimulation used for OSL and TT-OSL measurements. In some samples this takes a long time; in tests using 7 mm aliquots of south-east of South Australia quartz, the curve only became approximately linear after 200 seconds of illumination with blue diodes, and continued to bleach after half an hour (see chapter 6). However, after the first minute of illumination, the gradient of the exponential curve becomes low enough that over the time taken to read the TT-OSL signal it is approximately constant, and so the value of the light sum at the end of the OSL can be subtracted from the TT-OSL signal to get rid of any residual OSL signal.

After the OSL signal has been sufficiently bleached, a preheat to stimulate TT-OSL is given to the sample. The TT-OSL signal is then stimulated in the same way as the usual OSL signal. The signal is calibrated by the sample's response to a small test dose. After a preheat to 300 °C in order to empty the traps responsible for the DD-TT-OSL signal, the dose-independent TT-OSL (DI-TT-OSL) is measured and calibrated. Each dose-dependent TT-OSL measurement is calculated by the following equation:

$$DD\text{-}TT\text{-}OSL = \left[\frac{(TT\text{-}OSL - end\ of\ OSL\ signal)}{(signal\ from\ test\ dose - end\ of\ test\ dose\ signal)}\right] - \left[\frac{(DI\text{-}TT\text{-}OSL - end\ of\ OSL\ signal)}{(signal\ from\ test\ dose - end\ of\ test\ dose\ signal)}\right]$$

Creating a calibrated DD-TT-OSL dose point requires three to four extra measurements than an OSL measurement. This, in addition to TT-OSL's small signal strength means that the errors in a DD-TT-OSL measurement will in general be larger than the errors of an OSL measurement. It is in the range

where OSL signals are beginning to saturate and TT-OSL signals still have a relatively linear relationship to dose that TT-OSL equivalent dose results will begin to have smaller errors than their OSL equivalents, even though the individual data points will still have larger errors. As quartz OSL signals start to saturate at around 150 Gy, comparison tests between dose equivalents gained from the two procedures will have to include tests on samples with natural dose exposures well above this range.

-TT-OSL protocols-

	Basic TT-OSL protocol
Order	**Step**
1	Preheat
2	OSL measurement
3	Preheat to stimulate TT-OSL
4	TT-OSL measurement
5	Test dose
6	Preheat
7	OSL measurement of test dose
8	Preheat to stimulate TT-OSL
9	TT-OSL measurement of test dose
10	Annealing (high-temperature preheat)
11	OSL measurement
12	Preheat to stimulate DI-TT-OSL
13	DI-TT-OSL measurement
14	Test dose
15	Preheat
16	OSL measurement of test dose
17	Preheat to stimulate TT-OSL
18	TT-OSL measurement of test dose

Table 2.1: The basic protocol used to measure TT-OSL signals in quartz.

Protocols for measuring TT-OSL generally start with steps 1-7 from the table above. While most protocols measure the OSL response to the test dose, some protocols (such as the one used by Stevens et al, 2009) measure the TT-OSL response to the test dose, rather than just the OSL response, including steps 8-9 after step seven. The test dose is made to measure the sensitivity of the aliquot. Measuring the OSL response to the test dose assumes that the sensitivity of all the traps the TT-OSL samples are always in the same proportion to the OSL trap. Measuring the TT-OSL response to the test dose

assumes that steps 1-4 above do not create a sensitivity change large enough that the sensitivity in the first cycle cannot be recreated from measuring the sensitivity of the second cycle. While measuring the sensitivity of a measurement by repeating the same type of measurement would be the ideal, the low signals of TT-OSL stimulations and the small test doses given mean that using the TT-OSL signal for the test dose may give less accurate results than the OSL signal, which would have much better counting statistics and smaller errors.

Many protocols follow the first seven to nine steps with a measurement of the dose independent (DI) TT-OSL signal (shown in steps 10-18 of Table 1.1), though some simplified protocols such as that of Porat et al (2009) leave out this part. This part of the protocol assumes that the DI-TT-OSL is completely dose independent, and so the test dose in the first step does not increase the signal. As stated previously, the DI-TT-OSL has been shown to have a small dose dependence. Whether this dose dependence and the test dose are both large enough to significantly change the DI-TT-OSL light sum is uncertain. As the quartz metastable states relevant to this procedure may sensitise with dose exposure, this uncertainty highlights the need for small test doses.

As the DI-TT-OSL signal is in fact slightly dose dependent (Kim et al, 2009), it can also be used to find the natural dose of the signal. Jacobs et al (2011) compared DD-TT-OSL and DI-TT-OSL equivalent doses, and found that both gave similar results in most cases. As it is suggested that the DD-TT-OSL signal comes from a trap population with a smaller lifetime than DI-TT-OSL, it was suggested that DI-TT-OSL be used as a check on the suitability of DD-TT-OSL signals for dating. If the DD-TT-OSL and DI-TT-OSL signals give the same equivalent dose, it can be assumed that the sample was both adequately bleached at deposition, and that the lifetime of the DD-TT-OSL trap population is suitable for dating the sample.

In 2006, Wang et al found that an annealing temperature of 300 °C got rid of any dose dependent aspects of the TT-OSL signal. This temperature is commonly used in TT-OSL protocols, though the annealing temperature required to measure DI-TT-OSL may change with each sample. The annealing step of the protocol assumes that the dose independent part of the signal is much more thermally stable than the dose dependent part. This may not be the case if part of the dose

dependent signal comes from double transferred OSL as suggested by Shen et al (2011). If the hypothesis of Wang et al (2006b) that the OSL signal saturates because of a lack of recombination centres is wrong, double transferred OSL will be dose independent for large doses. If the dose dependent TT-OSL signal comes from high-temperature TL peaks, the 325 °C peak component of the DI-TT-OSL will be less thermally stable than the DD-TT-OSL component.

Wang et al (2007) performed some experiments on the suitability of different test doses, and for their samples were able to most closely reproduce specific doses when using a test dose of approximately 10% of the known or estimated dose. Shen et al (2011) suggest that around 10% of the TT-OSL signal is due to the double-transfer process. If the OSL signal is saturated, and the test dose in step five contributes to the less-dose-dependent signal measured in step 13, the results may be artificially corrected during this process. Though the artificial correction would be small, it may be possible to see if it occurs by observing results from samples with unsaturated and saturated OSL trap populations, and observing results from 0-dose (modern) samples. In this scenario, results from samples with unsaturated OSL trap populations would give overestimates of the age, and modern samples would have higher than expected results for the dose. Results for samples with trap populations saturated in OSL would be more accurate.

During data analysis, the DI-TT-OSL signal is subtracted from the full TT-OSL signal, taking into account the sensitivity changes between the two results (calculated from the test dose measurements).

Preheat steps before OSL, TT-OSL, and DI-TT-OSL measurements are usually done at 260 °C (as in the protocols of Wang et al (2007), Porat et al (2009), Tsukamoto et al (2008), Pagonis et al (2009), and Adamiec et al (2010)); or 280 °C (as in Burbidge et al (2011) and Jacobs et al (2011)). Burbidge et al (2011) noted that higher preheats gave rise to sharper dose dependency curves, and reduced the slower components of the signal more than the faster ones. Preheats before test doses were generally done at 220 °C.

For multiple-aliquot protocols, which use a separate aliquot for each cycle in order to reduce the impact of the quartz sensitivity changes after heating, the cycle stops here. For single-aliquot protocols, a "hot wash" in order to reset the

traps is undertaken as the last step of a cycle. The temperature and duration of the hot wash, and whether or not optical stimulation is included, varies widely between protocols. The temperature varies between 280 °C (Tsukamoto et al, 2008) and 350 °C (Adamiec et al, 2010). The duration varies between 100 seconds (Tsukamoto et al, 2008; Porat et al, 2009) and 400 seconds (Stevens et al, 2009).

-Comparing TT-OSL ages to other dating methods-

Ages obtained from sediment layers also dated with other techniques have had varied comparative results. The first, by Wang et al (2006b) attempted to date a number of different Chinese loess samples, whose approximate age was determined from the difference in magnetic susceptibility in glacial and interglacial samples. Their TT-OSL age overestimated a comparison OSL age for the Holocene sample, but for samples from the last glacial/interglacial period (15-130 ka) their results were in accord. TT-OSL results from the BM boundary sample appeared reasonable, but no other numerical ages existed for comparison.

Many studies have found TT-OSL compares favourably with other dating methods. Nian et al (2009) compared TT-OSL and various OSL results from a lakebed sample from Xychang, China. The TT-OSL results lay between those of well-tested OSL methods and an OSL method whose accuracy was in question. Kim et al (2010) compared optical and TT-OSL ages of various stratified layers of possible windblown soil and lakebed origins, and found that TT-OSL ages were in stratigraphic order, while their optical ages were not. In 2011, TT-OSL and optical ages were obtained for the sediment of a palaeolake from Oman, and agreed with each other within errors (Rosenberg et al, 2011). Sun et al (2013) compared TL and TT-OSL ages of a middle Pleistocene hominin site in Luonan Basin in Central China, and found the ages of both dating methods were in stratographic order and agreed with each other. Arnold et al (2013) compared TT-OSL and OSL dates for the Hotel California middle Paleolithic site in Spain, and found the ages were in good agreement, especially using single grain SAR protocols for both techniques. Pickering et al (2013) dated sea caves of around 1 million years, and found TT-OSL and U-Pb ages to

agree. Ryb et al (2013) dated with OSL and TT-OSL methods eroded hilltops, and ages compared favourably.

However, not all TT-OSL studies have had such agreeable results. Thiel et al (2012) compared TT-OSL ages to OSL ages and IRSL ages of raised costal-marine terraces. They gained mixed results for the TT-OSL OSL comparisons: two agreed with each other, but one TT-OSL age overestimated and one underestimated the OSL results. Of the older IRSL dated samples, two of three TT-OSL ages agreed with the IRSL ages. Athanassas and Zacharias (2010) compared OSL and TT-OSL results of marine sediments, and found a negative systematic trend when comparing TT-OSL ages to ones gained by OSL. It was not known whether the TT-OSL or optical ages were more accurate. Schmidt et al (2011) compared OSL, IRSL and TT-OSL ages for loess records from the late middle and upper Pleistocene. While OSL and IRSL results generally agreed with each other, TT-OSL ages overestimated the ages when compared with the other two methods. Brown and Forman (2012) studied the TT-OSL of loess deposited in the Missouri and Mississippi river valleys. Younger samples had TT-OSL ages that matched with previously publised IRSL and TL results, but TT-OSL underestimated the oldest sample.

The results seem to suggest that TT-OSL ages can be accurate in situations where optical dating fails (e.g. Kim et al (2010)). The results of Nian et al (2009) and Athanassas and Zacharias (2010), however, indicate a potential systematic trend away from optical ages. In these cases, whether the optical ages or the TT-OSL ages were more accurate is not known, as there were no known independent ages calculated for these sites.

-The importance of dating samples with an independent age control-

Tests of TT-OSL results have generally taken one of two forms: testing the protocol's dose recovery on a known experimental dose, or comparing it to luminescence ages of natural samples. Using experimental doses allows people to view any systematic error trend, but does not account for any changes or difficulties in comparing a natural dose to a set of experimental doses. Using a natural dose more completely

shows the behaviour of results from a natural system, but when the age of the sample is uncertain, the validity of any TT-OSL result is unknown. In their review of TT-OSL, Duller and Wintle (2012) indicate that the reliability of TT-OSL sediment dating is still undetermined, and could be demonstrated by using samples with an independent age control.

THE SOUTH-EAST OF SOUTH AUSTRALIA STRANDED DUNE SEQUENCE

The south-east of South Australia stranded dune sequence is a set of parallel, modern to Pliocene-age stranded dunes many kilometres in length, representing changes in the position of the coast. The oldest inland ancient coast lies between Renmark and Loxton. The dunes were formed by a slow tectonic uplift stranding series of former coastal beaches pertaining to various sea level stands of the Pleistocene glacial/inter-glacial cycle (see fig 2.6). The highest uplift from sea level was approximately 200 metres (Sprigg, 1979).

The dunes can be grouped into two sub-sequences: the older dunes, made of sandstone, free of shelly matter, and extensively weathered (Sprigg, 1979); and the younger set, from 0-800 ka, positioned between Robe and Naracoorte (see fig 2.7) (Twidale and Bourne, 2010). This younger subset consists almost entirely of calcium carbonate (50-95 %) and quartz (Huntley et al, 1993). After formation, most of these dunes developed a calcrete cap, which protected them from erosion. This has preserved the dunes until modern times (Sprigg, 1979). It is this younger subset of dunes which is of interest in this thesis, and from now on mention of the sequence will only refer to this subset.

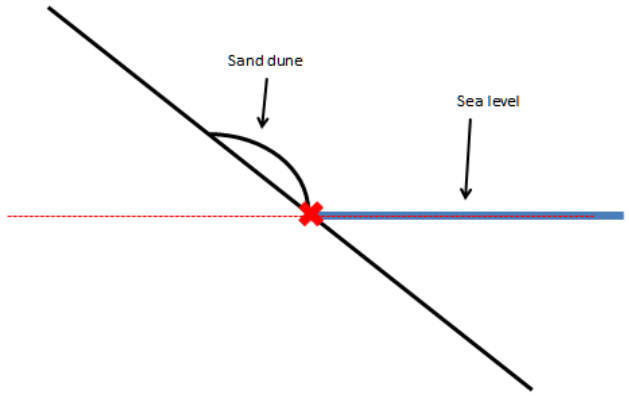

A)

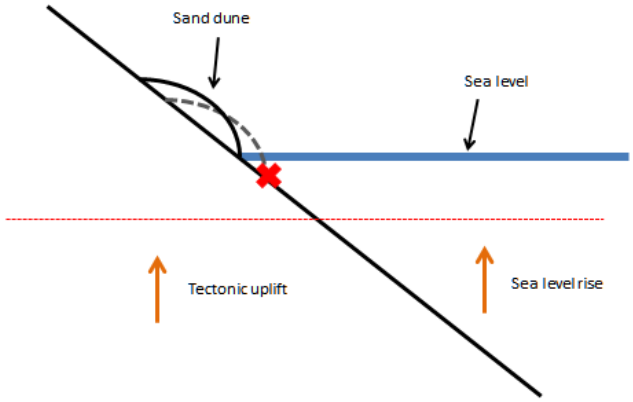

B)

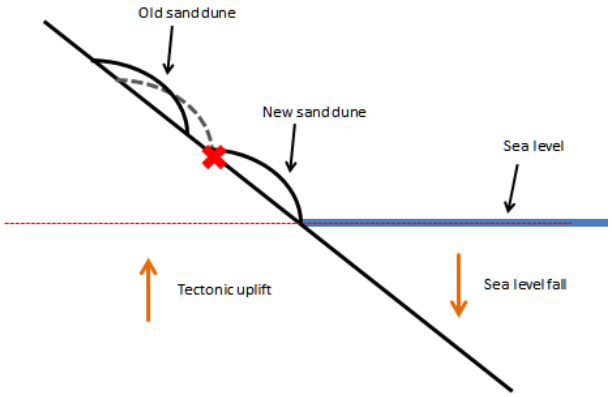

C)

Figure 2.6: A diagram showing how dunes can be sequentially stranded and formed by a combination of tectonic uplift and oscillating sea levels. The red 'X' shows one point on the land (slowly rising due to tectonic uplift), and the red dotted line shows the initial sea level. A) shows an initial sequence, with the sand dune being formed near the sea. B)

shows how rising sea levels reform sand dunes further up the beach, and C) shows how rising land and falling sea levels strand sand dunes higher than the current forming sand dune.

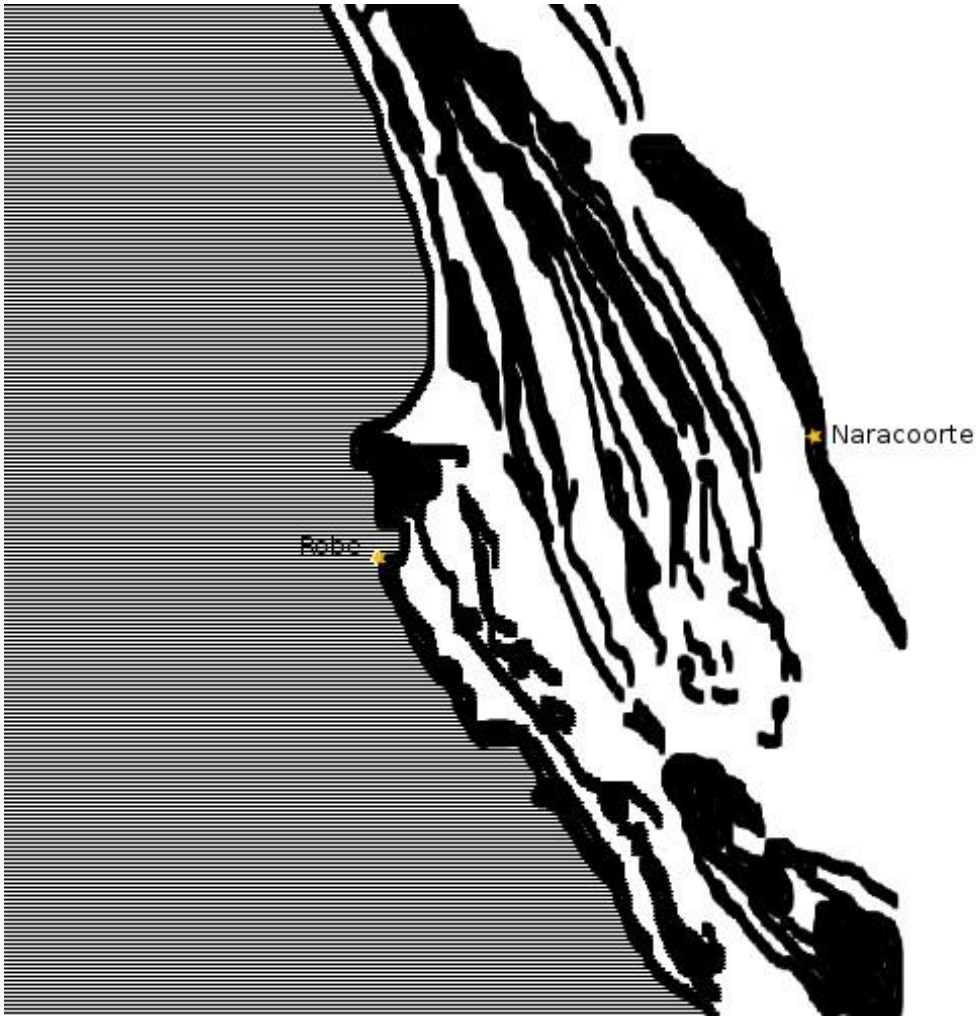

Figure 2.7: A map of the south-east of South Australia. Modern and stranded dunes are coloured black. Map details from Drexel and Preiss (1995).

In addition to the rising land, cyclic sea level changes created the formation of distinct dune ridges approximately 10 km apart (Huntley et al 1993). When in development, these were large, lagoon-backed wind-blown dunes, similar in form to the modern-day Coorong. Although these sea level changes mean that some of the dunes were partially reworked and have layers of development of differing age, such as the Woakwine Range (Sprigg 1979), these layers are relatively distinct, and many dunes are of approximately one particular age.

The calcium carbonate of the dunes has been formed mostly from marine shells, and shelly material is still found in many dunes (Blackburn et al, 1965). The quartz of the dunes may come from previous sea beds exposed by times of low sea level, though the ultimate formation of the dunes is thought to be at the high sea level part of the sea level cycle. In this scenario, previously formed dunes were reworked or destroyed by the raised sea (Blackburn et al, 1965), creating the set of distinct ridges seen today. A great deal of the sand deposits in the region are carried from inland by the Murray River, which is thought to have been more active in sediment transportation in the past (Sprigg, 1979). The source of this sand is primarily desert dunes. A fraction of the quartz of older dunes may have come from streams originating in the Mount Gambier region (Blackburn et al, 1965), providing younger, volcanic quartz. While the origin of the quartz for each dune is unknown, it is likely that fractions of the quartz in each dune are of varying origin, age and history.

The quartz of the dunes is suitable for luminescence dating. The OSL of a great deal of the quartz of the dunes is very sensitive to small doses, giving counts in the order of tens of thousands for doses less than 10 Gy. As the dune sands were wind-blown, it is likely that they were exposed to a great deal of sunlight, and were therefore adequately reset before burial. Due to the formation of a calcrete cap over the top of the dunes, weathering and re-exposure are unlikely. Bioturbation of the dunes is not very significant. A great deal of the dunes have large deposits of the same sample age, and before the development of topsoil the dunes would not have supported a very large component of burrowing life. Although the region has seen the introduction of rabbits, large-scale burrowing has been recent enough that any turbation of this kind is obvious. Solution pipes can be seen in the area, with a maximum depth of seven to eight metres (Blackburn et al, 1965). However, these pipes are distinct, perpendicular, do not branch, and can easily be avoided when collecting samples.

The dunes have been dated a number of times by independent dating methods. They have been dated by modelling (Huntley et al, 1993a), oxygen-isotopes (Schwebel, 1983 and 1984; Belperio and Cann, 1990), TL (Huntley et al, 1985 and 1994; Huntley and Prescott, 2001), OSL (Banerjee et al, 2003), OSL inclusions (Huntley et al, 1993b), and at Naracoorte by

magnetic reversal (Idnurm and Cook, 1980). The ages agree with each other within a few ka, though there has been some trouble dating the Naracoorte samples. It should be noted that the model and oxygen isotope date the dunes from their first formation, while TL and OSL methods date from the last burial of the sediments. As the dunes were windblown and were possibly reworked before the formation of their calcrete caps, TL and optical ages are expected to be slightly younger than oxygen isotope and model ages.

Due to the extensive, independent dating of the dunes and the dunes' distinct ages, the south-east of South Australia stranded dune sequence has been proposed as a quartz thermoluminescence test sequence (Huntley et al, 1985), and by extension a test sequence for other luminescence methods. The brightness of the OSL of the grains makes it a useful test sequence for TT-OSL, due to the decreased light output of this method. While the maximum natural background dose of the sequence has been calculated to be approximately 455 Gy, much lower than the kGy that TT-OSL is thought to be able to date, the sequence provides a test of TT-OSL against TL and ages found independently from luminescence techniques, and through the range at which OSL begins to become unreliable.

03-EQUIPMENT USED

Various machines and equipment were used for the experiments in this thesis. Below are listed their specifications, and to what purposes they were put.

-Risø TL/OSL DA-20-

This machine is an automated luminescence measuring device, with the ability to run series of programmable protocols. It has a computer-controlled β irradiator, a heating plate, and blue and IR diodes for stimulation. The automation of the luminescence protocols means that they can be followed with greater precision, and allows long protocols to be run continuously. Two of these machines were used, one for aliquot measurements, and the other for single grain (or small aliquots in single grain disc) measurements (Bøtter-Jensen, 1997; Bøtter-Jensen et al, 2000).

-Risø TL/OSL DA-8-

An earlier version of the Risø automated TL and OSL reader. This machine was only used for initial TT-OSL experiments. It uses a green lamp for optical stimulation, which requires a warm-up time before each use. In addition, the illumination is controlled by an electro-mechanical shutter, and is of lower intensity than the DA-20 model.

-Single grain reader-

The single grain reader module is an attachment to the Risø TL/OSL DA-20. Grains are placed in depressions on specialised discs, and stimulated individually with a green 532 nm laser, which has a maximum energy fluence rate at the sample of 50 W/cm^2. Due to the smaller signals gained and the power of the laser, OSL measurements for each grain may only take between 1 and 2 seconds before background levels are reached (Bøtter-Jensen et al, 2000).

-Filters-

In all experiments with stimulation by a blue diode or a green laser, a 7 mm Hoya U-340 filter was used, which transmits wavelengths between 250 and 390 nm, with a peak transmittance of 79.9 % at 340 nm. In experiments with IR

stimulation, a 3 mm Schott BG-39 filter was used, which transmits wavelengths between 310 and 810 nm, peaking at a 97% internal transmittance at 500 nm. A Corning 7-39 filter was used for TL measurements, which transmits wavelengths from 310 to 420 nm, with a peak transmission of 57 % at 365 nm. This filter begins to transmit light again at 685 nm, but the TL measurements made did not go to high enough temperatures that long-wavelength incandescence was a problem.

-Photomultiplier tubes (PMTs)-

The photomultiplier type used with both Risø machines is the bialkali EMI 9235QB, with a maximum detection efficiency in the range between 300 and 400 nm.

The photomultiplier used for aliquot measurements was exposed to an LED with increasing current levels (0-35 mA). Tests were done with the LED far from the photomultiplier tube and a 20 % neutral density filter between the LED and the PMT, with the LED near the photomultiplier and the neutral density filter in place, and the LED far from the photomultiplier and no neutral density filter in place. From these experiments, it was found that the PMT response increases linearly from 60 to 1,960,000 counts (see fig 3.1).

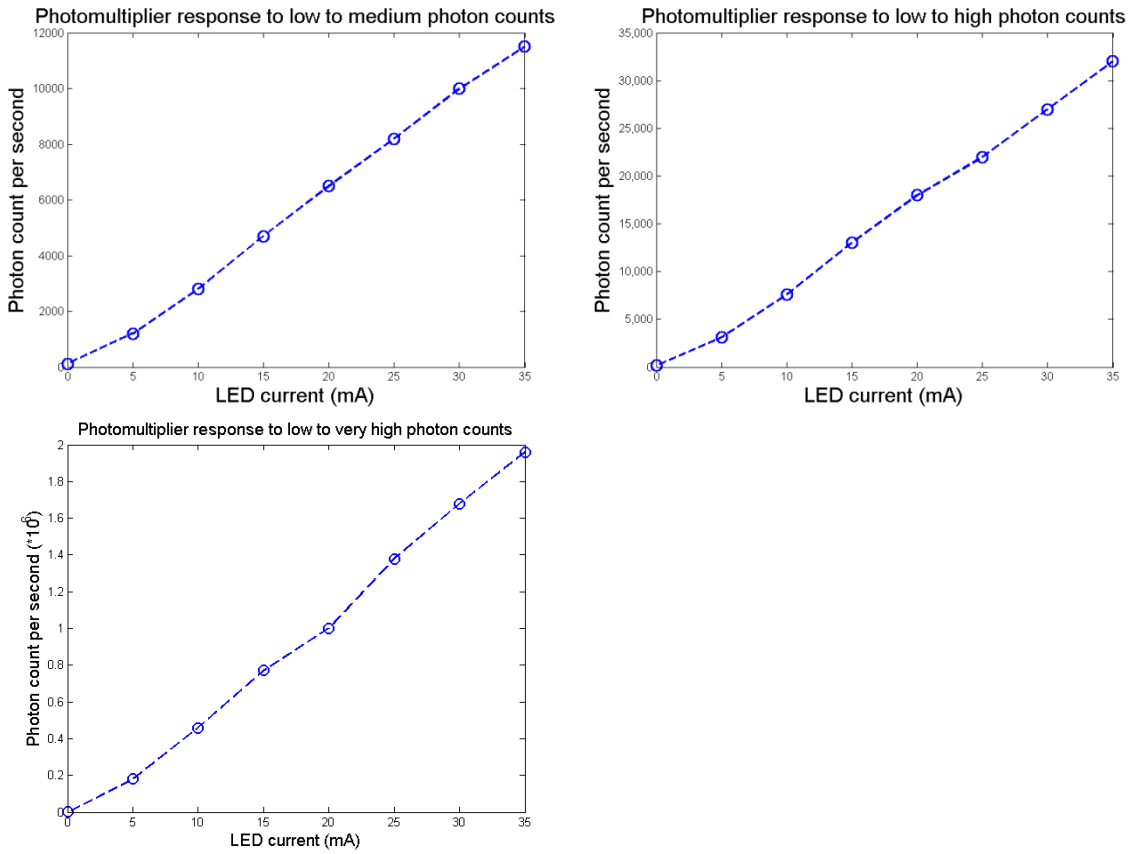

Figure 3.1: Photomultiplier response to an LED with increasing current. A) shows the response with low counts; B) shows the response up to high counts, and C) shows the response up to 2 million counts per second.

The dark counts for the photomultiplier tube were then measured while increasing the high voltage of the PMT from 500 to 1500 V. Counts vs high voltage level measurements were also done up to 1200 V with an LED far from the photomultiplier tube with and without a 20 % neutral density filter between the light source and the PMT (see fig 3.2). This was to simulate dim and bright signals. For each high voltage level, a calculation of (signal-dark noise)/dark noise was made, to find the high voltage level that maximised the signal to noise ratio of the PMT. For dim light, the signal to noise ratio plateaued at 980 V, while the bright light sample plateaued at 980 V. Both signal types had the signal-to-noise ratio begin to decrease at 1080 V. A high voltage level of 1050 V was used for the improved 5 mm SESA results (Chapter 11) and the Baldina Creek sample measurements (Chapter 13).

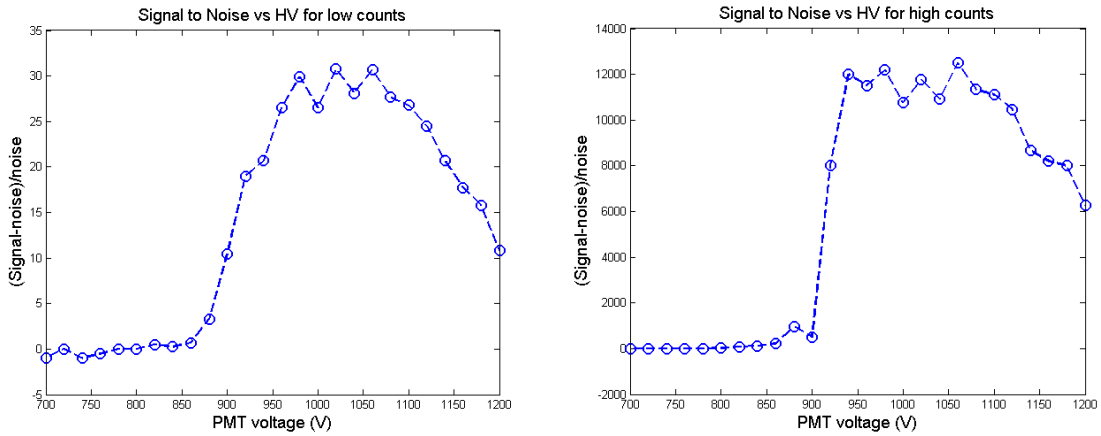

Figure 3.2: Signal-to-noise ratios for different High Voltage levels. A) uses low counts, and B) uses high counts. These are using the PMT used for aliquot measurements.

Signal to noise ratio vs high voltage measurements were also taken for the photomultiplier used with single grain discs, by Daniele Questiaux and Don Creighton (see fig 3.3). The signal to noise level plateaued at 1150 V.

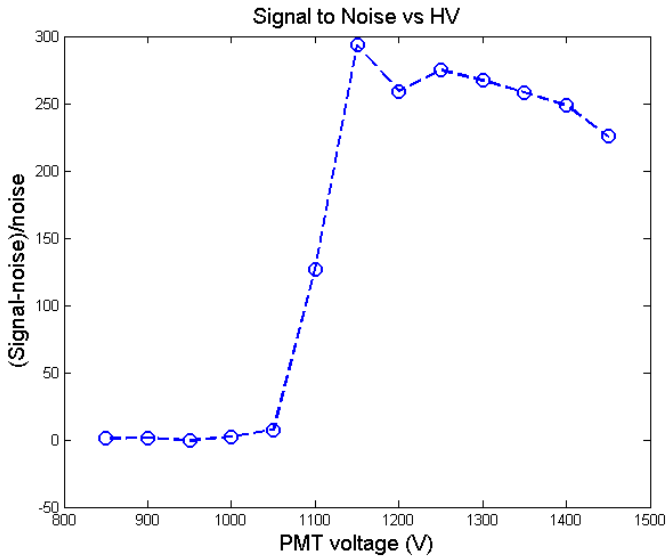

Figure 3.3: Signal-to-noise ratios for different High Voltage levels. This graph was made using the PMT used for small aliquot and single grain measurements.

The photomultiplier used with the Fourier Transform Spectrometer is a bialkali S20 EMI 9558 QB, which is a red sensitive photomultiplier. It has a maximum detection efficiency between 200 and 400 nm.

The photomultiplier used with the Risø TL/OSL DA-8 is an EMI 9635 QB. The detection efficiency peaks at 200-450 nm, and falls below 10 % at 550 nm.

-OSL stimulation-

Three types of OSL stimulation were used:
Blue diodes: 470 nm wavelength light with a maximum power of 80 $mW.cm^{-2}$
IR diodes: 870 nm wavelength light with a maximum power of 145 $mW.cm^{-2}$.
Green laser: 532nm 10 mW ND:YVO4 laser, used for single grain measurements.

Note that unless otherwise stated, stimulations were done at 90% power.

-Fourier Transform Spectrometer-

The Fourier Transform Spectrometer (FTS) is a custom-built piece of laboratory equipment initially designed and built by J R Prescott and Hans Jensen as part of H Jensen's PhD thesis (Jensen, 1982), and modified over the PhD projects of Riaz Akber (1986) and Phil Fox (1990). It is situated at the University of Adelaide, and is used for "three-dimensional" studies of thermoluminescence responses (Prescott et al, 1988). In essence, the FTS is a thermoluminescence reader with an interferometer situated between the sample and the photomultiplier. The moveable mirror of the interferometer is moved by a piezoelectric stack. The mirror is moved back and forth while the sample is heated, creating an interferogram. A "three-dimensional" response of light intensity vs photon energy vs temperature is created. The FTS has a wavelength response range from 250 to 740 nm with a resolution of 20 nm at 550 nm.

For further specifications, refer to Jensen H E (1982), Akber R A (1986), and Fox P J (1990) in the reference list.

-Notes:-

-Specifications for stimulation power and wavelengths and the EMI bialkali 9235QA photomultiplier detection efficiencies were gained from the Risø DTU website (Risø DTU 2011).
-Diode powers stated are maximum power measured from the sample position by the Risø laboratory.

04-THE SESA SAMPLES

Seven samples from the south-east of South Australia were used in experiments documented in this thesis. Six were collected previously by D. J. Huntley and J. R. Prescott. These samples were stored without processing in light-proof galvanised iron paint tins. Processed fractions of these samples were used previously for TL measurements of the dunes. A table of sample names, and previously-found ages and natural doses is shown below.

The eighth sample (LBST(P)) was used as a modern-age equivalent to the dunes, and collected from Long Beach, near Robe, in late February 2013. Grains were taken by collecting sand blown onto emplaced collecting surfaces by the wind. In this way, only grains that have been through the wind-blown bleaching process were collected.

The TL and OSL ages in the above table were gained using quartz grains, rather than other minerals. They are therefore a good reference for potential TT-OSL ages. As OSL and TL ages may be slightly younger than oxygen isotope and magnetic reversal ages gained from the same dunes, in this thesis TT-OSL ages are generally compared to the OSL and TL ages where possible. Although these ages generally match those gained by non-luminescence means, they are sometimes slightly younger, possibly due to the dunes being reworked before being permanently stranded.

-Sample processing-

All samples collected were mostly composed of quartz and calcium carbonate. The calcium carbonate in older samples was the matrix in which the quartz grains were held. In some younger samples calcium carbonate was contained in some identifiable shelly matter as well. In the modern-age sample, the calcium carbonate was present as shell grit. During processing the calcium carbonate was dissolved in HCl acid. Any clay-like (fine) material was taken out in suspension following dispersion in an ultrasonic bath with sodium hydroxide. The amount of such fine material in all samples was minimal.

Sample	Range/ place of collection	De (Gy)	Age (ka)	Source
LBST(P)	Long Beach		0	By definition
RB1s/2	Robe I/II			
		0.4 ± 0.3	0.8 ± 0.6	Huntley et al 1993b—quartz inclusions
WK4	Woakwine 1	65 ± 1.9	120 ± 8.7	Banerjee et al 2003
		69 ± 2	118 ± 4	Huntley et al 1994
		73 ± 3	132 ± 6	Huntley et al 1993a
		64 ± 6	114 ± 16	Huntley et al 1993b—quartz inclusions
		47 ± 7	116 ± 16	Huntley et al 1993b—quartz inclusions
			120	Belperio and Cann 1990
			120	Schwebel 1983
ED1Sa/1	East Dairy	128 ± 16	292 ± 25	Huntley and Prescott 2001
			309	Schwebel 1983
			200	Belperio and Cann 1990
BA2S/2	Baker	209 ± 16	456 ± 37	Huntley et al 1993a
		187 ± 16	390 ± 40	Huntley et al 1993b—quartz inclusions
			500	Belperio and Cann 1990
HA3S/2	Harper	282 ± 20	585 ± 44	Huntley et al 1993a
			650	Belperio and Cann 1990
NE4S	East Naracoorte	455 ± 44	720 ± 70	Huntley et al 1993a
			>860	Belperio and Cann 1990
			950	Huntley et al 1994b—oxygen isotope
			>780	Huntley et al 1994b—Magnetic reversal

Table 4.1: A table of the samples used (their laboratory codes and their place of origin) and a list of ages and equivalent doses previously found for them. Note that the Robe sample may be from the Robe 1 or Robe 2 range, but the specific range was not identified during sampling.

Samples also contained a small but significant proportion of feldspars and heavy grains. These were separated from the quartz by density separations at 2.58 and 2.67 g/cc. The first density separation floats potassium feldspars, while quartz sinks. The second density separation floats quartz and some feldspars, sinking heavier grains.

After density separation, samples were etched with 40% HF acid for forty minutes. This was done for two main reasons: to dissolve any remaining feldspar in the sample, and to etch away the outer 6-8 µm layer of the quartz grains. This outer layer of quartz has been subjected to typically 90 % of the α radiation dose received by the grains, and removing this layer reduces the complexity of dosimetry measurements and calculations. After etching, samples are rinsed in HCl acid to remove fluoride components created in the etching process, then rinsed in distilled water and dried.

When being readied for measurement for luminescence, samples were subdivided into separate aliquots in two different ways. One, used for small aliquot or single grain measurements, involves placing grains in depressions on an anodised aluminium disc. The other is used for larger aliquots, between one and seven mm in diameter. Stainless steel discs are placed under a mask of the desired aliquot size, and sprayed with silicone spray. The discs are then placed on a bed of grains, silicone layer-side-down. Loose grains are shaken off the disc. The resulting aliquot is a monolayer of grains, covering the same diameter as the aperture of the mask.

-Quartz TL analysis-

While the TL of many of the samples has been studied previously (Huntley et al, 1985; Huntley et al, 1993; Huntley et al, 1994; and Huntley and Prescott, 2001), it is instructive to undertake a quick comparison of their characteristics, and to directly compare TL output from each of the samples and the newly collected modern sample (Long Beach). The thermoluminescence characteristics of the etched quartz grains were studied from 0 to 450 °C (see fig 4.1).

Six 5 mm aliquots of 212-250 µm diameter grains were created for the Long Beach, Robe, Woakwine, East Dairy, Baker, Harper, and Naracoorte East samples. Three aliquots from each sample were given a dose close to the expected natural dose, while the others were untouched. The thermoluminescence of the aliquots was measured using a Risø TL/OSL DA-20 with a 7-59 filter, at 5 K/s. After the initial run, the background was taken; then each of the aliquots given a natural dose near the expected value for that sample, and the TL of the sample was measured again. Values were analysed by subtracting the background measurement from the natural or irradiated measurement, and dividing by the weight of the aliquot to obtain a value for counts per milligram.

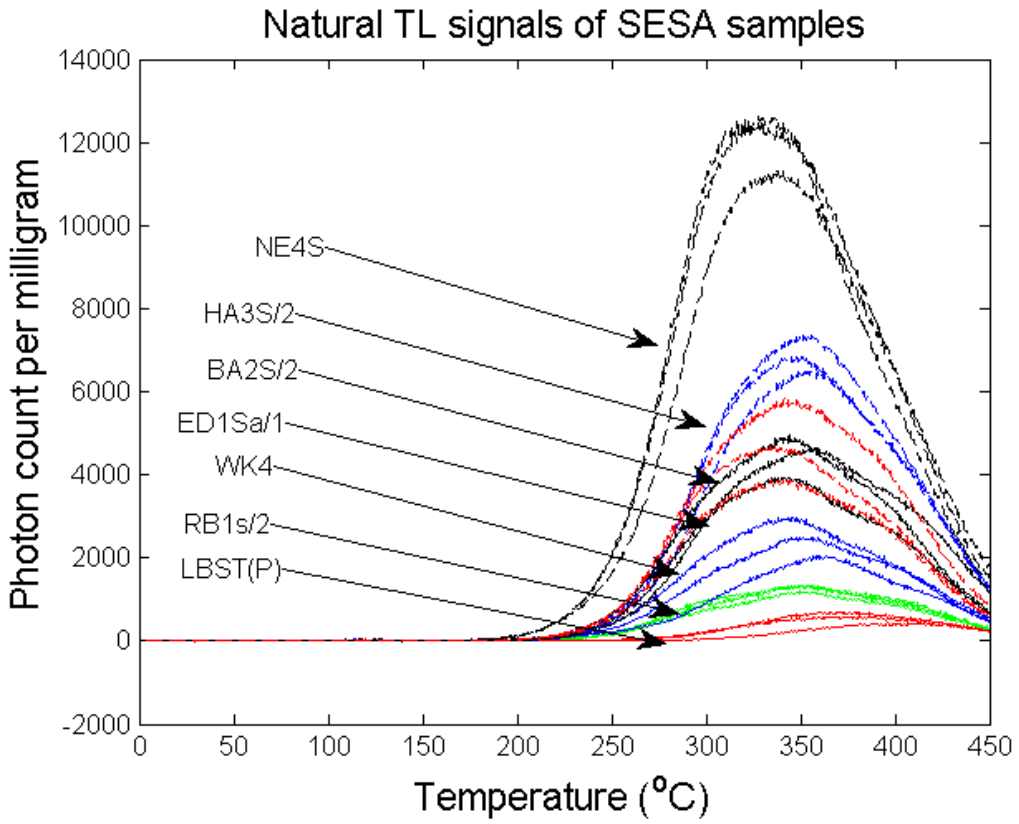

Figure 4.1: Natural thermoluminescence of the SESA samples.

The natural signals appear to increase with age, and the average total counts over the three aliquots for each sample increase with increasing age. The modern sample, LBST(P), had an average total photon count of around 130,000 per mg. The peak in which these counts come from is quite deep, peaking at around 365 °C for two aliquots, and 400 °C for another.

With most younger samples, it is obvious that the photon counts gained are from the addition of two or more peaks, the maximum counts between 300 and 400 °C. The Naracoorte East sample counts peak earlier than the rest, at around 325 °C.

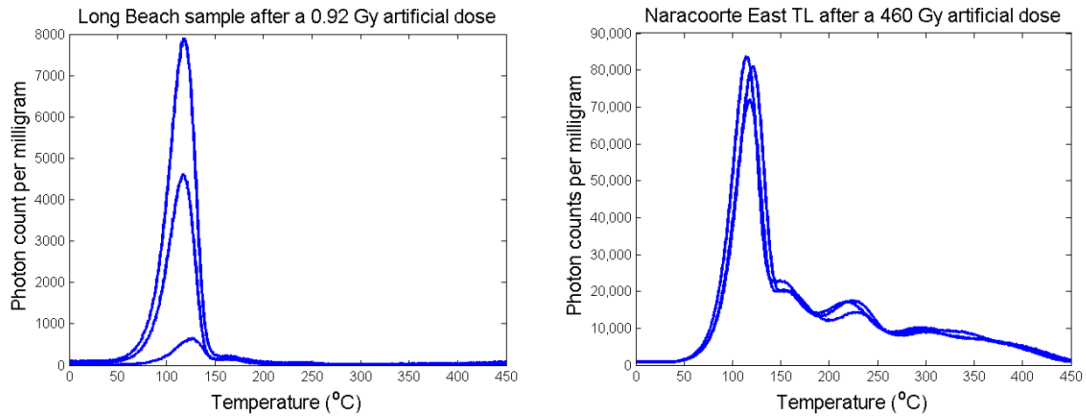

Figure 4.2: A) Long Beach and B) Naracoorte East thermoluminescence using samples that were irradiated after measuring the natural TL. Note that the irradiation given to the Long Beach sample was much smaller than that given to the Naracoorte East sample.

The Long Beach aliquots that were irradiated after the natural had been measured differed very significantly in photon counts for each aliquot (see fig 4.2), especially for the shallow peaks. While the shallow peaks thermally fade quickly due to their short lifetimes (fading to background (undetected) levels in the order of hours or days), the aliquots were irradiated and measured as part of an automated sequence, and the delay between the irradiation and measurement was approximately the same for each aliquot. Two had large peaks at approximately 120 °C; the other had a smaller peak at approximately 125 °C.

Other samples had initial photon counts varying in peak position. Most initial peaks were at 110, 112, 118, 120, 126, and 130 °C. Other distinguishable peaks were at 240 and 315 °C. There is a significant peak near the initial, large peak that is located between 150 and 180 °C.

The mass of the stainless steel discs used to place each aliquot on can affect the results gained. The Risø TL/OSL DA-20 measures temperature with respect to the heating plate, and different thicknesses of discs cause different lag times between the temperature of the heating plate and the temperature of the aliquot. Stray material on the heating plate or disc position can also cause temperature lags.

Although discs were chosen so that aliquots of the same sample were on discs with similar masses, and care was taken to clean the disc positions in the Risø machine before the placement of discs, this survey cannot be used to make specific analysis of the peak positions of the SESA samples' thermoluminescence structure. We can, however, make the following generalisations:

1) The natural thermoluminescence of the SESA sample is on average positively dependent on the age of the sample.

2) The modern (zero-age) sample has the smallest amount of thermoluminescence present. The peak of this thermoluminescence appears to be at a higher temperature than all the other samples.

3) Irradiation of the samples causes low-temperature peaks to appear in all samples.

The cause of number one is reasonably clear: the samples contain deep traps that do not saturate during the age sequence of samples observed. Thus the older the sample (and in general the greater the natural dose), the more thermoluminescence traps in the population are filled. Number three, too, can be easily explained: the low temperature peaks belong to shallow traps which do not have a sufficiently long lifetime to appear when samples are given natural doses at very low rates over thousands of years.

As the modern sample has been extensively bleached, traps that would still be filled in very old samples due to their long lifetimes will have been depopulated, and only extremely hard-to-bleach trap electron populations would remain. This is the most likely cause for the second point. Another, less likely explanation is that this sample has an abundance of a different type of quartz, with a smaller percentage of the lower temperature traps.

-Quartz Fourier Transform Spectrometer analysis-

The emission spectra of etched and unetched quartz fractions for the Robe, East Dairy, Baker, Harper, and Naracoorte East samples were measured by the Fourier Transform Spectrometer (FTS), giving a thermoluminescence reading of temperature vs photon energy vs photon count (Prescott et al, 1988) (see fig 4.3). Each measurement was taken from 0 to 425 °C at 5 K/s in

flowing nitrogen gas. Two aliquots of each fraction were made—one to examine the natural signal, and one to measure the natural signal plus a β dose of approximately 41 Gy. The irradiations were done the day before the measurements, so the shallow 110 °C peak was not present. Each aliquot had identifiable quartz peaks, with no extra peaks present. Unetched quartz samples were measured to compare with feldspar and etched quartz samples and to check for feldspar contamination. No feldspar signals were seen in either set of quartz samples.

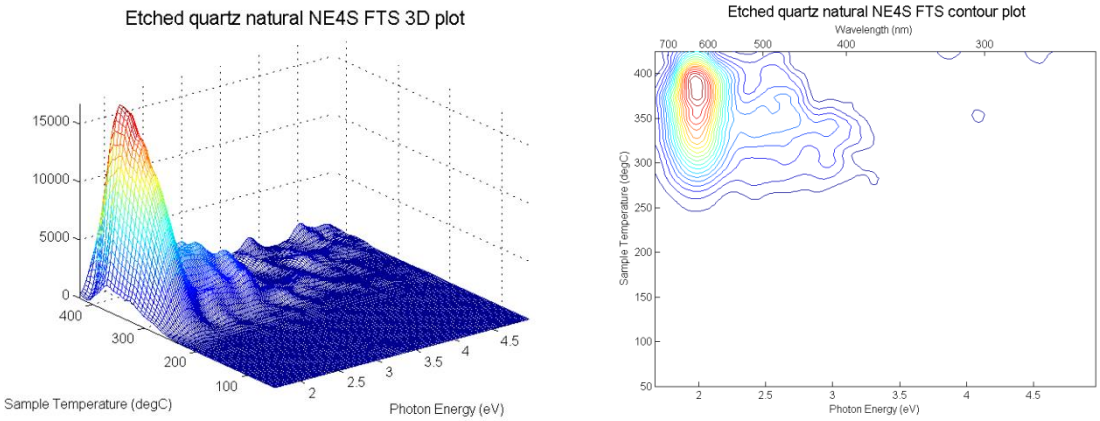

Figure 4.3: Fourier Transform Spectrometer results for natural etched quartz Naracoorte East aliquots. Results for other SESA samples can be found in the appendix.

-Feldspar survey-

Like quartz, feldspar grains, especially high-potassium feldspars (K-feldspars), can be used for sediment dating. They have some advantages over quartz, including higher saturation levels and brighter signals (Li and Li, 2011). However, feldspar signals suffer from anomalous fading, a phenomenon in which electrons are released from metastable states at a rate higher than that suggested by kinetics lifetime equations. It is thought that this phenomenon is due to quantum mechanical tunnelling effects (Wintle, 1973; Visocekas et al, 1976). While there are protocols such as post-infrared infrared stimulation (pIRIRSL) that are claimed to negate anomalous fading (Li and Li, 2011), the presence of feldspars in sediment used for quartz dating, whether as individual grains or as inclusions in quartz, may give anomalous signals or misleading results. Due to the possible usefulness of feldspars in long-range dating, and the possibility that sediment used in quartz dating may still

contain feldspars, a survey of feldspar presence in seven samples of varying ages was undertaken.

Fractions of the floated feldspar (density < 2.58 $g.cm^{-3}$), unetched quartz, and etched quartz were collected for the Robe, Baker, Harper, East Dairy, and Naracoorte East samples. Each fraction was observed under a microscope (e.g. figure 4.4). The feldspar float in each sample appeared to have significant amounts of feldspars, the overall colour of grains in these samples ranging from red to orange. The unetched samples contained a large amount of quartz-like clear grains, with some orange to pink grains present as well (e.g. fig. 4.4, yellow circle). Many of the clear, quartz-like grains had pink or orange veins running through them, or red to orange coloured inclusions (e.g. fig. 4.4, blue square). The etched samples were much cleaner, consisting almost entirely of white or clear quartz-like grains. Some of these contained dark inclusions.

A)

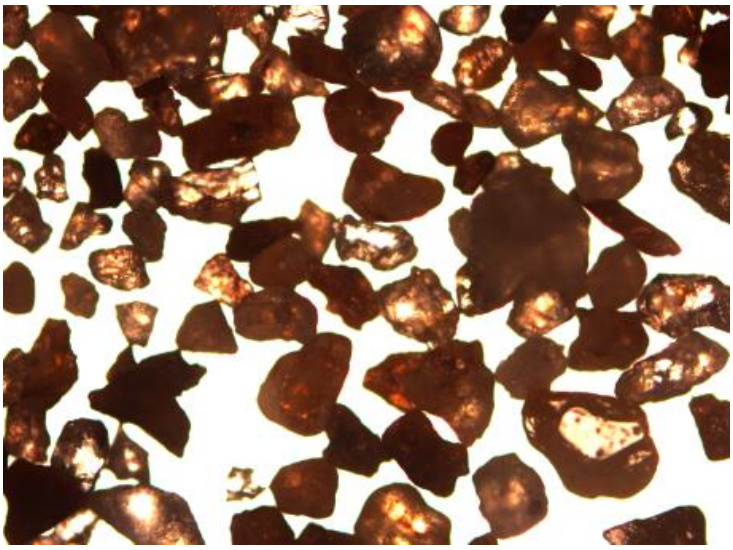

B)

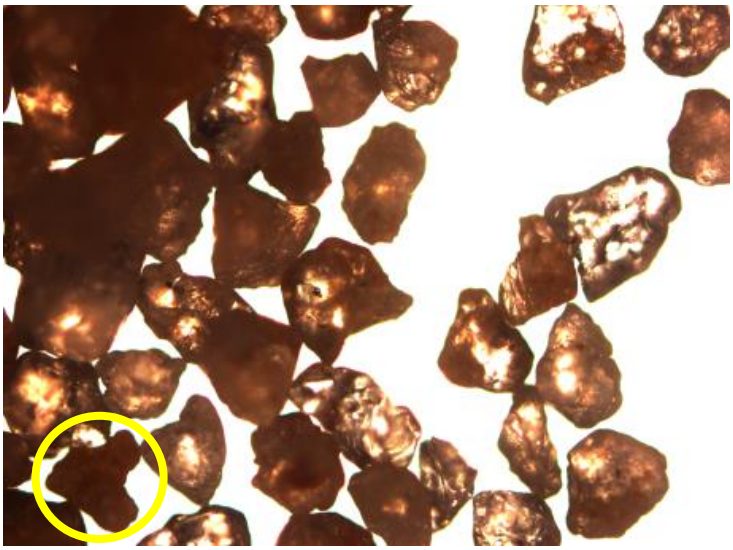

C)

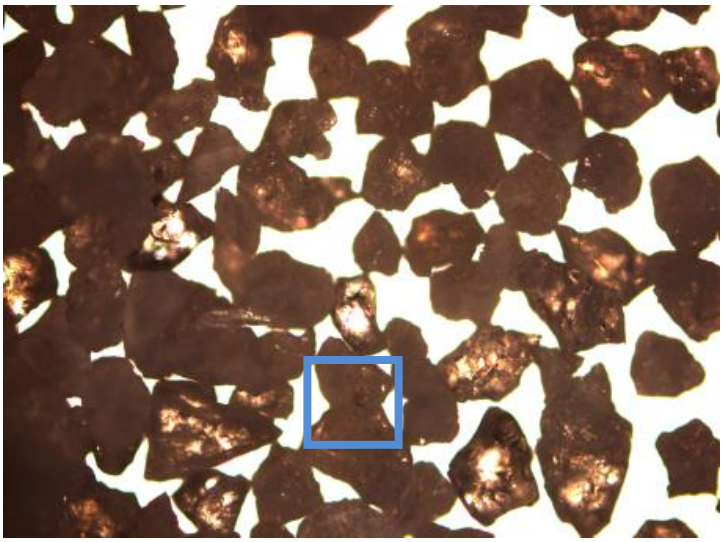

Figure 4.4: Magnified photos of the East Dairy sample. A) Feldspar float; B) Unetched quartz; C) Etched quartz. Photos of the other samples are shown in the appendix.

Experiments were done on the 15 samples to look for IRSL signals. Tests were performed on a Risø OSL/TL DA-20, with a 3 mm BG39 filter in place. Samples were first exposed to IR stimulation at 30 °C for 500 s, in order to view and erase any natural IRSL. The samples were then exposed to 92 Gy of β radiation. After a preheat to 290 °C, the samples were exposed to the same IR stimulation as before (at 30 °C for

500 s), then exposed to a post-IR-IR stimulation at 225 °C (see table 4.2).

Step	Use
500 s 90 % IR diode stimulation at 30°C.	Viewing natural IR signal
1000 s β dose (92 Gy)	Repopulating metastable states
Heat to 290 °C at 5 K/s	Depopulating shallow traps
500 s 90 % IR diode stimulation at 30°C.	Viewing IR signal
500 s 90 % IR diode stimulation at 225°C.	Viewing post-IR IR signal

Table 4.2: The procedure followed when measuring IR signals in this thesis.

The < 2.58 g/cc "K-feldspar" floats had large IR signals, indicating the presence of feldspars. All K-feldspar fractions showed significant signal, even the youngest sample (Robe). The heavy grain fractions (> 2.67 g/cc) had IR signals an order of magnitude lower than that of the light fractions, and apart from the East Dairy sample, unetched and etched samples had roughly the same signal strength. When normalised, K-feldspar fractions appeared to have a stimulation response positively correlated to age until the two oldest samples. The etched and unetched quartz fractions appeared to show no IR signal dependence on age.

While there was an IRSL response from the etched quartz fraction, this does not necessarily mean that there is a thermally transferred IRSL response. Experiments to find out the IRSL response of the etched quartz fraction after TT-OSL preheats were undertaken on a Risø TL/OSL DA-20 with the same filters as above. After a dose of approximately 37 Gy, etched quartz aliquots were preheated to 260 °C for 10 s, given a 30 s IR stimulation, preheated to 260 °C for 10 s, and given a 20 s IR stimulation. The first stimulation gave significant signal, peak photon counts for the first second being between two and eight thousand counts for 5 mm diameter aliquots with approximately 3.5-5.5 mg of quartz each. After the second preheat, no extra signal was found, indicating that there is no IR TT-OSL in these aliquots.

K-feldspar fractions were heated to 425 °C at 5 K/s in the Fourier Transform Spectrometer at the University of Adelaide (Prescott et al, 1988). K-feldspar fractions showed a large

peak at 350 °C and about 405 nm, suggesting the presence of microcline (see fig 4.5).

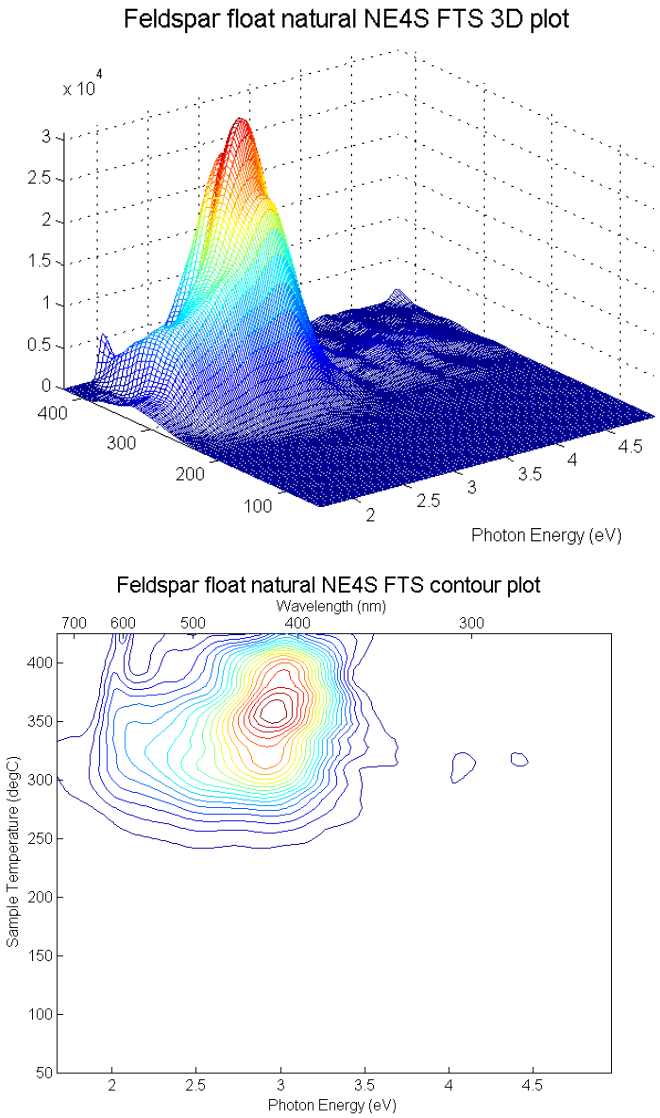

Figure 4.5: Naracoorte East natural K-feldspar FTS results. See the appendix for other FTS results.

It is evident that, although quartz is the predominant sediment grain mineral, there is a significant feldspar presence in the south-east of South Australian stranded dune sequence. The presence of a fraction of high potassium feldspar grains indicates that the sequence can be used as a test sequence for new feldspar dating protocols, such as post-IR IRSL (Buylaert et al, 2009). While unetched grains of quartz show significant amounts of feldspar inclusions, a 40 minute etching in HF leaves clear and for the most part inclusion-free grains. However, the presence of an IR signal

in the samples of etched grains indicates there may be K-feldspar still present, either as inclusions or as autonomous grains.

-Pulsed OSL measurements to assess feldspar and quartz contributions to OSL signals-

The IR tests on etched grains of quartz indicated that there is still feldspar present in the sample, most likely in inclusions. This feldspar presence is not very large in TL, else feldspar peaks would be seen on the FTS measurements, but to find out if the feldspar presence is significant in OSL from these grains compared to quartz, a sensitive comparison technique must be used, such as pulsed-OSL.

Pulsed OSL is a technique in which a light source, usually either a laser or a diode, is turned rapidly on and off, in the order of micro or milliseconds. It is used to study the relaxation times of luminescence materials, to capture OSL signals in materials with large fluorescence signals, and can also be used to separate luminescence components of a mixed-material sample (e.g. Denby et al, 2006 and Ankjaergaard et al, 2010).

The separation of signals is possible as each luminescence mineral has a different initial response to stimulation. Quartz has a relatively slow build-up of signal when the stimulation light is first turned on, and a slow decay when the stimulation light is turned off. Feldspar, on the other hand, has fast build-up and decay times (Denby et al, 2006). Thus the first few milliseconds of signal after the stimulation light has been turned on is a feldspar-dominated signal, and the signal after this time contains an increasing quartz-OSL component. After the stimulation light has been turned off, the signal becomes quartz dominant.

Feldspar and quartz signals have another major difference: feldspar traps empty relatively slowly under blue-light stimulation, translating to a slow decay curve under continuous wave OSL. Quartz OSL traps empty quite fast by comparison.

Using these two differences in quartz and feldspar luminescence signals, one can devise a technique to find feldspar signal in a sample that is quartz-dominated (e.g. Denby et al, 2006 and Ankjaergaard et al, 2010). If one uses pulsed-OSL for a significant amount of time (several

seconds), the pulse response shape of a mixed quartz-feldspar sample will become more feldspar-like in the later pulses than the earlier ones, as the quartz component becomes depleted.

To test this, samples of the < 2.58 g/cc feldspar float, etched quartz, and a mixture of feldspar and etched quartz were made into 5 mm diameter aliquots with approximately 3.5-5.5 mg of grains in each. Aliquots were given a β radiation dose of approximately 11 Gy. They were then given a preheat to 260 °C for 10 s, and then subjected to 12 s of pulsed OSL at 125 °C, with a pulse-on time of 4 ms and a pulse off time of 5 ms.

In the first few pulses, the etched quartz sample gave a typical quartz pulsed-OSL curve. The feldspar float results also looked like a quartz pulse curve in the first few pulses, indicating the presence of quartz in the feldspar float (see fig 4.6). The feldspar float pulse shapes began to look like feldspar curves after approximately 0.7 s. The feldspar-quartz mixture had a quartz-like curve in the first few pulses, and a feldspar-like curve at approximately three seconds. After the twelve seconds, both the feldspar and the feldspar-quartz mixtures both had definite feldspar shapes to their pulse curves. The etched quartz aliquots still had quartz-like curves after twelve seconds, but much lower signal intensity (see fig 4.7).

From this experiment we can see that quartz signal dominates the blue OSL stimulated output from SESA etched quartz samples for at least twelve seconds of pulsed OSL measurement (equivalent to 5.3 s of continuous stimulation). As the OSL output from the sample after twelve seconds was near residual levels, we can say that the total feldspar input to the blue OSL signal is not significant.

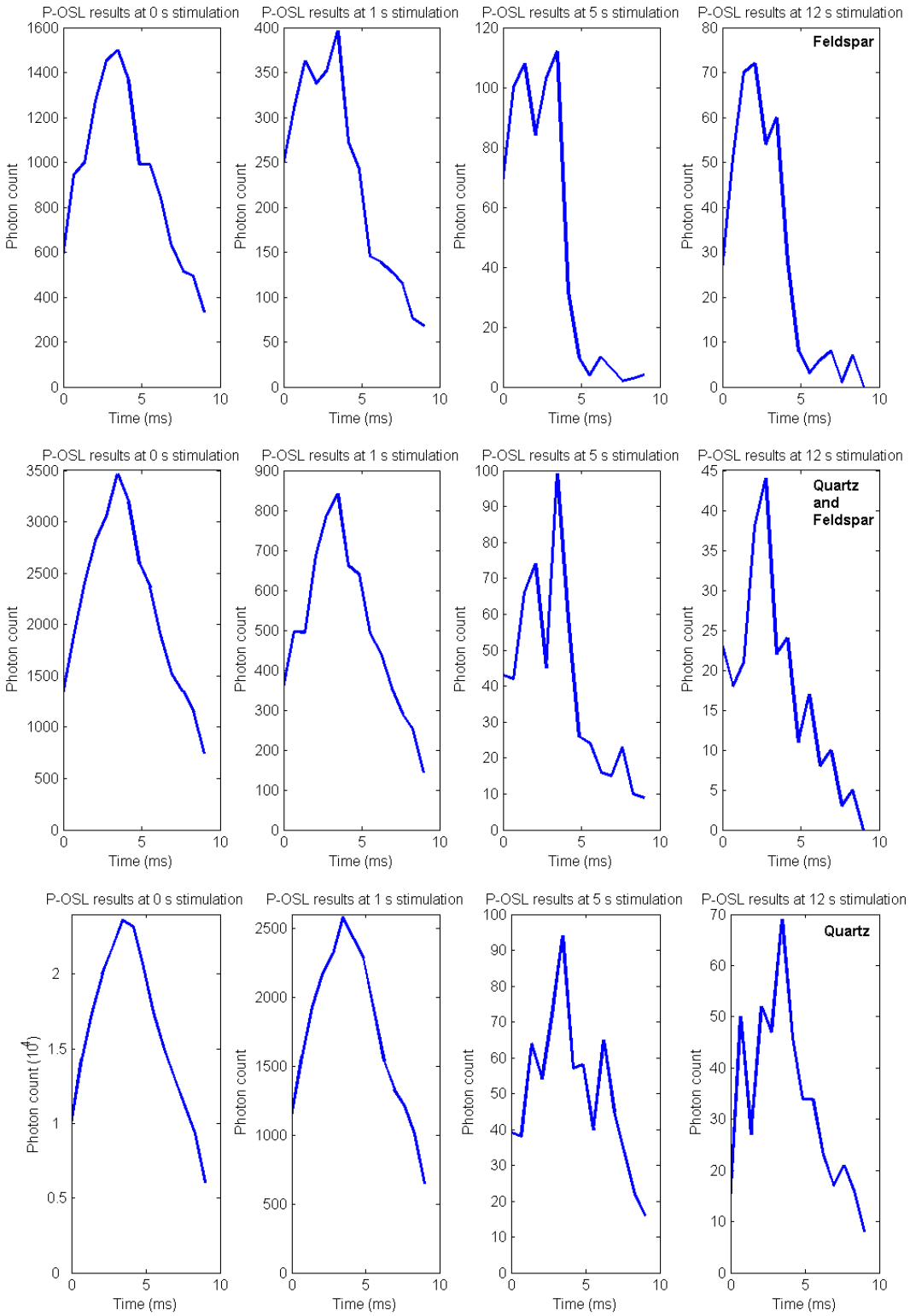

Figure 4.6: Pulsed-OSL results after different lengths of stimulation time. Figures in the top row are the results of the feldspar float; the middle row the quartz and feldspar mix; and the third row the etched quartz. Note that after 12

seconds of stimulation the quartz/feldspar mix peaks before 4 ms, while the etched quartz peaks at the end of the pulsed stimulation at 4 ms, indicating a slower rise in the etched quartz sample.

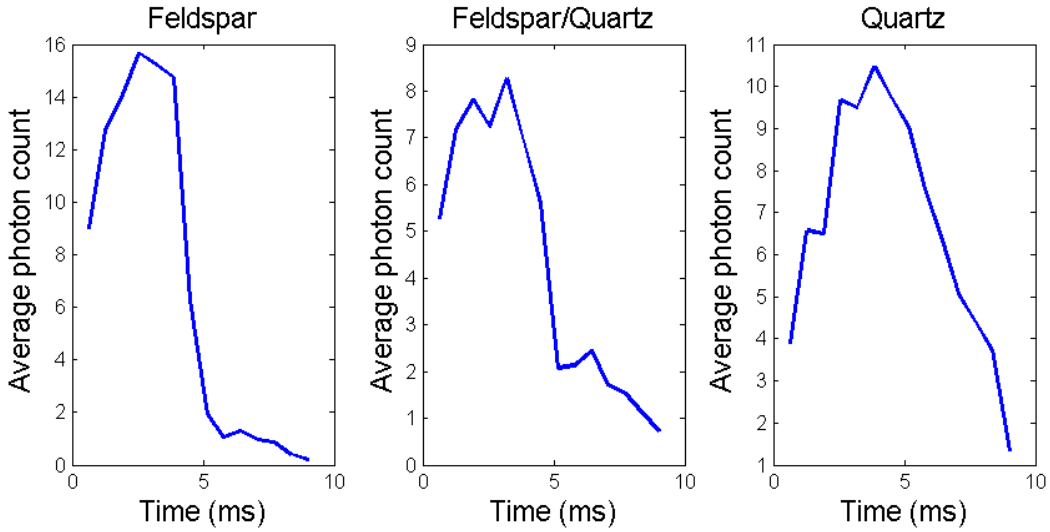

Figure 4.7: Pulsed-OSL results averaged from pulses starting at 11.87 s to 12 s. Note the shape of the quartz results looks the same as the quartz results at zero seconds in Figure 2.6.

-Dose rates-

To find the age of the samples, dose rates must be calculated. Dose rates for the Woakwine, East Dairy, Baker, and Harper samples had been calculated previously (Huntley et al, 1993; Huntley et al, 1994; Huntley and Prescott, 2001). Dose rates for the Long Beach and Naracoorte East samples were calculated for the first time during this thesis.

Dose given to a sample comes from three main sources: from cosmic rays, from radioactive material in the surrounding material, and from radioactive elements inside the grain itself. For quartz samples, the dose from within the grain is assumed to be near negligible unless there are inclusions of other minerals in the grain. Dose from radioactivity in the soil can be calculated using a gamma spectrometer to directly measure the radiation and so enable calculation of the radioactivity by using dose rate equations based on the proportion of uranium, thorium and potassium in the soil; the water content (water in the soil can transport away certain daughter products and provides a passive absorber medium to absorb radiation before it reaches a sample grain); and the density of the sample (which changes due to the sample's

mineral content and compactness). The calculation of radioactivity from the surrounding sediment is affected by the HF etching done when processing the sample, as it takes away most of the grain volume affected by external α radiation. The dose from cosmic rays depends on the location of the sample, its altitude, its density, and the mass of material on top of it.

The Long Beach samples location was found using Google Maps (using the latitude and longitude finding site <http://itouchmap.com/latlong.html>). The water content of this sample was measured directly. The latitude, longitude and altitude of other samples were taken from the 1:50 000 series of Australian Government topographic maps. Overburden measurements and the average water content for the area were taken from sample notes provided by J. R. Prescott and D. J. Huntley. Unprocessed SESA samples were sent to the company "Genalysis Laboratory Services Pty Ltd" (www.genalysis.com.au), for the uranium, thorium and potassium contents to be measured using XRF analysis.

The cosmic ray dose was calculated using the spreadsheet created by J. R. Prescott and J. T. Hutton. The total dose was calculated using the DOS program 'AGE99' created by R. Grün (Grün, 2009). Variables used are shown in the tables below.

Variables used for all samples	
Alpha Efficiency	0.05±0.02
Diameter	168.5±43.5 µm
Layer Removed	9±2 µm
Density	1.5 $g.cm^{-3}$
Average Water Content	5±2 %

Table 4.3: Variables used for all samples

Sample	Lat.(S)	Long. (E)	Altitude (m)	Burial depth (m)	U (ppm)	Th (ppm)	K (%)
Long Beach	37° 7' 60"	139° 47' 45"	0	0	0.92 ± 0.07	0.95 ± 0.07	0.16 ±0.007
Robe	37° 9'	139° 44'	5	2	1.05 ±0.07	0.82 ± 0.06	0.06 ± 0.003
Woakwine	37° 2'	139° 47'	20	0	0.92 ± 0.07	1.03 ± 0.07	0.12 ± 0.006
East Dairy	37° 7'	139° 59'	5	1	0.37 ± 0.04	0.86 ±0.06	0.12 ± 0.006
Baker	38° 54'	140° 21'	25	8	0.28 ± 0.03	1.49 ± 0.10	0.19 ± 0.008
Harper	36° 51'	140° 32'	40	2	0.51 0.04	1.72 ± 0.11	0.09 ± 0.005
Naracoorte East	37° 8'	140° 51'	90	2	1.4 ± 0.09	15.41 ± 0.89	0.24 ± 0.010

Table 4.4: Variables used for individual samples.

Results for the samples with previously calculated dose rates agreed with the previous dose rates within errors. The Naracoorte East sample dose rate was quite large compared to the others, and closely matched the previously calculated dose rate of the sample site NE3 (calculations from the SESA sample notes of D J Huntley), and the sample site NE5b (Huntley and Prescott, 2001) which are situated in the same unit feature of the sampled Naracoorte East site used in this study.

Sample Name	**Calculated dose (Gy/ka)**	**Previously calculated dose (Gy/ka)**
Long Beach	0.64±0.04	
Robe	0.55±0.03	
Woakwine	0.61±0.04	0.582±0.007
East Dairy	0.46±0.03	0.44±0.01
Baker	0.47±0.02	0.450±0.008
Harper	0.51±0.03	0.481±0.009
Naracoorte East	1.84±0.09	

Table 4.5: Results from dose rate calculations.

05-DATA ANALYSIS AND ERROR ANALYSIS

DATA ANALYSIS

-How to get a dose-dependent TT-OSL data point-

A dose-dependent TT-OSL (DD-TT-OSL) data point used to form the TT-OSL SAR growth curve is created by subtracting from the full TT-OSL result a measurement of the dose-independent TT-OSL (DI-TT-OSL) result:

DD-TT-OSL = TT-OSL − DI-TT-OSL

As each TT-OSL and DI-TT-OSL result come from separate measurements, each has their background subtracted from the signal, and is normalised by a separate measurement. Therefore, the DD-TT-OSL data point calculation is as shown below:

$$DD\text{-}TT\text{-}OSL = \frac{(TT\text{-}OSL\ signal) - (TT\text{-}OSL\ background)}{(TT\text{-}OSL\ normalisation\ factor)} - \frac{(DI\text{-}TT\text{-}OSL\ signal) - (DI\text{-}TT\text{-}OSL\ background)}{(DI\text{-}TT\text{-}OSL\ normalisation\ factor)}$$

Every part of the calculation—the signal, the background, and the normalisation factor—can be optimised to improve the accuracy and precision of the final DD-TT-OSL result. A discussion of each part is included below.

-The signal-

The signal gained is in the form photon counts per chosen time period, or bin. In this thesis, for aliquots stimulated by blue diodes, the time period (or bin width) in question is generally 0.1 s, and for single grains or small aliquots stimulated by a green laser, 0.02 s. For data collected in bins, the bin width is the smallest fraction of time photon counts can be resolved to, and so generally the smallest useful bin width is chosen.

The optically stimulated signal in quartz does not necessarily come from the same type of trap, and fast, medium, and slow components have been found that are mathematically separable. The slower components are thought to be from more optically stable, but less thermally stable

traps (see Bailey, 2001, where a comparison of the kinetics given for fast and medium OSL components shows that the medium component has a slightly larger energy gap between its metastable state and the conduction band (E value), and a much larger chance-to-escape rate (s value)). This means that the slower components are from traps with shorter lifetimes, which can interfere with dating measurements. In optical dating, generally the first fraction of the signal is used, to minimise the fraction of the slower components contributing to the result.

At the same time, the precision of a result is affected by the amount of signal selected, the counting error of a measurement being the square root of the result. Thus a balance has to be found between the purity of the signal and its strength.

-The background signal-

The background signal is made up of all the components of the measurement that are not connected to the desired signal. In luminescence measurements, there are various different components of the background signal. The first is the signal spontaneously emitted from the photomultiplier, called the dark count or instrumental background. How high this signal is depends on the setup of the photomultiplier including its high voltage setting, and the temperature of the room (the bialkali photomultiplier tubes used in the OSL measurements are uncooled, and so operate at ambient temperature). Usually the dark count is of the order of tens of counts per second; in some cases up to hundreds of counts per second.

A source of background signal in OSL measurements is the small amount of stimulation light that is reflected up to the photomultiplier and passes through the filters. Most filter setups render this portion of the background minimal, of the order of the PMT background or below.

In TL or high temperature measurements, background noise is also contributed by incandescence from the sample, its holder (a disc or planchet), and the instrumentation. In LM TL, this increases as the temperature increases, and so cannot be simply subtracted from the signal. In this case, the measurement is repeated after the luminescence signal has been depleted, which allows one to find the response of the system to the measurement environment without the luminescence signal.

Background signal also originates from the sample itself. Slow components of quartz OSL raise the level of light seen in a measurement by an order of magnitude. Some OSL and TL materials also fluoresce or phosphoresce, raising the background levels under stimulation by a significant, though usually stable, amount.

Other sources of background signal are the fluorescence or phosphorescence of some filters, and ambient light leaking into the instrumentation. In most cases these sources can be minimised by not exposing fluorescent filters to light before a measurement, and taking precautions such as lowering ambient light levels to darkroom conditions and covering up machinery that is not light-proof.

In luminescence measurements, how the background is subtracted differs between continuous-wave (CW) and linearly modulated (LM) measurements. In CW measurements, the background signal is approximately constant. Background measurements are therefore found by continuing to stimulate the sample until the signal has depleted, leaving the residual background signal. In LM measurements, the background signal is not constant, with stimulation light leakage increasing in OSL measurements and incandescence increasing in TL measurements. The background measurement is therefore obtained by repeating the same measurement after the luminescence has been depleted. This gives the background signal for each point in the measurement.

In TT-OSL measurements, how to measure the background signal is not as straightforward. There are three ways to do so:

1) Using the final portion of the conventional OSL shine-down (fig 5.1). This background measurement has the advantage of subtracting any signal from remaining charge in the OSL traps. This background subtraction assumes that the further 260 °C preheat to stimulate TT-OSL signal does not deplete the residual OSL charge, as it has already survived one preheat, though this may not be the case.

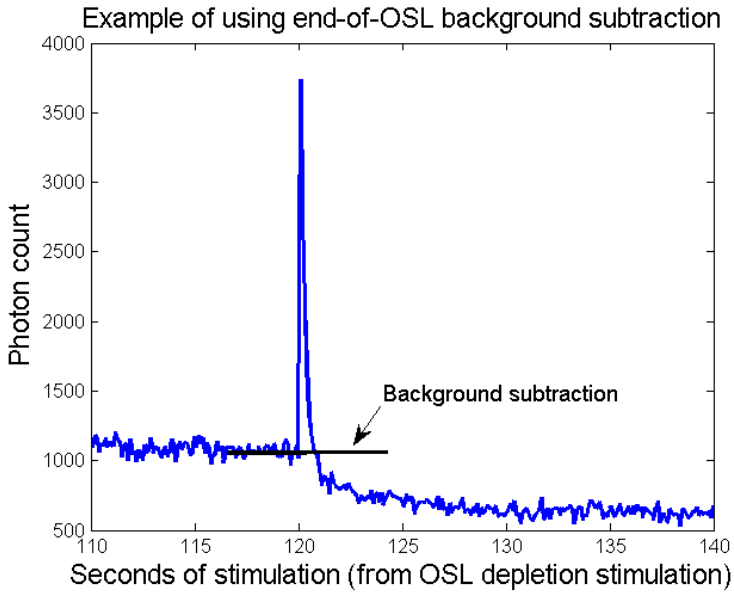

Figure 5.1: Example of where the background would be subtracted on a signal using the end-of-OSL background subtraction method. In this thesis, the signal whose background is being subtracted would be the first 0.1 s to 0.5 s of signal after preheating (at 120 s in the figure).

2) The TT-OSL signal near the TT-OSL measurement (fig 5.2). This uses the TT-OSL signal immediately after the measurement, before the TT-OSL signal is fully depleted. This can reduce the impact of medium and slow components on the signal, but reduces the amount of signal counted, resulting in larger counting errors.

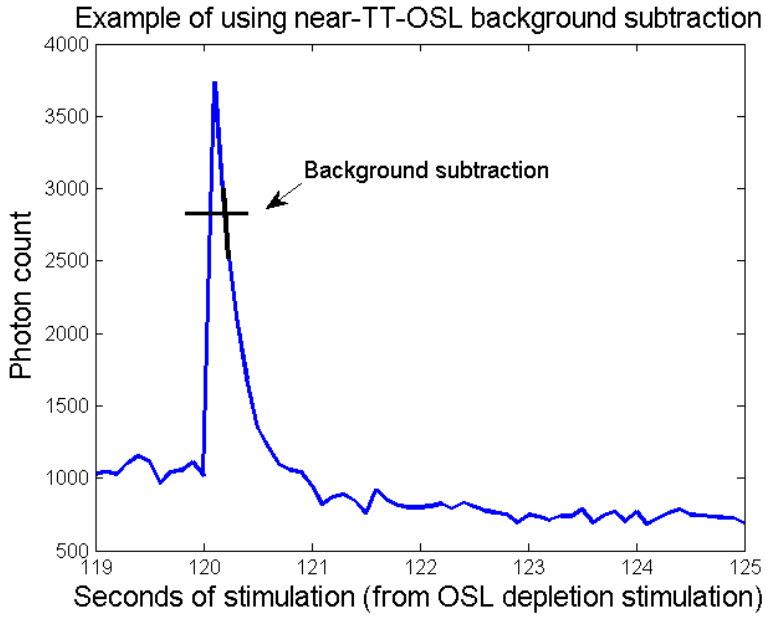

Figure 5.2: Example of where the background would be subtracted on a signal using the near-TT-OSL background subtraction method. In this thesis, the signal whose background is being subtracted would be the first 0.1 s to 0.5 s of signal after preheating (at 120 s in the figure).

3) The end of the TT-OSL measurement (fig 5.3). This uses the amount of signal when the TT-OSL signal is depleted. It maximises the amount of signal used, but may include extra signal from medium and slow components, or remaining charge in the OSL trap.

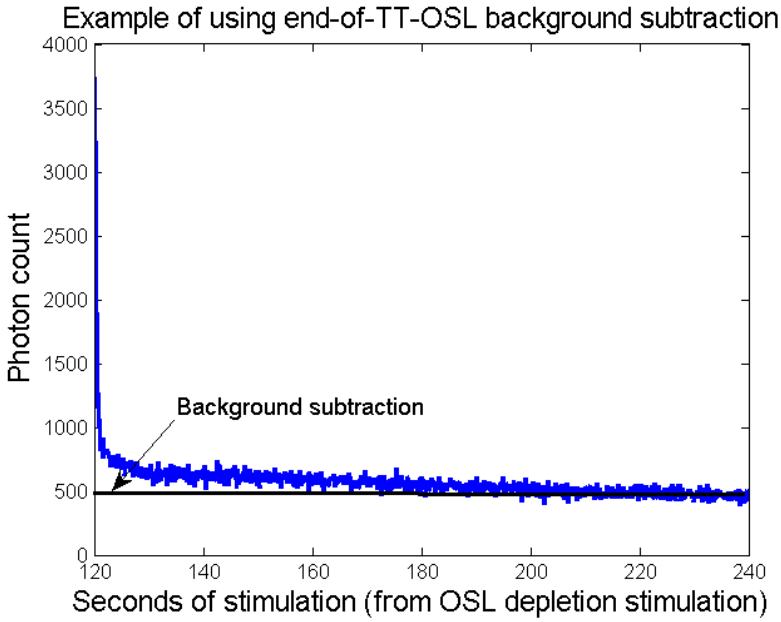

Figure 5.3: Example of where the background would be subtracted using the end-of-TT-OSL background subtraction method. In this thesis, the signal whose background is being subtracted would be the first 0.1 s to 0.5 s of signal after preheating (at 120 s in the figure).

-Normalisation-

Due to differences between aliquots and sensitivity changes in quartz grains due to heating and irradiation, each measurement in a TL or OSL protocol must be normalised in order to be compared with other measurements in the dating protocol used. In multiple-aliquot protocols, this can be done using the weight of the aliquot (giving a value of signal per unit weight), or by using the aliquot's response to a test dose (giving a value of signal per arbitrary (test) dose). Single aliquot or single grain protocols use a test dose to monitor sensitivity changes during cycles in the protocol.

Using the weight of a sample has long been practiced in TL measurements. It has the disadvantage in that it does not take into account varying average sensitivities of different aliquots, or of different traps. Normalising by weight is not used for OSL measurements, due to the relatively small aliquots used. Normalising by weight is only useful when using very large aliquots, where each aliquot gives the same statistical representation of the sample population (for instance, 5 mg of 90-125 µm quartz contains 3000-4000 grains); even so, the presence of a small population of

"bright" grains will cause "disc-to-disc scatter". A small population of grains contributing to the majority of luminescence in a sample has been found in TL (Huntley and Kirkey, 1985), and in OSL (Duller et al, 2000) measurements.

There are two ways of using a test dose to measure the sensitivity of a quartz aliquot or grain. One (Type 1) is by using the shallow 110 °C peak (Liritzis, 1980), a method that can be used for normalising both TL and OSL measurements. In this method, a test dose much smaller than the expected value is given to the aliquot. The aliquot is then heated to above 110 °C but stopped before any useful peaks. The TL measurement of the 110 °C peak is used for normalisation. This method has the advantage in that it measures the sensitivity of the aliquot before a measurement is made, which itself changes the sensitivity of the aliquot. However, this method does not directly measure the sensitivity of the trap population that is being measured, which can change in sensitivity at a different rate than the 110 °C peak. Using a test dose before the natural measurement can also interfere with the measurement of very young samples, and so is generally only used for normalising old samples.

The other way of normalising using a test dose (Type 2) can only be used for OSL measurements, and involves measuring a test dose response after the measurement (Strickertsson and Murray, 1999). In this method, the measurement is made again after a small test dose. This has the advantage that it is measuring the same signal for normalisation as the one being normalised. However, measuring the sensitivity of the grain or aliquot after the measurement neglects to take into account any sensitivity changes occurring due to the measurement itself.

While test doses in Type 2 normalisation are much smaller than expected doses to decrease sensitivity changes, for faint samples this can create resolvability issues. Often a smaller preheat is used to maximise the amount of signal gained. This however means that the normalising signal is not the same signal as the one measured, and different optically stimulated components with differing rates of change of sensitivity may be present in different proportions to the signal being normalised.

TT-OSL measurements are generally normalised using the Type 2 test dose method. However, protocols differ as to whether one uses the OSL or TT-OSL response to the test dose for

normalisation. The OSL normalisation measurement has the advantage in that it provides a much higher photon count than the TT-OSL measurement: as the proportion of TT-OSL to OSL signal is less than a percent in large aliquots, one can have resolvability problems when measuring small test doses with TT-OSL. TT-OSL normalisation also uses the whole TT-OSL signal, including the DI-TT-OSL signal, which may lead to inconsistencies if one is using the DD-TT-OSL signal which does not include this extra signal. TT-OSL normalisation also uses an extra step to OSL normalisation, including a preheat, which can further change the sensitivity of the trap populations. Measurements made during this thesis indicate that the SESA samples do not change sensitivity very much due to preheat temperatures of 280 °C and 300 °C, but do due to irradiation (see Figures 5.4 and 5.5). Therefore the TT-OSL normalisation signal does not overly change the sensitisation of the measured normalisation signal to the signal being normalised; however, the test dose must be much larger to resolve a TT-OSL signal than an OSL signal, and so in that respect the TT-OSL normalisation does cause a larger sensitivity change between the initial and normalisation measurements. While there are disadvantages to TT-OSL normalisation, OSL normalisation, however, only measures the sensitivity of the OSL trap populations, and not necessarily the sensitivity of the TT-OSL populations.

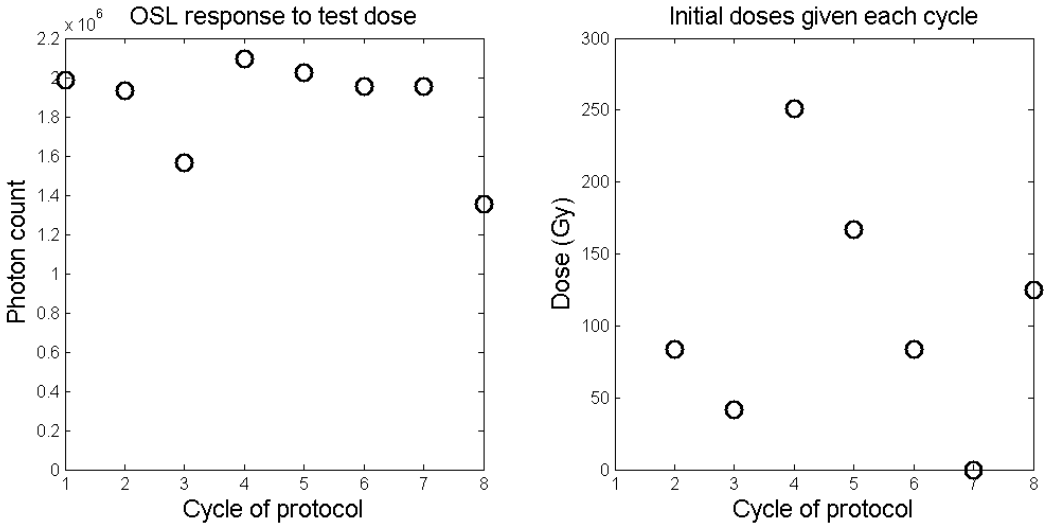

Figure 5.4: OSL response to a test dose after measurements of different doses. There appears to be a slight correlation between the dose measured and the response to a test dose. Note that cycle one was the measurement of the natural signal, and so the dose given is unknown and at a different dose rate.

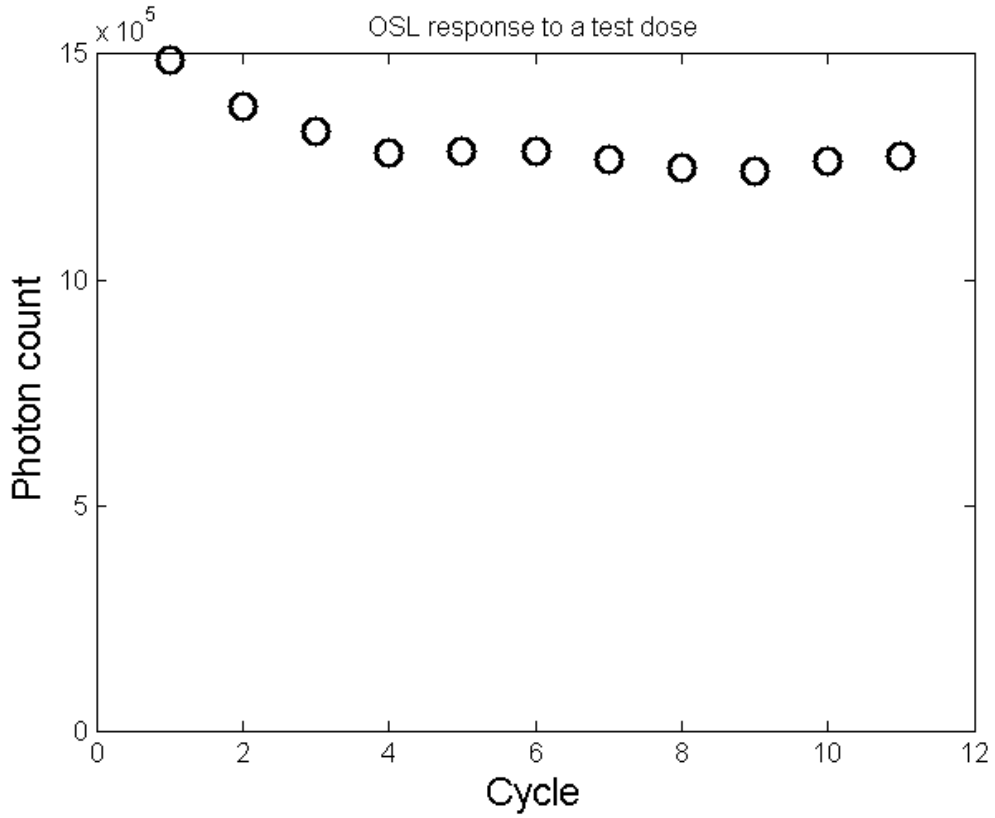

Figure 5.5: OSL response to a test dose after measurements of the same dose.

Note that measuring the DI-TT-OSL signal is done after three more preheats than the TT-OSL signal (two at 260 °C and one at 300 °C), and one test irradiation, which could potentially change the sensitivity of the signal. Thus protocols using this signal test the sample's response to dose after both the TT-OSL and DI-TT-OSL signals, giving them two normalising measurements per cycle.

-Fitting measurements to a growth curve-

The series of data points gained by finding the grain or aliquot's response to different doses must be fitted to a curve in order to gain a result for the equivalent dose that would give the same signal as the natural. In some protocols, such as the Australian Slide (Prescott et al, 1993), a fit does not have to be of any particular function; in most protocols, fitting to a set of defined functions is necessary to assess the validity of the results.

In this thesis, fitting was done using Matlab's 'fit' function, in its curve fitting toolbox. This can produce non-

linear least squares fits for both provided and inputted equations. The start points for fit iterations and their upper and lower bounds can be provided. While this limits the possible results to the provided fit, it makes the fitting function more likely to succeed, as it only goes through the non-linear least squares procedure a finite number of times. Start and bound values used can be found in the 'list of natdose input values' in the appendix of this thesis.

Fits can also be weighted, with weights provided by the user. More information about the weighting process can be found in the error analysis section of this chapter.

-Types of curves fitted-

A simple one-trap, one recombination centre process provides a saturating exponential photon count vs dose curve. In reality, other functions are used commonly in fitting curves to data points. Three functions were used in this thesis:

1) Linear function
$y = ax + b$ (coefficients are a, b)

Linear fits work best when the trap population is far from saturation, and the saturating exponential curvature is not yet evident. In the Matlab fitting program, this function is provided automatically for the user and its simplicity allows it to be fitted easily to functions.

2) Saturating exponential
$y = ae^{(-bx)} + c$ (coefficients are a, b, c)

This is the most commonly fitted function when measuring old samples. In these samples, the natural dose can be reasonably close to the saturation point, and the photon count vs dose data have a decreasing positive curve. In Matlab, this equation must be provided by the user, including starting points for a larger fitting success rate.

3) Saturating exponential plus linear
$y = ae^{(-bx)} + cx + d$ (coefficients are a, b, c, d)

This type of fit is needed if the trap population whose signal is being measured sensitises during dose deposition, adding a linear component to the signal vs dose curve, or if signal from two different sources are being measured at the same time, one which saturates and one which does not. It is

not recommended to use aliquots with this type of growth curve unless the natural signal is far from the linear component of the curve. This is due to the fact that the sensitising due to dose may have a limit, interfering with results, or may be dependent on the rate of the dose given, which is much smaller for natural doses than artificial lab-given doses. This equation must be provided by the user of the Matlab 'fit' function, and due to the large number of coefficients provided, does not tend to give very accurate results unless the data points have very small errors or the data points are not weighted in the fit.

-Finding the equivalent dose-

To find a result for the natural dose of a sample (also called equivalent dose), the best fit is chosen (if no fit is sufficiently good, the grain or aliquot is discarded). The goodness of a fit is calculated by using a number of different variables, including the sum of standard errors (SSE) value given automatically by the Matlab function, which gives one a rough idea of how close the fit is to the data points, and the residuals, which are the differences between the fit and the data for each data point. The residuals are particularly useful, as they can indicate whether the fit follows the data throughout the entirety of the length of the data string (in which case the residuals appear to be randomly distributed around zero), or whether it deviates from the data at points (indicated by trends up or down from zero, or strings of data points either above or below the zero point). This can help indicate whether data are linear, or slightly curved (in which case a saturating exponential fit is better than a linear one).

Once a fit has been decided on, one can interpolate what the value of the natural dose is by finding the dose value of the fit that would give one the value of the natural signal. It is this value for the equivalent dose, divided by the calculated dose rate of the sample site, that gives one a value for the age of the sample.

ERROR ANALYSIS

Each measurement has an associated error, which gives an indication of our confidence in the accuracy of the result. In OSL measurements, this error comes from a variety of sources. The simplest to define is the counting error of the

measurement, which follows Poisson statistics. This error is due to the statistical fluctuations inherent in any discrete counting measurement, and is estimated by the square root of the measurement (Bevington and Robinson, 2003). Most other random errors are instrumental errors, errors introduced by slight inaccuracies in the instrumentation used to heat, stimulate, dose, and read output of the sample. These errors are different for each machine, and different for each type of measurement. Most instrumental errors affect other instrumental errors, if more than one comes into play in a protocol. As they are not independent, they are difficult to assess individually, and it is best to empirically calculate a value for the instrumental error as a whole.

Systematic or non-random errors in measurements can come from a variety of sources. Light leakage through filters and changes in ambient temperature can affect the background of the measurement. If the light source is approximately stable, and the ambient temperature does not change significantly throughout the measurement, these changes do not affect the measurement after the background has been subtracted.

A systematic error is also provided by the calibration of the beta source used in measurements. Any error in the calibration means that an age gained via a dose recovery curve will be off by this amount. Calibration is done by creating dose recovery curves with quartz that has zero initial signal, and comparing it to quartz that has been dosed by a highly calibrated source.

Another systematic error—or rather, a difference between the instrumental readouts and reality—is due to the thermal lag between the heating plate and the sample. As long as the heating plate is clean and free of stray grains, this is generally defined by the thickness of the stainless steel disc used to store and carry the sample. This error can be minimised by heating at a slow rate, or by ensuring the thickness of the discs used remains relatively constant. Note that lack of thermal contact due to deformities in the disc shape, or stray grains or other material on the heating plate, cause random thermal lag errors rather than systematic

ones. These are minimised by ensuring the discs used are of good quality, and that the heating plate and the back of the disc used are clean.

In this thesis, the TT-OSL protocol used includes a preheat to 260 °C at 5 K/s, which is then held for 10 s. This preheat does two things: firstly, it empties shallow quartz traps that interfere with the dosimetric OSL signals; secondly, it transfers the TT-OSL signal into the OSL trap. The small lag times of the thin stainless steel discs used and the high temperature reached ensure that this preheat does its first job. As the lag is different for each aliquot, each aliquot will reach a temperature at which thermal transfer occurs at a slightly different time in the preheating process, and each will be kept at this temperature or higher for a slightly different time. This means that every aliquot is measuring a slightly different proportion of the TT-OSL signal. As the protocols tested in this thesis are single aliquot protocols, this difference does not overly affect results. If a multiple aliquot protocol was being used, however, this difference would add an extra uncertainty to results, and to minimise this signals would have to be normalised by the TT-OSL response to the test dose, and not the OSL response.

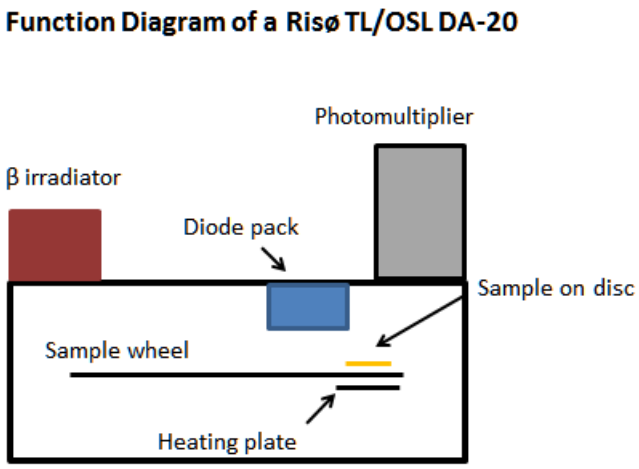

Figure 5.6: Diagram of a Risø TL/OSL DA-20. Error sources include the statistical nature of the β irradiation (source heterogeneity); fluctuations in the temperature of the

heating plate; thermal lag due to the thickness of the disc the sample is put on; fluctuations in the intensity and wavelength of the diode output; and counting and noise-related errors from the photomultiplier tube.

-Finding the instrumental error-

Each signal used to create a normalised TT-OSL datum uses the heating plate, blue LED optical stimulation, the β source, and the photomultiplier of the Risø TL/OSL DA-20 (see fig 5.6). An experiment to find the combined instrumental error of this type of measurement was devised, similar to that used in Thomsen (2004). Two 5 mm diameter aliquots of 125-180 μm diameter grains of crushed Pyrex were used for this experiment. Pyrex was chosen as each aliquot would contain grains with similar properties to each other, as Pyrex is a homogenous glass and the grains came from the same glass object. Pyrex has also been seen to be stable under repeated thermoluminescence measurements, and so would be unlikely to have very wildly changing OSL properties with repeated use. This experiment was done on the Risø TL/OSL DA-20 used for aliquot measurements of the TT-OSL protocol in this thesis. A 7 mm U340 UV band-pass filter was used.

Each aliquot underwent 300 iterations of the following cycle:

1 120 s β dose
2 Preheat to 75 °C at 5 K/s
3 Blue LED stimulation for 30 s
4 60 s β dose
5 Preheat to 75 °C at 5 K/s
6 Blue LED stimulation for 30 s

Both aliquots underwent sensitivity changes, the response to dose increasing with each step in the cycle. When the first measurement (step 3) was normalised by the second (step 6), a histogram of each aliquot could be estimated by a Gaussian (see Figure 5.7). The difference in the mean of each aliquot was small, but larger than the 69 % confidence interval of each distribution. The difference in the mean could be due to variations in the disc thickness, grain distribution, and the distribution of grain size of the two aliquots.

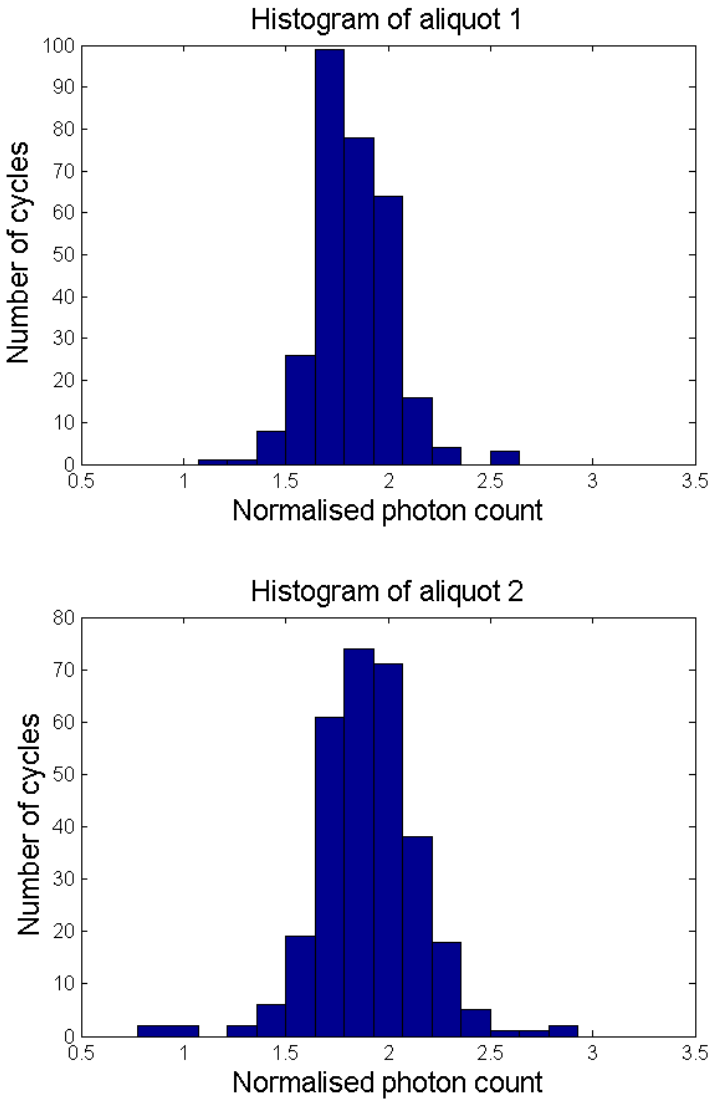

Figure 5.7: The histograms made of each Pyrex aliquot result.

The error of the mean of each of the two distributions can be found in two ways. One estimates the error using the variation of the points, and the other by using the calculated errors of each measured point.

Using the variation in the distribution, the error of the mean is:

Standard error = $\sqrt{\frac{1}{n(n-1)}\sum(x_i - \bar{x})^2}$ (Moore, D, and McCabe, G., 2003)

Where n is the number of data points.

Using the errors of individual points:

Error propagation equation for $x(x_i)$, assuming independent errors:

$$\sigma_x^2 = \sum \sigma^2 \left(\frac{\partial x}{\partial x_i}\right)^2$$ (Bevington, P. and Robinson, D., 2003)

for $x=\frac{1}{n}\Sigma x_i$, (n is the number of data points),

$$\sigma_x = \sqrt{\frac{1}{n^2}\sum {\sigma_{x_i}}^2}$$

If the calculated errors are accurate, these two equations should give similar results. As expected, the error of the mean using the errors of individual points is consistently lower than the error via variation in the distribution, if the counting error is used as the only error present. We need an extra error term, the instrumental error, in order to have an error that reflects the true variability of the measurements.

The instrumental error is dependent on a number of variables, including:

- -The temperature to which the sample was heated
- -The heating rate
- -The time the sample was kept at a constant temperature
- -The optical stimulation time
- -The time taken to dose the sample
- -The reflecting properties of the aliquot and disc.
- -Drift in the PMT detector efficiency
- -Drift in PMT dark noise

While some instrumental errors are approximately constant, like the error in the time the aliquot is exposed to a radiation source (due to shutter speed and timing errors), other errors 'average out' with increased time, such as the statistical fluctuations in the dose rate of the source. The instrumental error in the exposed dose should then be:

$$Error(exposed\ dose)^2 = error(shutter\ speed)^2 + error(timing)^2 + \frac{variability(dose\ rate\ per\ unit\ time)^2}{\sqrt{(measured\ unit\ time)-1}}$$

Where (measured unit time)-1 is the number of degrees of freedom of the error of the dose rate.

If all sources of error were independent of each other, we could write the instrumental error as:

$$Instrumental\ error^2 = constant + \sum \frac{variability(source_x)}{\sqrt{degrees\ of\ freedom_x}}^2$$

In reality, all instrumental errors are affected by the errors that came before it in the sequence, and so the instrumental error equation is more complex.

A first experiment to find the instrumental error for each aliquot assumed that the instrumental error could be approximated by a constant. An iterative Matlab function (see Appendix A) was used to find the instrumental error for each aliquot. Errors of the mean gained via the two error equations mentioned above were compared. The instrumental error was increased until both errors of the mean were the same, giving the instrumental error needed to raise the error to that indicated by the scatter of the distribution.

The instrumental error result gained by the two aliquots differed significantly from each other. The instrumental error gained when the number of seconds of signal integrated was changed was also different, increasing with bin size (each bin was set with a 0.1 s width). One major difference between the two aliquots was that one was significantly dimmer than the other. This indicated that the instrumental error may be proportional to both the signal measured and the number of bins used.

The instrumental error term was changed to be:

$$Instrumental\ error = constant_1 + \frac{constant_2}{\sqrt{(signal-1)}}$$

Where (signal-1) is the number of degrees of freedom of the signal. The iterative process was run again, this time with two variables. Values for the constants that gave small differences in the means for all distributions were collected, and the result that gave the smallest total difference was used as the instrumental error result. The differences were calculated using the following equation:

$$(difference)^2 = difference(distribution_1)^2 + difference(distribution_2)^2$$

(See Appendix A for a transcript of the Matlab function)

Results were found for values using 0.1, 0.2, 0.3, and 0.4 seconds of integrated signal for each measurement. For all minimum results, $constant_1$ was zero, indicating that all or most of the instrumental error is proportional to $\frac{1}{\sqrt{(signal-1)}}$. For all values, the secondmost, thirdmost and fourthmost smallest differences were very similar values to the result used, indicating that the result is near a true minimum of the difference. A plot of the instrumental error vs the number of bins used for the signal could be fitted to a saturating exponential, giving an instrumental error of:

$$Instrumental\ error = \frac{580-563e^{-0.2617b}}{\sqrt{(signal-1)}}$$

Where b is the number of bins used (with bins of 0.1 s width).

Note that the distributions used in this estimation of the instrumental error do not have differing dose or temperatures, and so any variation in the error due to heating times or rates, or time exposed to dose are not accounted for in this estimation. This estimation of the instrumental error found here is only valid for other measurements if the errors due to heating and dose are very small, or approximately constant.

-Error propagation-

Each DD-TT-OSL signal is comprised of a number of different measurements:

-End of OSL measurement (Oe) (or other background subtraction measurement)
-TT-OSL measurement (TT)
-Test dose measurement (either an OSL test dose (Ot) or a TT-OSL test dose (TTt-Ote) Note that this includes an additional background subtraction element.
-End of OSL measurement (Oe_2)
-DI-TT-OSL measurement (BT)
-Test dose measurement (either an OSL test dose (Ot_2) or a TT-OSL test dose (Btt-OT_2e)

Each of these measurements has a different error, which can be propagated through calculations by using the error propagation formula:

$$error(F(x,y,\ldots))^2 = (error(x)^2(\frac{dF}{dx})^2 + error(y)^2(\frac{dF}{dy})^2 + \ldots)$$

Assuming that the errors are independent. Specific error propagation equations used in finding a DD-TT-OSL measurement are given below.

Addition/subtraction:
$F = x + y$
$error(F)^2 = error(x)^2 + error(y)^2$

Multiplication/division:
$F = xy$
$error(F)^2 = F^2[(\frac{error(x)}{x})^2 + (\frac{error(y)}{y})^2]$

Using these equations, we can find the error of each measurement:

TT-OSL measurement with OSL test dose:

$$TT\text{-}OSL = \frac{(TT - Oe)}{Ot}$$

$$error(TT\text{-}OSL) = \sqrt{\{ (\frac{(TT\text{-}Oe)}{Ot})^2 [\frac{\sqrt{(error(TT)^2 + error(Oe)^2)}^2}{(TT - Oe)} + (\frac{error(Ot)}{Ot})^2] \}}$$

TT-OSL measurement with TT-OSL test dose:

$$TT\text{-}OSL = (\frac{TT - Oe)}{(TTt - Oet)}$$

$$error(TT\text{-}OSL) = \sqrt{\{ (\frac{(TT - Oe)}{(TTt - Oet)})^2 [(\frac{\sqrt{(error(TT)^2 + error(Oe)^2)}}{(TT - Oe)})^2 + (\frac{\sqrt{(error(TTt)^2 + error(Oet)^2)}}{(TTt - Oet)})^2] \}}$$

And similarly with the DI-TT-OSL measurement.

To get the error of the DD-TT-OSL measurement:

$$DD\text{-}TT\text{-}OSL = TT\text{-}OSL - DI\text{-}TT\text{-}OSL$$

$$error(DD\text{-}TT\text{-}OSL) = \sqrt{error(TT\text{-}OSL)^2 + error(DI\text{-}TT\text{-}OSL)^2}$$

-Error of natural dose-

The error of each normalised data point given above is used to weight each data point used in fitting the dose response curve for each aliquot. Weights are calculated by using the following equation:

$$w = \frac{1}{err^2}$$

Where w is the weighting and err is the error. Weighting each data point is important, as changes in sensitivity throughout the cycles of the protocol as well as the dose given for each cycle changes the error of each data point. This means that data points we have more confidence in are given more weight in the fit than those with large errors. Weighting is only useful, however, if one is confident in the values for their errors.

The fit gained has an error (automatically provided for the user by the Matlab fit function), and this combined with the natural dose point error is used to estimate the y-axis error of the equivalent dose. The x-axis error is estimated by translating the y-axis points to the x-axis using the fit (see fig 5.8). This error can then be combined with any applicable dose-related errors to give a total estimated error of the equivalent dose.

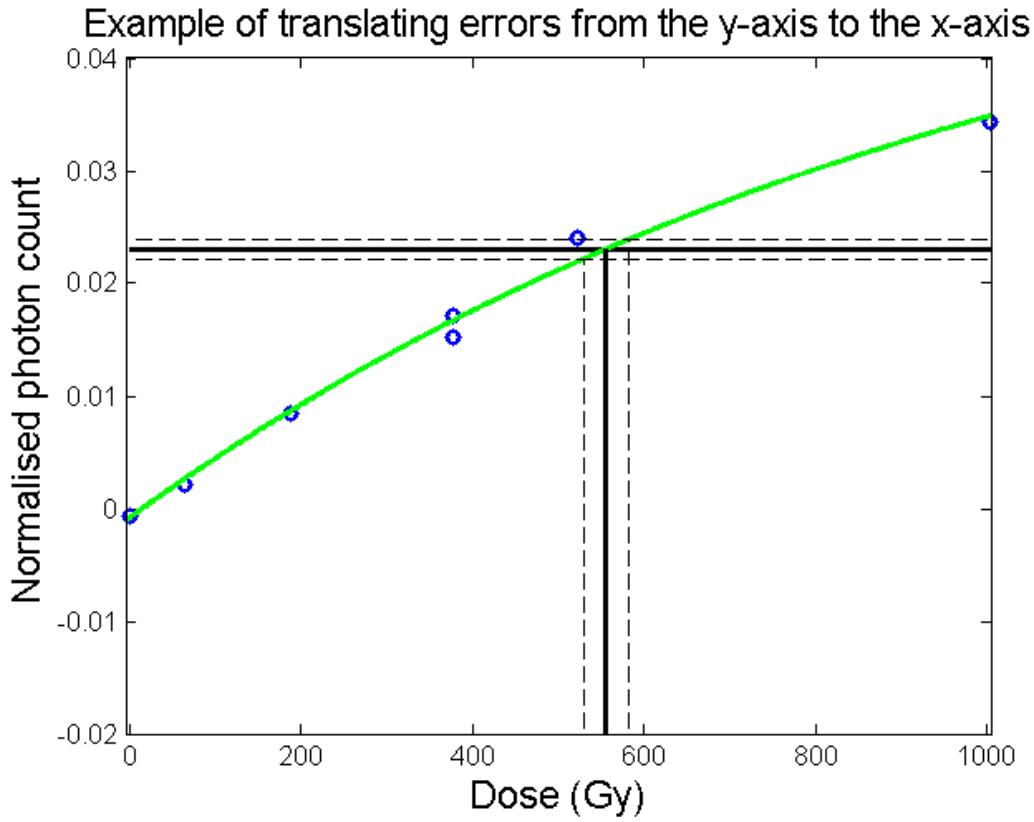

Figure 5.8: Translating errors from the y-axis to the x-axis. The x-axis error is estimated to be where the y-axis error meets the fitted curve.

Note that in a linear fit, the errors of the equivalent dose should be symmetrical. However, in the case of a saturating exponential fit, and large errors or a natural result close to the saturation point of the growth curve, the errors may be significantly asymmetrical, with the larger of the errors to the positive side of the result.

-Other errors-

The errors calculated above for the natural dose only include errors created in measuring the sample. There are other errors and uncertainties involved, some of which are listed below:

-Systematic errors
Systematic errors could be introduced to the measurements gained in a number of ways. These include:

-The normalisation method not taking into account part of the sensitivity changes.

-The normalisation method not taking into account differences in sensitivity changes between the natural measurement and the artificial dose measurements.

-A change in the deposition of electrons in metastable states due to differences in natural and artificial dose rates.

-Interference by other OSL components
While the 325 °C TL peak is the main source of OSL signal, other, less bleachable components are also present (Murray, 1996). These may not be completely bleached after the OSL reduction part of the protocol, and may not be completely separable from the TT-OSL signal. Certain background subtractions may reduce the influence of these components, and mathematically separating components can be attempted if the interference is high.

-Sample population purity
Errors may be gained, especially in aliquot results, by samples made from more than one population of grains. Grains from different ages or different natural equivalent doses can be mixed into the population, due to incomplete bleaching of all grains of the sample or sediment mixing. The subsequent result gained from an aliquot is a mean value of the different equivalent doses, weighted by the population's prevalence in the aliquot and the sensitivity of individual grains.

-Sample purity
The results gained are assumed to be from pure quartz samples. Inclusions in grains can skew results, either by adding signal to the measurements that are not in proportion to the quartz dose response, or, if the inclusions are radioactive, increasing the dose rate for individual grains, making a bulk dose rate result for the sample, used to find the sample's age, inaccurate for that particular grain and positively skewing the result for the age.

-Sample history
While some sediment beds are laid down quickly, others, such as the wind and wave formed dune systems of the SESA range, were formed over a reasonably long time, being extensively reworked before being stranded by the coast rising. This means that a precise value for the age of the sediment is physically impossible as there is no true single age, and adds an extra uncertainty to the final result.

06-INITIAL RESEARCH INTO THE TT-OSL BEHAVIOUR OF SESA SAMPLES

-Testing for TT-OSL-

Initial tests were done on the WK4 sample, which is from the Woakwine 1 dune system. Previous doses obtained for this dune have been 65 Gy (Banerjee et al, 2003), 69 Gy (Huntley et al, 1994), 73 Gy (Huntley et al, 1993a), and 64 and 47 Gy (Huntley et al, 1993b). Aliquots of sample were prepared by creating a 5 mm diameter monolayer of grains on a stainless steel disc.

A first experiment to see whether the sample had TT-OSL signals was done on a Risø TL-DA-8, with a 7 mm Hoya U340 filter, and a green lamp for stimulation. Samples were preheated to 260 °C for 10 s, stimulated to deplete the OSL trap, then given the same preheat and stimulated to measure the TT-OSL signal. To measure the dose-independent TT-OSL signal, the aliquot was heated to 300 °C, depleted of OSL signal by optical stimulation, preheated to 260 °C for 10 s, and then stimulated to measure the dose independent TT-OSL. It was found that WK4 had peak DD-TT-OSL (also called ReOSL) and DI-TT-OSL (BT-OSL) responses up to five hundred times smaller than the OSL measurements. DD-TT-OSL was resolvable once the DI-TT-OSL was subtracted in medium-sized doses (around 35 Gy), but not in small doses (around 7 Gy). This indicates that, if using TT-OSL to normalise, one has a minimum resolvable test dose one cannot go under, even though Wang et al (2006a) indicate that a test dose of 10 % of the expected value is ideal.

A question arises: is the phenomenon seen above actually TT-OSL? An experiment was done on four previously bleached and heated Rb1s 5 mm aliquots on a Risø TL/OSL DA-20. OSL stimulation was by blue diodes at 90 % power. Each aliquot was given a β dose of around 37 Gy, and given a 260 °C preheat, then a blue diode stimulation for 120 s. After this each aliquot was subjected to a slightly different protocol before another blue diode stimulation at 260 °C, as shown below.

Protocol 1	**Protocol 2**	**Protocol 3**	**Protocol 4**	**Protocol 5**
β dose of 37 Gy	β dose of 37 Gy	β dose of 37 Gy	β dose of 37 Gy	β dose of 37 Gy
260 °C preheat for 10 s at 5 K/s	260 °C preheat for 10 s at 5 K/s	260 °C preheat for 10 s at 5 K/s	260 °C preheat for 10 s at 5 K/s	260 °C preheat for 10 s at 5 K/s
Blue diode stimulation for 120 s	Blue diode stimulation for 120 s	Blue diode stimulation for 120 s	Blue diode stimulation for 120 s	Blue diode stimulation for 120 s
	Pause for 180 s	Pause for 600 s	Pause for 180 s	Pause for 600 s
260 °C preheat for 10 s at 5 K/s			260 °C preheat for 10 s at 5 K/s	260 °C preheat for 10 s at 5 K/s
Blue diode stimulation for 120 s	Blue diode stimulation for 120 s	Blue diode stimulation for 120 s	Blue diode stimulation for 120 s	Blue diode stimulation for 120 s

Table 6.1: the protocols used to find out if the signal found is thermally transferred.

Aliquots subjected to a preheat showed a rise in signal from the end of the first stimulation to the start of the subsequent signal (see fig 6.1). Aliquots that were not given a preheat before a subsequent stimulation did not have any change in signal. This indicates that the preheat is necessary for the creation of the signal shown.

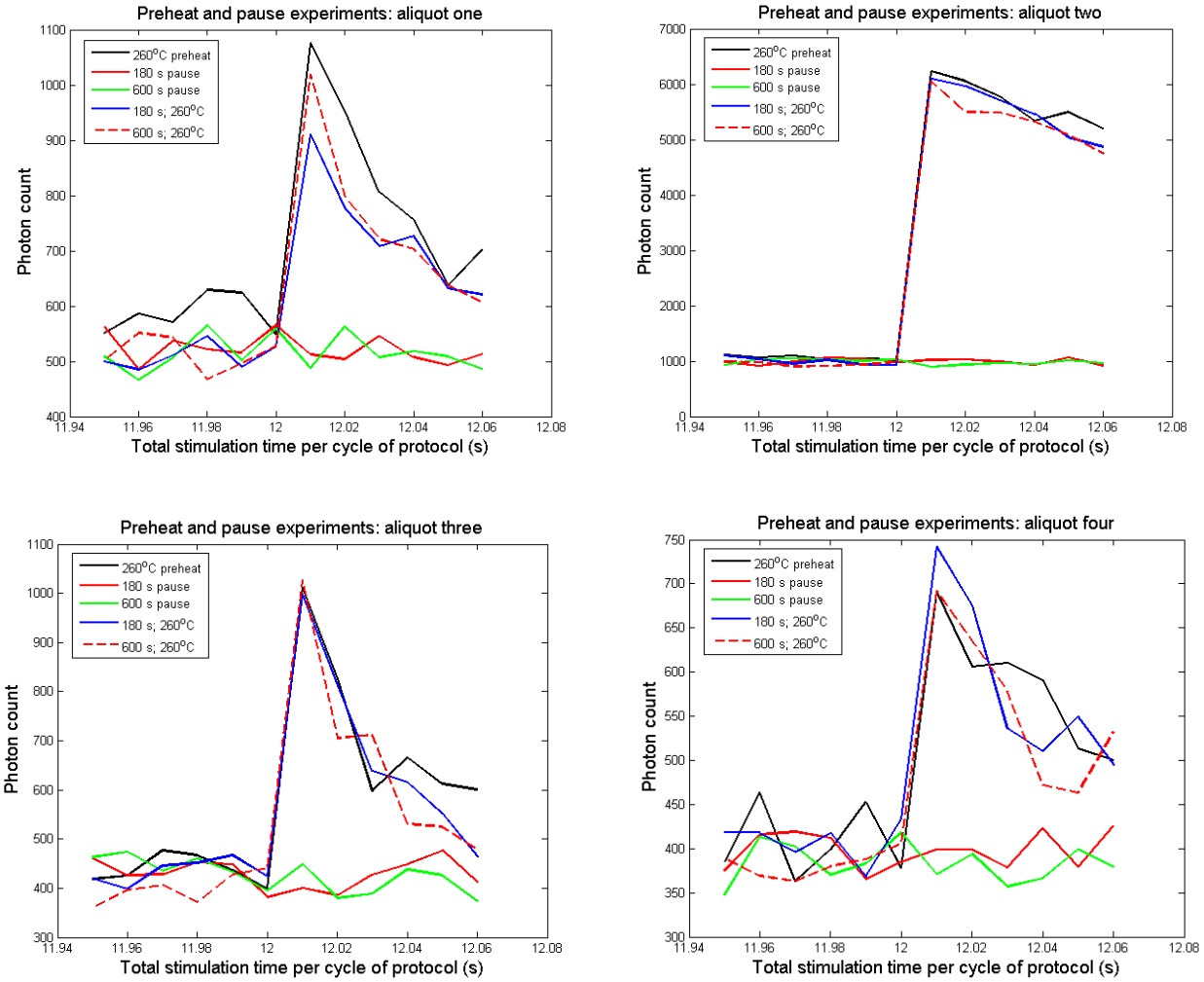

Figure 6.1: Results for four aliquots exposed to preheats, pauses, or both. In all four aliquots, a preheat was necessary to see an extra signal.

-What proportion of TT-OSL is there in a sample?-

Observations were made of the proportion of TT-OSL to OSL, and the peak TT-OSL photon count in different-sized aliquots of sample. The results are shown below.

Single grains: the natural signal from one hundred 180-250 µm grains of the East Naracoorte sample were assessed, using the protocol detailed in Table 6.2 below. The grains were optically stimulated by a green laser for two seconds. Measurements were done in a Risø TL/OSL DA-20 with a single-grain reader attachment. A 7 mm Hoya U340 filter was used. Of the one hundred grains, twenty had both OSL and TT-OSL signals, and six had an identifiable dose dependence. Peak photon counts for the first 0.02 s of stimulation time ranged from tens to thousands of counts. The ratio of TT-OSL peak counts to OSL counts in the first 0.02 of measurement ranged from 0.51 to 16%.

Protocol for each cycle of TT-OSL SAR measurements.
Preheat to 260 °C at 5 K/s, holding for 10 s
Stimulation by green laser for 2 s (at 125 °C)
Preheat to 260 °C at 5 K/s, holding for 10 s
Stimulation by green laser for 1 s (at 125 °C)
~7.5 Gy β dose
Preheat to 260 °C at 5 K/s, holding for 10 s
Stimulation by green laser for 1 s (at 125 °C)
Preheat to 300 °C at 5 K/s, holding for 10 s
Stimulation by green laser for 2 s (at 125 °C)
Preheat to 260 °C at 5 K/s, holding for 10 s
Stimulation by green laser for 1 s (at 125 °C)
~7.5 Gy β dose
Preheat to 260 °C at 5 K/s, holding for 10 s
End-of-cycle TT-OSL depletion at 290 °C with blue diodes at 90 % power, holding for 400 s

Table 6.2: The protocol used for single grain measurements.

Small aliquots: grains of 125-180 µm diameter from the Woakwine sample were placed in a single grain disc, which consists of an array of 10 x 10 cylindrical pits of 300 µm diameter and depth. Around eight to twelve grains were in each hole, forming a small aliquot. The aliquots were measured with a Risø TL/OSL DA-20 with a single-grain attachment, and 7mm Hoya U340 filter, and stimulated with a green laser. Using the protocol detailed in chapter 8, peak TT-OSL photon counts were in the hundreds in the first 0.02 s of stimulation. The ratio of TT-OSL peak counts to OSL counts

ranged from 0.9 to 13 % when including all 100 aliquots. A ratio between 1.1 and 3.8 % was found for the ten aliquots whose growth curves met the following criteria:

- a linear, saturating exponential or saturating exponential + linear curve could be fitted to the regenerated dose points
- the natural signal was not beyond the saturation point of the fit, or below the signal of a 'zero' regenerated dose point.
- a repeated dose measurement was not more than 50 % more or less than the original measurement.

Large Aliquots: aliquots of the Naracoorte East sample were made using silicone spray to stick a monolayer of grains onto a stainless steel disc. 125-180 µm grains were used. Eight aliquots were made each of a diameter of 1, 3, 5, and 7 mm. Aliquot TT-OSL response was measured on a Risø TL/OSL DA-20, and stimulated with blue diodes. Using the protocol detailed in chapter 9, peak TT-OSL photon counts per second ranged from thousands for the 1 mm aliquots, to tens of thousands for the 7 mm aliquot. The average ratio between the TT-OSL and OSL peaks was around 1 % for the 1 mm and 7 mm aliquots, and 0.7 % for the 3 mm and 5 mm aliquots. All large aliquots had resolvable TT-OSL signals, and signals positively dependent to dose.

Size of aliquot	**Ratio of TT-OSL to OSL (%)**
single grain	0.51 to 16
8-12 grains	0.9 to 13
1 mm diameter	0.8 to 1
3 mm diameter	0.4 to 1
5 mm diameter	0.7 to 1
7 mm diameter	0.7 to 2

Table 6.3: Summary of the proportion of TT-OSL to OSL for various aliquot sizes. Note that the single grain result only counts those grains with resolvable TT-OSL signals.

-How long does it take for OSL to deplete?-

The first few steps of a TT-OSL protocol are made to deplete the OSL trap or traps, before transferring the TT-OSL signal. Six aliquots of WK4 grains were made. The aliquots were made quite large, 7 mm in diameter, to provide enough grains that each aliquot was representative of the sample as a whole. Each sample was given a separate preheat of either 240, 250,

260, 270, 280 or 290 °C, then stimulated with blue LEDs for half an hour (see fig 6.2). The protocols were done on a Risø TL/OSL DA-20, with a U340 filter in place.

Mass normalised responses indicate that low temperature preheats of 240 °C and 250 °C have larger residual OSL levels after 200 s, and the 290 °C preheat gave smaller residual OSL levels. The 260 °C, 270 °C, and 280 °C preheats had similar residual levels. When normalised by the first data point after stimulation rather than the mass of the aliquots, the responses for each preheat had the same decay shape, and could be directly compared.

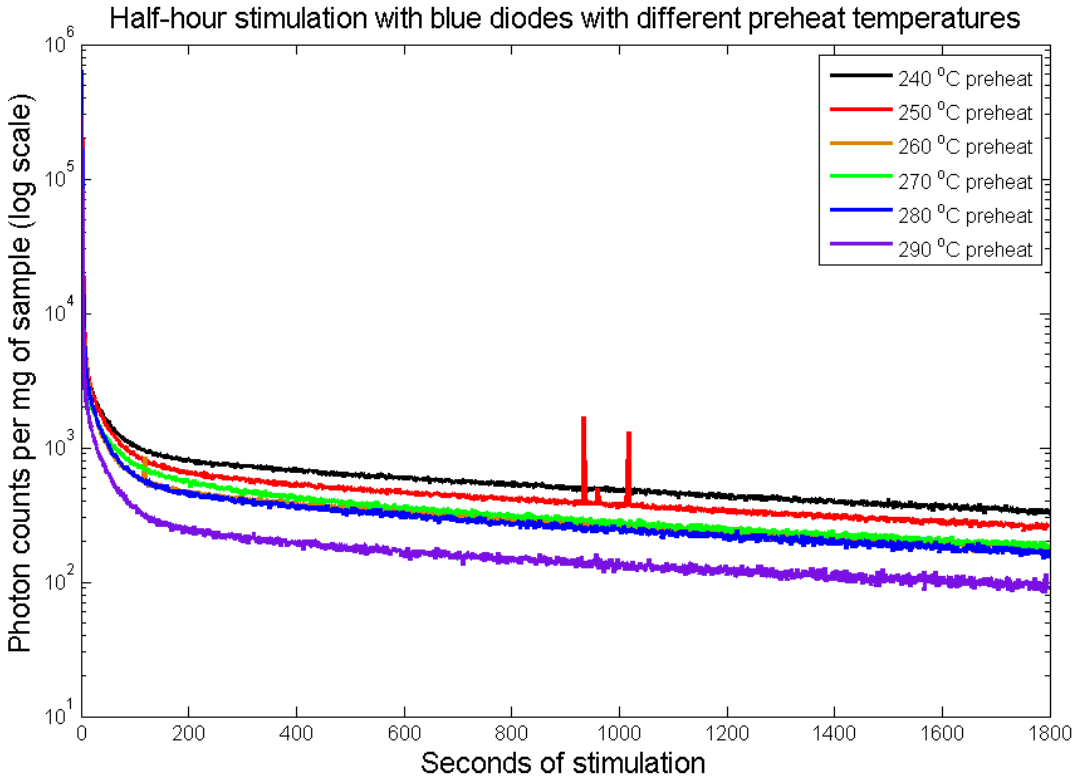

Figure 6.2: Mass-normalised stimulations with various preheats. Note that the spikes in the 250 °C preheat aliquot results are most likely instrumental aberrations caused by RF interference or point line "spikes".

All aliquot responses were characterised by a large initial signal, quickly depleting until evening out to a slow decay. The slow decay did not flatten out completely throughout the half hour, though after a minute, one can say that the signal is approximately constant over five seconds, and there is no visible negative gradient within a five second period after

two minutes (see fig 6.3). This indicates that the total OSL depletion times must be quite long, despite the fact that most of the signal is depleted in the first few seconds. Minimum times for OSL depletion (using blue LEDs at 90% power) should be one minute, while two minutes or more are preferable.

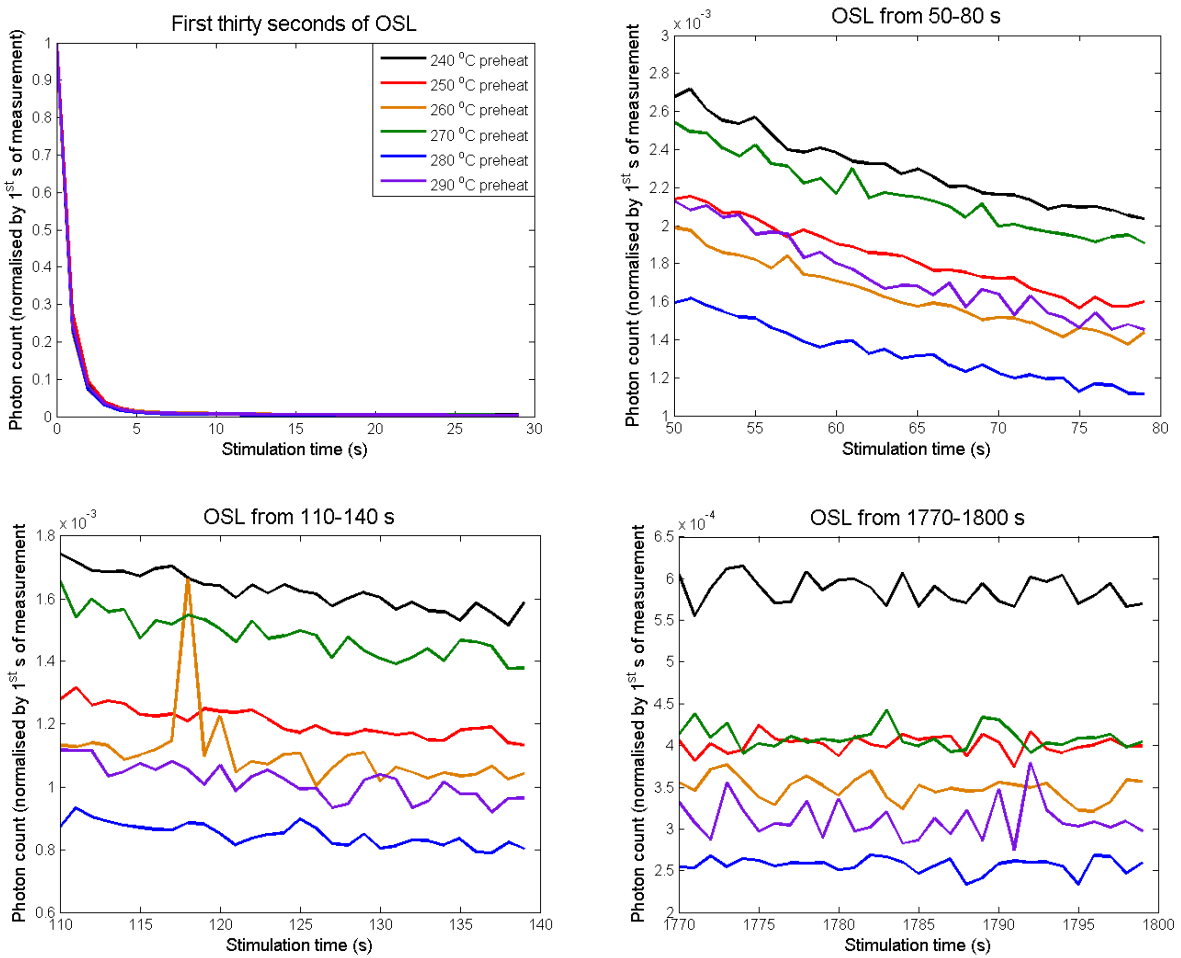

Figure 6.3: results for the long stimulation after various preheats, normalised by the first data point. A) is from 0-30 s; B) is near one minute; C) is near two minutes; and D) is near 30 minutes.

—What proportion of TT-OSL grains are useful?-

Twelve single grain discs of small aliquots were made of the WK4 sample. These were measured using the TT-OSL protocol detailed in chapter 8, using a Risø TL/OSL DA-20 with a single grain attachment. Stimulation light was from a green (532 nm) laser, and light to the EMI 9235QB photomultiplier was passed through a 7 mm Hoya U340 filter. After the 1200 small aliquots were analysed, 80 had saturating exponential or linear, unsaturated TT-OSL growth curves. Of these, 62 met all selection criteria, which included whether repeated doses gave similar results, and whether natural results were within the parameters of the growth curve (e.g., were not negative or above saturation). For small aliquots of eight to 12 grains, therefore, just over 5 % of them are useful for this sample.

-Is the TT-OSL signal dependent on age?-

A quick test often used on sequences of samples with the same sample source is to see whether the natural signals increase with age. The natural OSL signals of the Naracoorte East, Harper, Baker, East Dairy, Woakwine, and Long Beach samples were compared to one another. Results from six 5 mm diameter Long Beach aliquots, and eight each of the other samples were used. The aliquots were stimulated with blue diodes at 90 % power for 120 seconds. A Risø TL/OSL DA-20 with a 7 mm Hoya U340 filter was used for measurements. The background of each TT-OSL measurement was subtracted using the average of the last half a second of the previous OSL measurement. When OSL measurements were used for normalisation, the background was subtracted using the average of the last half a second of the same OSL measurement. Sample results were averaged and then compared to each other.

Protocol step	**Reason for step**
Preheat at 260 °C for 10 s	To remove the trapped charge populations of shallow traps
Blue diode stimulation at 90% power for 120 s	To deplete the population of the OSL traps
Preheat at 260 °C for 10 s	To induce thermal transfer
Blue diode stimulation at 90% power for 120 s	To measure the thermally transferred OSL
18.4 Gy β dose	A test dose
Preheat at 260 °C for 10 s	To remove the populations of shallow traps
Blue diode stimulation at 90% power for 120 s	To measure the aliquot's OSL response to the test dose
Preheat at 260 °C for 10 s	To induce thermal transfer
Blue diode stimulation at 90% power for 120 s	To measure the aliquot's TT-OSL response to the test dose

Table 6.4: the protocol used in finding the natural TT-OSL signals for each sample.

Results were normalised by both OSL and TT-OSL responses to a test dose, and the average signal of each sample compared with the average of the others (see fig 6.4). In the OSL normalised results, all but the Woakwine and Long Beach samples (which were reversed) were in order increasing with age. This reversal may be due to an increased background with age—the results without background subtraction are all in order of age.

TT-OSL normalised results with end-of-OSL background subtraction (see Chapter 5 for details) were in order of age at the peak result, although the Baker and Harper results were very close to each other, and over the course of the stimulation time the photon counts per 0.1 s changed order of age twice. The graph of the Long Beach result crossed over all the other results, at the end of the stimulation time ending up with the highest counts. The East Dairy, Baker, and Harper results all had very similar counts at the end of the stimulation time, while the Woakwine result had much lower counts, and the Naracoorte East much higher ones. Without background subtraction the results were in order of age along the entire length of the signal, apart from the Woakwine signal which appeared to have a higher residual background than the others.

From these results we can see that there is a general trend

of increasing TT-OSL signal with age, when normalised either with OSL or TT-OSL responses to a test dose. It also can be noted that a residual OSL component can be seen in all but the Long Beach sample, indicating both that the residual OSL can be bleached almost completely by sunlight (unlike TT-OSL, which has a residual amount after bleaching), and that proper background subtraction is important in getting an accurate TT-OSL measurement.

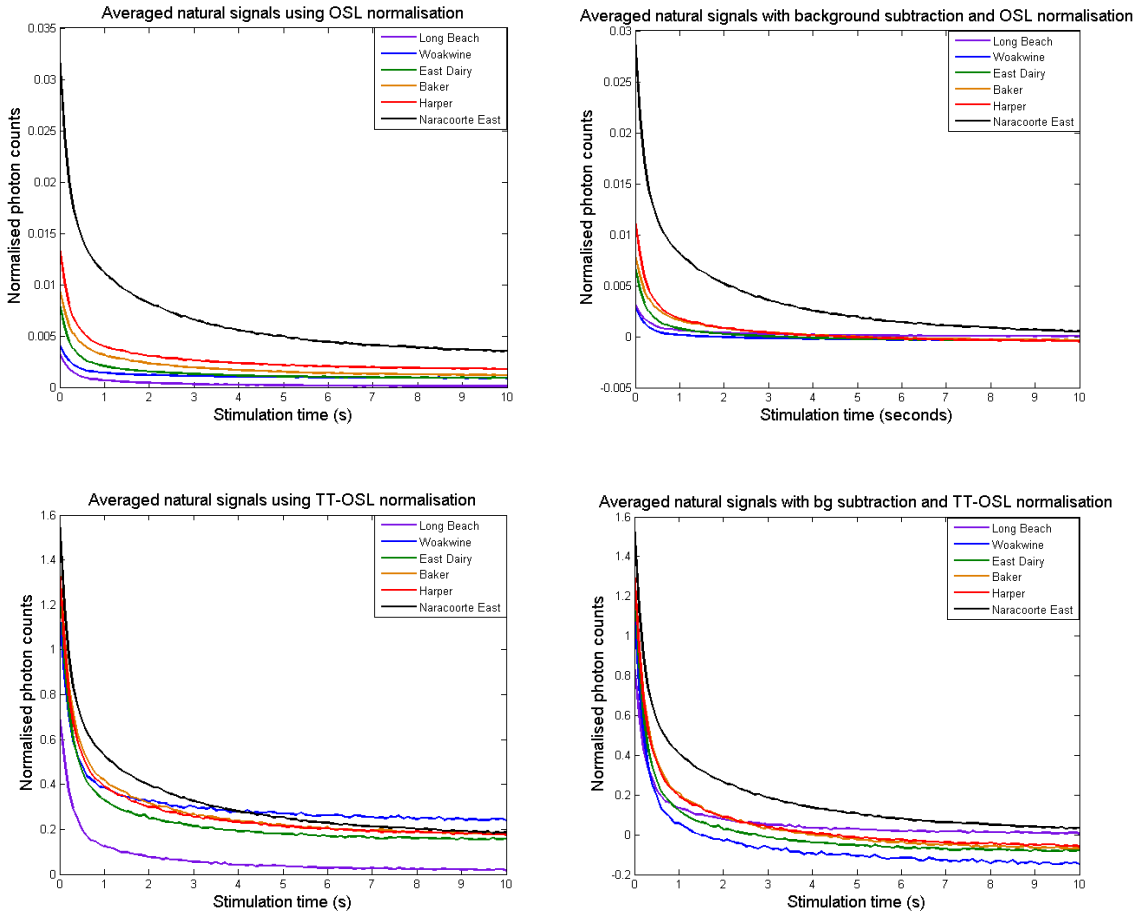

Figure 6.4: Graphs showing the first ten seconds of the averaged natural TT-OSL signals. A) With OSL normalisation and without background subtraction; B) with OSL normalisation and background subtraction; C) with TT-OSL normalisation and without background subtraction; D) with TT-OSL normalisation and background subtraction. Samples are listed in order of increasing age.

07-ZERO-AGE SAMPLE RESULTS

An important requirement for a dating method is that the method gives a value of zero for the age of a modern sample. This ensures that the method does not systematically over-estimate the age of older samples. Previous experiments on various samples have had differing results. Wang et al (2006b) tested three young samples which gave OSL ages of around 1 ka. The DD-TT-OSL results for the same samples were higher, up to 5 ka. However, this difference was not particularly significant when compared to the measurement of samples of tens to hundreds of ka.

Porat et al (2006) also found a near-modern sample to give small equivalent doses, as did Tsukamoto et al (2008), although one of their modern samples had a high DI-TT-OSL result. Hu et al (2010), when searching for thermally transferred signals that could interfere with their OSL measurements of young samples, did not find any of significance. However, Stevens et al found a loess sample with an OSL SAR equivalent dose of 1.1 Gy gave 13.3 Gy when measured by TT-OSL. Jacobs et al (2011) found significant DD-TT-OSL signals in zero-age samples.

Experiments on the bleachability of the DD-TT-OSL signal generally show a sharp drop in signal followed by a slow decay of a significant residual signal. Different samples, however, show widely varying bleaching times. For example, after half an hour, two quartz samples exposed to a SOL2 solar simulator by Tsukamoto et al (2008) retained around 60 % and 50 % of their original signal, while a different quartz sample exposed to direct sunlight by Athanassas and Zacharias (2010) only retained 13 % of its original signal. Athanassas and Zacharias concluded that an hour's exposure to sunlight would be sufficient to reduce their sample's DD-TT-OSL signal to residual levels, while the samples of Tsukamoto et al (2008) retained 18 % and 10 % of their signal after seven days continuous exposure. Kim et al (2009) had similar results to Tsukamoto et al, having significant residual signal left after optical stimulation for seven days. Brown and Foreman (2012) found that after stimulation under a sunlamp for 95 hours, 20 % to 40 % of the original signal remained in their samples. It should be noted that the solar simulator may be missing key wavelengths needed for bleaching TT-OSL signals, or may expose the sample to a lower intensity

of light than natural sunlight. While the results of Tsukamoto et al (2008), Kim et al (2009) and Brown and Foreman (2012) indicate that the TT-OSL signals of some samples may not deplete completely after a full day's worth of exposure to light, the results of Athanassas and Zacharias (2010) indicate that, after a day's exposure to natural sunlight, at least some samples have TT-OSL signals depleted to residual levels.

A zero-age sample from the south east of South Australia was collected on the 19th of February, 2013, from the Long Beach surfing beach, near Robe. Winds were blowing from south to north along the beach. The volume of sand moved by the wind was sufficient to collect only immediately wind-blown samples. The sample was collected by placing a bag in a purpose-dug depression and collecting sand blown into it (see fig 7.1). Samples were taken in daylight, at approximately 5:00 PM. As the samples were collected near the middle of summer, it was thought that they would have received near the maximum amount of exposure to sunlight reasonable to assume for any windblown sand.

Figure 7.1: The 'sand trap' used to collect the sample. Wind was blowing sand from the left to the right of the picture.

An experiment to observe both the OSL and TT-OSL signals remaining in a zero-age sample was undertaken. Eight 5 mm aliquots of 125-180 µm grains were made. Four of the samples underwent a 120 s OSL stimulation by blue LEDs at 125 °C. The remaining four were heated to 260 °C for 10 s, then the same OSL stimulation was administered. Both sets of aliquots were normalised by the OSL response to a 1.4 Gy test dose, after a 10 s preheat to 260 °C.

All but one of the aliquots that was not given a preheat had small initial signals, less than 300 counts in the first second. One of the aliquots had a large signal of about 15,500 counts in the first second. The aliquots which had a preheat before optical stimulation varied in initial counts from 7,800 to 20,000. The test dose response was much higher (from 120,000 to 350,000 per second) in all cases than the response to the natural dose, indicating that the initial natural dose equivalent is less than the given laboratory dose of 1.4 Gy.

Six 5mm 125-180 µm aliquots were measured using the Woakwine SAR TT-OSL protocol (see Chapter 11). DD-TT-OSL results were much higher than expected, the weighted mean of the six results ranging from 10 to 76 Gy, using different data analysis methods. Results using the end-of-TT-OSL background subtraction were in all cases smaller than results using other background subtractions, although all results were similar for each background subtraction when using a 0.5 s integral. Using 0.1 s integral and OSL normalisation, using the near-TT-OSL background subtraction gave larger results than the other background subtractions. The smallest palaeodoses were found using TT-OSL normalisation and the initial 0.5 s of signal. The largest results were found using OSL normalisation and the initial 0.1 s of signal. Ages gained for TT-OSL signals were larger than those of the DD-TT-OSL signal, and results for the DI-TT-OSL signal were larger again (see table 7.1).

Data analysis method	**Average (Gy)**	**Weighted mean* (Gy)**	**Error weighted mean**	**Age from weighted mean (ka)**
OSL normalisation	62	46.5	1.3	73 ± 5
end-of-OSL background subtraction	71	57.4	1.1	90 ± 6
0.1 s integral	107	83.8	3.6	131 ± 10

OSL normalisation end-of-OSL background subtraction 0.5 s integral	23 31 79	16.4 23.8 71.2	0.63 0.65 2.3	25 ± 2 38 ± 3 111 ± 8
TT-OSL normalisation end-of-OSL background subtraction 0.1 s integral	36 39 45	26.6 39.5 31.6	2.1 1.5 2.9	42 ± 4 62 ± 5 50 ± 5
TT-OSL normalisation end-of-OSL background subtraction 0.5 s integral	12 19 43	10.9 17.6 39.1	0.69 0.92 1.6	17 ± 2 28 ± 2 61 ± 5
OSL normalisation near-TT-OSL background subtraction 0.1 s integral	77 83 124	76.5 82.0 108	2.5 1.8 8.3	118 ± 8 128 ± 8 169 ± 17
OSL normalisation near-TT-OSL background subtraction 0.5 s integral	22 30 78	16.8 23.7 78.4	0.71 0.71 2.9	27 ± 2 38 ± 3 122 ± 9
TT-OSL normalisation near-TT-OSL background subtraction 0.1 s integral	24 43 79	25.1 42.8 45.4	4.0 2.5 6.8	39 ± 7 67 ± 6 70 ± 12
TT-OSL normalisation near-TT-OSL background subtraction 0.5 s integral	12 18 44	10.4 17.0 40.2	0.71 0.95 1.8	16 ± 2 27 ± 2 63 ± 5
OSL normalisation end-of-TT-OSL background subtraction 0.1 s integral	42 50 103	31.7 42.2 82.8	0.82 0.74 3.8	50 ± 3 66 ± 4 130 ± 10
OSL normalisation end-of-TT-OSL background subtraction 0.5 s integral	21 29 78	15.5 22.6 71.0	0.67 0.67 2.3	25 ± 2 36 ± 2 111 ± 8
TT-OSL normalisation end-of-TT-OSL background subtraction 0.1 s integral	20 28 55	16.2 25.9 38.7	1.2 1.2 2.4	25 ± 2 40 ± 3 61 ± 5
TT-OSL normalisation end-of-TT-OSL background subtraction 0.5 s integral	11 18 44	9.96 16.5 40.3	0.63 0.90 1.7	16 ± 1 26 ± 2 63 ± 5

Table 7.1: Results for six aliquots using the SAR TT-OSL method and different data analysis methods. Results in each cell are for DD-TT-OSL, TT-OSL, and DI-TT-OSL respectively.

The dose rate of this sample is 0.64 ± 0.04 Gy/ka (details in Chapter 4).

**Weighted means were calculated using a weight of $\frac{1}{se^2}$, where se is the total measurement error value calculated for each aliquot.*

The results gained for the zero-age sample indicate that there is residual TT-OSL in a wind-blown sample, indicating that this sample more closely follows the findings of Tsukamoto et al (2008) and Jacobs et al (2011) that the TT-OSL signal takes a very long time to bleach. The residual TT-OSL will artificially increase the dose result in SAR TT-OSL signals. Using these results as a guide, we can find the approximate overestimation of similar wind-blown sands using the SAR TT-OSL protocol. Calculations were made using the average of the weighted mean results for different background subtractions: Using the DD-TT-OSL signal, TT-OSL normalisation and the first 0.5 s of signal, 10.4 Gy; using OSL normalisation and the first 0.5 s of signal, 16.2 Gy. As the OSL trap population saturates at approximately 150 Gy, at the point where TT-OSL protocols begin to become useful TT-OSL normalisation using the first 0.5 s of signal will give approximately a 6.5 % overestimation of the dose, while OSL normalisation with 0.5 s of integral will give a 10 % overestimation of the dose. The oldest sample used in this thesis was the Naracoorte East sample, with an estimated age of over 900 ka. Another sample from the Naracoorte East range (with lower natural dose rates) gave a TL-calculated natural dose of 455 Gy, which with the above residual natural doses would have a 2 % and 3 % overestimation of the dose respectively. Using the TT-OSL signal rather than the DD-TT-OSL signal will increase the overestimations to 10 and 13 % for 150 Gy, and 4 and 5 % for 455 Gy. Using the first 0.1 s of the DD-TT-OSL signal will give an overestimate of 13 and 25 % for 150 Gy, and 5 and 10 % for 455 Gy.

The 'dose equivalent' age found for the zero-age sample range from the tens to the hundreds of ka, nearing in the case of some DI-TT-OSL results and some results using the near-TT-OSL background subtraction the expected age of the Woakwine 1 range. From these results alone, one would conclude that TT-OSL dating could only be accurate when measuring large natural doses (or potentially samples bleached further than the zero-age sample measured), via the first 0.5 s of DD-TT-OSL signal, with normalisation by the TT-OSL response to the test dose and using either the end-of-OSL or end-of-TT-OSL

background subtraction. Whether this "residual" dose influences the older samples will be found in Chapter 11.

08-INITIAL RESULTS FOR WOAKWINE SMALL ALIQUOTS

The Woakwine sample was used as a test sample for the TT-OSL SAR procedure, as the Woakwine range has been dated extensively by TL, OSL, and oxygen isotope methods, which give an age of around 120 ka. Small "aliquots" were made by putting 125-180 µm grains into the 300 µm diameter depressions in single-grain discs, giving approximately 8-12 grains per aliquot. Small aliquots were chosen as they would give an idea of the distribution of the natural equivalent doses (though in a less resolvable form than single-grain dating) while still giving enough light to detect the very small TT-OSL signals. A Risø TL/OSL DA-20 with a single-grain reader attachment was used, with a 7 mm thick Hoya U340 filter interposed between the sample and the photomultiplier. Doses were given using a 1.48 GBq Sr^{90}/Y^{90} beta source, at a dose rate of approximately 0.15 ±0.01 Gy/s. The protocol used is shown below (tables 8.1 and 8.2). Note that the "hot wash" at the very end of each cycle was done at 290 °C. This was because the air inside the machine with the single grain attachment could not be pumped out (as this module cannot hold vacuum), and continuous higher temperatures would oxidise the heating plate in the presence of oxygen. To compensate, the temperature was held for 400 s, as in Stevens et al (2009).

Protocol for each cycle of TT-OSL SAR measurements.
Artificial β dose (zero for first cycle)
Preheat to 260 °C at 5 K/s, holding for 10 s
Stimulation by green laser for 2 s (at ambient temperature)
Preheat to 260 °C at 5 K/s, holding for 10 s
Stimulation by green laser for 1 s (at ambient temperature)
~7.5 Gy β dose
Preheat to 260 °C at 5 K/s, holding for 10 s
Stimulation by green laser for 1 s (at ambient temperature)
Preheat to 300 °C at 5 K/s, holding for 10 s
Stimulation by green laser for 2 s (at ambient temperature)
Preheat to 260 °C at 5 K/s, holding for 10 s
Stimulation by green laser for 1 s (at ambient temperature)
~7.5 Gy β dose
Preheat to 260 °C at 5 K/s, holding for 10 s
End-of-cycle TT-OSL depletion at 290 °C with blue diodes at 90 % power, holding for 400 s

Table 8.1: The protocol used for gaining TT-OSL measurements. Note that stimulations were done at ambient temperatures. As

the Woakwine sample has a large photon count to dose ratio and a small natural dose, the loss of signal and artificial saturation effects due to retrapping at shallow traps was not deemed significant enough to effect results for this experiment.

Cycle	β dose administered (Gy)
2	45
3	90
4	150
5	300
6	450
7	0
8	45

Table 8.2: The dose used in each cycle of the protocol. Note that the first cycle does not include an artificial dose, as it is measuring the natural signal.

The signals were quite small, and the last portion of the OSL trap emptying stimulation measurements were used for background subtraction (called the end-of-OSL background subtraction in chapter 6), thereby removing OSL signal while maximising the signal retained (when compared with background subtractions such as the near-TT-OSL background subtraction). All of the signal from the start of stimulation until the signal reached the background level was used. OSL responses to test doses were used for normalisation, as the TT-OSL responses were generally too small to be resolved.

A number of selection criteria were chosen, as listed below:

-Positive dose dependence: the normalised signal must increase with dose.

-Good fit to equation with physical meaning: the response to artificial doses must be able to be fit to either a linear, saturating exponential, or saturating exponential plus linear function. Results that were too scattered or did not appear to have a trend were discarded.

-Natural dose within bounds: the natural dose must not be negative, or lie at or beyond the saturation point of the growth curve.

-Good recycling ratio: an artificial dose that was repeated cannot have a large difference between the two normalised

signals. In this case, 'large differences' were said to be repeated signals in which one was 100 % more discrepant from the other.

Twelve discs with a total of 1200 aliquots were made and measured using the protocol. Results were found using the Matlab code "allparts2" (see Appendix A). Of the 1200 small aliquots, 69 met the selection criteria (see fig 8.1 for example).

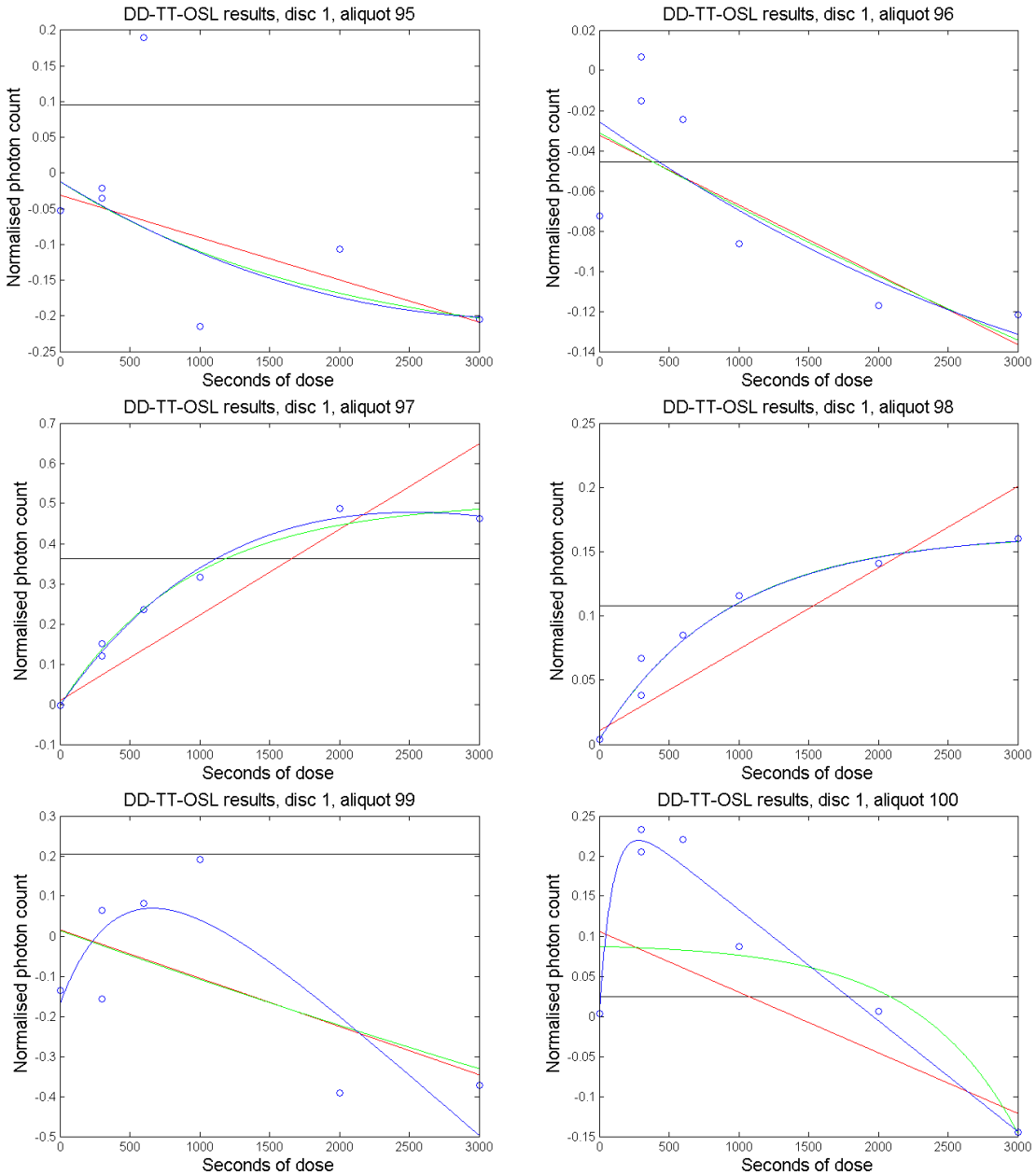

Figure 8.1: Examples of dose recovery curves. The last six small aliquot results for the first disc are shown. The

natural signal's normalised photon count is shown as a black line. Regenerative dose points are shown as blue circles. Three fits are shown: linear (red), saturating exponential (green), and saturating exponential plus linear (blue). Of these six, only aliquots 97 and 98 were accepted.

-Results using weighted mean and average-

The weighted mean of the age of the 69 accepted aliquots was 83 ± 4 ka, while the average value was 150 ka, indicating that the errors were in general proportionally smaller for smaller values. This may be due in part to the fact that instrumental errors for this machine had been previously calculated to be 1.7% of the value of the result, and using a percentage error means that the instrumental error trends towards zero the smaller the result becomes. The instrumental errors found experimentally for a different but similar machine (see Chapter 5), by contrast, included a constant value. If the actual and estimated errors differ in this way, it would negatively skew a weighted value for the mean.

-Results using histograms-

Histograms of the results (see fig 8.2) indicate that there is a relatively asymmetrical distribution of results. Different edge points of the histogram lead to different peak values, but in general the distribution peaks between 100 and 140 ka. There is a long tail of very old ages, which may have positively skewed the average value.

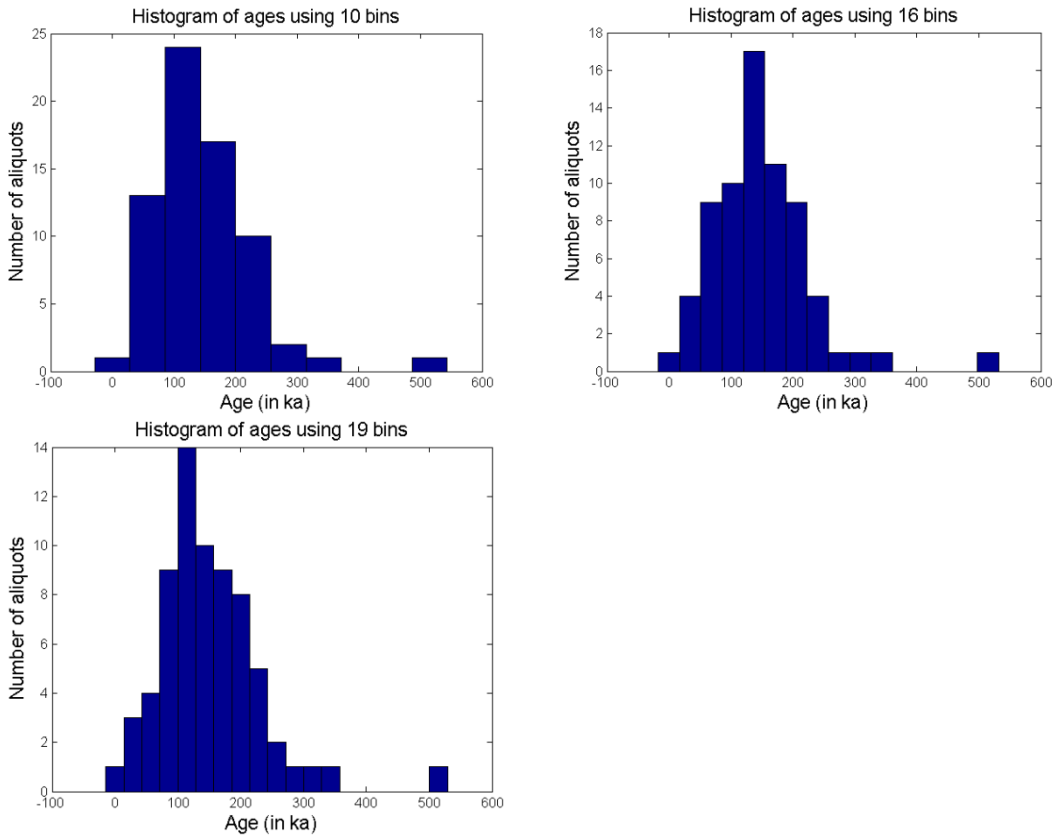

Figure 8.2: Histograms of aliquot ages, using different bin widths.

-Results using 'gradient isolation'-

If all results are sorted from smallest to largest and graphed, there appears to be a pattern in the data, wherein there is a smooth progression of data points followed by a discontinuity (see fig 8.3). The two main discontinuities split the population into three parts, with weighted means of 56 ± 6, 119 ± 10, and 207 ± 17 ka. Average values were the same as the weighted means within errors. It is noted that the middle value is equal to the expected age of the Woakwine range within errors. Whether selecting parts of populations in this way is a feasible method is not known.

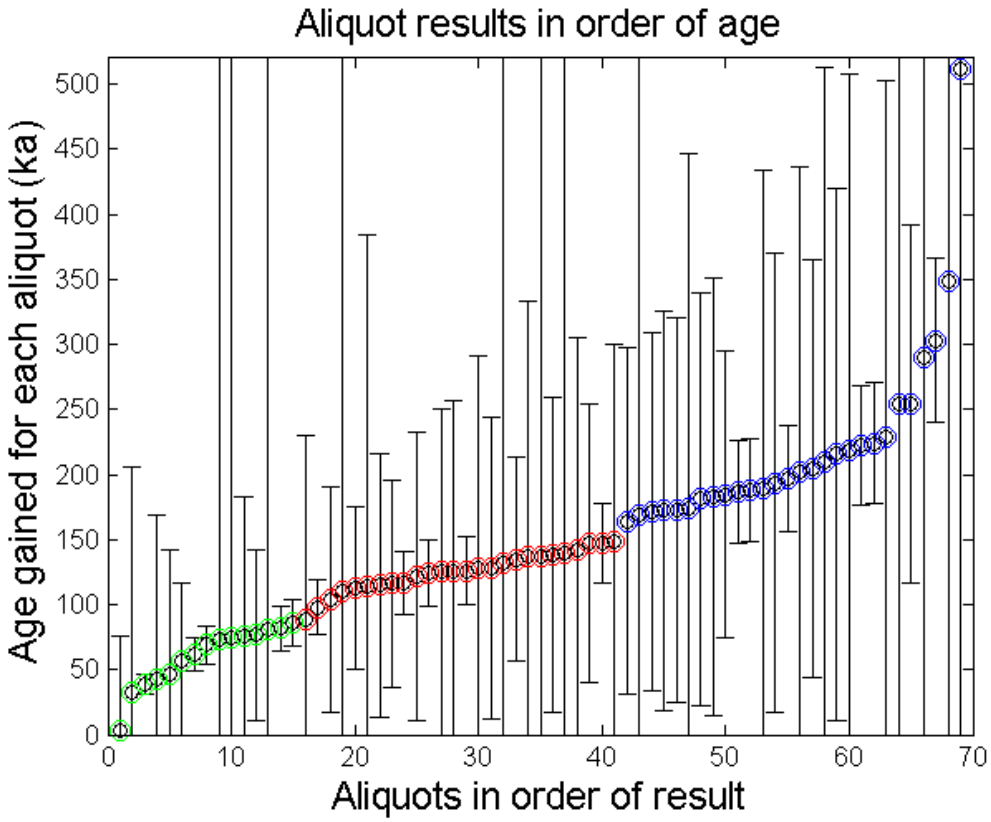

Figure 8.3: Aliquots in order of age. Results ringed in different colours indicate those before or after discontinuities. Results ringed in red give a weighted mean near the expected result for the Woakwine Range based on independent dating evidence.

-Results summing aliquot signals-

Another method of acquiring a result from a distribution of grains is to combine the normalised signal of all accepted results together, and fit a curve to the results. The normalised signal of the 69 accepted small aliquots were summed, and the dose rate of the β source was taken to be the average dose rate over the disc (0.15 Gy/s). This gave a saturating exponential curve, with the natural signal far from the saturation point (see Fig. 8.4). The natural signal had an equivalent dose of 95 ± 12 Gy, which corresponds to an age of 155 ± 22 ka, near to the average value of the individual small aliquot results.

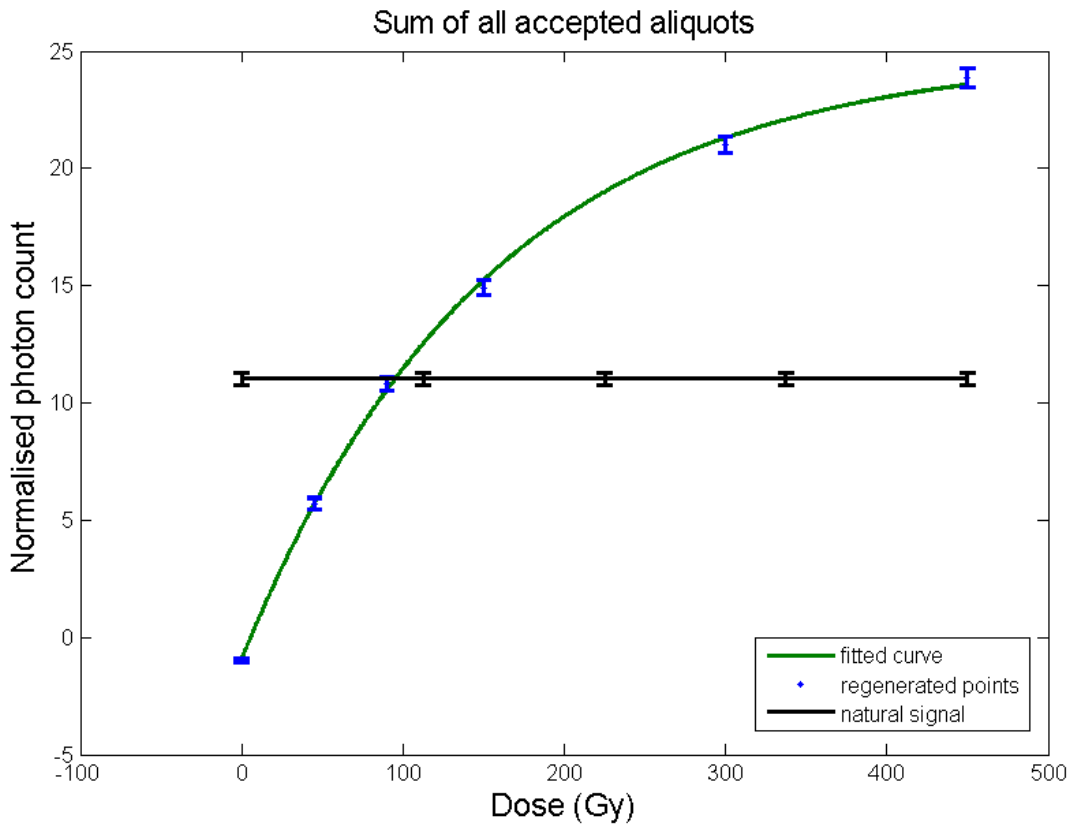

Figure 8.4: Regenerative dose curve using the sum of all normalised DD-TT-OSL signals for the 69 accepted small aliquots. The fitted curve (in green) was created using Matlab's Curve Fitting Toolbox.

-Summary-

The weighted mean of this distribution was skewed away from the mean and median values of the distribution. When looking at a histogram of the distribution, the peak value of age is much higher than the weighted mean, and is generally around the expected age of the sample. It is possible that in this instance the weighted mean is skewed by non-real instrumental error values, and so cannot be used. In addition, the distribution appears to be asymmetrical, which would make a result for the (non-weighted) mean skewed away from the peak value. It appears that the best way to find a value for the age of the sample from this distribution is to find the peak value from a histogram of the results, although this is not a very precise method. Ordering results and finding areas of approximately the same gradient to isolate and find the mean from also gives results at the expected value, though this

process can be subjective, and may introduce bias into the results.

Using the gradient isolation method and the histogram method give results at the expected value. We can therefore say that, for the Woakwine sample, it is possible to find an age that matches the expected value using TT-OSL. Other methods, however, give ages above and below the expected value, and so more experimentation must be done to see whether there is a data analysis method that consistently gives the expected dose for different samples.

09-INITIAL RESULTS FOR 5 mm ALIQUOTS

The Adelaide laboratory (Prescott Environmental Luminescence laboratory) holds a large number, almost 150, of samples collected from the stranded beach ridges of the SESA region. From these, a subset of samples widely spaced in time and with independent dating evidence are chosen to review the SAR TT-OSL dating protocol. These were the Woakwine, East Dairy, Baker, Harper, and Naracoorte East samples. The protocol was applied to 5 mm diameter aliquots of 125-180 µm diameter grains. The TT-OSL protocol used for initial aliquot results is shown in the tables below (9.1 and 9.2). It includes the 350 °C end-of-cycle "hot wash" for 200 s (as in Adamiec (2010)), and 260 °C preheats. The DI-TT-OSL component was measured, as was the TT-OSL response to the test doses. A Risø TL/OSL DA-20 was used for measurements, with a 7 mm Hoya U340 filter interposed between the sample and the photomultiplier. Selection criteria used were the same as in the previous section. Data analysis was done via Version 5 of the 'natdose' Matlab program found in Appendix A of this thesis.

Protocol for each cycle
β dose (0 at natural)
Preheat to 260°C (5 K/s; held for 10 s)
OSL stimulation at 125 °C for 60 s with Blue diodes at 90% power
Preheat to 260°C (5 K/s; held for 10 s)
OSL stimulation at 125 °C for 60 s with Blue diodes at 90% power
Test dose (8.3 Gy β)
Preheat to 260°C (5 K/s; held for 10 s)
OSL stimulation at 125 °C for 60 s with Blue diodes at 90% power
Preheat to 260°C (5 K/s; held for 10 s)
OSL stimulation at 125 °C for 60 s with Blue diodes at 90% power
Preheat to 300°C (5 K/s; held for 10 s)
OSL stimulation at 125 °C for 60 s with Blue diodes at 90% power
Preheat to 260°C (5 K/s; held for 10 s)
OSL stimulation at 125 °C for 60 s with Blue diodes at 90% power
Test dose (8.3 Gy β)
Preheat to 260°C (5 K/s; held for 10 s)

OSL stimulation at 125 °C for 60 s with Blue diodes at 90% power
Preheat to 260°C (5 K/s; held for 10 s)
OSL stimulation at 125 °C for 60 s with Blue diodes at 90% power
Heat to 350°C for 200 s

Table 9.1: The TT-OSL SAR protocol used for each aliquot.

Cycle	**Naracoorte East**	**Harper**	**Baker**	**East Dairy**	**Woakwine**
2	63	84	42	42	8
3	188	167	84	84	25
4	376	251	167	125	50
5	523	335	251	167	75
6	1004	502	335	209	151
7	0	0	0	0	0
8	376	251	167	84	50

Table 9.2: The dose (in Gy) used in each cycle of the TT-OSL SAR protocol for each sample. The first cycle is to measure the natural signal, and so no dose is given to the sample.

Protocols using the TT-OSL signal (e.g., Stevens et al, 2009) and the DI-TT-OSL signal (Jacobs et al, 2011) have been used in the past. The equivalent dose was therefore found using the DD-TT-OSL, TT-OSL, and DI-TT-OSL signals, for comparison. The results were computed using various data analysis variables, as listed below:

Signal integration: using the first 0.1 s and first 0.5 s of signal.

Background subtraction: using the end-of-OSL, end-of-TT-OSL, and near-TT-OSL background subtraction methods.

Normalisation: using the OSL and TT-OSL response to a test dose for normalisation.

-Individual results-

A list of individual sample results is shown below. OSL normalisation and the end-of-OSL background subtraction were used in the figures shown.

Woakwine (see Fig 9.1): DD-TT-OSL and TT-OSL results are in general lower than the expected age, though five of nine DD-TT-OSL results fall into the expected age range within errors, the rest are lower than the expected age range by

more than 20 ka. All but one DI-TT-OSL result falls within the expected age range within errors, though this may be due to their large errors and not the accuracy of the measurements.

East Dairy (see Fig 9.2): DI-TT-OSL results lie within the expected age range, though the errors in the results are very large. Six of nine DD-TT-OSL results are in the expected range within errors, although they are all in the lower half of the expected range.

Baker (see Fig 9.3): DD-TT-OSL and TT-OSL results are much smaller than the expected age range. DI-TT-OSL results are in general around the expected age range, although the scatter and errors of the values is large.

Harper (see Fig 9.4): DD-TT-OSL and TT-OSL results are in general much smaller than the expected age range. DI-TT-OSL results are very scattered, with the expected value lying approximately in the middle of the scatter.

Naracoorte East (see Fig 9.5): DD-TT-OSL and TT-OSL results are in general much smaller than the expected age range. DI-TT-OSL results have large error bars, and at best the results are near the lower end of the range of previously gained ages.

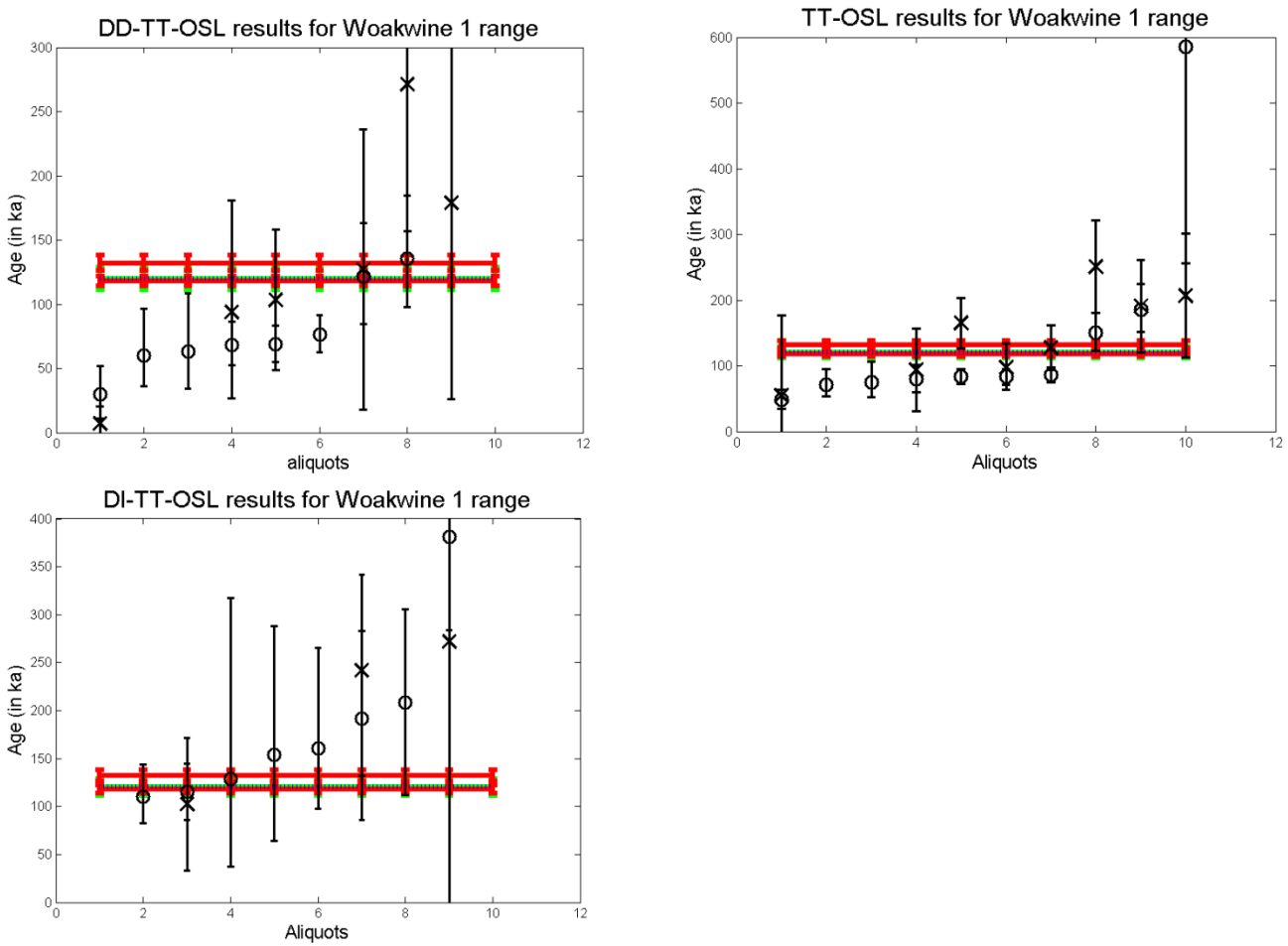

Figure 9.1: Results for individual Woakwine 1 aliquots. Previous results are shown: Oxygen isotope results in blue (dashed), OSL results in green, and thermoluminescence results in red. Circles represent results using 0.5 s of signal, while crosses represent results using 0.1 s of signal. A) DD-TT-OSL results; B) TT-OSL results; C) DI-TT-OSL results.

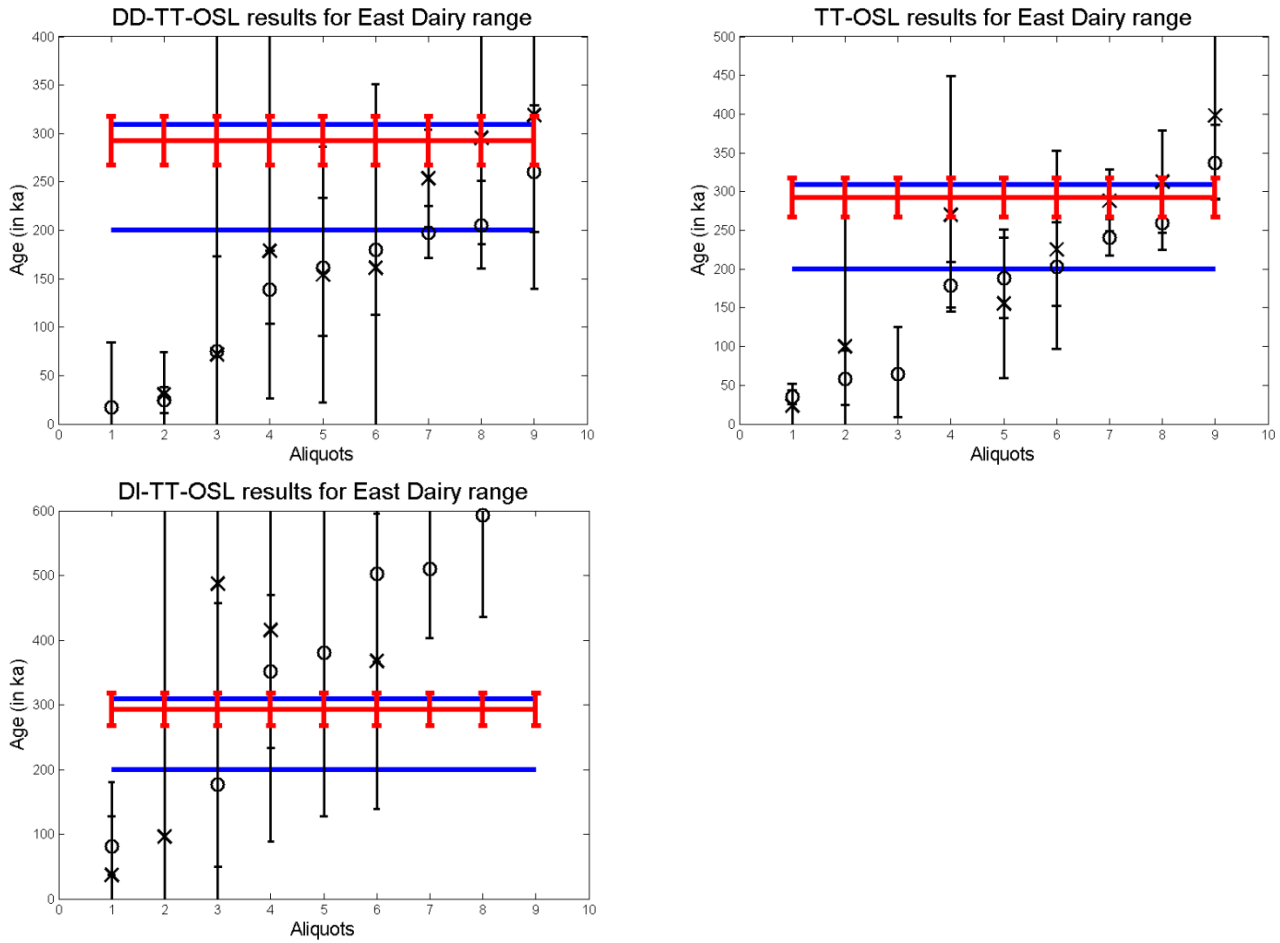

Figure 9.2: Results for individual East Dairy aliquots. Previous results are shown: Oxygen isotope results in blue, and thermoluminescence results in red. Circles represent results using 0.5 s of signal, while crosses represent results using 0.1 s of signal. A) DD-TT-OSL results; B) TT-OSL results; C) DI-TT-OSL results.

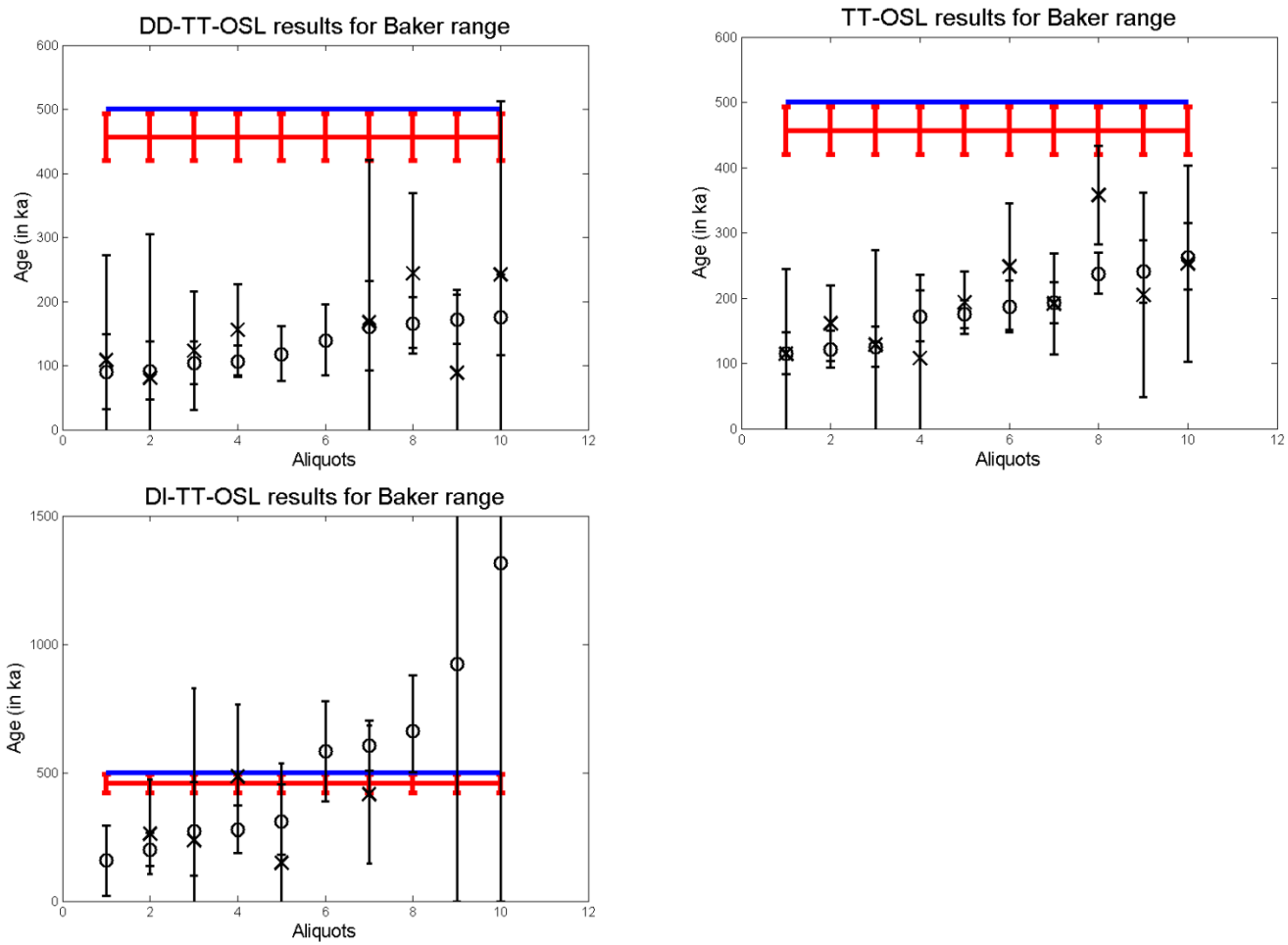

Figure 9.3: Results for individual Baker aliquots. Previous results are shown: Oxygen isotope results in blue, and thermoluminescence results in red. Circles represent results using 0.5 s of signal, while crosses represent results using 0.1 s of signal. A) DD-TT-OSL results; B) TT-OSL results; C) DI-TT-OSL results.

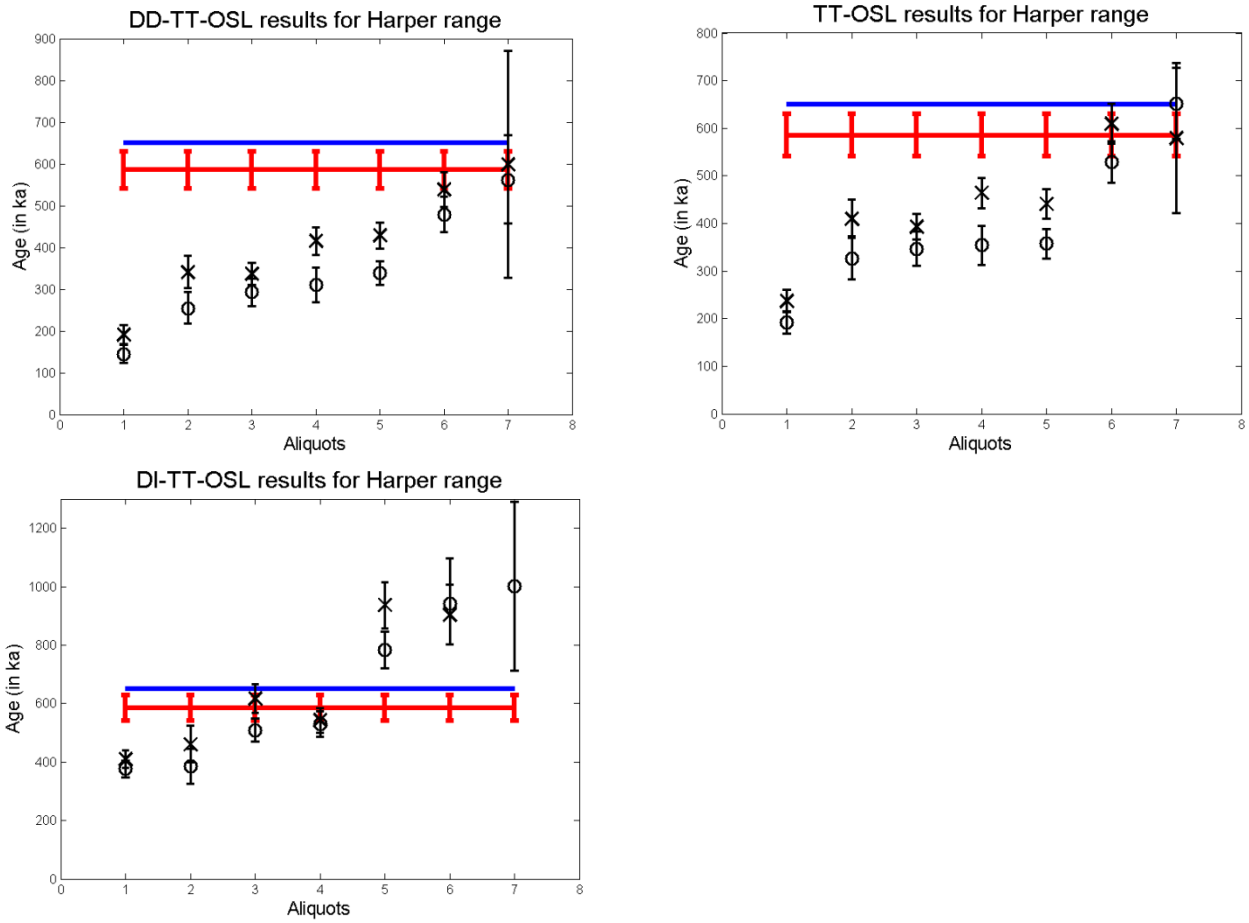

Figure 9.4: Results for individual Harper aliquots. Previous results are shown: Oxygen isotope results in blue, and thermoluminescence results in red. Circles represent results using 0.5 s of signal, while crosses represent results using 0.1 s of signal. A) DD-TT-OSL results; B) TT-OSL results; C) DI-TT-OSL results.

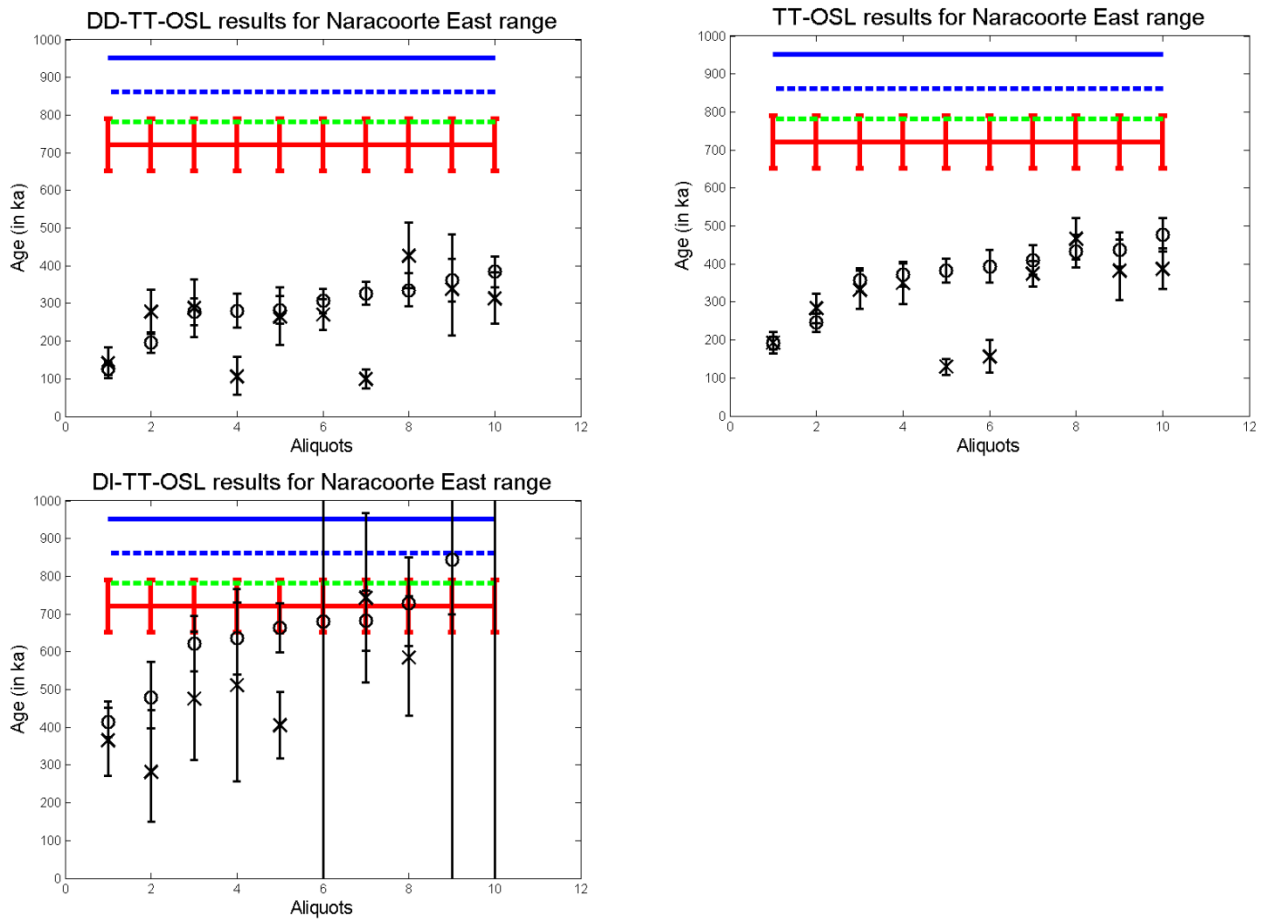

Figure 9.5: Results for individual Naracoorte East aliquots. Previous results are shown: Oxygen isotope results in blue, palaeomagnetic data results in green, and thermoluminescence results in red. Circles represent results using 0.5 s of signal, while crosses represent results using 0.1 s of signal. A) DD-TT-OSL results; B) TT-OSL results; C) DI-TT-OSL results.

-Comparisons of results gained from various data analysis variables:-

Results were affected by the signal and data analysis methods used, as summarised below:

Signal used: In general, DD-TT-OSL and TT-OSL results underestimated the age of the sample. Results were generally scattered and had large errors. DI-TT-OSL results were more closely aligned with the expected results. However, they had very large errors, often more than 50 % of the signal's value.

Integral of signal: Use of the 0.1 s of signal for calculations in general gave more linear dose recovery curves than the 0.5 s of signal calculations. Some of the 0.1 s calculations did not have recognisable dose response curves, and so a result could not be obtained. Whether or not a result could be obtained did not correspond to the signal's strength (as determined by the un-normalised natural signal) when compared to other 0.1 s calculations, although all were much smaller than 0.5 s calculations. There appeared to be no trend up or down in the difference between 0.1 s and 0.5 s results. The 0.5 s results, however, were less scattered (having an average difference from the mean value of 77 ka vs 127 ka for 0.1 s integral results). In addition, 0.5 s results had smaller errors, having an average percentage error of 39 % of the value, as opposed to the 99 % of 0.1 s results.

Background subtractions:
The background subtraction used did not appear to influence the results gained, although it heavily influenced whether a result could be obtained. This appears to be a resolution issue, and is seen most clearly when using the first 0.1 s of signal. For the Woakwine sample, of the 10 aliquots analysed, dose response curves were able to be obtained for eight of the OSL-normalised 0.1 s signal aliquots with end-of-TT-OSL background subtraction, which maximises the signal used. End-of-OSL background subtraction, which uses less proportion of the signal, gave six viable results from the ten aliquots, while near-TT-OSL background subtractions gave only one viable result. To contrast, the Naracoorte East sample whose protocol uses much higher artificial doses (and had higher photon counts overall) had 10, 10, and six out of 10 aliquots respectively with viable results.

Normalisation: TT-OSL normalisation gave fewer viable results, and the dose response curves saturated earlier than those created using OSL normalisation. Using the OSL response to the test dose gave straighter curves, often behaving linearly throughout the doses given.

-Conclusions-

A major problem in obtaining a result from a TT-OSL protocol is the lack of TT-OSL signal produced. Small photon counts create large errors, and do not allow for a great deal of flexibility during the data analysis stage. Using the first 0.1 s of signal, and using the near-TT-OSL background subtraction technique are procedures which are supposed to minimise interference in the measured signal by slower OSL components. However, as they lower the available signal, in these measurements they gave scattered data points with large errors. TT-OSL normalisation is also subject to large errors and scatter of the data, as it relies on a TT-OSL signal from a small dose, hence introduces a second significant source of large errors from poor counting statistics. As DI-TT-OSL signals are smaller than TT-OSL signals, DD-TT-OSL results are also affected by large counting errors.

While DI-TT-OSL results in general appear to give the best correlation to known ages of the three proposed TT-OSL dating signals, their lack of precision means that their true accuracy for dating is unclear. A way to increase the total photon counts of a sample must be used in order to determine the suitability of these TT-OSL-derived signals for dating.

10-IMPROVEMENTS TO MEASURING TECHNIQUES

Before further measurements were made, a number of improvements were introduced to optimise instrument and hence use, and the protocol. These focused on improving signal strength, the reliability of results, and enabling a flexibility in choosing how to analyse the data. Details of these improvements are shown below.

-Instrumentation-

Optimising the instrumentation in general does little other than improve the recorded signal strength, which while decreasing counting errors can also increase background noise levels and may not do anything to increase the reliability of results. As seen in the initial results, however, a lack of signal strength can prevent the use of certain methods of data analysis. To find out whether these methods produce more accurate results than those that can be used for dim samples, one has to increase the signal output, whether by increasing the amount of sample being measured or by increasing the amount of signal captured by the instrumentation. A list of instrumentation and procedural improvements is listed below.

-Cleaning: It was found that a layer of salt (apparently electrostatically attracted to the quartz window) had built up on the quartz window situated between the sample and the photomultiplier, from independent measurements on that material by other researchers. The quartz window is used to protect the photomultiplier from damage (as shown necessary by the salt build-up). When the salt was removed, signals recorded increased by about a factor of ten.

-Photomultiplier HV optimisation: The signal-to-noise ratio of the photomultiplier was measured for different high voltage levels. This was done with a large signal (with millions of counts per second) and a small signal (with thousands of counts per second). The HV level with the largest signal-to-noise ratio for both high and low signals was chosen. More information can be found in Chapter 3. While HV optimisation lowers the amount of 'dark' noise measured in relation to the signal, it does not account for other background noise sources, such as very slow OSL components or phosphorescence. Dark noise in this case has two contributors: spontaneous signal from the photomultiplier

itself, and low-level light leakage (in general this is zero).

-Warming up the machine: It was noted that the first measurement in any protocol was much smaller than the others, often causing the first aliquot in a sequence of aliquot measurements to be discarded due to having natural TT-OSL counts smaller than the counts after no dose. After this was noted, before every sequence was run, as a practical step, the photomultiplier, heating plate, nitrogen, and stimulation diodes were used in order to ensure that all parts of the machine were working and warmed up. This prevented further 'negative dose' measurements being recorded.

-Changes to the protocol-

The protocol used for the initial study was chosen to represent current best-practice, being a combination of the most commonly used and most recent innovations of the general TT-OSL SAR protocol. However, other versions of the protocol may be more suitable for the SESA samples.

An experiment to test the reproducibility of a measurement using various SAR protocols was devised. Woakwine, Naracoorte East, and Robe samples were used. 5 mm aliquots were bleached in the sun for approximately four hours on a day with a top temperature of 33 °C, the aliquots were given approximately 73 Gy of β radiation dose, then run through a TT-OSL cycle. This was repeated 12 times, then a cycle with no dose was done. The protocol remained the same as for the 5 mm aliquot results in the previous section, but with changes to the preheat temperature and the end-of-cycle wash to bleach out any remaining TT-OSL signal (see table below). The changes were:

-Preheat temperature of 260 °C or 280 °C

-End-of-cycle wash for 200 s, using blue diodes at 90 % power at 290 °C, blue diodes at 90 % power at 350 °C, and no optical stimulation at 350 °C.

Protocol Step		**Alternate protocol step**	**Purpose of step**
73 Gy β dose	or	0 β dose (for cycle 13)	
Preheat to 260°C (5 K/s; held for 10 s)	or	Preheat to 280°C (5 K/s; held for 10 s)	Preheat to empty shallow traps
OSL stimulation 60 s Blue diodes at 90% power			OSL stimulation to deplete OSL trap
Preheat to 260°C (5 K/s; held for 10 s)	or	Preheat to 280°C (5 K/s; held for 10 s)	Preheat to stimulate thermal transfer
OSL stimulation 60 s Blue diodes at 90% power			OSL stimulation to measure TT-OSL
Test dose (8.3 Gy β)			Test dose for normalisation
Preheat to 260°C (5 K/s; held for 10 s)	or	Preheat to 280°C (5 K/s; held for 10 s)	Preheat to empty shallow traps
OSL stimulation 60 s Blue diodes at 90% power			OSL stimulation to deplete OSL trap
Preheat to 260°C (5 K/s; held for 10 s)	or	Preheat to 280°C (5 K/s; held for 10 s)	Preheat to stimulate thermal transfer
OSL stimulation 60 s Blue diodes at 90% power			OSL stimulation to measure TT-OSL
Preheat to 300°C (5 K/s; held for 10 s)			High temperature preheat to deplete DD-TT-OSL
OSL stimulation 60 s Blue diodes at 90% power			OSL stimulation to deplete OSL trap
Preheat to 260°C (5 K/s; held for 10 s)	or	Preheat to 280°C (5 K/s; held for 10 s)	Preheat to stimulate thermal transfer
OSL stimulation 60 s Blue diodes at 90% power			OSL stimulation to measure DI-TT-OSL
Test dose (8.3 Gy β)			Test dose for normalisation
Preheat to 260°C (5 K/s; held for 10 s)	or	Preheat to 280°C (5 K/s; held for 10 s)	Preheat to empty shallow traps

OSL stimulation 60 s Blue diodes at 90% power			OSL stimulation to deplete OSL trap
Preheat to 260°C (5 K/s; held for 10 s)	or	Preheat to 280°C (5 K/s; held for 10 s)	Preheat to stimulate thermal transfer
OSL stimulation 60 s Blue diodes at 90% power			OSL stimulation to measure TT-OSL
Heat to 350°C for 200 s with or without Blue diodes at 90% power	or	Heat to 290°C for 200 s with Blue diodes at 90% power	High temperature heat to deplete all TT-OSL signal

Table 10.1: TT-OSL SAR protocols with alternative steps.

Each preheat was used with each end-of-cycle wash, making six protocol variants tested in all. Four aliquots were used for each protocol, one from the Woakwine range, two from the Robe range, and one from Naracoorte East. Each set of results was calculated using all three background subtractions (end-of-OSL, near-to-signal TT-OSL, and end-of-TT-OSL), using both the TT-OSL and OSL responses to test doses for normalisation, and using the first 0.1 s and 0.5 s of signal.

For all results using OSL normalisation, the first data point is much higher than subsequent results, indicating that either four hours of sun exposure is not enough to fully bleach the TT-OSL signal, or that the normalisation method used is not sufficient to normalise the first cycle with subsequent ones. Results were put into two categories, 'good' and 'bad'. 'Bad' results had positive or negative gradients in the results of cycles two to 12, had scattered results, or the dosed results could not be resolved as distinct from the zero-dose result (cycle 13). 'Good' results had results from cycles two to 12 in a straight line with a gradient of zero, which was distinct from the zero result. Positive gradients were found in DD-TT-OSL and TT-OSL results, and negative gradients were found only in TT-OSL results (see fig 10.1). Only one protocol variant had 'good' results for all four aliquots: the protocol with the 260 °C preheat to stimulate TT-OSL and the end-of-cycle "hot wash" using 200 s blue diode stimulation at 350 °C. The data analysis methods which gave 'good' results for the protocol above used TT-OSL and OSL normalisation with end-of-OSL background subtraction, and OSL normalisation with near-to-signal TT-OSL background subtraction, using the first 0.1 s of TT-OSL signal.

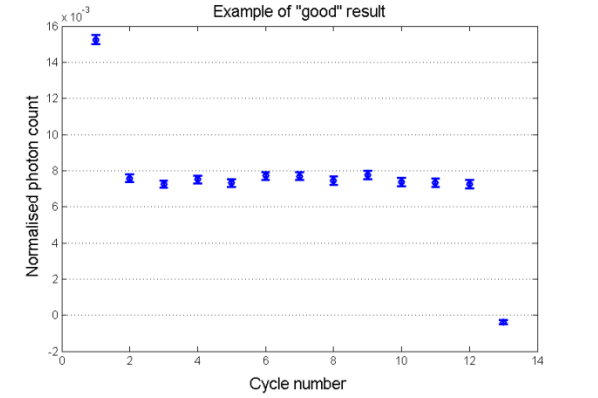

DD-TT-OSL result of the Robe sample, using 260 °C preheat, 290 °C illuminated wash, OSL normalisation, 0.1 s signal and end-of-TT-OSL bg subtraction

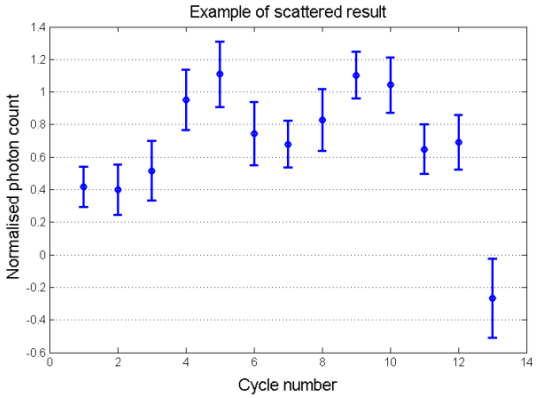

DD-TT-OSL signal of the Robe sample, using 260 °C preheat, 290 °C illuminated wash, TT-OSL normalisation, 0.1 s signal, and near-TT-OSL bg subtraction

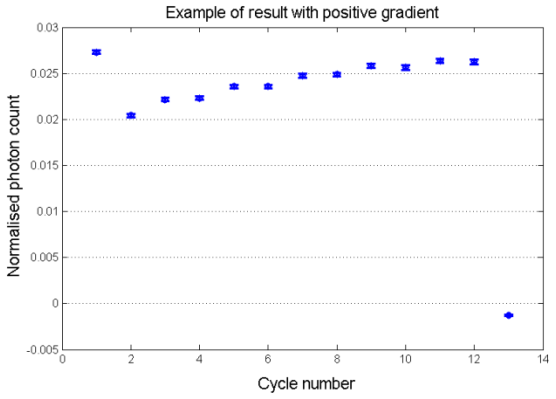

DD-TT-OSL signal of the Woakwine sample, using 260 °C preheat, 290 °C illuminated wash, OSL normalisation, 0.5 s signal, and end-of-OSL bg subtraction

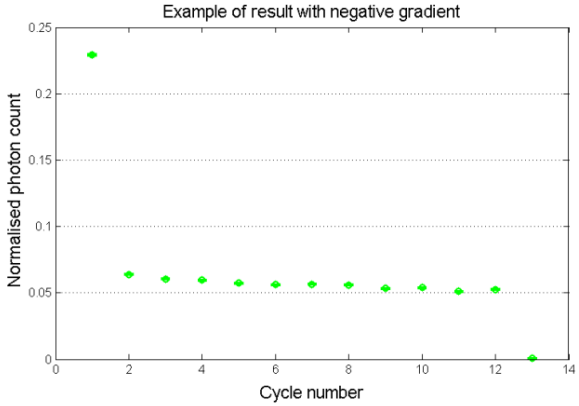

TT-OSL signal of the Naracoorte sample, using 260 °C preheat, 350 °C wash, OSL normalisation, 0.5 s of signal, and end-TT-OSL bg subtraction

Figure 10.1: Examples of A) 'good' results; B) scattered results; C) results with a positive trend; and D) results with a negative trend. A, B, and C are from DD-TT-OSL results, while D is from TT-OSL results.

Following the observations above, the protocol was changed to include blue diode stimulation with the 350 °C end-of-cycle trap resetting. Three further changes to the protocol were also made:

-OSL and TT-OSL stimulation for two minutes: previous protocols had OSL and TT-OSL stimulation times of one minute. Two minutes gives end-of-stimulation readings closer to a zero-gradient straight line, and so gives more accurate background subtractions for longer integrals, such as the 0.5 s TT-OSL integral.

-Randomising doses: the previous 5 mm aliquot results were done with doses in order of increasing size. This can give artificial dose dependence to growth curves if the normalising method does not work. The modified protocol uses a non-progressive dose for each cycle, and has the repeated dose just before the zero-dose cycle, to ensure that any un-normalised changes to the dose dependence during successive cycles is easily visible.

-Larger test doses: TT-OSL responses to test doses previously did not give good normalisation results, most likely due to the signals being too small to be resolved properly. The test dose was increased from around 8 Gy to around 18 Gy of β dose, to ensure the resolvability of the signal. This will mean that the sensitivity change in the sample due to the test dose will be larger, but that more accurate TT-OSL normalisation will be gained.

A comparison of the old protocol and the new one is shown in table 10.2.

Old Protocol Step	**New Protocol Step**
β dose (0 at natural)	β dose (0 at natural)
Preheat to 260°C (5 K/s; held for 10 s)	Preheat to 260°C (5 K/s; held for 10 s)
OSL stimulation 60 s Blue diodes at 90% power	OSL stimulation **120** s Blue diodes at 90% power
Preheat to 260°C (5 K/s; held for 10 s)	Preheat to 260°C (5 K/s; held for 10 s)
OSL stimulation 60 s Blue diodes at 90% power	OSL stimulation **120 s** Blue diodes at 90% power
Test dose (8.3 Gy β)	Test dose (**18.4** Gy β)
Preheat to 260°C (5 K/s; held for 10 s)	Preheat to 260°C (5 K/s; held for 10 s)
OSL stimulation 60 s Blue diodes at 90% power	OSL stimulation **120 s** Blue diodes at 90% power
Preheat to 260°C (5 K/s; held for 10 s)	Preheat to 260°C (5 K/s; held for 10 s)
OSL stimulation 60 s Blue diodes at 90% power	OSL stimulation **120 s** Blue diodes at 90% power
Preheat to 300°C (5 K/s; held for 10 s)	Preheat to 300°C (5 K/s; held for 10 s)
OSL stimulation 60 s Blue diodes at 90% power	OSL stimulation **120 s** Blue diodes at 90% power
Preheat to 260°C (5 K/s; held for 10 s)	Preheat to 260°C (5 K/s; held for 10 s)
OSL stimulation 60 s Blue diodes at 90% power	OSL stimulation **120 s** Blue diodes at 90% power
Test dose (8.3 Gy β)	Test dose (**18.4** Gy β)
Preheat to 260°C (5 K/s; held for 10 s)	Preheat to 260°C (5 K/s; held for 10 s)
OSL stimulation 60 s Blue diodes at 90% power	OSL stimulation **120 s** Blue diodes at 90% power
Preheat to 260°C (5 K/s; held for 10 s)	Preheat to 260°C (5 K/s; held for 10 s)
OSL stimulation 60 s Blue diodes at 90% power	OSL stimulation **120 s** Blue diodes at 90% power
Heat to 350°C for 200 s	Heat to 350°C for 200 s **with Blue diodes at 90% power**

Table 10.2: The old protocol and revised protocol. Pertinent changes are in bold.

11-IMPROVED RESULTS

After improving the protocol, eight 125-180 µm grain diameter 5mm aliquots each of the Naracoorte East, Harper, Baker, East Dairy and Woakwine samples were made, and run through the improved protocol presented at the end of Chapter 10 (table 10.2) with the dose per cycle given in table 11.1. Measurements were done on a Risø TL/OSL DA-20 with an evacuated chamber filled with nitrogen. A 7.5 mm HOYA U340 filter was interposed between the sample and the photomultiplier. An EMI 9235QB PMT was used for photon counting, and a Sr^{90}/Y^{90} β irradiation source with an approximate strength of 1.48 GBq (a dose rate for quartz of approximately 0.092 Gy/s) was used to irradiate samples. Much larger signals were seen than before, and near-TT-OSL background subtracted results and TT-OSL normalised results were able to be analysed. Analysis sets (of particular normalisation, background subtraction, and integral of signal used) were deemed successful if at least half of the aliquots gave a result. Results were found by taking the weighted mean of successful aliquots.

Cycle	Naracoorte East	Harper	Baker	East Dairy	Woakwine
2	376	84	167	84	75
3	63	167	42	42	50
4	1004	502	251	251	8
5	188	251	84	167	25
6	376	167	167	84	50
7	0	0	0	0	0
8	524	3095	335	125	276

Table 11.1: The dose (in Gy) used in each cycle of the TT-OSL SAR protocol for each sample. The first cycle is to measure the natural signal, and so no dose is given to the sample.

-Results-

TT-OSL normalisation appeared to give reasonable results, though for DD-TT-OSL and TT-OSL results they saturated very quickly (see Fig 11.1 for an example). Results were found for the Woakwine and East Dairy samples, but for other samples natural signals were at the saturation point of the signal-to-dose curve. TT-OSL normalisation gave DI-TT-OSL results for all samples but the Naracoorte East sample, which did not

have any successful DI-TT-OSL results for either normalisation method.

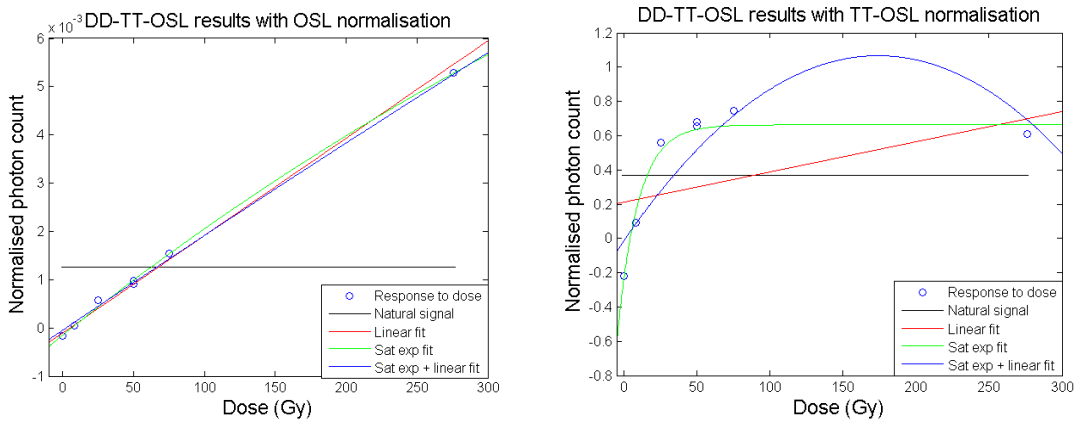

Figure 11.1: Examples of the growth curves of an aliquot using OSL and TT-OSL signals for normalisation. The aliquot results shown are from the Woakwine sample, and use 0.1 s of signal and end-of-TT-OSL background subtraction.

Near-TT-OSL background subtractions still did not have many successful aliquots when using the first 0.1 s of the signal. It was successful using DD-TT-OSL with the Woakwine and Naracoorte East samples, but not the others. In general, all results were less scattered than those from the initial results chapter (see Fig 11.2), and more data analysis methods were successful.

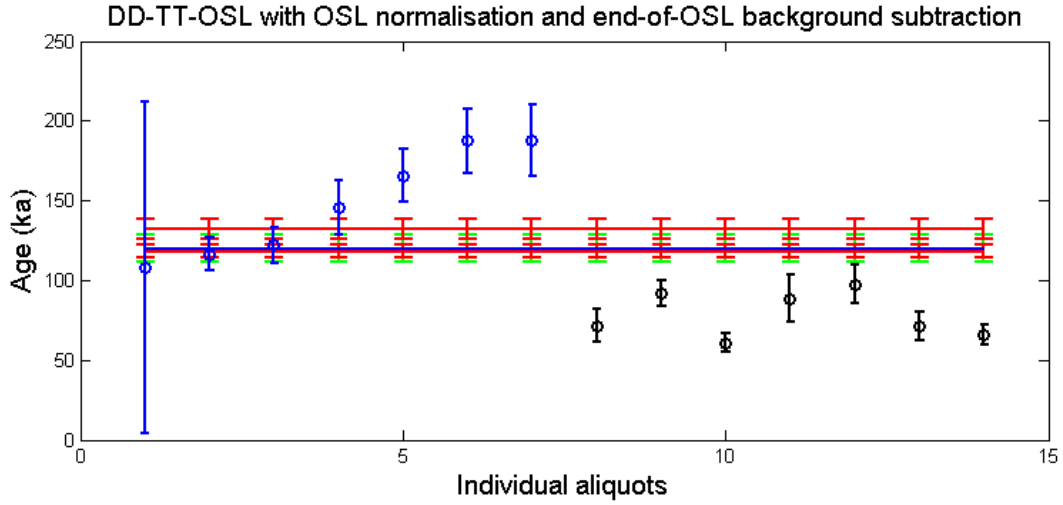

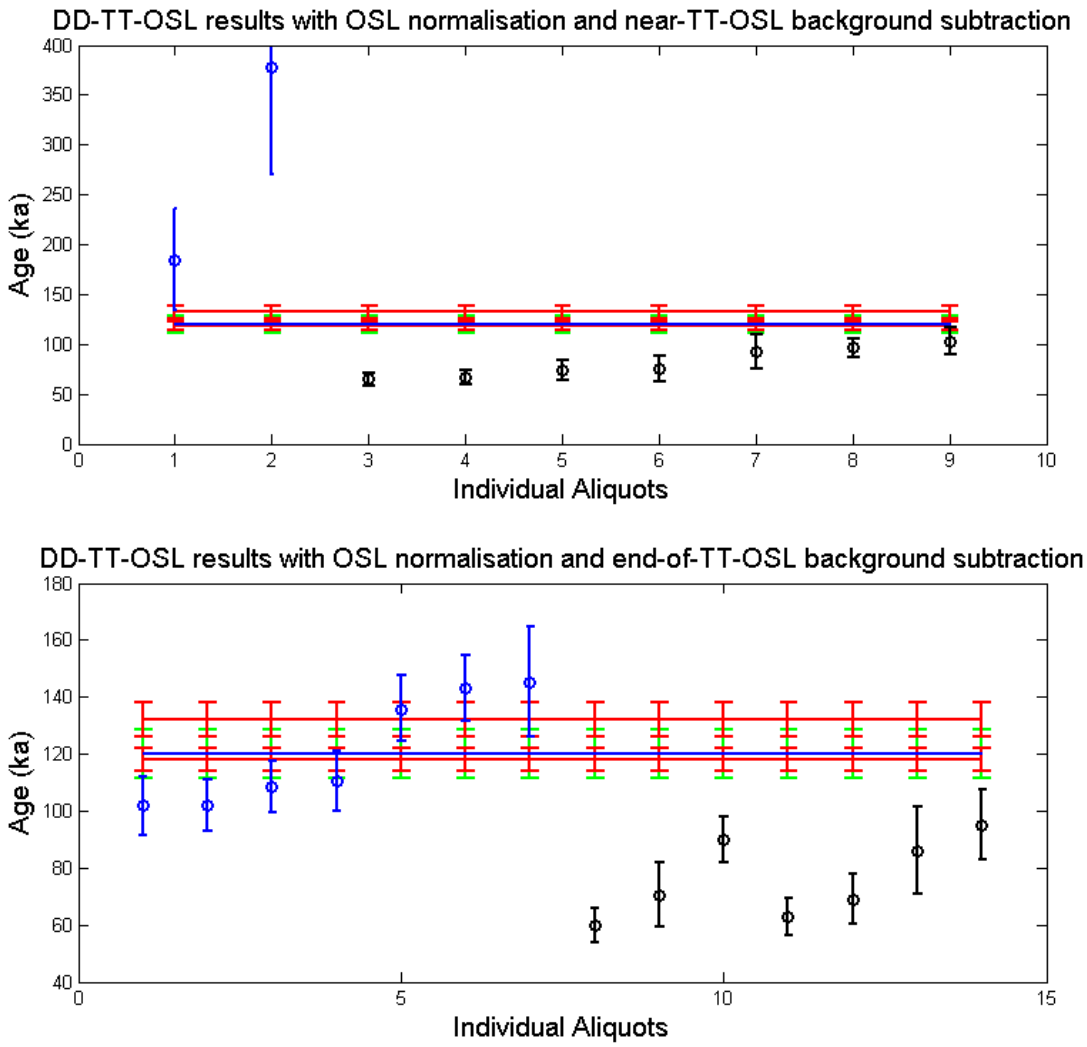

Figure 11.2: Example of the scatter of results. Shown are the DD-TT-OSL results of the Woakwine sample, using OSL normalisation and a) end-of-OSL; b) near-TT-OSL; and c) end-of-TT-OSL background subtraction. Blue data points are with 0.1 s of signal, and black data points are with 0.5 s of signal. Previously gained results are shown: in red, TL results; in green, OSL results; in blue, oxygen isotope results.

DD-TT-OSL					
		end-of-OSL background subtraction	**near-TT-OSL background subtraction**	**end-of-TT-OSL background subtraction**	**Expected range (ka)**
Naracoorte East	**OSL normalisation**				>780
	0.1 s	240±7	78±11	243±7	
	0.5 s	211±7	219±8	209±7	
Harper	**OSL normalisation**				580-650
	0.1 s	251±10		292±12	
	0.5 s	229±11	257±12	233±12	
Baker	**OSL normalisation**				450-500
	0.1 s	237±7		230±6	
	0.2 s	195±6	209±7	198±6	
East Dairy	**OSL normalisation**				200-300
	0.1	241±9		243±8	
	0.5	174±7	190±7	173±6	
	TT-OSL normalisation				
	0.1 s	77±8			
Woakwine	**OSL normalisation**				118-130
	0.1 s	138±6	220±46	115±4	
	0.5 s	72±3	76±4	71±3	
	TT-OSL normalisation				
	0.1 s	89±9		42±3	
	0.5 s	26±1	27±2	26±1	

Table 11.2: Results for DD-TT-OSL signals using various data analysis methods. All results are in ka.

DD-TT-OSL results, as seen in the table above, did not give accurate results for most samples, in the case of the Naracoorte East sample underestimating the minimum sample age by an average of 580 ka. For the East Dairy and Woakwine samples, OSL normalisation with 0.1 s of signal using end-of-OSL and end-of-TT-OSL background subtractions were in the range of previous results. However using OSL normalisation and 0.5 s of signal gave results that underestimated both sample ages by around 30 ka.

TT-OSL					
		end-of-OSL background subtraction	near-TT-OSL background subtraction	end-of-TT-OSL background subtraction	Expected range (ka)
Naracoorte East	OSL normalisation				>780
	0.1 s	288±8		277±8	
	0.5 s	248±8	254±9	245±8	
Harper	OSL normalisation				580-650
	0.1 s	347±12		358±13	
	0.5 s	298±13	323±14	299±13	
Baker	OSL normalisation				450-500
	0.1 s	280±6		274±7	
	0.5 s	223±7	238±7	226±7	
East Dairy	OSL normalisation				200-300
	0.1 s	282±6		274±7	
	0.5 s	214±5	228±5	226±7	
Woakwine	OSL normalisation				118-130
	0.1 s	161±6		137±4	
	0.5 s	91±4	93±4	88±4	
	TT-OSL normalisation				
	0.1 s	100±6		72±4	
	0.5 s	50±3	50±3	48	

Table 11.3: Results for TT-OSL signals using various data analysis methods. All results are in ka.

TT-OSL results are on average around 20 % larger than their DD-TT-OSL counterparts; however the Naracoorte East, Harper, and Baker results still underestimate the results by hundreds of ka. All East Dairy results lie within the expected range, though that range is broad (see table 11.3). Woakwine results either lie under or over the expected range. Two results come close to the expected range: Using OSL normalisation, end-of-TT-OSL background subtraction, and 0.1 s of signal; and using TT-OSL normalisation, end-of-OSL background subtraction, and 0.1 s of signal.

DI-TT-OSL					
		end-of-OSL background subtraction	**near-TT-OSL background subtraction**	**end-of-TT-OSL background subtraction**	**Expected range (ka)**
Harper	**OSL normalisation**				580-650
	0.1 s	582±22		562±23	
	0.5 s	488±19	506±20	490±19	
	TT-OSL normalisation				
	0.5 s	298±13	296±16		
Baker	**OSL normalisation**				450-500
	0.1 s	158±9		355±9	
	0.5 s	306±7	315±8	306±7	
	TT-OSL normalisation				
	0.1 s	321±20			
	0.5 s	359±14		369±14	
East Dairy	**OSL normalisation**				200-300
	0.1 s	396±9		393±10	
	0.5 s	319±7	340±7	322±7	
	TT-OSL normalisation				
	0.1 s	283±13		320±13	
	0.5 s	267±6	279±8	273±6	
Woakwine	**OSL normalisation**				118-130
	0.1 s	192±7	309±40	192±7	
	0.5 s	166±6	170±6	166±6	
	TT-OSL normalisation				
	0.1 s	95±12		142±8	
	0.5 s	138±5	147±6	143±5	

Table 11.4: Results for DI-TT-OSL signals using various data analysis methods. All results are in ka.

Compared with TT-OSL and DD-TT-OSL results, TT-OSL normalisation was more sucessful for DI-TT-OSL results (see table 11.4), with results gained up to the Harper sample. Woakwine and East Dairy results using TT-OSL normalisation and end-of-OSL background subtractions were within the expected age ranges, but were overestimated using OSL

normalisation by 96 and 19 ka for East Dairy, and 62 and 36 ka for Woakwine, for 0.1 s and 0.5 s results respectively.

In contrast, most Baker and Harper results underestimated the age, albeit by 300 ka less than DD-TT-OSL results for Harper, and 100 ka less for the Baker sample. Two data analysis combinations (OSL normalisation, end-of-OSL and end-of-TT-OSL background subtractions, 0.1 s of signal) gave ages within errors in the expected range for the Harper sample, though as no other sample gave equally good results for these data analysis combinations, the result cannot be said to be useful or indicative of a trend. No results for the Naracoorte East sample were gained, due to the saturation of the dose response curve.

-Conclusions-

For younger samples, DD-TT-OSL signals appear to give the best approximation for the age, when using 0.1 s of signal and a background subtraction that maximises the amount of signal used. Results for older samples appear to remain between 200 and 300 ka, though the samples are much older. For the same data analysis methods TT-OSL signals give slightly higher results, in general around 30 ka higher. DI-TT-OSL results are much more scattered, but ages increase beyond the apparent limits of DD-TT-OSL and TT-OSL. DI-TT-OSL results, however, in general do not match previously gained results for the age of the samples.

Of the three signals used (DD-TT-OSL, TT-OSL, and DI-TT-OSL), DD-TT-OSL signals gave results that most closely matched previously calculated ages for the younger samples. The fact that older samples give the same age results—i.e., that the method appears to "plateau" at approximately 200-250 ka, suggest that DD-TT-OSL signals may not be able to be used for "long-range" dating. The asymptotic effect could be age-related rather than related to the trap population saturating, as the three oldest samples have different background radiation dose rates. From the results it is unclear whether the East Dairy sample, which has an expected age at the range the others asymptote at, gives good results

due to chance or not. These results, therefore, only indicate that one can acquire DD-TT-OSL results in the expected range for samples not above 120 ka. DD-TT-OSL signals, however, still saturate at much larger doses than does OSL (note the linear nature of the OSL normalised dose recovery curve in Figure 11.1, up to 300 Gy). TT-OSL dating may, therefore, be useful for dating young sites with very high natural dose rates, and so, while not very old, the quartz in the sample has already reached saturation. This probability was investigated in later chapters in two ways: (1) dating of a palaeontological (megafaunal) site where conventional OSL signals were saturated, and (2) A kinetic analysis of the TT-OSL signal. It should be noted that as the SESA samples all have the same general history and origin, the TT-OSL behaviour of these samples may not necessarily be general quartz TT-OSL behaviour, and other samples may behave differently.

12-Baldina Creek

While most sites with saturated natural OSL signals are quite old, others saturate due to high natural dose rates. Baldina Creek is one such site, with a natural dose rate of approximately 2.5 Gy/ka. One sediment layer is thought to be within 40-100 ka old, due to the presence of remains of certain megafauna. Electron-spin resonance (ESR) dating has previously dated diprotodon teeth in the area to around 50-70 ka in age (Grün et al, 2008). Due to its high dose rate and low age, this layer is useful for testing TT-OSL's usefulness in dating young samples that display saturated OSL signals.

The Baldina Creek megafaunal layer was sampled in late 2012. The layer is defined by fine red silt and clay containing megafaunal remains. The sample was taken to the right of a washout revealing "Diprotodon opatum" remains in situ (see fig 12.1). Gamma spectrometry measurements were taken for one hour using a portable NaI gamma-ray spectrometer. The average depth of the sample site is thought to be two metres.

Figure 12.1: The Baldina Creek sampling site. To the right of the tools is the sample in the process of being collected; to the left is a washout exposing megafaunal remains.

The sample was prepared as described for the SESA samples in the 'Sample' chapter of this thesis. Thirty seven 5 mm aliquots of 125-180 µm grains were prepared and tested using the protocol shown in the 'Improved results' chapter, with the doses given in table 12.1. Doses given each cycle are shown in the table below.

Cycle	Dose (Gy)
1	Natural (0)
2	167
3	251
4	502
5	335
6	167
7	0
8	84

Table 12.1: Doses given to each aliquot in each cycle of the TT-OSL SAR protocol.

-Dosimetry-

The dose rate for the Baldina Creek sample was calculated in the same way as the SESA samples. Uranium, thorium, and potassium levels were found using a one-hour in situ gamma spectrometry measurement, subsequently analysed by "Minty Geophysics", and by XRF soil analysis by "Genalysis Pty Ltd". While the two methods roughly agreed with each other, they did not agree within errors (see 12.2), and so each were used to create a separate result for the dose rate. The dose rate was calculated using the J. R. Prescott and J. T. Hutton Cosmic Ray spreadsheet, and by the AGE program by R Grün. The dose rate using the gamma spectrometry measurements was 2.94 ± 0.11 Gy/ka, while the dose rate using the Genalysis soil analysis was 3.48 ± 0.14 Gy/ka. This difference in dose rate using different methods may be due to a disequilibrium of parent to daughter isotopes, due to a wet period of the sample's life allowing soluble daughter isotopes to be removed from the surrounding sediment. A way to allow for this difference in soil analysis is to use the gamma spectrometry measurements for the gamma radiation part of the dose rate calculation, and the soil analysis measurements for the alpha and beta part of the dose rate calculation. This gives a dose rate of 3.29 ± 0.084 Gy/ka.

	Uranium (ppm)	Thorium (ppm)	Potassium (%)
Gamma Spectrometry	1.77±0.06	10.18±0.14	1.90±0.01
Genalysis soil analysis (ICPMS)	2.24±0.14	12.77±0.74	2.37±0.09

Table 12.2: Uranium, Thorium and Potassium results from gamma spectrometry measurements and soil analysis.

-Results-

All results using TT-OSL normalisation were saturated. Initial results were found using three different methods of data analysis, previously found to give expected results for a sample of similar age:

1) DD-TT-OSL results with end-of-OSL background subtractions using the first 0.1 s of signal,

2) DD-TT-OSL results with end-of-TT-OSL background subtractions using the first 0.1 s of signal,

3) TT-OSL results with end-of-TT-OSL background subtractions using the first 0.1 s of signal.

These data analysis methods were chosen as they gave reasonable results for the Woakwine SESA sample, the closest well-dated SESA sample in age to the expected age of the Baldina Creek sample. This would mean that age-related discrepancies in Baldina Creek results would probably be similar to those of the Woakwine sample. Other problems associated with TT-OSL are saturation and resolvability issues. Both the Woakwine and Baldina Creek samples have bright signals, and so the signals can be resolved from the backgrounds in both cases. The Baldina Creek samples appear saturated when using TT-OSL normalisation, whereas the Woakwine sample does not in all cases. Other discrepancies that are sample specific cannot be compared between SESA and Baldina Creek samples, due to their different history, origins and locations.

Aliquot results were ordered and graphed for all three data analysis methods. Results in order looked for the most part like a straight line, with curved drops at the start and end. A straight line was drawn from the median point, and weighted means were found using all data points that fell on the

straight line section within errors, unless there was a discontinuity in the line of data points.

The weighted means of the three data analysis methods were 289 ± 4 Gy, 268 ± 3 Gy, and 272 ± 3 Gy respectively. Graphs of the aliquot results and the results used are shown in figure 12.2 below.

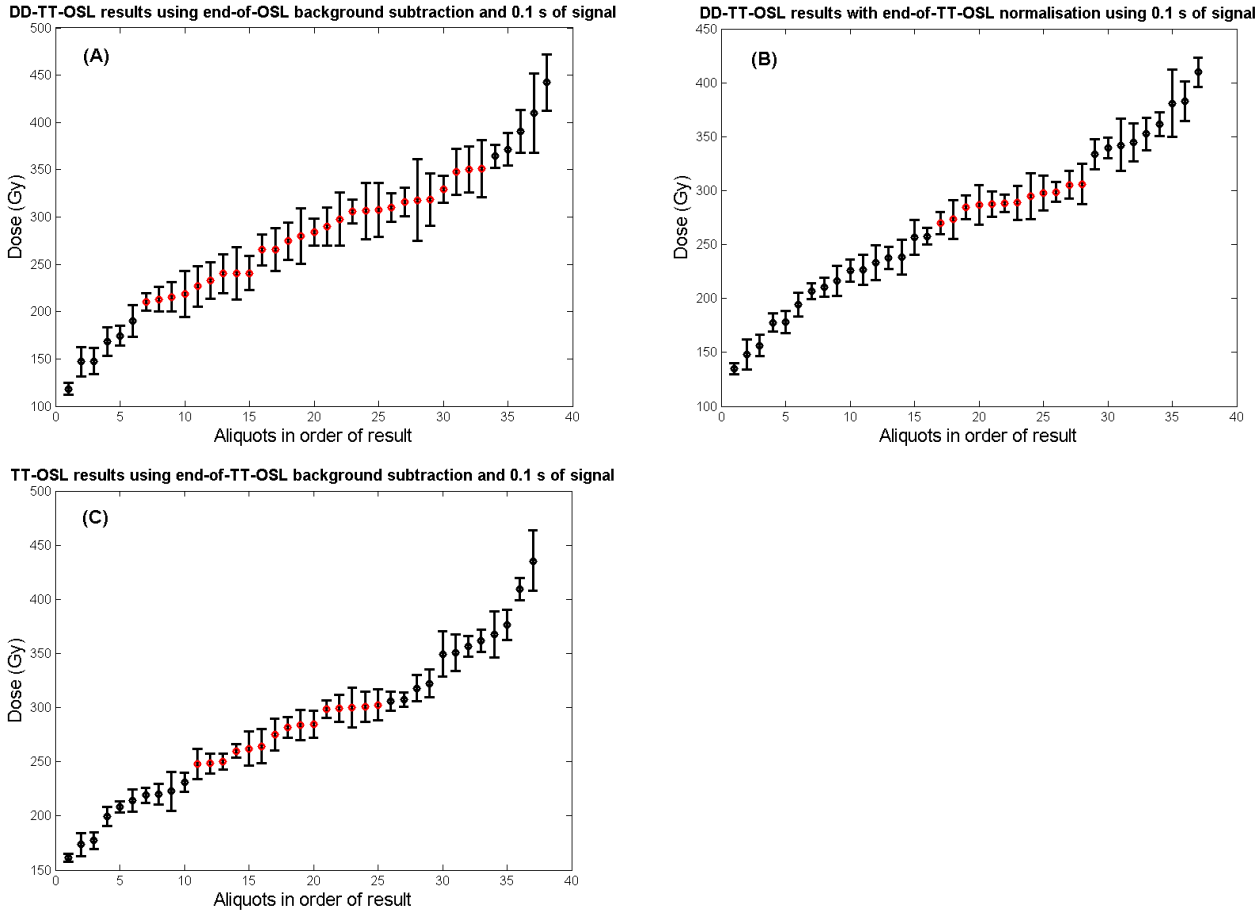

Figure 12.2: the results for each aliquot using A) DD-TT-OSL results with end-of-OSL background subtractions; B) DD-TT-OSL results with end-of-TT-OSL background subtractions; and C) TT-OSL results with end-of-TT-OSL background subtractions. All three used OSL normalisation and the first 0.1 s of signal. Results used in weighted mean calculations are highlighted in red.

Histograms were made of all DD-TT-OSL and TT-OSL results using OSL normalisation, and the peak values recorded. The main peak appeared around 250 Gy. In some results, there appears to be two or three peaks, but this may be due to the small amount of aliquots appearing in each bin. When only five bins are used, the histogram results approximate a Gaussian (see fig 12.3). Using weighted fitting (where the weights are the reciprocal of the number of aliquots in the bin), the 5-bin results for the three methods of data analysis used in the above section were fitted to a Gaussian using the Matlab curve fitting toolbox. The peak of the Gaussians gave the following results: 268 Gy (for DD-TT-OSL results using end-of-OSL background subtraction); 264 Gy (for DD-TT-OSL results using end-of-TT-OSL background subtraction); and 275.2 Gy (for TT-OSL results using end-of-TT-OSL background subtraction).

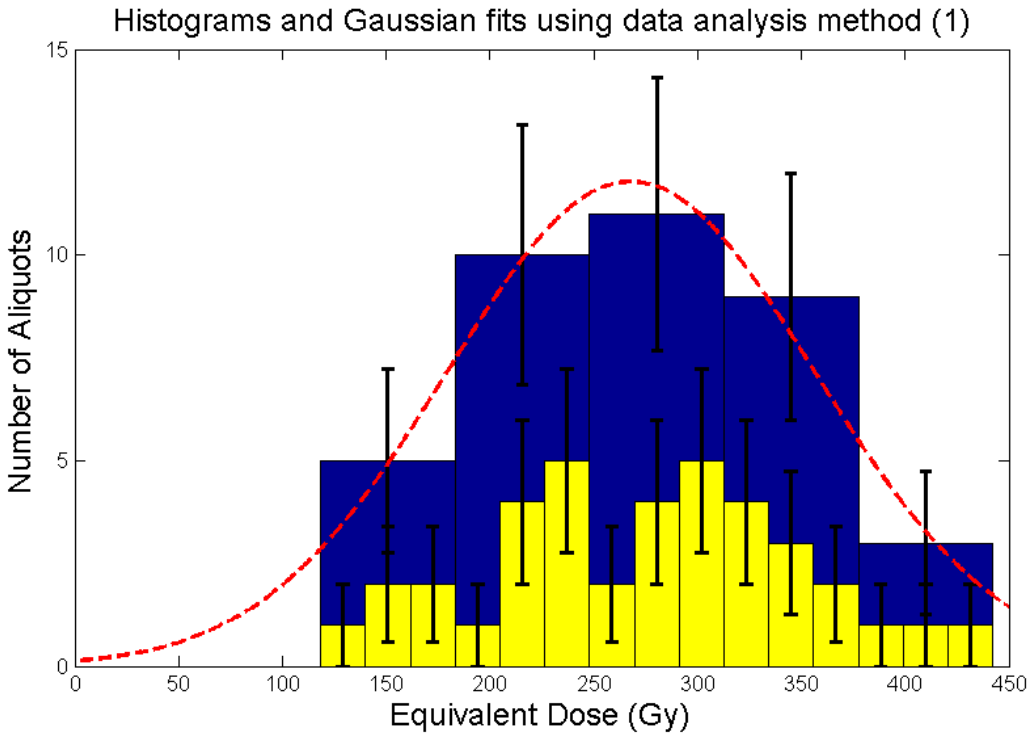

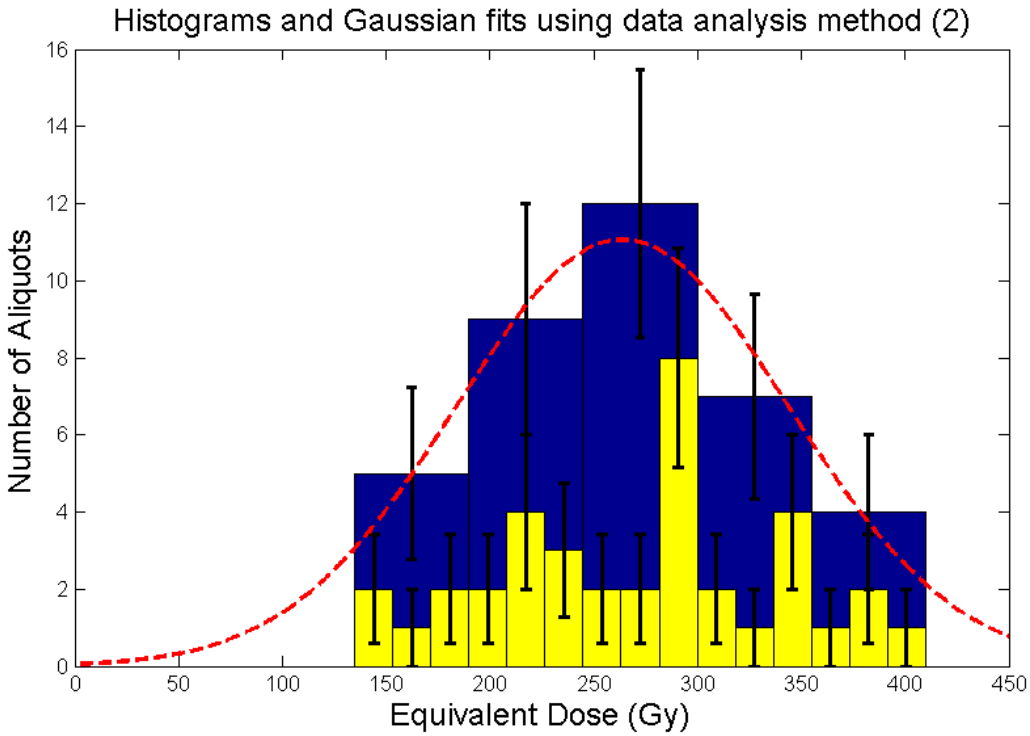

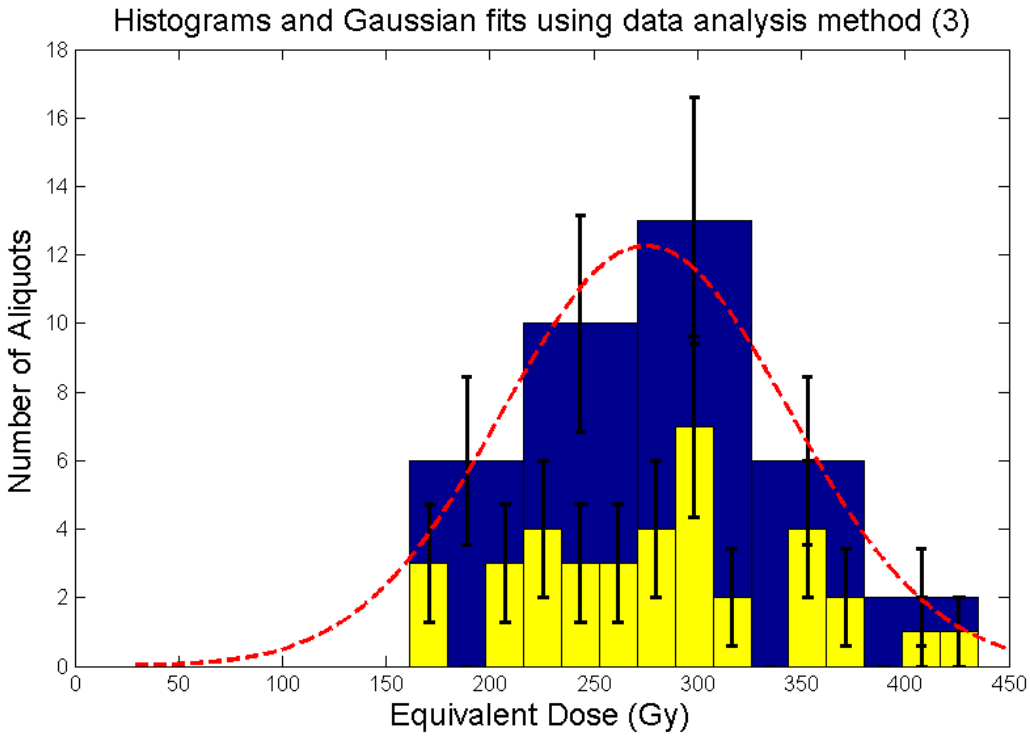

Figure 12.3: Histograms of the three data analysis methods as described on page 145. Yellow histograms divide the data into 15 bins, the first bin at the lowest result and the last bin at the highest. Blue histograms divide the data into five

bins. The red dashed line shows a Gaussian fitted to the 5-bin results.

As the Baldina Creek samples were done on a machine that had its instrumental error calculated (see Chapter 5, section 2), unlike for the Woakwine small aliquots in chapter eight, it is appropriate to use analysis that depends heavily on the calculated error. The R. Galbraith program "cdose-prf.s" was used. This program uses the "central age model" (Galbraith et al, 1999), which calculates the central peak in a distribution of discrete results, taking into account their errors. A dispersion value of 5 % (how far the peaks are off a Gaussian distribution) was used. Results are shown below in table 12.3.

Data Analysis methods	Peak value (Gy)	Error (Gy)
DD-TT-OSL 0.1 s signal end-of-OSL bg subtraction	265	75
DD-TT-OSL 0.1 s signal end-of-TT-OSL bg subtraction	262	68
TT-OSL 0.1 s signal end-of-TT-OSL bg subtraction	275	62

Table 12.3: Peak values gained using the "cdose-prf.s" program by R. Galbraith.

To test whether there was more than one peak in the distribution of results, the R. Galbraith "fmix.s" program was used. This program uses a "finite mixture model" (Galbraith and Laslett, 1993), and identifies and calculates where a given number of peaks is likely to occur in a distribution, for a given dispersion value. The program also gives a relative likelihood of the number of peaks chosen being accurate for the distribution. For a dispersion value of 5 %, four peaks was the most likely result. For a dispersion of 15 %, the two DD-TT-OSL data analysis methods gave 2 peaks as the most likely result, while the TT-OSL data analysis method gave a likely result of 3 peaks. A dispersion of 25-30 % gave the most likely result as one peak. This indicates that the 37 aliquots used do not give a sharp peak, and a greater number of aliquots would be needed to give a highly defined result. While 5 % dispersion rates give a result of four peaks, each peak would have an average of 9 aliquots attributed to it, which is not enough to discount

counting errors as the source of variability in the distribution.

As seen for the Woakwine results, the DD-TT-OSL results using end-of-TT-OSL background subtraction gives the smallest of the three results for Baldina Creek, and as this data analysis method also gave the closest result to the expected age in the Woakwine results, it was chosen for the Baldina Creek result, giving 262 ± 68 Gy for the equivalent dose. Using the combined gamma spectrometry and soil analysis dose rate results, this gives an age of 80 ± 21 ka for the sediment unit in which the Diprotodon Opatum was discovered. This result is considered by the palaeontologists to be in very good accord with expectation, which spanned approximately 40-110 ka, and agrees within errors with the ESR dating ages by Grün et al (2006).

13-KINETICS OF THE TT-OSL SIGNAL

KINETIC MEASUREMENTS OF THE TT-OSL SIGNAL

Obtaining kinetic measurements for TT-OSL signals can be difficult, as the signal is only measured indirectly. A number of different methods have been previously used. Li and Li (2006) used isothermal studies and pulsed annealing tests to study the kinetics of different thermally transferred signals. They identified one signal thermally transferred at temperatures between 260 and 320 °C, and another thermally transferred at temperatures higher than 500 °C. The signal transferred at lower temperatures was found to have an E value of 1.14 ± 0.05 eV, and an s value of 1.6 ± 2.4 $*10^{6}$ s^{-1}, giving a lifetime of 0.76 Ma at 20 °C. This would indicate that this signal will underestimate old samples. It should be noted that s values for quartz tend to be between 10^{12} to 10^{13} s^{-1} (McKeever, 1985), and so an s value of the order of 10^{6} is physically unlikely. Similarly, 1.14 eV is an unusually shallow trap to require 260 °C for thermal drainage.

Adamiec et al (2008) studied the kinetics of the thermally transferred signal used in TT-OSL dating protocols (the signal transferred from heating to 260 °C for 10 s). This was done by comparing TT-OSL and TL depletion and growth curves. Adamiec et al concluded that the TT-OSL signal is transferred from a trap not related to the 325 °C peak, but that had a similar thermal stability.

Adamiec et al (2010) studied the kinetics of the thermally transferred signal from a 260 °C preheat for 10 s by looking at the depletion of TL signals after successive TT-OSL measurements. Kinetic measurements were made of the depleted TL signal by measuring the TL signals at different heating rates and using Hoogenstraaten's method. The lifetime at 10 °C gained for the DD-TT-OSL signal was 4.5 Ma, and the lifetime of the DI-TT-OSL signal 48000 Ma. This would mean that for older samples, the TT-OSL signal would give an underestimation of the age, but the DI-TT-OSL signal would not (although it may have disadvantages for dating of its own, including slow optical decay rates, hence doubt about effective resetting by sunlight).

An experiment to observe the depletion of TT-OSL signal gained from a 260 °C preheat was devised. A 26-cycle SAR

protocol was used, with an approximately 73.6 Gy β dose administered each cycle (see table 13.1). The preheat before the OSL depletion stimulation was varied from 150 to 400 °C (see table 13.2). Results were analysed using the end-of-TT-OSL background subtraction. Results for TT-OSL and OSL normalisation, and 0.1 s and 0.5 s initial integrals were determined. Three 5 mm aliquots of 180-212 µm grains were used, one each of the Robe, Woakwine, and Naracoorte samples.

Protocol Steps
73.6 Gy β dose
Preheat to varying temperatures at 5 K/s for 10 s.
OSL stimulation at 125 °C: blue diodes at 90% for 120 s
Preheat to 260 °C, 5 K/s, 10 s
OSL stimulation at 125 °C: blue diodes at 90% for 120 s
Test dose (approx. 13.8 Gy β dose)
Preheat to 260 °C, 5 K/s, 10 s
OSL stimulation at 125 °C: blue diodes at 90% for 120 s
Preheat to 260 °C, 5 K/s, 10 s
OSL stimulation at 125 °C: blue diodes at 90% for 120 s
Preheat to 300 °C, 5 K/s, 10 s
OSL stimulation at 125 °C: blue diodes at 90% for 120 s
Preheat to 260 °C, 5 K/s, 10 s
OSL stimulation at 125 °C: blue diodes at 90% for 120 s
Test dose (approx. 13.8 Gy β dose)
Preheat to 260 °C, 5 K/s, 10 s
OSL stimulation at 125 °C: blue diodes at 90% for 120 s
Preheat to 260 °C, 5 K/s, 10 s
OSL stimulation at 125 °C: blue diodes at 90% for 120 s
Heat to 350 °C for 200 s with blue diodes at 90% power

Table 13.1: Protocol used for kinetics testing

OSL Preheats (in °C)
150
175
200
225
250
275
300
325
350
375
400
250
275
200
210
220
230
240
250
260
270
280
290
300
310
320

Table 13.2: Preheats used in above protocol, in order of use.

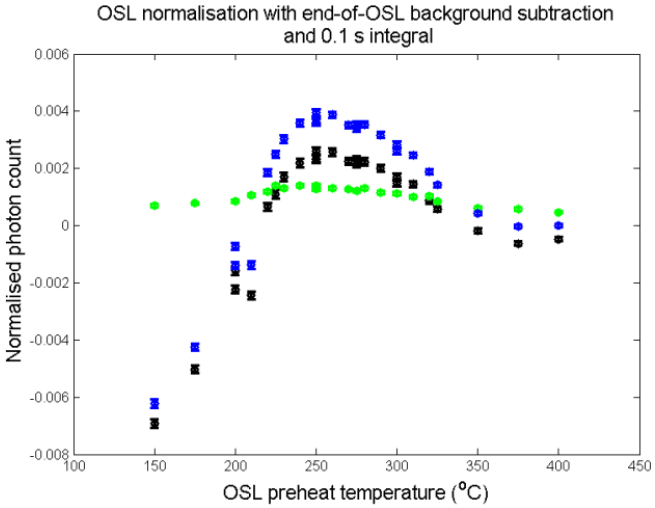
OSL normalisation with end-of-OSL background subtraction
and 0.1 s integral
Normalised photon count
OSL preheat temperature (°C)

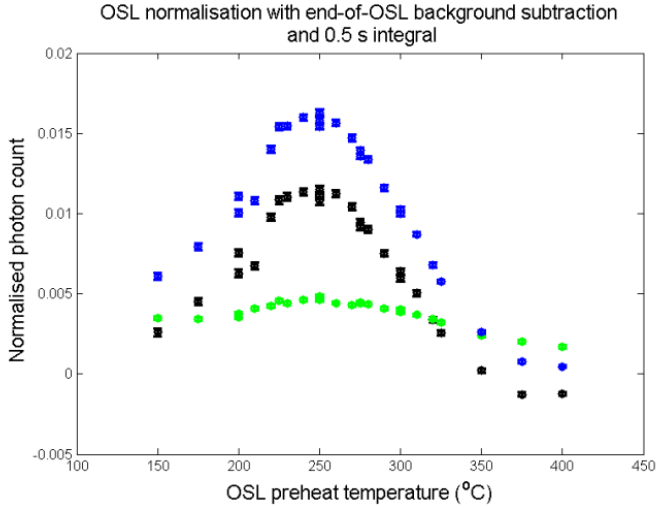
OSL normalisation with end-of-OSL background subtraction
and 0.5 s integral
Normalised photon count
OSL preheat temperature (°C)

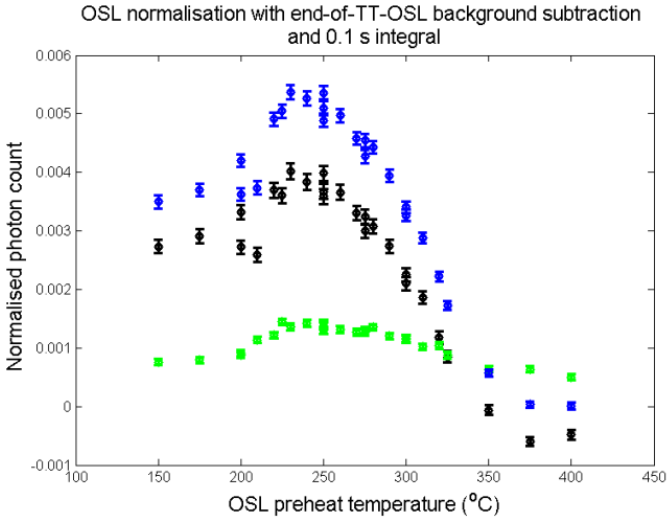
OSL normalisation with end-of-TT-OSL background subtraction
and 0.1 s integral
Normalised photon count
OSL preheat temperature (°C)

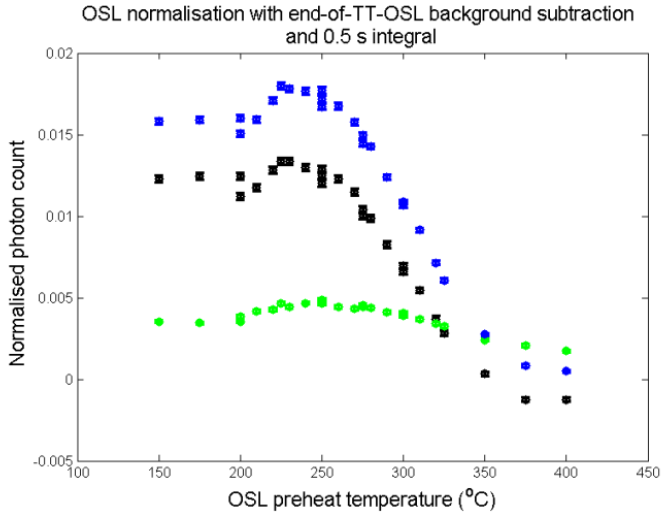
OSL normalisation with end-of-TT-OSL background subtraction
and 0.5 s integral
Normalised photon count
OSL preheat temperature (°C)

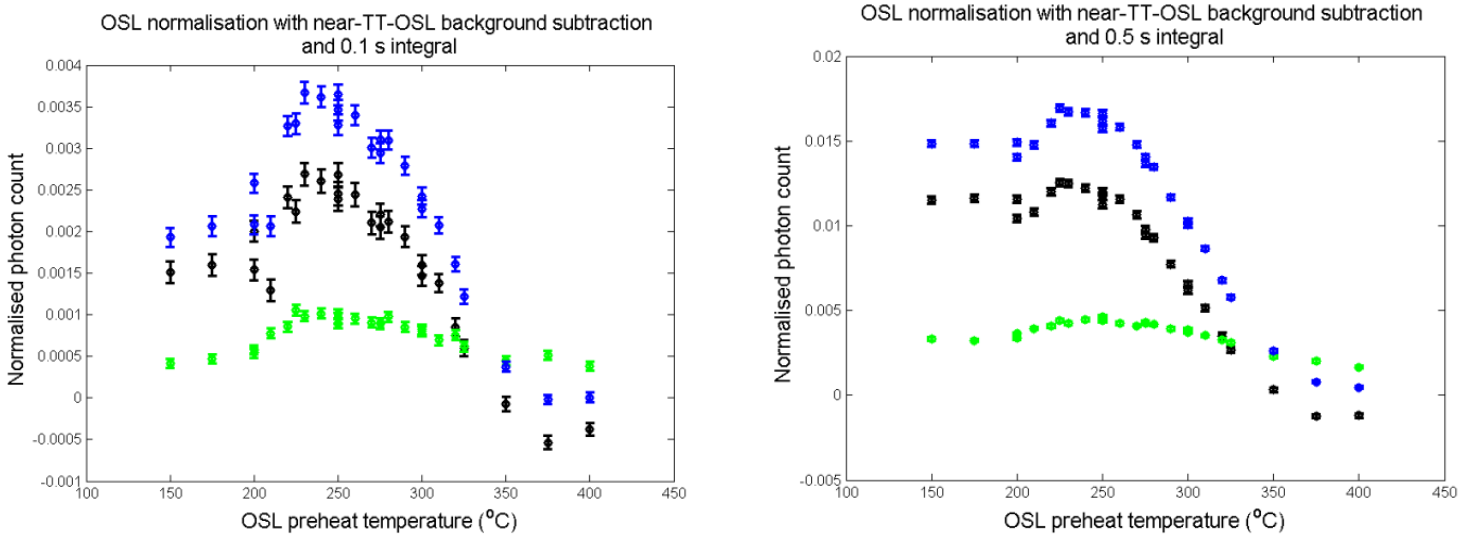

Figure 13.1: Decay vs OSL preheat results for the Robe aliquot, using OSL normalisation and various background subtractions. Black data points: DD-TT-OSL; blue data points: TT-OSL; green data points: DI-TT-OSL.

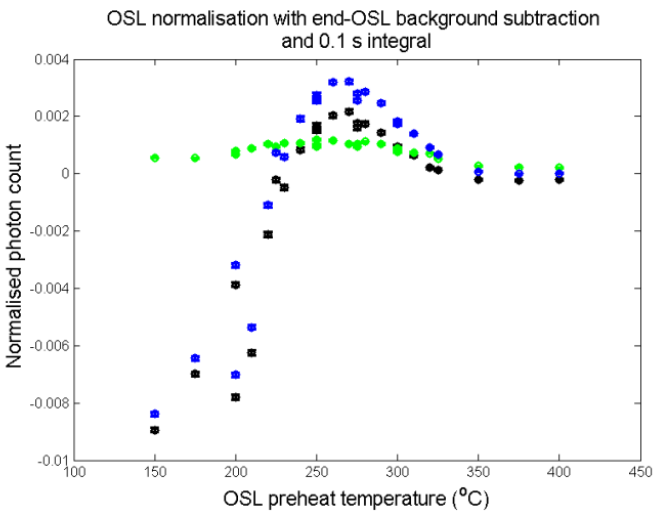
OSL normalisation with end-OSL background subtraction
and 0.1 s integral
Normalised photon count
OSL preheat temperature (°C)

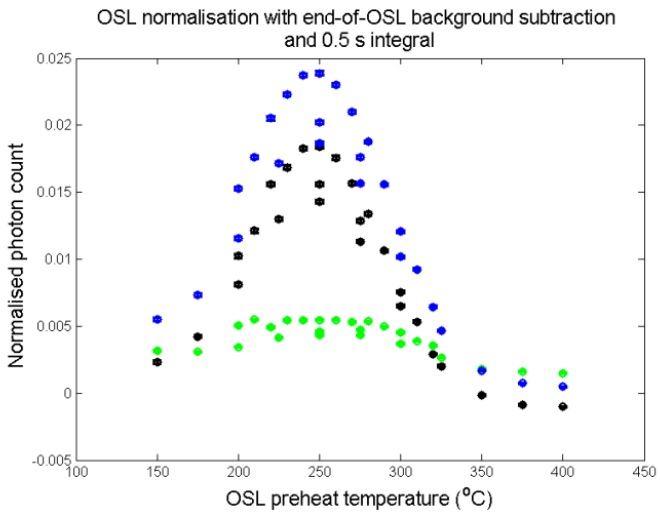
OSL normalisation with end-of-OSL background subtraction
and 0.5 s integral
Normalised photon count
OSL preheat temperature (°C)

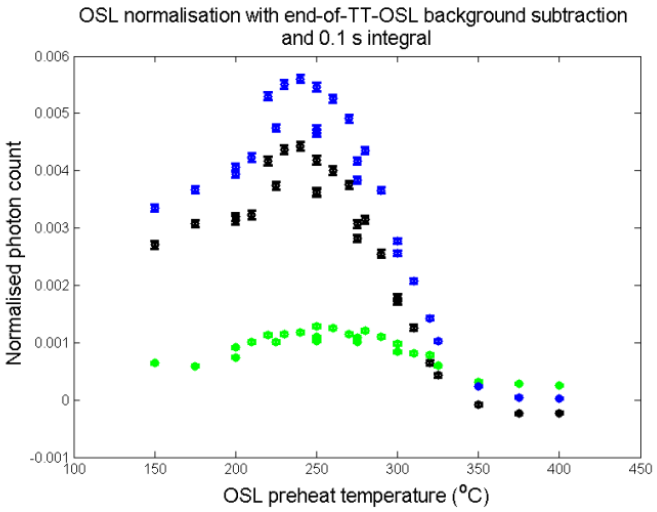
OSL normalisation with end-of-TT-OSL background subtraction
and 0.1 s integral
Normalised photon count
OSL preheat temperature (°C)

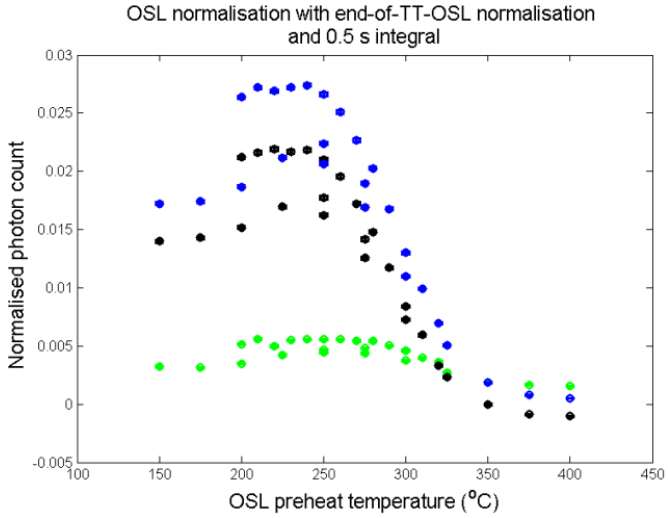
OSL normalisation with end-of-TT-OSL normalisation
and 0.5 s integral
Normalised photon count
OSL preheat temperature (°C)

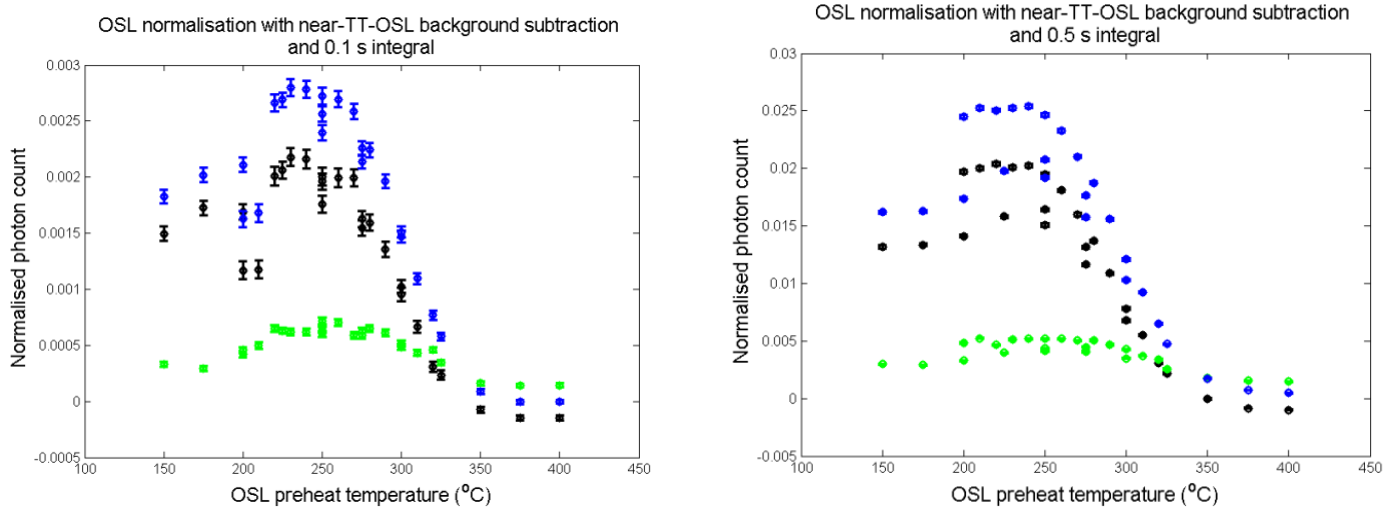

Figure 13.2: Decay vs OSL preheat results for the Woakwine aliquot, using OSL normalisation and various background subtractions. Black data points: DD-TT-OSL; blue data points: TT-OSL; green data points: DI-TT-OSL.

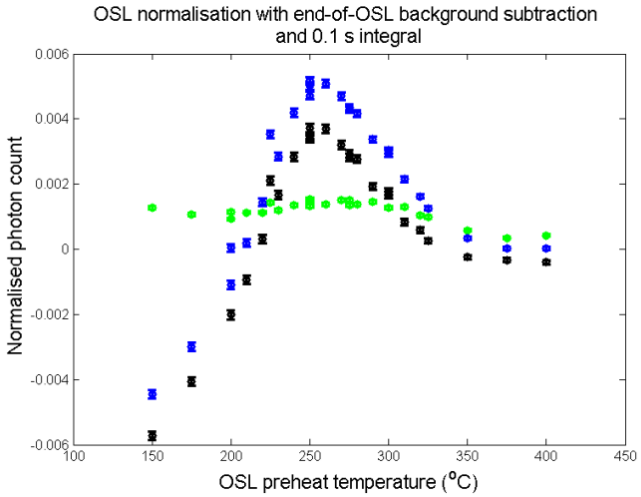
OSL normalisation with end-of-OSL background subtraction
and 0.1 s integral
Normalised photon count
OSL preheat temperature (°C)

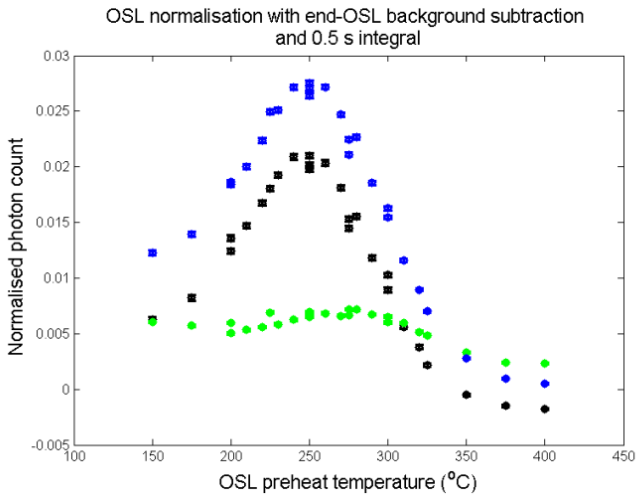
OSL normalisation with end-OSL background subtraction
and 0.5 s integral
Normalised photon count
OSL preheat temperature (°C)

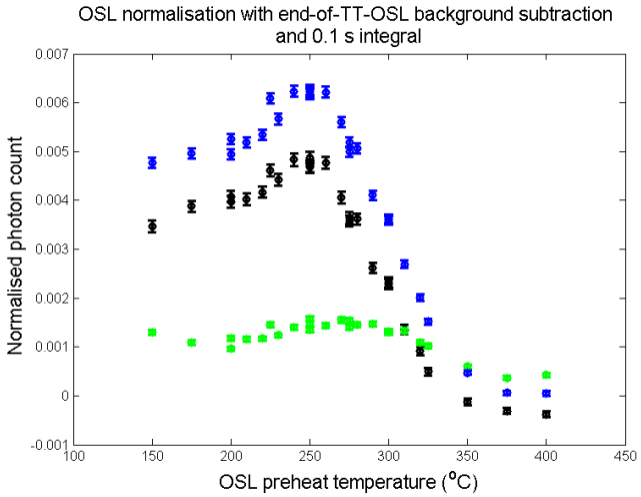
OSL normalisation with end-of-TT-OSL background subtraction
and 0.1 s integral
Normalised photon count
OSL preheat temperature (°C)

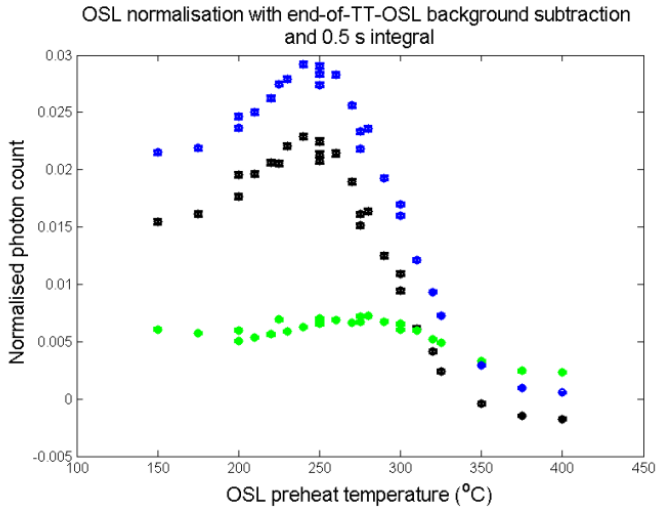
OSL normalisation with end-of-TT-OSL background subtraction
and 0.5 s integral
Normalised photon count
OSL preheat temperature (°C)

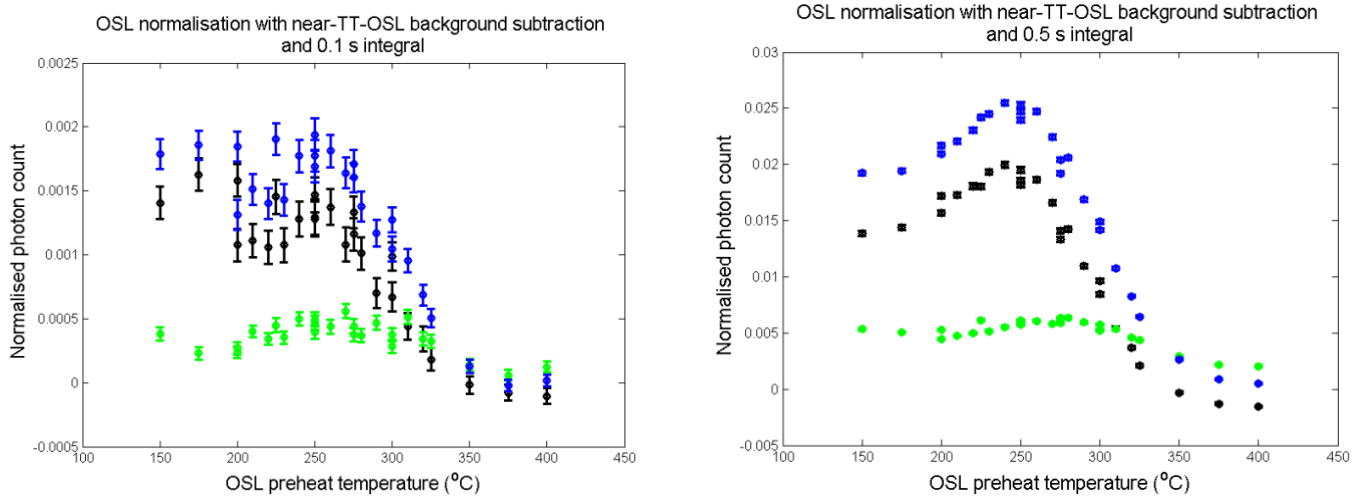

Figure 13.3: Decay vs OSL preheat results for the Naracoorte East aliquot, using OSL normalisation and various background subtractions. Black data points: DD-TT-OSL; blue data points: TT-OSL; green data points: DI-TT-OSL.

-Results-

Using OSL normalisation, the TT-OSL and DD-TT-OSL results are distinguished by measurements that are flat or slowly rising until 200 °C, then a sharp rise to a plateau at 225 °C, and a decay at 260 °C. Results reach a zero value between 350 and 375 °C. DI-TT-OSL results do not reach zero, but have a rise to a plateau at 225 °C and a fall to initial levels from 300 °C (see figs 13.1-13.3).

One cannot use end-of-OSL background subtractions in this method of kinetic study before the OSL preheat and TT-OSL preheat reach the same temperature, as there will be shallow traps present in the OSL signal as slow components, which will increase the OSL background. As expected, for OSL normalisation the end-of-OSL background subtraction creates an increasing result with temperature to 260 °C. After 260 °C, the result drops with respect to temperature, reaching a zero level at 350 °C while using the first 0.1 s of signal, and 375 °C using the first 0.5 s. Using the near-TT-OSL background subtraction using OSL normalisation gives results wherein a negative gradient is formed at 250-260 °C, with a zero value at 350-375 °C. Results using the end-of-TT-OSL background subtraction rise at around 220 °C, and fall to zero between 350 °C and 375 °C.

The Woakwine aliquot did not initially have the rise-and-fall TT-OSL and DD-TT-OSL characteristics between 225 and 260 °C, but this phenomenon was gained during repeat measurements further in the cycle. This could be an unexplained experimental artefact. However, if it is an effect from the sample and not the instrumentation, it indicates that what causes this rise-and-fall is not necessarily present in all aliquots of a sample, and can be caused by repeated measurements, indicating it is a sensitivity effect.

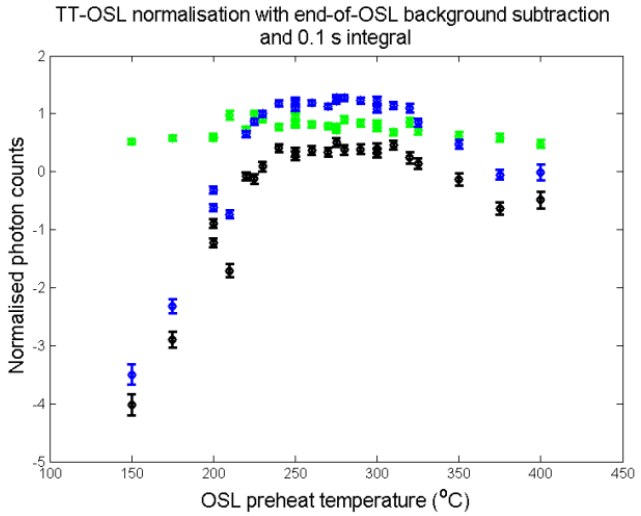
TT-OSL normalisation with end-of-OSL background subtraction and 0.1 s integral
Normalised photon counts
OSL preheat temperature (°C)

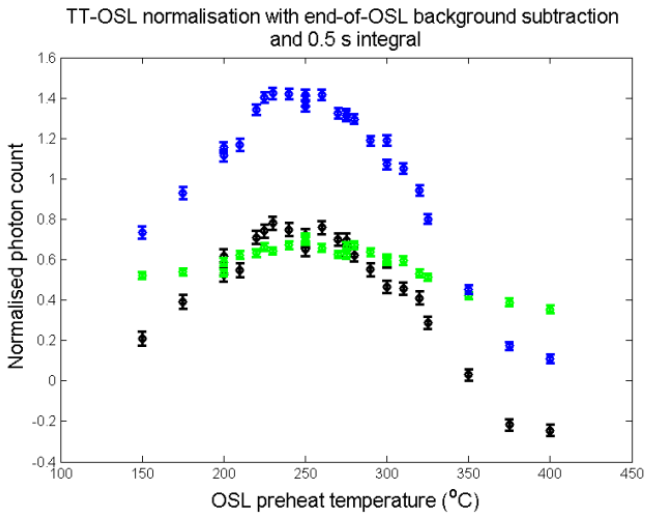
TT-OSL normalisation with end-of-OSL background subtraction and 0.5 s integral
Normalised photon count
OSL preheat temperature (°C)

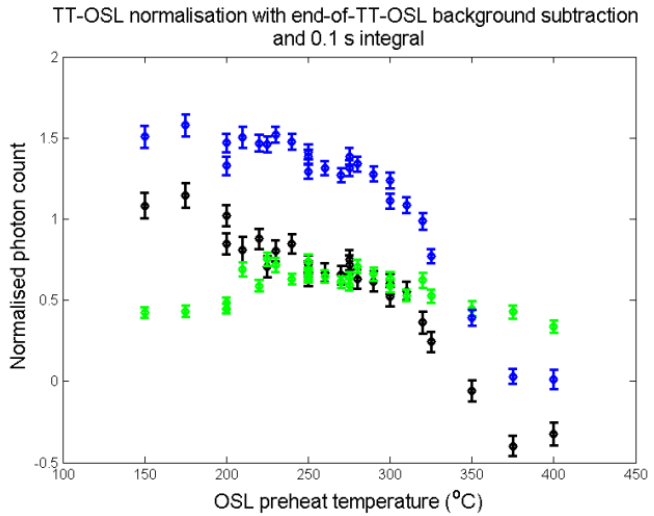
TT-OSL normalisation with end-of-TT-OSL background subtraction and 0.1 s integral
Normalised photon count
OSL preheat temperature (°C)

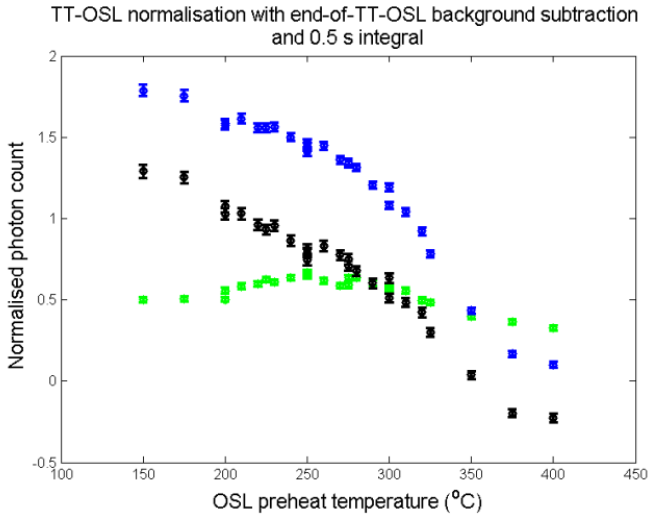
TT-OSL normalisation with end-of-TT-OSL background subtraction and 0.5 s integral
Normalised photon count
OSL preheat temperature (°C)

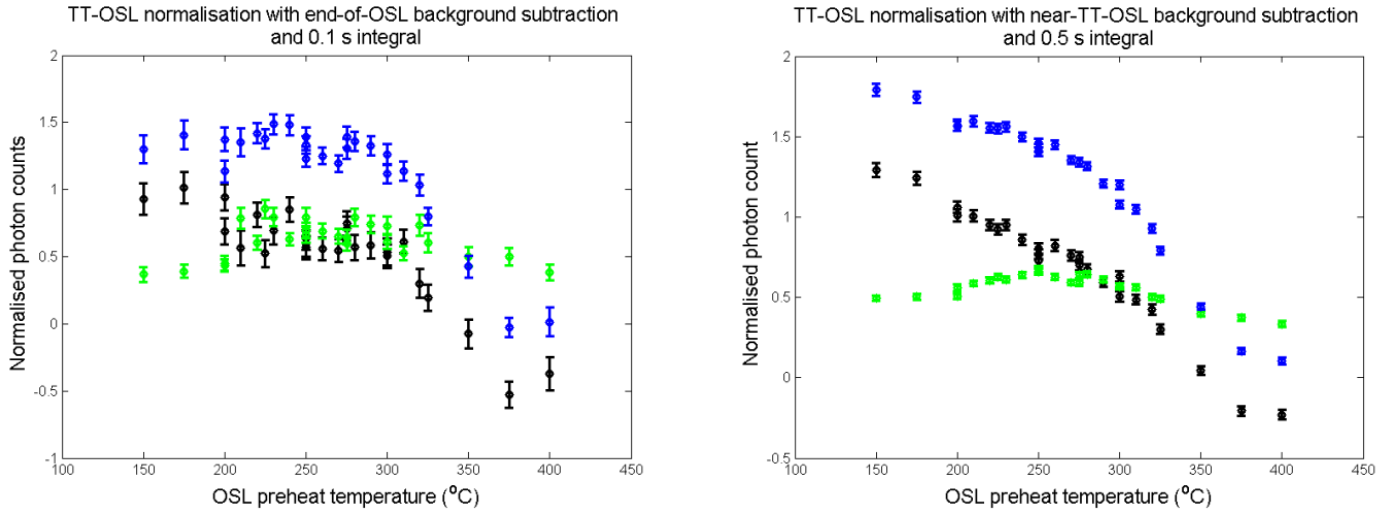

Figure 13.4: Decay vs OSL preheat results for the Robe aliquot, using TT-OSL normalisation and various background subtractions. Black data points: DD-TT-OSL; blue data points: TT-OSL; green data points: DI-TT-OSL.

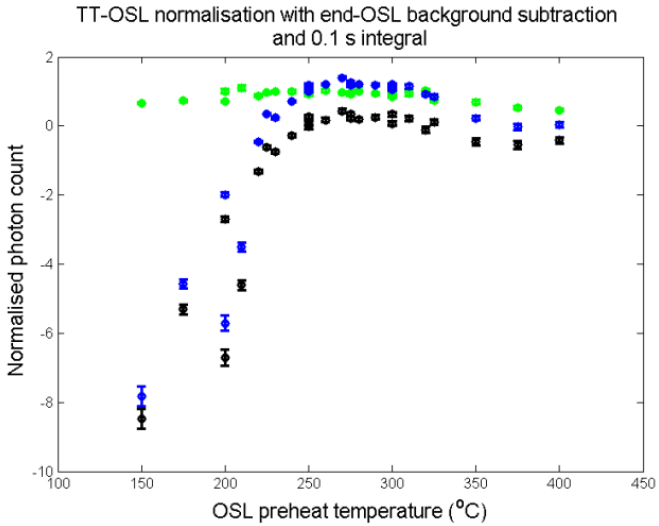
TT-OSL normalisation with end-OSL background subtraction
and 0.1 s integral
Normalised photon count
OSL preheat temperature (°C)

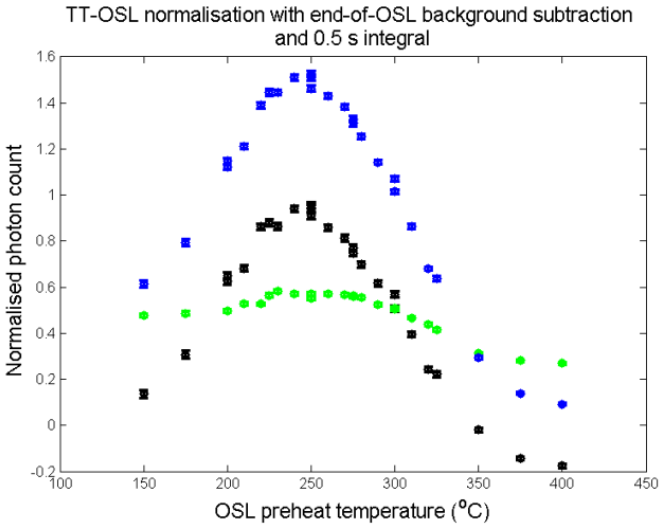
TT-OSL normalisation with end-of-OSL background subtraction
and 0.5 s integral
Normalised photon count
OSL preheat temperature (°C)

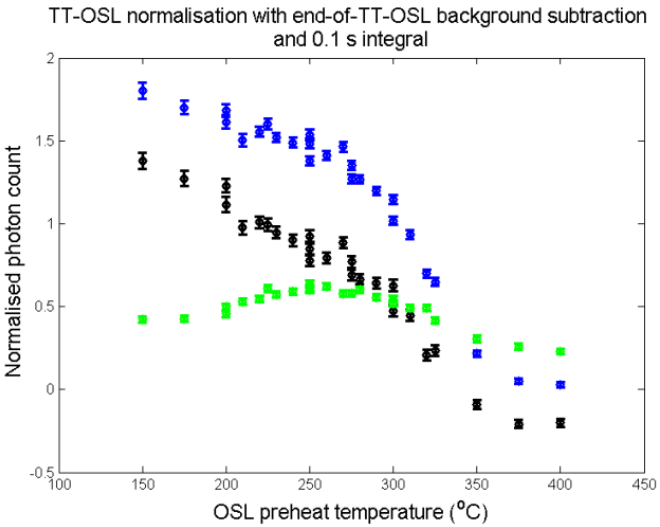
TT-OSL normalisation with end-of-TT-OSL background subtraction
and 0.1 s integral
Normalised photon count
OSL preheat temperature (°C)

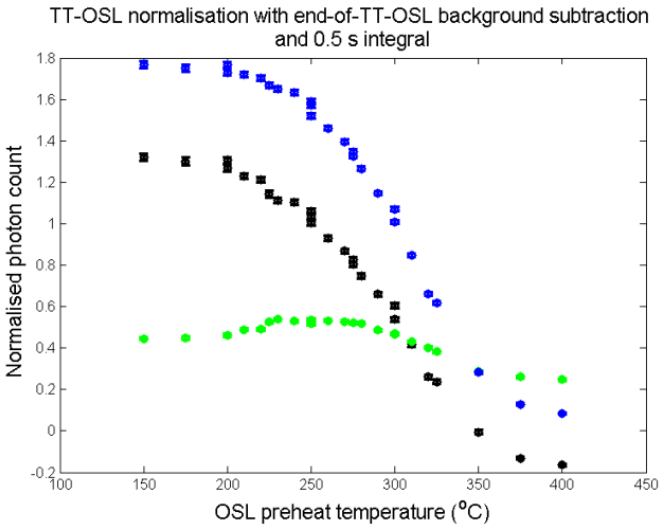
TT-OSL normalisation with end-of-TT-OSL background subtraction
and 0.5 s integral
Normalised photon count
OSL preheat temperature (°C)

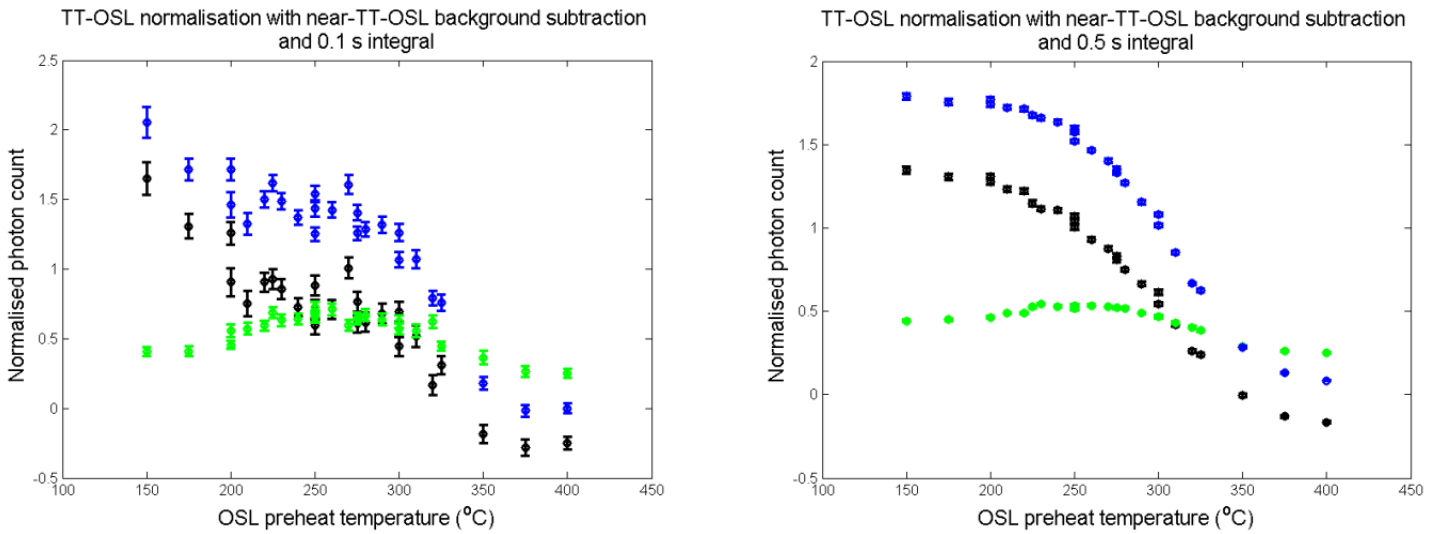

Figure 13.5: Decay vs OSL preheat results for the Woakwine aliquot, using TT-OSL normalisation and various background subtractions. Black data points: DD-TT-OSL; blue data points: TT-OSL; green data points: DI-TT-OSL.

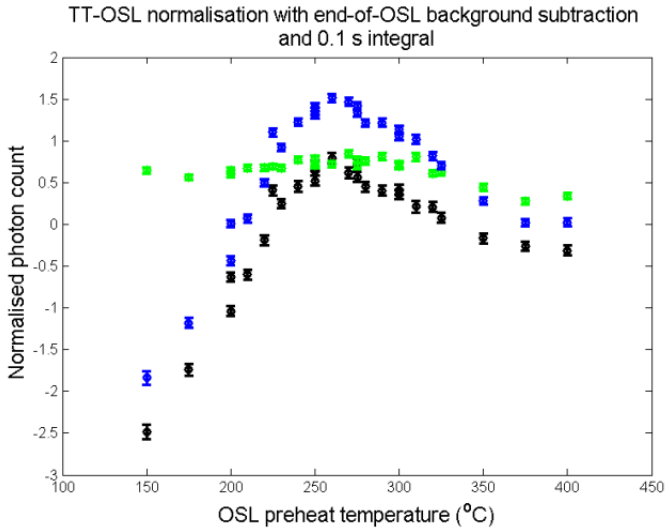
TT-OSL normalisation with end-of-OSL background subtraction and 0.1 s integral
Normalised photon count
OSL preheat temperature (°C)

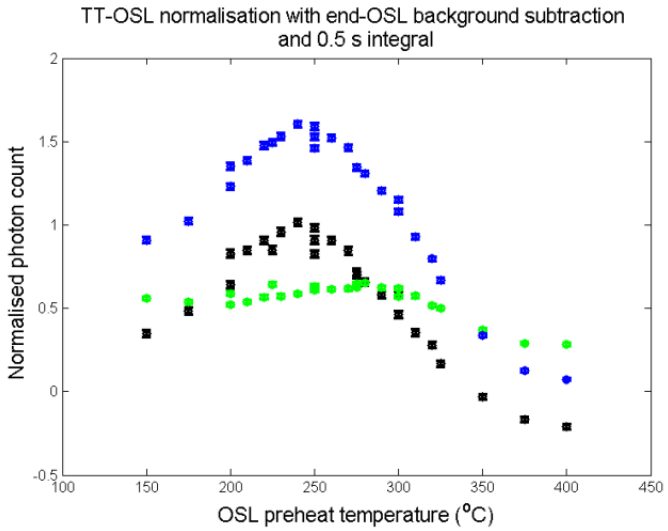
TT-OSL normalisation with end-OSL background subtraction and 0.5 s integral
Normalised photon count
OSL preheat temperature (°C)

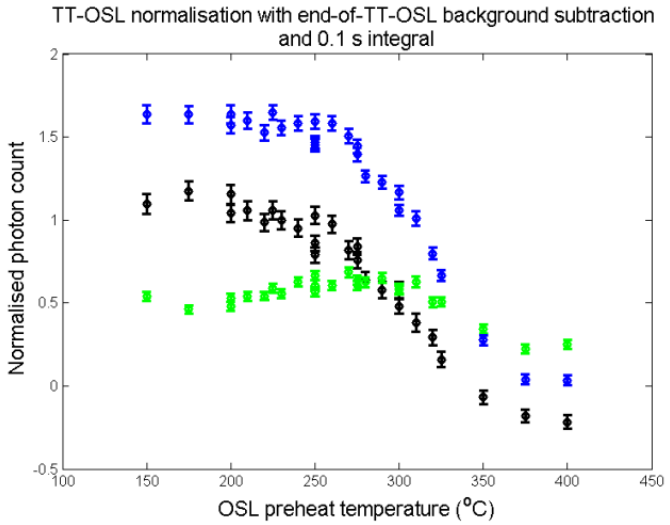
TT-OSL normalisation with end-of-TT-OSL background subtraction and 0.1 s integral
Normalised photon count
OSL preheat temperature (°C)

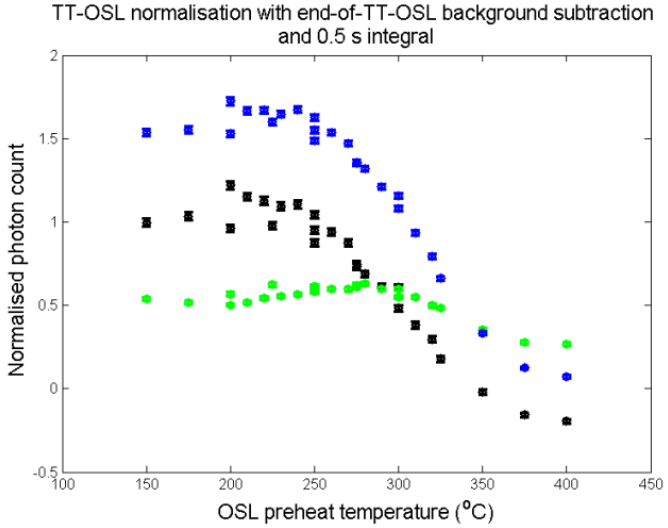
TT-OSL normalisation with end-of-TT-OSL background subtraction and 0.5 s integral
Normalised photon count
OSL preheat temperature (°C)

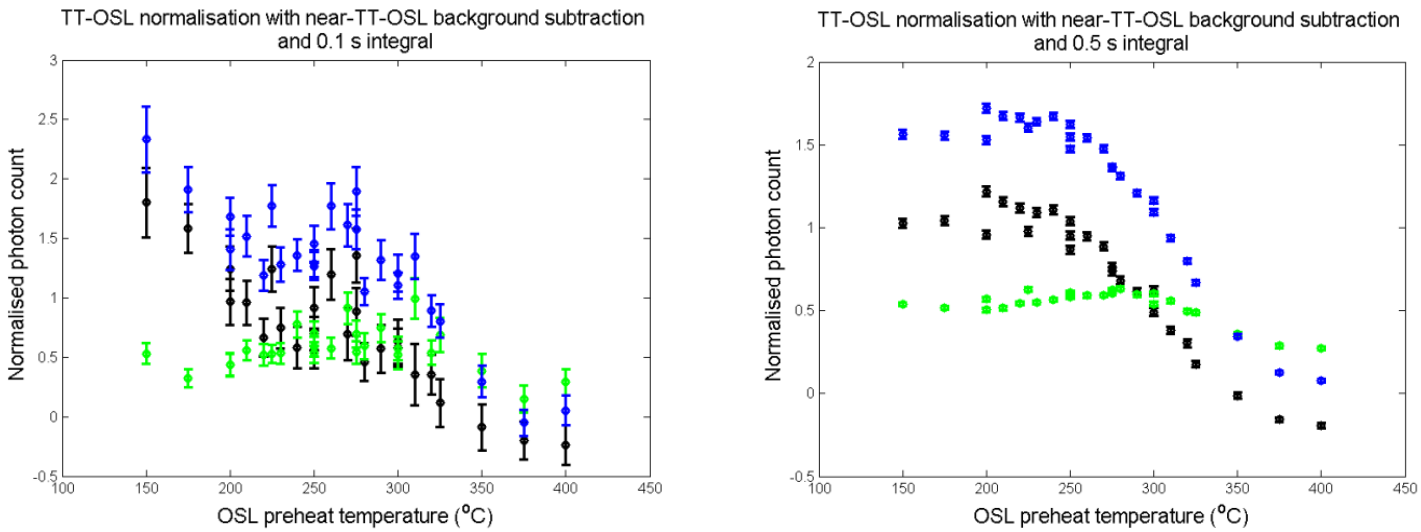

Figure 13.6: Decay vs OSL preheat results for the Naracoorte East aliquot, using TT-OSL normalisation and various background subtractions. Black data points: DD-TT-OSL; blue data points: TT-OSL; green data points: DI-TT-OSL.

Using TT-OSL normalisation, the DD-TT-OSL and TT-OSL results for the Robe and Woakwine aliquots have the signal decreasing with OSL preheat temperature, with the signal decreasing at a faster rate between 270 and 300 °C (see figs 13.4-13.6). The Naracoorte East aliquot has results that are approximately flat until 270 °C, after which they decrease until they reach zero signal at 375 °C. DI-TT-OSL results behaved the same as those with OSL normalisation.

Using the first 0.1 s of signal creates a result that drops with temperature around 320-325 °C for the first two aliquots, and 260 for the third with a discontinuity in the gradient at 300 °C. Using a 0.5 s integral, one finds an initial drop in gradient between 260 and 275 °C, with a discontinuity between 290 and 300 °C. The normalised photon count drops to zero at 375 °C.

Using TT-OSL normalisation gives results that are a little scattered due to low counting statistics for 0.1 s results, but general features are still visible: the normalised photon count vs OSL preheat temperature graph remains steady or slowly declining until 300-310 °C, after which there is a sharper decline until one reaches the zero value at 375 °C. For the Robe aliquot, the general features remain the same when using the 0.5 s integral, although the 0.1 s results from 150 to 310 °C are flat, while the 0.5 s integral results are slowly declining. For the Woakwine and Naracoorte East aliquots, the change to a sharper negative gradient occurs at 270 °C. The results reach zero at 270 °C.

-Modelling-

In order to discover the thermal depletion properties of different metastable states, a model for thermal depletion was constructed, using the simple model for lifetime:

$$t = s^{-1}e^{(\frac{E}{kT})}$$

And the depletion equation:

$$L = e^{\frac{-t'}{s^{-1}e^{\frac{E}{kT}}}}$$

Where t is the lifetime of the trap, s is the frequency factor (in s^{-1}), E is the energy difference between the metastable state and the conduction band (in eV), k is Boltzmann's constant, T is the ambient temperature (in K), L is the proportion of charge left in a trap population, and t' is the time spent at a particular temperature. The

probability of an electron remaining in the trap for ten seconds with a beginning ramp of 5 K/s from 0 °C was found for different ending temperatures and different E and s values, and then plotted using a Matlab code (see Appendix A).

For the E and s values found in Li and Li (2006), the model suggests that the trap population fully depopulates at around 575°C, indicating that our samples do not have TT-OSL signals transferred by a 260 °C preheat that originate from a metastable state with these kinetic values.

Values of E and S were taken from Spooner and Questiaux (2000), Bailey (2001), Spooner and Franklin (2002), and Kitis (2002) and used in the model (see fig. 13.7). The experimental results fit between the 325 °C trap and the 375 °C trap depletion values, fitting in between the depletion rates for the OSL UV signal (Spooner and Questiaux, 2000) and the 375 °C trap as calculated by Kitis (2002).

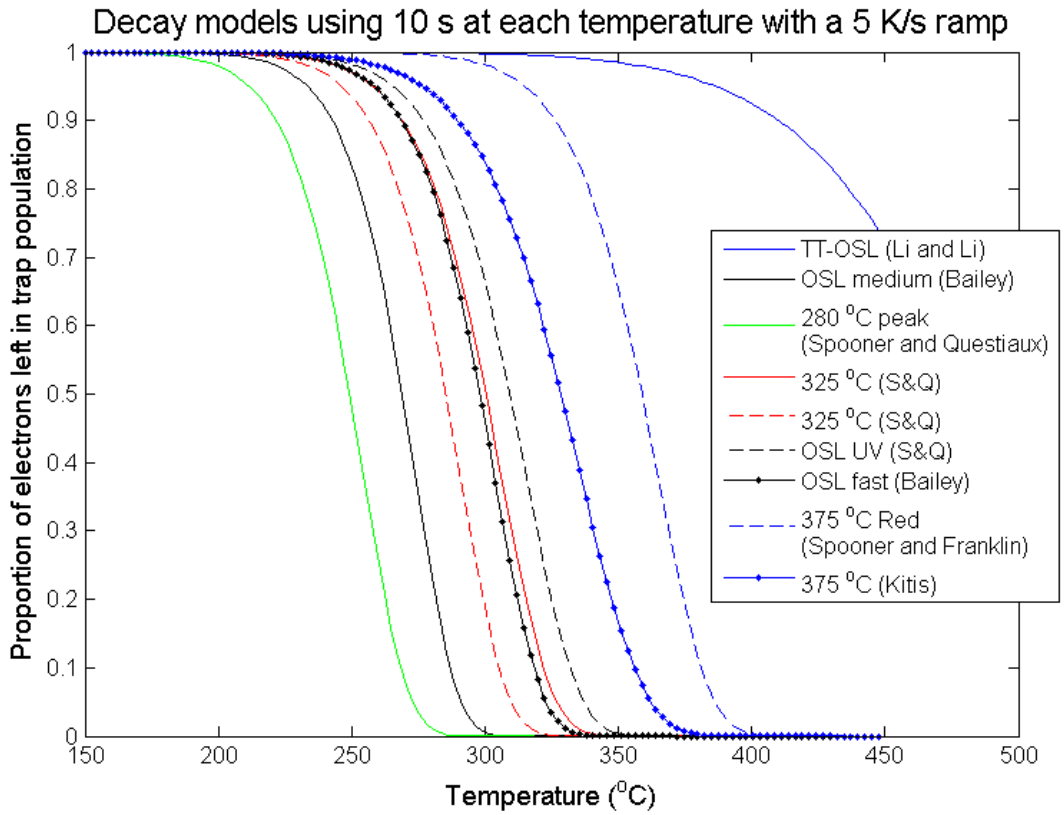

Figure 13.7: Thermal decay model results for various E and s values from Spooner and Questiaux (2000), Bailey (2001), Spooner and Franklin (2002), Kitis (2002), and Li and Li (2006).

-Fitting to the model-

It is theoretically possible to use this model to find E and s values for the origins of the DD-TT-OSL signal. However, this assumes that the DD-TT-OSL signal originally comes from only one trap, which may not be the case. The TT-OSL signal is made up of two distinct signals, the DD-TT-OSL and the DI-TT-OSL signals, which come from two different origins. Even if the DD-TT-OSL signal does only come from one trap, there may be a small amount of DI-TT-OSL signal in the experimental results due to the DI-TT-OSL subtraction process not being completely efficient.

To minimise the effects of other signals, the TT-OSL normalised, near-TT-OSL background subtracted, 0.1 s integral signal was used to attempt to find E and s values for the DD-TT-OSL signal. Iterations of E values from 0.5 to 3.0 eV, and s values from $1*10^{9}$ to $1*10^{15}$ were put through the modelling calculations, and the one with the lowest least squares value was found, using the "simdepopfit.m" Matlab code (see Appendix). Experimental results from 260 °C and onwards were used, as increased backgrounds due to the presence of shallow traps in the OSL signal may have influenced earlier results. It was assumed that at 150 °C the TT-OSL thermal depletion rate is near zero, and so the TT-OSL signals were normalised by this data point. The results are shown in table 13.3, and figure 13.8 below.

Aliquot	E (eV)	s (s^{-1})	R^2 value
Robe	1.8	10^{9}	0.72
Woakwine	1.9	10^{10}	0.65
Naracoorte East	1.9	10^{10}	0.76

Table 13.3: Modelling results for the simdepopfit.m function, including E, s, and R-squared values.

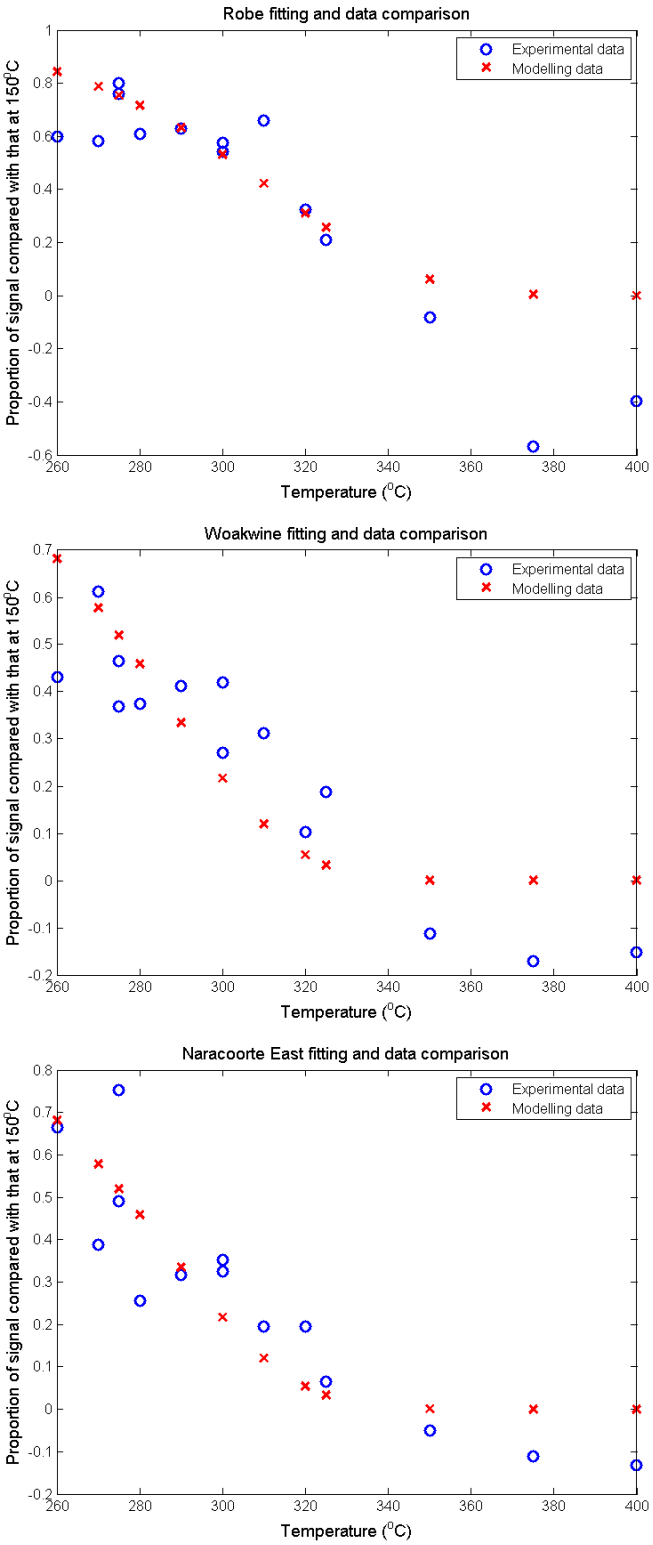

Figure 13.8: Comparisons of the experimental results (blue circles) and the fitting model (red crosses) for TT-OSL normalisation, near-TT-OSL background subtractions, and 0.1 s of signal.

Note that the normalisation of the DD-TT-OSL values (by the value of depletion at 150 °C) heavily influences the result of these results, and may not be accurate. In addition, the near-TT-OSL background subtraction with 0.1 s of signal has large counting errors, and the scatter of the data could effect the results. More experimental work must be done in this area to find accurate kinetic values for the DD-TT-OSL signal.

14-DISCUSSION AND SUMMARY

-Unusual signals-

Natural dose order

The TT-OSL SAR protocol did not produce results consistent with other results for SESA samples older than East Dairy (approximately 200-300 ka). However, the test in the 'Initial research into the TT-OSL behaviour of SESA samples' chapter of this thesis, which compared the natural TT-OSL response of each sample, showed that even up to the oldest sample, the TT-OSL response increased with age. This may mean that the inability of the approaches tested here to date older SESA samples is due to the protocol used, rather than the TT-OSL signal itself.

Another explanation for this phenomenon is that the sample's sensitivity is dependent on age. Looking at the signal received after the first test dose, which is the test dose directly after measuring the natural TT-OSL signal, this appears to be the case (see fig 14.1). The fact that the older samples' natural TT-OSL response increases under the same test dose when its equivalent dose results do not may mean that the test dose normalisation techniques used here do not take into account all of the sensitivity changes in the sample.

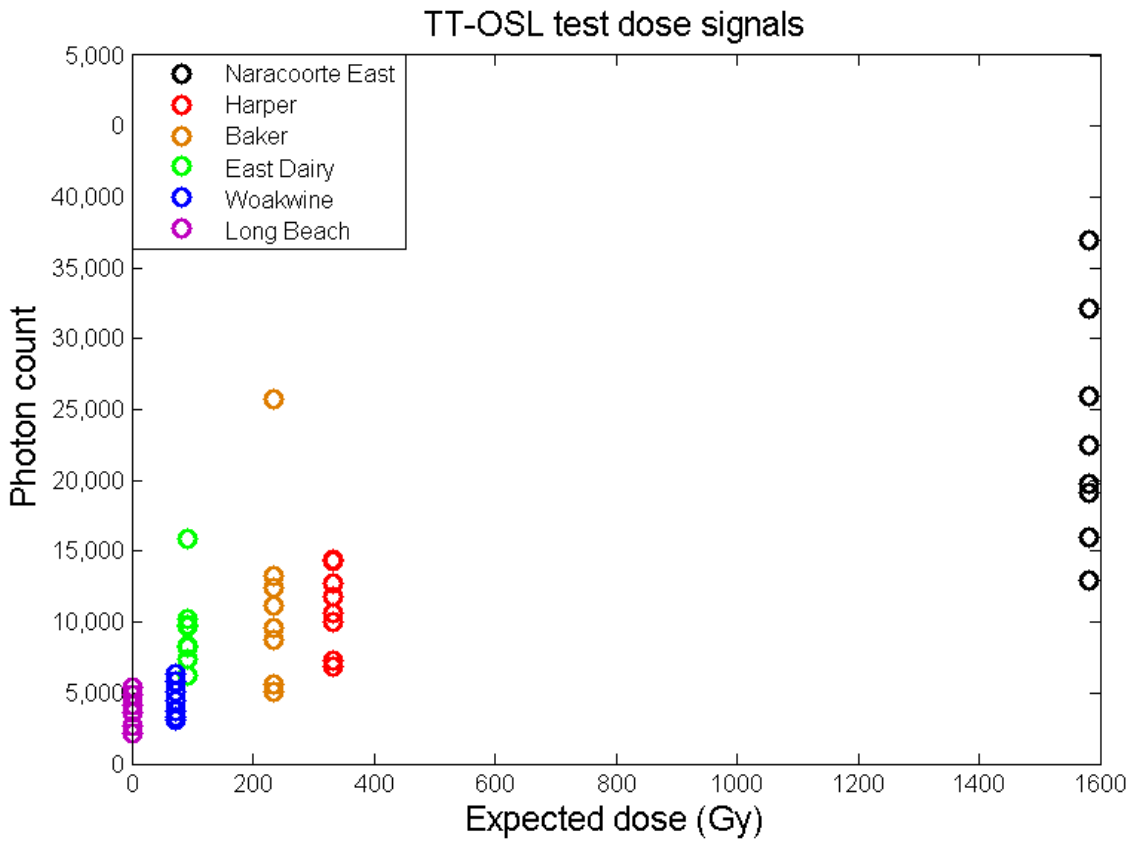

Figure 14.1: TT-OSL test dose signals from eight aliquots for each sample, using 0.1 s of signal and no background subtraction. Expected doses were calculated using the Belperio and Cann (1990) oxygen-isotope ages and the dosimetry of the individual samples.

Anomalous dose response curves

Some dose response curves using OSL normalisation, end-of-OSL background subtraction, and the first 0.1 s of signal, rather than being linear or saturating exponential in shape, had a 'tick' shape (see fig 14.2), where the zero-dose was larger than the next few doses. This may be a peculiarity of the samples or the TT-OSL signal, or may be a sign that normalisation using a test dose was not correcting for all the sensitivity changes in the sample, or possibly due to "dose quenching". For these samples there was in general an increase in sensitivity throughout the cycles (though the bulk of the sensitivity change of a cycle was dependent on the dose of that cycle and the previous one). In the sequences used, the signal with zero dose was always measured

second-to-last, and the sample at that point could potentially be much more sensitive than for cycles situated earlier in the protocol.

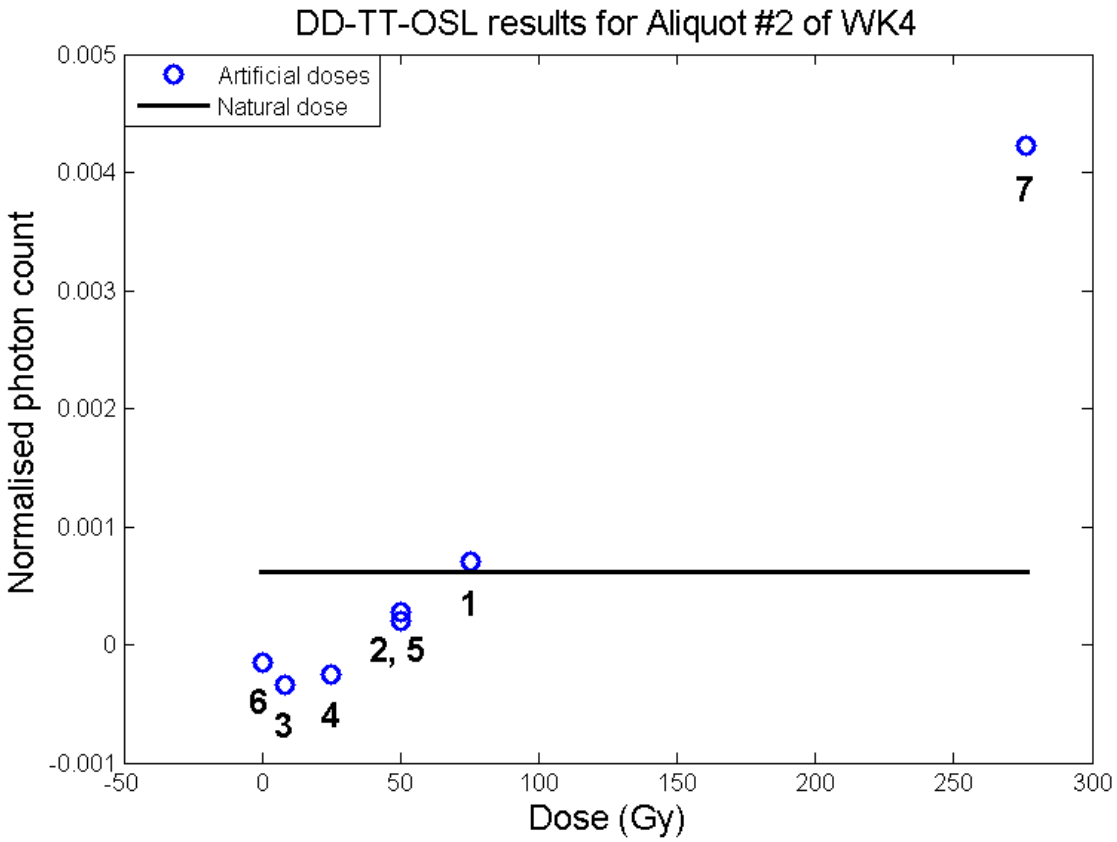

Figure 14.2: Example of 'tick' behaviour in a Woakwine sample. The numbers below each data point indicate the cycle of the single-aliquot regenerative dose protocol in which they were measured.

-Measurement precision-

The experimental errors of the equivalent dose for the Woakwine sample, using the signal and data analysis methods that best matched previous Woakwine results (DD-TT-OSL results using OSL normalisation, end-of-TT-OSL background subtraction, and the first 0.1 s of signal) were quite small, between 5 and 12 %. Similar results for the Baldina Creek sample gave errors between 3 and 9 %. However, the spread of results was much larger, the average Woakwine sample result deviating 18 Gy from the mean value (15 %), and the average Baldina Creek result deviating 56 Gy from the mean value (21

%). The spread of data is obviously dependent on the sample (the Woakwine results had a smaller spread with seven aliquots than the Baldina Creek results with 37), and this more than the experimental error determines the precision of the result.

TT-OSL signals are almost always much dimmer than their OSL counterparts (barring residual signals at nominally zero doses), and so suffer from greater counting errors. Results in chapter nine (where light from the samples was artificially dimmed due to salt build-up on the apparatus (see Chapter 10 for details)) show the effect very dim samples can have on the results. Experimental errors were extremely large, and a much greater number of aliquots would have been needed to gain a similar precision to the results in chapter 11. Also of note from Chapter nine, it was much less likely to gain a result when using the first 0.1 s of signal, and the first 0.5 s of signal had to be used in order to gain more results for a given number of aliquots. As using the first 0.1 s of signal gave better results for the Woakwine sample, it is possible that the accuracy of dim samples would be affected as well as the precision.

-Analysis variables-

In this thesis different signals and data analysis methods were used on each sample, and each variable had a different effect on the final aliquot result, as discussed below.

Signal used (DD-TT-OSL, TT-OSL, or DI-TT-OSL)

Different workers have previously used DD-TT-OSL (Wang et al, 2006a), TT-OSL (Porat et al, 2009), and DI-TT-OSL (Jacobs et al, 2011) signals to gain TT-OSL age results. For young SESA samples, DD-TT-OSL results were closer to expected results, while TT-OSL results in general overestimated the age of these young samples. DI-TT-OSL results were not near expected values, but results increased with age when TT-OSL and DD-TT-OSL results did not. It might be that the SESA samples need a higher temperature anneal to remove all the DD-TT-OSL signal, and that DI-TT-OSL signals could be more accurate for older SESA samples than results suggest, if analysed in a different way.

Portion of signal used
In this thesis, both the first 0.1 s of signal and the first 0.5 s of signal were used to gain results. The 0.1 s signal results were more scattered, as is to be expected as the counting errors would be larger for these results. The 0.5 s of signal results were further from the expected value than the 0.1 s signal results, indicating that the 0.1 s of signal results are more reliable. This may be because there is a slower OSL signal interfering with the TT-OSL signal that is minimised in the 0.1 s signal results.

Background subtraction
Three different types of background subtraction were used in this thesis: end-of-OSL, end-of-TT-OSL, and near-TT-OSL methods. In general, near-TT-OSL background subtractions led to scattered data points that could not be fit to a dose curve, probably due to the small amount of signal remaining after the background subtraction. In contrast, end-of-OSL and end-of-TT-OSL background subtractions resulted in dose curves that were easily fitted. In general, results with end-of-TT-OSL background subtraction were the nearest to the expected age. It should also be noted that end-of-TT-OSL background subtraction maximises the amount of signal used, giving smaller counting errors and hence greater precision.

Normalisation method
For all samples, including those that did not give expected results, OSL normalisation gave dose response curves that could be fit well to a linear or saturating exponential fit. Using TT-OSL normalisation gave more scattered data points and in addition, except for the very young samples (Long Beach and Woakwine), growth curves saturated before the natural dose. OSL normalisation, however, may not normalise all components of the signal reliably, as discussed in the 'unusual signals' section above.

-Overview of sample results-
SESA results
Woakwine and East Dairy ages were measured to be within the expected age range when using DD-TT-OSL signals with OSL normalisation, giving the best results when using the first

0.1 s of signal, and end-of-TT-OSL background subtraction. The Long Beach sample, from the modern beach, gave results larger than zero, suggesting that a residual signal may also be present in the other samples. Baker, Harper, and Naracoorte East results significantly underestimated the age of the samples when compared to previous results, no matter what TT-OSL signal was used.

Baldina Creek

Baldina Creek results gave answers that were within the expected age range: stratigraphic correlation suggests an approximate age range of 40-110 ka. Errors of the TT-OSL signals are larger than typical OSL errors, although decreasing the error of the final result is possible by using more aliquots.

Large errors in a dating technique can limit its usefulness in answering questions people may have about the dated sample. One major question posed by palaeontologists is whether the megafauna of Australia became extinct due to human hunting or climactic change. Due to the larger errors of this technique, the age measured here straddles both the climate change event (last ice age) and the migration of humans to Australia, and so using TT-OSL to date this megafaunal skeleton does not support either theory.

15-CONCLUSIONS

In the introduction to this thesis, I outlined a number of questions I wished to answer, the answers to which are below:

Is TT-OSL suitable for dating buried sediments at natural doses where optical dating fails?
As shown from the Baldina Creek sample, the TT-OSL signal has the potential to date relatively "young" sediments with large natural doses that are saturated when measured by conventional OSL. Care must be taken, however, to ensure that the sediment's environment and age are suitable for use with the TT-OSL signal.

Is TT-OSL suitable for dating buried sediments older than can be dated using conventional OSL (more than half a million years)?
While the TT-OSL signal was successful at matching age results from younger samples, no TT-OSL dating method used was able to date SESA samples older than 250 ka.

How precise are TT-OSL measurements, and how much time and sample is needed to obtain a result?
As mentioned in the previous chapter, the precision of the TT-OSL measurements are effected mainly by the variability of dose given in the sample, unless the TT-OSL signals are very dim. As the signal strength is also sample dependent, it is not possible to make any generalisations about the precision of TT-OSL measurements.

Using a Sr^{90}/Y^{90} beta source which doses quartz at a rate of 0.092 Gy/s in an automated Risø TL/OSL DA-20, the full Woakwine SAR protocol took approximately eight hours to run one 5 mm (3.5—5.5 mg) sample, while the Baldina Creek protocol took 12 hours, due to the large natural dose. To obtain results for the 37 Baldina Creek aliquots in this thesis, therefore, took approximately 18.5 days of machine time, and 0.1665 g of sample. For comparison, an OSL protocol with the same doses given would take approximately 7 hours to complete one sample, or 10.8 days for 37.

Is TT-OSL more suitable for dating older sediments than other luminescence methods, such as thermoluminescence (TL)?
As seen in chapters 11 and 13, the TT-OSL signal does not have a large lifetime suitable for dating old sediments. In chapter 7, it was shown that wind-blown sands that have had significant exposure to sunlight still contained a residual TT-OSL dose, and TT-OSL is therefore not suitable for dating very young sediments. According to the research done in this thesis on the SESA samples, TT-OSL has a small window of usefulness: for dating samples of approximately 50-150 ka, that have dose rates large enough for conventional OSL signals to be saturated. TT-OSL protocols require high temperature preheats and signal depletion steps, and so need the same specialised equipment as thermoluminescence procedures. In addition, resetting of TT-OSL in nature is problematic: TT-OSL does not have the advantage of short resetting times that conventional OSL does. If there is a TL peak with a suitable lifetime to date in this range and a similar dose saturation level, TL dating would be preferable to TT-OSL, as it would give brighter signals, and the signal is much more readily identifiable as coming from only one peak.

16-APPENDIX

A: MATLAB CODES

Contents of Appendix A:

1) "iner"

The function used to find and collect instrumental errors which create mean values with small differences.

2) "differences1"

The function used to find the smallest differences between the means and the corresponding instrumental error values.

3) "allparts2"

The function used to gain natural dose results when using single grain discs.

4) "natdose"

The function used to gain natural dose results for large aliquots.

5) "variations"

The function used to process the reproducibility experiments in Chapter 9. A variation was also used to process the kinetic data in Chapter 12.

6) "simdepop"

The function used to model preheat depletion of traps using previously published E and s values.

7) "simdepopfit"

The function used to find E and s values that fit experimental thermal depletion data.

"INER"

```
function iner

%A function to find the most probable instrumental error.

close all
clear all

%inporting data

whichdata=input('Which data file do you want to use? (1=d3; 2=d5)');

if whichdata==1;
    points=300;
sdata=csvread('alld3.txt');
%whichd='alld3';
end

if whichdata==2;
    points=300;
sdata=csvread('alld5.txt');
%whichd='alld5';
end

%results=zeros(4,4);
results=zeros(1,4);

%Defining ie
ie=linspace(0,1000,1001);
%res=ie(2)-ie(1);
ie2=ie;
%l=length(ie);

%mean=zeros(1,l);
%meanerr=zeros(1,l);
%err=zeros(1,l);

for intergral=4:5%2:5;
disp(intergral-1);
    data=sdata;
%Stripping to wanted data
data(1,:)=[];
data(:,1)=[];
data(:,intergral:600)=[];

data=sum(data,2);

y=zeros(1,points);
```

```
yerrsquared=zeros(1,points);

%Finding ie
for qq=1:length(ie)
    for rr=1:length(ie2)

    for aa=0:(points-1);
%02/08/2012 changed yerrsquared--had ie2 dependent on data(aa.*2+1),
rather than being +1 and then +2.
%02/08/2012 changed yerrsquared--now ie2/(data(aa.*2+X)-1) (instead of
sans
%-1)
        y(aa+1)=data(aa.*2+1)./data(aa.*2+2);
        yerrsquared(aa+1)=y(aa+1).^2.*(  ((sqrt(data(aa.*2+1)) + ie(qq) +
(ie2(rr)./sqrt(data(aa.*2+1)-1))) ./ (data(aa.*2+1))).^2  +
((sqrt(data(aa.*2+2)) + ie(qq) + (ie2(rr)./sqrt(data(aa.*2+2)-1))) ./
(data(aa.*2+2))).^2);
        %yerr(aa+1)=sqrt(yerrsquared(aa+1));

    end

   %
   %
l=length(y);
mean=sum(y)/length(y);
ytakemeansquared=(y-mean).^2;
%meanerr=sqrt((1/(length(y)-1))*sum(ytakemeansquared)/sqrt(length(y)));
meanerr=sqrt((1/(l*(l-1)))*sum(ytakemeansquared));
err=sqrt((1/length(y))^2 * (sum(yerrsquared)));

    if (err <= meanerr) && ((err+0.01) > meanerr);
    results(1)=ie(qq);
    results(2)=ie2(rr);
    results(3)=err;
    results(4)=meanerr;
    if intergral==2;
        dlmwrite('test2int1da.txt',results,'-append','newline','pc');
    end
    if intergral==3;
        dlmwrite('test2int2da.txt',results,'-append','newline','pc');
    end
    if intergral==4;
        dlmwrite('test2int3da.txt',results,'-append','newline','pc');
    end
    if intergral==5;
        dlmwrite('test2int4da.txt',results,'-append','newline','pc');
    end
    end
```

```
    end
end

end

%Recording errors of means and instrumental errors.

%dlmwrite('ies_nodatadep.txt',whichd,'-append','newline','pc');
%dlmwrite('ies_nodatadep.txt',results,'-append','newline','pc');

end
```

"DIFFERENCES1"

```
function differences1

%A function to find the ie and ie2 values with the smallest deviation
from
%the ideal errormean=statmean.
%Note: the text document written in the for and if loops and read in
%'matches' needs to be reset each time.

close all
clear all

disp('Please ensure that the results_differences1 text document has been
reset, and then press any key.');
pause

data1=csvread('test2int4d3.txt');

data2=csvread('test2int4d5.txt');


length1=length(data1(:,1));
length2=length(data2(:,2));

for aa=1:length1
    for bb=1:length2
                if data1(aa,1)==data2(bb,1) && data1(aa,2)==data2(bb,2);
            result=[data1(aa,:),data2(bb,3:4)];

            dlmwrite('results_differences1_20120802.txt',result,'-
append','newline','pc');
                end

    end
end

matches=csvread('results_differences1_20120802.txt');

differences=[abs(matches(:,3)-matches(:,4)),abs(matches(:,5)-
matches(:,6))];

diffvec=sqrt(differences(:,1).^2+differences(:,2).^2);


[~,jj]=min(diffvec);

disp('The numbers with minimum error are:');
res1=matches(jj,1:2);
```

```
disp(res1);

disp('The differences of the means are:');
res2=differences(jj,:);
disp(res2);

%To find next lowest:
% delete lowest
diffvec(jj)=[];
matches(jj,:)=[];
differences(jj,:)=[];

% find minimum as before.

[~,jj]=min(diffvec);


disp('The numbers with secondmost minimum error are:');
res1=matches(jj,1:2);
disp(res1);

disp('The differences of the means are:');
res2=differences(jj,:);
disp(res2);

%To find next lowest:
% delete lowest
diffvec(jj)=[];
matches(jj,:)=[];
differences(jj,:)=[];

% find minimum as before.

[~,jj]=min(diffvec);


disp('The numbers with thirdmost minimum error are:');
res1=matches(jj,1:2);
disp(res1);

disp('The differences of the means are:');
res2=differences(jj,:);
disp(res2);

%To find next lowest:
% delete lowest
diffvec(jj)=[];
matches(jj,:)=[];
differences(jj,:)=[];
```

```
% find minimum as before.

[~,jj]=min(diffvec);


disp('The numbers with fourthmost minimum error are:');
res1=matches(jj,1:2);
disp(res1);

disp('The differences of the means are:');
res2=differences(jj,:);
disp(res2);


end
```

"ALLPARTS2"

```
function allparts2


%a function to redo cleanly and create a function that:
%-finds 8pt TT-OSL, BT-OSL, ReOSL
%-finds recycling ratio
%-fits growth curve and finds age with errors
%
%
%#1: select and crop aliquot, OSL, TT-OSL, BT-OSL, test doses
%#2: plot ReOSL, TT-OSL, BT-OSL data.
%#3: select fits
%#4: from fits find dose (seconds) equivalent, and errors
%#5: from De and errors find age and errors, and write down information.
%
%
%Things different from findingx calculatingDe:
%*An escape clause if no fit is good.
%
%
%*outputs:
%-disc number
%-aliquot number
%-ReOSL age
%-ReOSL error
%-TT-OSL age
%-TT-OSL error
%-fit type
%-recycling ratio
%-natural peak TT-OSL
%number of data points (0.02 seconds) in TTOSL and BTOSL intergrals

%THINGS TO REMEMBER:
%*Instrumental error is set as 1.7%
%*R2 values are created by the following equation:
%R2=1-{(sum[(Y(point)-Y(fit))^2]/sum(variances^2)}

%CHANGES:
%-NOTE 23/01/12 CHANGED '0' NUMBERS TO '0.1' NUMBERS TO AVOID 0 ERRORS
AND
%NaN WEIGHTS. NOTE THAT THE SMALLEST NATURAL VALUE WOULD BE 1 (CANNOT
%NATURALLY HAVE 0.1 OF A PHOTON)
%
%-Note 23/01/12 CHANGED ERROR EQUATIONS FROM 'AVERAGE ERROR' TERMS TO
%'VARIANCE' TERMS.
%
%-Note 23/01/12 Changed the system of viewing so one has to look at all
%fits possible. Note that the fit bounds had to be changed to do this, to
%prevent 'Inf computed by model function, fitting cannot continue.' error
%messages that stop the code.
%
%-Note 23/01/12 Legends were turned off to make viewing graphs easier.
%
%-Note 24/01/12 Ttestintergral was changed so that 0 numbers turn to 0.1,
```

```
%to prevent NaN error messages that stop the code. (Tintergral is divided
%by Ttestintergral and then plotted.)

close all
clear all


%*******Things that stay the same for each disc and each aliquot:
cycles=[300 600 1000 2000 3000 0 300];
x=[300;600;1000;2000;3000;0;300];
%Defining dose rate per grain:
dose=[0.16 0.16 0.154 0.154 0.145 0.145 0.135 0.135 0.135 0.135 0.145
0.145 0.145 0.145 0.145 0.135 0.135 0.135 0.125 0.12 0.145 0.145 0.145
0.145 0.145 0.135 0.135 0.125 0.125 0.115 0.145 0.145 0.145 0.145 0.145
0.135 0.125 0.125 0.125 0.111 0.145 0.145 0.145 0.145 0.135 0.135 0.135
0.125 0.125 0.111 0.135 0.135 0.135 0.135 0.135 0.135 0.125 0.125 0.111
0.111 0.135 0.135 0.135 0.135 0.135 0.125 0.125 0.111 0.111 0.111 0.125
0.125 0.125 0.120 0.120 0.120 0.1 0.1 0.1 0.1 0.11 0.11 0.11 0.11 0.11
0.11 0.11 0.1 0.105 0.105 0.105 0.105 0.105 0.1 0.1 0.1 0.1 0.09 0.09
0.086];
%WK4 dose rate and errors
WK4dr=0.5823;
WK4drerror=0.075;

xnat=linspace(0,3000,9);
ynat=ones(1,9);
xtestTT=[0 1 2 3 4 5 6 7];
xtestBT=[0.5 1.5 2.5 3.5 4.5 5.5 6.5 7.5];

lastaliquot=csvread('lastaliquot.txt');

%Fit types (linear, saturating exponential (zero variable), saturating
%exponential plus linear (zero variable).
F1=fittype('poly1');
F2=fittype('-a.*exp(-b.*x) + c','coeff',{'a','b','c'});
F3=fittype('-a.*exp(-b.*x) + c*x + d','coeff',{'a','b','c','d'});
%************************************************************
%First item: which disc? This will also be the disc number output.
disc=input('Which disc?');
q1=input('Do you want to start at the beginning? (aliquot 1) (y=1)');
if q1==1
    ali=1;
else
    q2=input('Do you want to start at the last uncalculated aliquot?
(y=1)');
    if q2==1
        ali=lastaliquot;
    else
        ali=input('Which aliquot would you like to start at?');
    end
end

%reading off disc data
if disc==1
    data=csvread('8pt01.txt');
```

```
end

if disc==2
    data=csvread('8pt02.txt');
end

if disc==3
    data=csvread('8pt03.txt');
end

if disc==4
    data=csvread('8pt04.txt');
end

if disc==5
    data=csvread('8pt05.txt');
end

if disc==6
    data=csvread('8pt06.txt');
end

if disc==7
    data=csvread('8pt07.txt');
end

if disc==9
    data=csvread('8pt09.txt');
end

if disc==10
    data=csvread('8pt10.txt');
end

if disc==11
    data=csvread('8pt11.txt');
end

if disc==12
    data=csvread('8pt12.txt');
end

if disc==13
    data=csvread('8pt13a.txt');
end


%************************************************************************
%After this, everything will be for a specific aliquot.

for aliquot=ali:100


%************************************************************************
```

```
    %******************    PART ONE
************************************

%*************************************************************************

    %Part one reads off variable strings, crops them, and processes them
for
%calculating intergrals.
%It also calculates peak TTOSL and BOSL and the number of points in TT
and BT vectors.

%getting all data for each point.

%Preallocating matrices:
TOSL=zeros(8,111);
TTOSL=zeros(8,111);
Ttest=zeros(8,111);
BTOSL=zeros(8,111);
BOSL=zeros(8,111);
Btest=zeros(8,111);


for point=1:8

TOSL(point,:)=data(aliquot+(600*(point-1)),:);

TTOSL(point,:)=data(100+aliquot+(600*(point-1)),:);

Ttest(point,:)=data(200+aliquot+(600*(point-1)),:);

BTOSL(point,:)=data(400+aliquot+(600*(point-1)),:);

BOSL(point,:)=data(300+aliquot+(600*(point-1)),:);

Btest(point,:)=data(500+aliquot+(600*(point-1)),:);

end

%cropping ends of each data string

TOSL(:,107:111)=[];
TOSL(:,1:6)=[];

TTOSL(:,107:111)=[];
TTOSL(:,1:6)=[];

%finding peak TT-OSL (natural)
peakT=TTOSL(1,1) + TTOSL(1,2);

Ttest(:,107:111)=[];
Ttest(:,1:6)=[];

BTOSL(:,107:111)=[];
```

```
BTOSL(:,1:6)=[];

peakB=BTOSL(1,1) + BTOSL(1,2);

BOSL(:,107:111)=[];
BOSL(:,1:6)=[];

Btest(:,107:111)=[];
Btest(:,1:6)=[];


%Creating test dose values: Will be using first four points of each test
%curve.

%Note that Ttest intergral has its own error, as found below:

Ttest=Ttest(:,1:4);
Ttestintergral=sum(Ttest,2);
Ttesterror=sqrt(Ttestintergral + (0.017.*Ttestintergral).^2);

for fixit=1:8
    if Ttestintergral(fixit)==0
        Ttestintergral(fixit)=0.1
    end
end

Btest=Btest(:,1:4);
Btestintergral=sum(Btest,2);
Btesterror=sqrt(Btestintergral + (0.017.*Btestintergral).^2);


%Creating values for the end of OSL curve. Note that these are made from
%the average of the two ends of the OSL curve.

endTOSL=TOSL(:,99:100);
endTOSL=sum(endTOSL,2);
endTOSLerror=sqrt(endTOSL*1/4 + 1/4*(0.017.*endTOSL).^2);
endTOSL=endTOSL./2;

endBOSL=BOSL(:,99:100);
endBOSL=sum(endBOSL,2)/2;
%before=(sqrt(endBOSL) + 0.017.*endBOSL)./2
endBOSLerror=sqrt(endBOSL*1/4 + 1/4*(0.017.*endBOSL).^2);
endBOSL=endBOSL./2;


%Creating TTOSL and BTOSL intergrals
for pp=1:8
TTOSL(pp,:)=TTOSL(pp,:)-endTOSL(pp);

BTOSL(pp,:)=BTOSL(pp,:)-endBOSL(pp);

end
```

```
%Note cannot delete parts of matrix
TTOSLn=TTOSL(1,:);
TTOSL1=TTOSL(2,:);
TTOSL2=TTOSL(3,:);
TTOSL3=TTOSL(4,:);
TTOSL4=TTOSL(5,:);
TTOSL5=TTOSL(6,:);
TTOSL6=TTOSL(7,:);
TTOSL7=TTOSL(8,:);

BTOSLn=BTOSL(1,:);
BTOSL1=BTOSL(2,:);
BTOSL2=BTOSL(3,:);
BTOSL3=BTOSL(4,:);
BTOSL4=BTOSL(5,:);
BTOSL5=BTOSL(6,:);
BTOSL6=BTOSL(7,:);
BTOSL7=BTOSL(8,:);


for ee=0:99

    if TTOSLn(100-ee)<=0
    TTOSLn(100-ee)=[];
    end

    if TTOSL1(100-ee)<=0
    TTOSL1(100-ee)=[];
    end

    if TTOSL2(100-ee)<=0
    TTOSL2(100-ee)=[];
    end

    if TTOSL3(100-ee)<=0
    TTOSL3(100-ee)=[];
    end

    if TTOSL4(100-ee)<=0
    TTOSL4(100-ee)=[];
    end

    if TTOSL5(100-ee)<=0
    TTOSL5(100-ee)=[];
    end

    if TTOSL6(100-ee)<=0
    TTOSL6(100-ee)=[];
    end

    if TTOSL7(100-ee)<=0
    TTOSL7(100-ee)=[];
    end
```

```
    if BTOSLn(100-ee)<=0
    BTOSLn(100-ee)=[];
    end

    if BTOSL1(100-ee)<=0
    BTOSL1(100-ee)=[];
    end

    if BTOSL2(100-ee)<=0
    BTOSL2(100-ee)=[];
    end

    if BTOSL3(100-ee)<=0
    BTOSL3(100-ee)=[];
    end

    if BTOSL4(100-ee)<=0
    BTOSL4(100-ee)=[];
    end

    if BTOSL5(100-ee)<=0
    BTOSL5(100-ee)=[];
    end

    if BTOSL6(100-ee)<=0
    BTOSL6(100-ee)=[];
    end

    if BTOSL7(100-ee)<=0
    BTOSL7(100-ee)=[];
    end
end

%Calculating number of seconds of TTOSL and BTOSL.
lengthT=length(TTOSLn);
lengthB=length(BTOSLn);




%**********************************************************************
    %******************    PART TWO
************************************

%**********************************************************************

    %Part two creates ReOSL, TT-OSL and BT-OSL intergrals and plots them.


%Calculating intergrals for TTOSL
TTOSLint(1)=sum(TTOSLn);
lengthTTn=length(TTOSLn);
if length(TTOSLn)==0
```

```
    lengthTTn=0.1;
end
if TTOSLint(1)==0
    TTOSLint(1)=0.1;
end
%(to prevent 0 errors and NaN weights.)
errorTTOSLint(1)=sqrt(TTOSLint(1) + (0.017*TTOSLint(1))^2 +
(lengthTTn*endTOSLerror(1))^2);

TTOSLint(2)=sum(TTOSL1);
lengthTT1=length(TTOSL1);
if length(TTOSL1)==0
    lengthTT1=0.1;
end
if TTOSLint(2)==0
    TTOSLint(2)=0.1;
end

%(to prevent 0 errors and NaN weights.)
errorTTOSLint(2)=sqrt(TTOSLint(2) + (0.017*TTOSLint(2))^2 +
(lengthTT1*endTOSLerror(2))^2);

TTOSLint(3)=sum(TTOSL2);
lengthTT2=length(TTOSL2);
if length(TTOSL2)==0
    lengthTT2=0.1;
end
if TTOSLint(3)==0
    TTOSLint(3)=0.1;
end
%(to prevent 0 errors and NaN weights.)
errorTTOSLint(3)=sqrt(TTOSLint(3) + (0.017*TTOSLint(3))^2 +
(lengthTT2*endTOSLerror(3))^2);

TTOSLint(4)=sum(TTOSL3);
lengthTT3=length(TTOSL3);
if length(TTOSL3)==0
    lengthTT3=0.1;
end
if TTOSLint(4)==0
    TTOSLint(4)=0.1;
end
%(to prevent 0 errors and NaN weights.)
errorTTOSLint(4)=sqrt(TTOSLint(4) + (0.017*TTOSLint(4))^2 +
(lengthTT3*endTOSLerror(4))^2);

TTOSLint(5)=sum(TTOSL4);
lengthTT4=length(TTOSL4);
if length(TTOSL4)==0
    lengthTT4=0.1;
end
if TTOSLint(5)==0
    TTOSLint(5)=0.1;
end
%(to prevent 0 errors and NaN weights.)
```

```
errorTTOSLint(5)=sqrt(TTOSLint(5) + (0.017*TTOSLint(5))^2 +
(lengthTT4*endTOSLerror(5))^2);

TTOSLint(6)=sum(TTOSL5);
lengthTT5=length(TTOSL5);
if length(TTOSL5)==0
    lengthTT5=0.1;
end
if TTOSLint(6)==0
    TTOSLint(6)=0.1;
end
%(to prevent 0 errors and NaN weights.)
errorTTOSLint(6)=sqrt(TTOSLint(6) + (0.017*TTOSLint(6))^2 +
(lengthTT5*endTOSLerror(6))^2);

TTOSLint(7)=sum(TTOSL6);
lengthTT6=length(TTOSL6);
if length(TTOSL6)==0
    lengthTT6=0.1;
end
if TTOSLint(7)==0
    TTOSLint(7)=0.1;
end
%(to prevent 0 errors and NaN weights.)
errorTTOSLint(7)=sqrt(TTOSLint(7) + (0.017*TTOSLint(7))^2 +
(lengthTT6*endTOSLerror(7))^2);

TTOSLint(8)=sum(TTOSL7);
lengthTT7=length(TTOSL7);
if length(TTOSL7)==0
    lengthTT7=0.1;
end
if TTOSLint(8)==0
    TTOSLint(8)=0.1;
end
%(to prevent 0 errors and NaN weights.)
errorTTOSLint(8)=sqrt(TTOSLint(8) + (0.017*TTOSLint(8))^2 +
(lengthTT7*endTOSLerror(8))^2);

%Calculating intergrals for BTOSL

BTOSLint(1)=sum(BTOSLn);
lengthBTn=length(BTOSLn);
if length(BTOSLn)==0
    lengthBTn=0.1;
end
if BTOSLint(1)==0
    BTOSLint(1)=0.1;
end
%(to prevent 0 errors and NaN weights.)
errorBTOSLint(1)=sqrt(BTOSLint(1) + (0.017*BTOSLint(1))^2 +
(lengthBTn*endBOSLerror(1))^2);



BTOSLint(2)=sum(BTOSL1);
```

```
lengthBT1=length(BTOSL1);
if length(BTOSL1)==0
    lengthBT1=0.1;
end
if BTOSLint(2)==0
    BTOSLint(2)=0.1;
end
%(to prevent 0 errors and NaN weights.)
errorBTOSLint(2)=sqrt(BTOSLint(2) + (0.017*BTOSLint(2))^2 +
(lengthBT1*endBOSLerror(2))^2);

BTOSLint(3)=sum(BTOSL2);
lengthBT2=length(BTOSL2);
if length(BTOSL2)==0
    lengthBT2=0.1;
end
if BTOSLint(3)==0
    BTOSLint(3)=0.1;
end
%(to prevent 0 errors and NaN weights.)
errorBTOSLint(3)=sqrt(BTOSLint(3) + (0.017*BTOSLint(3))^2 +
(lengthBT2*endBOSLerror(3))^2);

BTOSLint(4)=sum(BTOSL3);
lengthBT3=length(BTOSL3);
if length(BTOSL3)==0
    lengthBT3=0.1;
end
if BTOSLint(4)==0
    BTOSLint(4)=0.1;
end
%(to prevent 0 errors and NaN weights.)
errorBTOSLint(4)=sqrt(BTOSLint(4) + (0.017*BTOSLint(4))^2 +
(lengthBT3*endBOSLerror(4))^2);

BTOSLint(5)=sum(BTOSL4);
lengthBT4=length(BTOSL4);
if length(BTOSL4)==0
    lengthBT4=0.1;
end
if BTOSLint(5)==0
    BTOSLint(5)=0.1;
end
%(to prevent 0 errors and NaN weights.)
errorBTOSLint(5)=sqrt(BTOSLint(5) + (0.017*BTOSLint(5))^2 +
(lengthBT4*endBOSLerror(5))^2);

BTOSLint(6)=sum(BTOSL5);
lengthBT5=length(BTOSL5);
if length(BTOSL5)==0
    lengthBT5=0.1;
end
if BTOSLint(6)==0
    BTOSLint(6)=0.1;
end
%(to prevent 0 errors and NaN weights.)
```

```
errorBTOSLint(6)=sqrt(BTOSLint(6) + (0.017*BTOSLint(6))^2 +
(lengthBT5*endBOSLerror(6))^2);

BTOSLint(7)=sum(BTOSL6);
lengthBT6=length(BTOSL6);
if length(BTOSL6)==0
    lengthBT6=0.1;
end
if BTOSLint(7)==0
    BTOSLint(7)=0.1;
end
%(to prevent 0 errors and NaN weights.)
errorBTOSLint(7)=sqrt(BTOSLint(7) + (0.017*BTOSLint(7))^2 +
(lengthBT6*endBOSLerror(7))^2);

BTOSLint(8)=sum(BTOSL7);
lengthBT7=length(BTOSL7);
if length(BTOSL7)==0
    lengthBT7=0.1;
end
if BTOSLint(8)==0
    BTOSLint(8)=0.1;
end
%(to prevent 0 errors and NaN weights.)
errorBTOSLint(8)=sqrt(BTOSLint(8) + (0.017*BTOSLint(8))^2 +
(lengthBT7*endBOSLerror(8))^2);

%Creating TTOSL (dose dependent+dose independent) points for plotting.
Ttestintergral=Ttestintergral';
Ttesterror=Ttesterror';
TTOSLplot=TTOSLint./Ttestintergral;
TTOSLploterror=sqrt(TTOSLplot.^2.*((errorTTOSLint./TTOSLint).^2 +
(Ttesterror./Ttestintergral).^2));



%Creating BTOSL (less dose dependent?) points for plotting
Btestintergral=Btestintergral';
Btesterror=Btesterror';
BTOSLplot=BTOSLint./Btestintergral;
BTOSLploterror=sqrt(BTOSLplot.^2.*((errorBTOSLint./BTOSLint).^2 +
(Btesterror./Btestintergral).^2));

%Creating ReOSL (dose dependent TT-OSL) points.
ReOSLplot=TTOSLplot-BTOSLplot;
ReOSLploterror=sqrt(TTOSLploterror.^2 + BTOSLploterror.^2);

%Defining Naturals and cropping plots
TTnat=TTOSLplot(1);
TTnaterror=TTOSLploterror(1);
TTOSLplot(1)=[];
TTOSLploterror(1)=[];
Trecyclingratio=TTOSLplot(1)/TTOSLplot(7);
if Trecyclingratio<1
    Trecyclingratio=1/Trecyclingratio;
```

```
end
ynatTT=ynat.*TTnat;
ynatTTerror=ynat.*TTnaterror;

BTnat=BTOSLplot(1);
BTnaterror=BTOSLploterror(1);
BTOSLplot(1)=[];
BTOSLploterror(1)=[];
Brecyclingratio=TTOSLplot(1)/TTOSLplot(7);
if Brecyclingratio<1
    Brecyclingratio=1/Brecyclingratio;
end
ynatBT=ynat.*BTnat;
ynatBTerror=ynat.*BTnaterror;

Renat=ReOSLplot(1);
Renaterror=ReOSLploterror(1);
ReOSLplot(1)=[];
ReOSLploterror(1)=[];
Rrecyclingratio=ReOSLplot(1)/ReOSLplot(7);
if Rrecyclingratio<1
    Rrecyclingratio=1/Rrecyclingratio;
end
ynatRe=ynat.*Renat;
ynatReerror=ynat.*Renaterror;


%Plotting
subplot(4,1,1), errorbar(xnat,ynatRe,ynatReerror,'k-')
hold on
subplot(4,1,1), errorbar(cycles,ReOSLplot,ReOSLploterror,'bo');
hold off
title(aliquot)
xlim([-1 3001]);
subplot(4,1,2), errorbar(xnat,ynatTT,ynatTTerror,'k-');
hold on
subplot(4,1,2), errorbar(cycles,TTOSLplot,TTOSLploterror,'bo');
hold off
title('All thermally transferred signal')
xlim([-1 3001]);
subplot(4,1,3), errorbar(xnat,ynatBT,ynatBTerror,'k-');
hold on
subplot(4,1,3), errorbar(cycles,BTOSLplot,BTOSLploterror,'bo');
hold off
xlim([-1 3001]);
title('Less dose dependent(?) signal');
subplot(4,1,4),
plot(xtestTT,Ttestintergral,'bx',xtestBT,Btestintergral,'bx');
title('Sensitivity changes');
xlim([-1 8]);


%**********above this was tested (and modified) to success on 08/12/2011.
```

```
%    good=input('Good aliquot? (y=1)');
%    if good ==1


%**********************************************************************
    %******************    PART THREE
**********************************

%**********************************************************************

    %Part three fits curves to data, and finds out whether the curves are
%reasonable.

%This part is much improved from earlier versions (pre 10/02/2012) by
'try'
%and 'catch' functions. Thanks to Tilanka.

goflin=0;
gofsate=0;
gofsatelin=0;

%Fitting grains

%if Rgood==1
    Rfit=ReOSLplot';
    Rw=(1./(ReOSLploterror.^2))';

    %Creating start points for saturating exponential
%
RstartptF2(1)=Rfit(4);
RstartptF2(2)=0.0001;
RstartptF2(3)=Rfit(6);
RstartptF2=RstartptF2';

RlowF2(1)=RstartptF2(1)-2;
RuppF2(1)=RstartptF2(1)+2;
RlowF2(2)=RstartptF2(2)-5;
RuppF2(2)=RstartptF2(2)+5;
RlowF2(3)=RstartptF2(3)-2;
RuppF2(3)=RstartptF2(3)+2;

%Creating start points for saturating exponential plus linear

RstartptF3(1)=Rfit(3);
RstartptF3(2)=0.01;
RstartptF3(3)=0.001;
RstartptF3(4)=Rfit(3);
RstartptF3=RstartptF3';

%RlowF3(1)=RstartptF3(1)-100;
%RuppF3(1)=RstartptF3(1)+100;
%RlowF3(2)=0;
%RuppF3(2)=RstartptF3(2)+5;
```

```
%RlowF3(3)=0;
%RuppF3(3)=RstartptF3(3)+1;
%RlowF3(4)=RstartptF3(4)-100;
%RuppF3(4)=RstartptF3(4)+100;

R1=0;
try
    [Rf1,goflin]=fit(x,Rfit,F1,'Weights',Rw);
catch
    disp('Rf1 cannot be fitted')
    R1=1;
end
R2=0;
try
    [Rf2,gofsate]=fit(x,Rfit,F2,'StartPoint',
RstartptF2,'Weights',Rw,'Lower', RlowF2, 'Upper', RuppF2);
catch
    disp('Rf2 cannot be fitted')
    R2=1;
end
R3=0;
try
    [Rf3,gofsatelin]=fit(x,Rfit,F3,'StartPoint',RstartptF3,'Weights',Rw);
    %'Lower', RlowF3, 'Upper', RuppF3, 'Weights',Rw);
catch
    disp('Rf3 cannot be fitted')
    R3=1;
end
%    R1R2=(1/7)*((abs(Rfit(1)-Rf1(
%R1R2=0.125*(abs(Rfit(1)-Rf1(300))/ReOSLploterror(1)+abs(Rfit(2)-
Rf1(600))/ReOSLploterror(2) + abs(Rfit(3)-Rf1(1000))/ReOSLploterror(3) +
abs(Rfit(4)-Rf1(2000))/ReOSLploterror(4) + abs(Rfit(5)-
Rf1(3000))/ReOSLploterror(5) + abs(Rfit(6)-Rf1(0))/ReOSLploterror(6) +
abs(Rfit(7)-Rf1(300))/ReOSLploterror(7))
%R2R2=0.125*(abs(Rfit(1)-Rf2(300))/ReOSLploterror(1)+abs(Rfit(2)-
Rf2(600))/ReOSLploterror(2) + abs(Rfit(3)-Rf2(1000))/ReOSLploterror(3) +
abs(Rfit(4)-Rf2(2000))/ReOSLploterror(4) + abs(Rfit(5)-
Rf2(3000))/ReOSLploterror(5) + abs(Rfit(6)-Rf2(0))/ReOSLploterror(6) +
abs(Rfit(7)-Rf2(300))/ReOSLploterror(7))
%R3R2=0.125*(abs(Rfit(1)-Rf3(300))/ReOSLploterror(1)+abs(Rfit(2)-
Rf3(600))/ReOSLploterror(2) + abs(Rfit(3)-Rf3(1000))/ReOSLploterror(3) +
abs(Rfit(4)-Rf3(2000))/ReOSLploterror(4) + abs(Rfit(5)-
Rf3(3000))/ReOSLploterror(5) + abs(Rfit(6)-Rf3(0))/ReOSLploterror(6) +
abs(Rfit(7)-Rf3(300))/ReOSLploterror(7))
%The higher the number the less good the fit.

%R1R2numer=(Rfit(1)-Rf1(300))^2+(Rfit(2)-Rf1(600))^2 + (Rfit(3)-
Rf1(1000))^2 + (Rfit(4)-Rf1(2000))^2 + (Rfit(5)-Rf1(3000))^2 + (Rfit(6)-
Rf1(0))^2 + (Rfit(7)-Rf1(300))^2;
%R1R2denom=sum(ReOSLploterror.^2);

%R1R2=1-R1R2numer/R1R2denom

figure
plot(xnat,ynatRe,'k-');
hold on
```

```
plot(cycles,ReOSLplot,'bo');
if R1~=1
plot(Rf1,'r-');
end
if R2~=1
plot(Rf2,'g-');
end
if R3~=1
plot(Rf3,'b-');
end
legend off
hold off

fitgoodR=0;
fitgoodR=input('Do the curves fit? (1=yes)');
if fitgoodR==1
try
    goflin
    gofsate
    gofsatelin
catch
    disp('Some fits did not work.')
end
    %end
goflin=0;
gofsate=0;
gofsatelin=0;
%resetting fitgood
fitgoodR=0;
fitgoodR=input('which fit is good? (red=1, green=2, blue=3, none=0');
end
    %below modded 23/01/11
if fitgoodR==1
    Rgood=1;
elseif fitgoodR==2
        Rgood=1;
elseif fitgoodR==3
        Rgood=1;
else
    Rgood=0;
end

close figure 2

%Note that the coefficient variances are assuming a normal distribution
if fitgoodR==1
    coeffsR=coeffvalues(Rf1);
    variancescoeffsR=confint(Rf1,0.682689);
    variancescoeffsR=variancescoeffsR(2,:)-coeffsR;
    optionsR=fitoptions('Method','LinearLeastSquares','Weights',Rw);
    goodfitR=F1;
end

%RlowF2=RstartptF2-50;
%RuppF2=RstartptF2+50;
```

```
%Changed 13/04/12
try
RlowF2=coeffvalues(Rf2)-25;
RuppF2=coeffvalues(Rf2)+25;
RstartptF2=coeffvalues(Rf2);
end

if fitgoodR==2
    coeffsR=coeffvalues(Rf2);
    variancescoeffsR=confint(Rf2,0.682689);
    variancescoeffsR=variancescoeffsR(2,:)-coeffsR;

optionsR=fitoptions('Method','NonlinearLeastSquares','Weights',Rw,'StartP
oint',RstartptF2,'Lower',RlowF2,'Upper',RuppF2);
    goodfitR=F2;
end

%RlowF3=RstartptF3-50;
%RuppF3=RstartptF3+50;

%Changed 13/04/12
try
RlowF3=coeffvalues(Rf3)-25;
RuppF3=coeffvalues(Rf3)+25;
RstartptF3=coeffvalues(Rf3);
end

if fitgoodR==3
    coeffsR=coeffvalues(Rf3);
    variancescoeffsR=confint(Rf3,0.682689);
    variancescoeffsR=variancescoeffsR(2,:)-coeffsR;

optionsR=fitoptions('Method','NonlinearLeastSquares','Weights',Rw,'StartP
oint',RstartptF3,'Lower',RlowF3,'Upper',RuppF3);
    goodfitR=F3;
end
%end for 'if Rgood =1
%end


%if Tgood==1
Tfit=TTOSLplot';
Tw=(1./(TTOSLploterror.^2))';

%Creating start points for saturating exponential
TstartptF2(1)=Tfit(4);
TstartptF2(2)=0.0001;
if Tfit(6) > 0
TstartptF2(3)=Tfit(6);
else
    TstartF2(3) = 0;
end
TstartptF2=TstartptF2';

TlowF2(1)=TstartptF2(1)-2;
```

```
TuppF2(1)=TstartptF2(1)+2;
TlowF2(2)=TstartptF2(2)-5;
TuppF2(2)=TstartptF2(2)+5;
TlowF2(3)=0;
TuppF2(3)=TstartptF2(3)+2;

%Creating start points for saturating exponential plus linear
TstartptF3(1)=Tfit(4);
TstartptF3(2)=0.01;
TstartptF3(3)=0.001;
TstartptF3(4)=Tfit(4);
TstartptF3=TstartptF3';

%TlowF3(1)=TstartptF3(1)-100;
%TuppF3(1)=TstartptF3(1)+100;
%TlowF3(2)=0;
%TuppF3(2)=TstartptF3(2)+5;
%TlowF3(3)=0;
%TuppF3(3)=TstartptF3(3)+1;
%TlowF3(4)=TstartptF3(4)-100;
%TuppF3(4)=TstartptF3(4)+100;

T1=0;
try
[Tf1,goflin]=fit(x,Tfit,F1,'Weights',Tw);
catch
    disp('Tf1 cannot be fitted')
    T1=1;
end
T2=0;
try
[Tf2,gofsate]=fit(x,Tfit,F2,'Weights',Tw,'StartPoint',TstartptF2,
'Lower',TlowF2,'Upper',TuppF2);
catch
    disp('Tf2 cannot be fitted')
    T2=1;
end
T3=0;
try
[Tf3,gofsatelin]=fit(x,Tfit,F3,'Weights',Tw,'StartPoint',TstartptF3);
%,'Lower',TlowF3,'Upper',TuppF3);
catch
    disp('Tf3 cannot be fitted')
    T3=1;
end

figure
plot(xnat,ynatTT,'k-');
hold on
plot(cycles,TTOSLplot,'bo');
if T1~=1;
plot(Tf1,'r-');
end
if T2~=1
plot(Tf2,'g-');
end
```

```
if T3~=1
plot(Tf3,'b-');
end
legend off
hold off

%reset seegof
seegof=0;
fitgoodT=input('Do the curves fit? (1=yes)');
if fitgoodT==1
try
    goflin
    gofsate
    gofsatelin
catch
    disp('Some fits did not work.')
end
    %end
goflin=0;
gofsate=0;
gofsatelin=0;

%resetting fitgood
fitgoodT=0;
fitgoodT=input('Which fit is good? (red=1, green=2, blue=3, none=0');
end

if fitgoodT==1
    Tgood=1;
elseif fitgoodT==2
    Tgood=1;
elseif fitgoodT==3
    Tgood=1;
else Tgood=0;
end

close figure 2

%Note that the coefficient variances are assuming a normal distribution.
if fitgoodT==1
    coeffsT=coeffvalues(Tf1);
    variancescoeffsT=confint(Tf1,0.682689);
    variancescoeffsT=variancescoeffsT(2,:)-coeffsT;
    optionsT=fitoptions('Method','LinearLeastSquares','Weights',Tw);
    goodfitT=F1;
end

%TlowF2=TstartptF2-50;
%TuppF2=TstartptF2+50;

%Changed 13/04/12
try
TlowF2=coeffvalues(Tf2)-25;
TuppF2=coeffvalues(Tf2)+25;
TstartptF2=coeffvalues(Tf2);
```

```
end

if fitgoodT==2
    coeffsT=coeffvalues(Tf2);
    variancescoeffsT=confint(Tf2,0.682689);
    variancescoeffsT=variancescoeffsT(2,:)-coeffsT;

optionsT=fitoptions('Method','NonlinearLeastSquares','Weights',Tw,'StartP
oint',TstartptF2,'Lower',TlowF2,'Upper',TuppF2);
    goodfitT=F2;
end

%TlowF3=TstartptF3-50;
%TuppF3=TstartptF3+50;

%Changed 13/04/12
try
TlowF3=coeffvalues(Tf3)-25;
TuppF3=coeffvalues(Tf3)+25;
TstartptF3=coeffvalues(Tf3);
end

if fitgoodT==3
    coeffsT=coeffvalues(Tf3);
    variancescoeffsT=confint(Tf3,0.682689);
    variancescoeffsT=variancescoeffsT(2,:)-coeffsT;

optionsT=fitoptions('Method','NonlinearLeastSquares','Weights',Tw,'StartP
oint',TstartptF3,'Lower',TlowF3,'Upper',TuppF3);
    goodfitT=F3;
end

%endifTgood==1
%end

%resetting fitgood
%if Bgood==1
    Bfit=BTOSLplot';
    Bw=(1./(BTOSLploterror.*2))';

    %Creating start points for saturating exponential
%BstartptF2(1)=Bfit(3);
%BstartptF2(2)=0.01;
%BstartptF2(3)=Bfit(3);
%BstartptF2=BstartptF2';

%BstartptF2(1)=Bfit(3);
%BstartptF2(2)=0.1;
%if Bfit(4) > 0
%BstartptF2(3)=Bfit(4);
%else
%    BstartF2(3) = 0;
%end
%BstartptF2=BstartptF2';
```

```
%BlowF2(1)=BstartptF2(1)-0.5;
%BuppF2(1)=BstartptF2(1)+0.5;
%BlowF2(2)=BstartptF2(2)-20;
%BuppF2(2)=BstartptF2(2)+20;
%BlowF2(3)=0;
%BuppF2(3)=BstartptF2(3)+0.01;

BstartptF2(1)=Bfit(4);
BstartptF2(2)=0.0001;
if Bfit(6) > 0
BstartptF2(3)=Bfit(6);
else
    BstartF2(3) = 0;
end
BstartptF2=BstartptF2';

BlowF2(1)=BstartptF2(1)-2;
BuppF2(1)=BstartptF2(1)+2;
BlowF2(2)=BstartptF2(2)-5;
BuppF2(2)=BstartptF2(2)+5;
BlowF2(3)=0;
BuppF2(3)=BstartptF2(3)+2;


%Creating start points for saturating exponential plus linear
BstartptF3(1)=Bfit(3);
BstartptF3(2)=0.01;
BstartptF3(3)=0.001;
BstartptF3(4)=Bfit(3);
BstartptF3=BstartptF3';

%BlowF3(1)=BstartptF3(1)-25;
%BuppF3(1)=BstartptF3(1)+25;
%BlowF3(2)=0;
%BuppF3(2)=BstartptF3(2)+1;
%BlowF3(3)=0;
%BuppF3(3)=BstartptF3(3)+1;
%BlowF3(4)=BstartptF3(4)-2;
%BuppF3(4)=BstartptF3(4)+2;

B1=0;
try
    [Bf1,goflin]=fit(x,Bfit,F1,'Weights',Bw);
catch
    disp('Bf1 cannot be fitted.')
B1=1;
end
B2=0;
try
[Bf2,gofsate]=fit(x,Bfit,F2,'Weights',Bw,'StartPoint',BstartptF2,'Lower',
BlowF2,'Upper',BuppF2);
catch
    disp('Bf2 cannot be fitted.')
    B2=1;
```

```
end
B3=0;
try
    [Bf3,gofsatelin]=fit(x,Bfit,F3,'Weights',Bw,'StartPoint',BstartptF3);
    %,'Lower',BlowF3,'Upper',BuppF3);
catch
    disp('Bf3 cannot be fitted.')
    B3=1;
end

figure
    plot(xnat,ynatBT,'k-');
    hold on
    plot(cycles,BTOSLplot,'bo');
    if B1~=1
    plot(Bf1,'r-');
    end
    if B2~=1
        plot(Bf2,'g-');
    end
    if B3~=1
        plot(Bf3,'b-');
    end
    legend off
    hold off

    fitgoodB=0;
    fitgoodB=input('Do the curves fit? (1=yes)');
    if fitgoodB==1
    try
        goflin
        gofsate
        gofsatelin
    catch
        disp('Some fits did not work.')
    end
 %   end
goflin=0;
gofsate=0;
gofsatelin=0;

    fitgoodB=0;
    fitgoodB=input('Which fit is best? red=1, green=2, blue=3, none=0');

    end

    if fitgoodB==1
        Bgood=1;
    elseif fitgoodB==2
        Bgood=1;
    elseif fitgoodB==3
        Bgood=1;
    else Bgood=0;
    end

    close figure 2
```

```
    if fitgoodB==1
        coeffsB=coeffvalues(Bf1);
        variancescoeffsB=confint(Bf1,0.682689);
        variancescoeffsB=variancescoeffsB(2,:)-coeffsB;
        optionsB=fitoptions('Method','LinearLeastSquares','Weights',Bw);
        goodfitB=F1;
    end

%BlowF2=BstartptF2-50;
%BuppF2=BstartptF2+50;

%Changed 13/04/12
try
BlowF2=coeffvalues(Bf2)-25;
BuppF2=coeffvalues(Bf2)+25;
BstartptF2=coeffvalues(Bf2);
end

    if fitgoodB==2
        coeffsB=coeffvalues(Bf2);
        variancescoeffsB=confint(Bf2,0.682689);
        variancescoeffsB=variancescoeffsB(2,:)-coeffsB;

optionsB=fitoptions('Method','NonlinearLeastSquares','Weights',Bw,'StartP
oint',BstartptF2,'Lower',BlowF2,'Upper',BuppF2);
        goodfitB=F2;
    end

%BlowF3=BstartptF3-50;
%BuppF3=BstartptF3+50;

%Changed 13/04/12
try
BlowF3=coeffvalues(Bf3)-25;
BuppF3=coeffvalues(Bf3)+25;
BstartptF3=coeffvalues(Bf3);
end

    if fitgoodB==3
        coeffsB=coeffvalues(Bf3);
        variancescoeffsB=confint(Bf3,0.682689);
        variancescoeffsB=variancescoeffsB(2,:)-coeffsB;

optionsB=fitoptions('Method','NonlinearLeastSquares','Weights',Bw,'StartP
oint',BstartptF3,'Lower',BlowF3,'Upper',BuppF3);
        goodfitB=F3;
    end

    %endifBgood==1
%end

%end part three
```

```
%*********************************************************************
    %******************    PART FOUR
***********************************

%*********************************************************************

    %part five creates x-values, variances, covariances, and errors.
%Clearing variables that have variable size
clear covarR covarT covarB
%creating estimation of covariance via jackknife-like calculation.

if Rgood==1
    %Exclusion value things
    %creating logical vectors for excluding points.
ee1=[1;0;0;0;0;0;0];
ee1=logical(ee1);
e1=excludedata(x,Rfit,'indices',ee1);

ee2=[0;1;0;0;0;0;0];
ee2=logical(ee2);
e2=excludedata(x,Rfit,'indices',ee2);

ee3=[0;0;1;0;0;0;0];
ee3=logical(ee3);
e3=excludedata(x,Rfit,'indices',ee3);

ee4=[0;0;0;1;0;0;0];
ee4=logical(ee4);
e4=excludedata(x,Rfit,'indices',ee4);

ee5=[0;0;0;0;1;0;0];
ee5=logical(ee5);
e5=excludedata(x,Rfit,'indices',ee5);

ee6=[0;0;0;0;0;1;0];
ee6=logical(ee6);
e6=excludedata(x,Rfit,'indices',ee6);

ee7=[0;0;0;0;0;0;1];
ee7=logical(ee7);
e7=excludedata(x,Rfit,'indices',ee7);

%Creating coefficient matrix:
options1=fitoptions(optionsR,'Exclude',e1);
fitr1=fit(x,Rfit,goodfitR,options1);
covarR(1,:)=coeffvalues(fitr1);
covarR(1,:)=covarR(1,:)-coeffsR;

options2=fitoptions(optionsR,'Exclude',e2);
fitr2=fit(x,Rfit,goodfitR,options2);
covarR(2,:)=coeffvalues(fitr2);
covarR(2,:)=covarR(2,:)-coeffsR;
```

```
options3=fitoptions(optionsR,'Exclude',e3);
fitr3=fit(x,Rfit,goodfitR,options3);
covarR(3,:)=coeffvalues(fitr3);
covarR(3,:)=covarR(3,:)-coeffsR;

options4=fitoptions(optionsR,'Exclude',e4);
fitr4=fit(x,Rfit,goodfitR,options4);
covarR(4,:)=coeffvalues(fitr4);
covarR(4,:)=covarR(4,:)-coeffsR;

options5=fitoptions(optionsR,'Exclude',e5);
fitr5=fit(x,Rfit,goodfitR,options5);
covarR(5,:)=coeffvalues(fitr5);
covarR(5,:)=covarR(5,:)-coeffsR;

options6=fitoptions(optionsR,'Exclude',e6);
fitr6=fit(x,Rfit,goodfitR,options6);
covarR(6,:)=coeffvalues(fitr6);
covarR(6,:)=covarR(6,:)-coeffsR;

options7=fitoptions(optionsR,'Exclude',e7);
fitr7=fit(x,Rfit,goodfitR,options7);
covarR(7,:)=coeffvalues(fitr7);
covarR(7,:)=covarR(7,:)-coeffsR;

%Covariances: (a-A)(b-B), like variances are (a-A)(a-A)
%No. coefficients:
%linear:2 (covariances=1)
%exponential: 3 (covariances=3)
%saturating exponential plus linear: 4 (covariances=6)
VarsR=zeros(1,5);


covarR1=covarR(:,1).*covarR(:,2);
covarR1=6/7.*(sum(covarR1));

if fitgoodR==1
    covarR2=0;
    covarR3=0;
    VarsR(2:3)=variancescoeffsR;
else
    covarR2=covarR(:,1).*covarR(:,3);
    covarR2=6/7.*abs(sum(covarR2));

    covarR3=covarR(:,2).*covarR(:,3);
    covarR3=6/7.*abs(sum(covarR3));
    VarsR(2:4)=variancescoeffsR(1:3);
end

if fitgoodR==3
    covarR4=covarR(:,1).*covarR(:,4);
    covarR4=6/7.*abs(sum(covarR4));
```

```
    covarR5=covarR(:,2).*covarR(:,4);
    covarR5=6/7.*abs(sum(covarR5));

    covarR6=covarR(:,3).*covarR(:,4);
    covarR6=6/7.*abs(sum(covarR6));

    VarsR(5)=variancescoeffsR(4);
else
    covarR4=0;
    covarR5=0;
    covarR6=0;
end

%Rvariances for coefficients:

VarsR(1)=Renaterror;
VarsR=VarsR.^2;
end

%TT-OSL
%creating estimation of covariance via jackknife-like calculation.

if Tgood==1
    %Exclusion value things
    %creating logical vectors for excluding points.
ee1=[1;0;0;0;0;0;0];
ee1=logical(ee1);
e1=excludedata(x,Tfit,'indices',ee1);

ee2=[0;1;0;0;0;0;0];
ee2=logical(ee2);
e2=excludedata(x,Tfit,'indices',ee2);

ee3=[0;0;1;0;0;0;0];
ee3=logical(ee3);
e3=excludedata(x,Tfit,'indices',ee3);

ee4=[0;0;0;1;0;0;0];
ee4=logical(ee4);
e4=excludedata(x,Tfit,'indices',ee4);

ee5=[0;0;0;0;1;0;0];
ee5=logical(ee5);
e5=excludedata(x,Tfit,'indices',ee5);

ee6=[0;0;0;0;0;1;0];
ee6=logical(ee6);
e6=excludedata(x,Tfit,'indices',ee6);

ee7=[0;0;0;0;0;0;1];
ee7=logical(ee7);
e7=excludedata(x,Tfit,'indices',ee7);

%Creating coefficient matrix:
```

```
options1=fitoptions(optionsT,'Exclude',e1);
fitt1=fit(x,Tfit,goodfitT,options1);
covarT(1,:)=coeffvalues(fitt1);
covarT(1,:)=covarT(1,:)-coeffsT;

options2=fitoptions(optionsT,'Exclude',e2);
fitt2=fit(x,Tfit,goodfitT,options2);
covarT(2,:)=coeffvalues(fitt2);
covarT(2,:)=covarT(2,:)-coeffsT;

options3=fitoptions(optionsT,'Exclude',e3);
fitt3=fit(x,Tfit,goodfitT,options3);
covarT(3,:)=coeffvalues(fitt3);
covarT(3,:)=covarT(3,:)-coeffsT;

options4=fitoptions(optionsT,'Exclude',e4);
fitt4=fit(x,Tfit,goodfitT,options4);
covarT(4,:)=coeffvalues(fitt4);
covarT(4,:)=covarT(4,:)-coeffsT;

options5=fitoptions(optionsT,'Exclude',e5);
fitt5=fit(x,Tfit,goodfitT,options5);
covarT(5,:)=coeffvalues(fitt5);
covarT(5,:)=covarT(5,:)-coeffsT;

options6=fitoptions(optionsT,'Exclude',e6);
fitt6=fit(x,Tfit,goodfitT,options6);
covarT(6,:)=coeffvalues(fitt6);
covarT(6,:)=covarT(6,:)-coeffsT;

options7=fitoptions(optionsT,'Exclude',e7);
fitt7=fit(x,Tfit,goodfitT,options7);
covarT(7,:)=coeffvalues(fitt7);
covarT(7,:)=covarT(7,:)-coeffsT;

%Covariances: (a-A)(b-B), like variances are (a-A)(a-A)
%No. coefficients:
%linear:2 (covariances=1)
%exponential: 3 (covariances=3)
%saturating exponential plus linear: 4 (covariances=6)

covarT1=covarT(:,1).*covarT(:,2);
covarT1=6/7.*abs(sum(covarT1));


VarsT=zeros(1,5);

if fitgoodT==1
    covarT2=0;
    covarT3=0;

    VarsT(2:3)=variancescoeffsT;
else
    covarT2=covarT(:,1).*covarT(:,3);
```

```
    covarT2=6/7.*abs(sum(covarT2));

    covarT3=covarT(:,2).*covarT(:,3);
    covarT3=6/7.*abs(sum(covarT3));

    VarsT(2:4)=variancescoeffsT(1:3);
end

if fitgoodT==3
    covarT4=covarT(:,1).*covarT(:,4);
    covarT4=6/7.*abs(sum(covarT4));

    covarT5=covarT(:,2).*covarT(:,4);
    covarT5=6/7.*abs(sum(covarT5));

    covarT6=covarT(:,3).*covarT(:,4);
    covarT6=6/7.*abs(sum(covarT6));

    VarsT(5)=variancescoeffsT(4);
else
    covarT4=0;
    covarT5=0;
    covarT6=0;
end

end
VarsT(1)=TTnaterror;
VarsT=VarsT.^2;

%BB-OSL
%creating estimation of covariance via jackknife-like calculation.

if Bgood==1
    %Exclusion value things
    %creating logical vectors for excluding points.
ee1=[1;0;0;0;0;0;0];
ee1=logical(ee1);
e1=excludedata(x,Bfit,'indices',ee1);

ee2=[0;1;0;0;0;0;0];
ee2=logical(ee2);
e2=excludedata(x,Bfit,'indices',ee2);

ee3=[0;0;1;0;0;0;0];
ee3=logical(ee3);
e3=excludedata(x,Bfit,'indices',ee3);

ee4=[0;0;0;1;0;0;0];
ee4=logical(ee4);
e4=excludedata(x,Bfit,'indices',ee4);

ee5=[0;0;0;0;1;0;0];
ee5=logical(ee5);
e5=excludedata(x,Bfit,'indices',ee5);
```

```
ee6=[0;0;0;0;0;1;0];
ee6=logical(ee6);
e6=excludedata(x,Bfit,'indices',ee6);

ee7=[0;0;0;0;0;0;1];
ee7=logical(ee7);
e7=excludedata(x,Bfit,'indices',ee7);

%Creating coefficient matrix:
options1=fitoptions(optionsB,'Exclude',e1);
fitb1=fit(x,Bfit,goodfitB,options1);
covarB(1,:)=coeffvalues(fitb1);
covarB(1,:)=covarB(1,:)-coeffsB;

options2=fitoptions(optionsB,'Exclude',e2);
fitb2=fit(x,Bfit,goodfitB,options2);
covarB(2,:)=coeffvalues(fitb2);
covarB(2,:)=covarB(2,:)-coeffsB;

options3=fitoptions(optionsB,'Exclude',e3);
fitb3=fit(x,Bfit,goodfitB,options3);
covarB(3,:)=coeffvalues(fitb3);
covarB(3,:)=covarB(3,:)-coeffsB;

options4=fitoptions(optionsB,'Exclude',e4);
fitb4=fit(x,Bfit,goodfitB,options4);
covarB(4,:)=coeffvalues(fitb4);
covarB(4,:)=covarB(4,:)-coeffsB;

options5=fitoptions(optionsB,'Exclude',e5);
fitb5=fit(x,Bfit,goodfitB,options5);
covarB(5,:)=coeffvalues(fitb5);
covarB(5,:)=covarB(5,:)-coeffsB;

options6=fitoptions(optionsB,'Exclude',e6);
fitb6=fit(x,Bfit,goodfitB,options6);
covarB(6,:)=coeffvalues(fitb6);
covarB(6,:)=covarB(6,:)-coeffsB;

options7=fitoptions(optionsB,'Exclude',e7);
fitb7=fit(x,Bfit,goodfitB,options7);
covarB(7,:)=coeffvalues(fitb7);
covarB(7,:)=covarB(7,:)-coeffsB;

%Covariances: (a-A)(b-B), like variances are (a-A)(a-A)
%No. coefficients:
%linear:2 (covariances=1)
%exponential: 3 (covariances=3)
%saturating exponential plus linear: 4 (covariances=6)

covarB1=covarB(:,1).*covarB(:,2);
covarB1=6/7.*abs(sum(covarB1));
```

```
VarsB=zeros(1,5);

if fitgoodB==1
    covarB2=0;
    covarB3=0;

    VarsB(2:3)=variancescoeffsB;
else
    covarB2=covarB(:,1).*covarB(:,3);
    covarB2=6/7.*abs(sum(covarB2));

    covarB3=covarB(:,2).*covarB(:,3);
    covarB3=6/7.*abs(sum(covarB3));

    VarsB(2:4)=variancescoeffsB(1:3);
end

if fitgoodB==3
    covarB4=covarB(:,1).*covarB(:,4);
    covarB4=6/7.*abs(sum(covarB4));

    covarB5=covarB(:,2).*covarB(:,4);
    covarB5=6/7.*abs(sum(covarB5));

    covarB6=covarB(:,3).*covarB(:,4);
    covarB6=6/7.*abs(sum(covarB6));

    VarsB(2:5)=variancescoeffsB(4);

else
    covarB4=0;
    covarB5=0;
    covarB6=0;
end

VarsB(1)=BTnaterror;
VarsB=VarsB.^2;

end


%Note that partial derivatives depend on x for saturating exponential
plus
%linear part. Therefore x must be found at least for this fit before
%partial derivates are calculated.

%Finding x:

%For Re-OSL
if Rgood==1
    if fitgoodR==1
        RX=(Renat-coeffsR(2))/coeffsR(1);
    end
    if fitgoodR==2
```

```
        RX=-1/coeffsR(2)*log((coeffsR(3)-Renat)/coeffsR(1));
    end
    if fitgoodR==3
   %Note that there are these restrictions in the sat exp plus lin
result:
   %-No extrapolation
   %-'Digital' type result with resolution 0.001.
   %-Always rounds up, not down (for positive slope).
        RX3=linspace(0.001,3000,300000);
        RY3=-coeffsR(1).*exp(-coeffsR(2).*RX3) + coeffsR(3).*RX3 +
coeffsR(4);
        RX=0;
        for hh=1:300000
            if RY3(300001-hh)>Renat;
                RX=RX3(300001-hh);
            end
        end
    end
end

%For TT-OSL
if Tgood==1
    if fitgoodT==1
        TX=(TTnat-coeffsT(2))/coeffsT(1);
    end
    if fitgoodT==2
        TX=-1/coeffsT(2)*log((coeffsT(3)-TTnat)/coeffsT(1));
    end
    if fitgoodT==3
   %Note that there are these restrictions in the sat exp plus lin
result:
   %-No extrapolation
   %-'Digital' type result with resolution 0.001.
   %-Always rounds up, not down (for positive slope).
        TX3=linspace(0.001,3000,300000);
        TY3=-coeffsT(1).*exp(-coeffsT(2).*TX3) + coeffsT(3).*TX3 +
coeffsT(4);
        TX=0;
        for hh=1:300000
            if TY3(300001-hh)>TTnat;
                TX=TX3(300001-hh);
            end
        end
    end
end


%For BT-OSL
if Bgood==1
    if fitgoodB==1
        BX=(BTnat-coeffsB(2))/coeffsB(1);
    end
    if fitgoodB==2
        BX=-1/coeffsB(2)*log((coeffsB(3)-BTnat)/coeffsB(1));
    end
    if fitgoodB==3
```

```
   %Note that there are these restrictions in the sat exp plus lin
result:
   %-No extrapolation
   %-'Digital' type result with resolution 0.001.
   %-Always rounds up, not down (for positive slope).
        BX3=linspace(0.001,3000,300000);
        BY3=-coeffsB(1).*exp(-coeffsB(2).*BX3) + coeffsB(3).*BX3 +
coeffsB(4);
        BX=0;
        for hh=1:300000
            if BY3(300001-hh)>BTnat;
                BX=BX3(300001-hh);
            end
        end
    end
end



%Creating Partial Derivatives

%For Re-OSL
if Rgood==1
    if fitgoodR==1
        Rdxdy=1/coeffsR(1);
        Rdxda=-1/coeffsR(1);
        Rdxdb=(coeffsR(2)-Renat)/(coeffsR(1)^2);
        Rdxdc=0;
        Rdxdd=0;
    end
    if fitgoodR==2
        Rdxdy=1/(coeffsR(2)*(coeffsR(3)-Renat));
        Rdxda=1/(coeffsR(1)*coeffsR(2));
        Rdxdb=(log((coeffsR(3)-Renat)/coeffsR(1)))/(coeffsR(2)^2);
        Rdxdc=-1/(coeffsR(2)*(coeffsR(3)-Renat));
        Rdxdd=0;
    end
   if fitgoodR==3
       Rdxdy=1/(coeffsR(1)*coeffsR(2)*exp(-coeffsR(2)*RX) + coeffsR(3));
       Rdxda=1/(exp(coeffsR(2)*RX)*(-Renat*coeffsR(2) +
coeffsR(4)*coeffsR(2) + coeffsR(3)*(1+(coeffsR(2)*RX))));
       %changed 13/12/11 on all R,T,B.
       %Rdxda=1/((coeffsR(3)*(RX/coeffsR(2))-Renat +
coeffsR(4))*coeffsR(2)*exp(coeffsR(2)*RX));
       Rdxdb=1/(RX^-2*log((coeffsR(3)*RX + coeffsR(4) -
Renat)/coeffsR(3)) - (1/RX)*(coeffsR(3)/(coeffsR(3)*RX + coeffsR(4) -
Renat)));
       Rdxdc=1/(-(Renat/(RX^2))+(coeffsR(4)/(RX^2))-((coeffsR(1)*exp(-
coeffsR(2)*RX))/(RX^2))-((coeffsR(2)*coeffsR(1)*exp(-
coeffsR(2)*RX))/(RX)));
       Rdxdd=1/(-(coeffsR(3) - coeffsR(1)*coeffsR(2)*exp(-
coeffsR(2)*RX)));
   end
end

%For TT-OSL
```

```
if Tgood==1
    if fitgoodT==1
        Tdxdy=1/coeffsT(1);
        Tdxda=-1/coeffsT(1);
        Tdxdb=(coeffsT(2)-TTnat)/(coeffsT(1)^2);
        Tdxdc=0;
        Tdxdd=0;
    end
    if fitgoodT==2
        Tdxdy=1/(coeffsT(2)*(coeffsT(3)-TTnat));
        Tdxda=1/(coeffsT(1)*coeffsT(2));
        Tdxdb=(log((coeffsT(3)-TTnat)/coeffsT(1)))/(coeffsT(2)^2);
        Tdxdc=-1/(coeffsT(2)*(coeffsT(3)-TTnat));
        Tdxdd=0;
    end
   if fitgoodT==3
       Tdxdy=1/(coeffsT(1)*coeffsT(2)*exp(-coeffsT(2)*TX) + coeffsT(3));
       Tdxda=1/(exp(coeffsT(2)*TX)*(-TTnat*coeffsT(2) +
coeffsT(4)*coeffsT(2) + coeffsT(3)*(1+(coeffsT(2)*TX))));
       Tdxdb=1/(TX^-2*log((coeffsT(3)*TX + coeffsT(4) -
TTnat)/coeffsT(3)) - (1/TX)*(coeffsT(3)/(coeffsT(3)*TX + coeffsT(4) -
TTnat)));
       Tdxdc=1/(-(TTnat/(TX^2))+(coeffsT(4)/(TX^2))-((coeffsT(1)*exp(-
coeffsT(2)*TX))/(TX^2))-((coeffsT(2)*coeffsT(1)*exp(-
coeffsT(2)*TX))/(TX)));
       Tdxdd=1/(-(coeffsT(3) - coeffsT(1)*coeffsT(2)*exp(-
coeffsT(2)*TX)));
   end
end


%For BT-OSL
if Bgood==1
    if fitgoodB==1
        Bdxdy=1/coeffsB(1);
        Bdxda=-1/coeffsB(1);
        Bdxdb=(coeffsB(2)-BTnat)/(coeffsB(1)^2);
        Bdxdc=0;
        Bdxdd=0;
    end
    if fitgoodB==2
        Bdxdy=1/(coeffsB(2)*(coeffsB(3)-BTnat));
        Bdxda=1/(coeffsB(1)*coeffsB(2));
        Bdxdb=(log((coeffsB(3)-BTnat)/coeffsB(1)))/(coeffsB(2)^2);
        Bdxdc=-1/(coeffsB(2)*(coeffsB(3)-BTnat));
        Bdxdd=0;
    end
   if fitgoodB==3
       Bdxdy=1/(coeffsB(1)*coeffsB(2)*exp(-coeffsB(2)*BX) + coeffsB(3));
       Bdxda=1/(exp(coeffsB(2)*BX)*(-BTnat*coeffsB(2) +
coeffsB(4)*coeffsB(2) + coeffsB(3)*(1+(coeffsB(2)*BX))));
       Bdxdb=1/(BX^-2*log((coeffsB(3)*BX + coeffsB(4) -
BTnat)/coeffsB(3)) - (1/BX)*(coeffsB(3)/(coeffsB(3)*BX + coeffsB(4) -
BTnat)));
```

```
       Bdxdc=1/(-(BTnat/(BX^2))+(coeffsB(4)/(BX^2))-((coeffsB(1)*exp(-
coeffsB(2)*BX))/(BX^2))-((coeffsB(2)*coeffsB(1)*exp(-
coeffsB(2)*BX))/(BX)));
       Bdxdd=1/(-(coeffsB(3) - coeffsB(1)*coeffsB(2)*exp(-
coeffsB(2)*BX)));
   end
end



%Have partial derivatives eg "Rdxdy", variances eg "VarsR(1)",
covariances
%eg "covarR1", x values eg "RX". Now to find variances:

if Rgood==1
    Rvariance=VarsR(1)*(Rdxdy.^2) + VarsR(2)*(Rdxda.^2) +
VarsR(3)*(Rdxdb.^2) + VarsR(4)*(Rdxdc.^2) +
VarsR(5)*(Rdxdd.^2)+2*covarR1*Rdxda*Rdxdb + 2*covarR2*Rdxda*Rdxdc +
2*covarR3*Rdxdb*Rdxdc + 2*covarR4*Rdxda*Rdxdd + 2*covarR5*Rdxdb*Rdxdd +
2*covarR6*Rdxdc*Rdxdd;
Rerror=real(sqrt(Rvariance));
end

if Tgood==1
    Tvariance=VarsT(1)*(Tdxdy.^2) + VarsT(2)*(Tdxda.^2) +
VarsT(3)*(Tdxdb.^2) + VarsT(4)*(Tdxdc.^2) + VarsT(5)*(Tdxdd.^2) +
2*covarT1*Tdxda*Tdxdb + 2*covarT2*Tdxda*Tdxdc + 2*covarT3*Tdxdb*Tdxdc +
2*covarT4*Tdxda*Tdxdd + 2*covarT5*Tdxdb*Tdxdd + 2*covarT6*Tdxdc*Tdxdd;
Terror=real(sqrt(Tvariance));
end

if Bgood==1
    Bvariance=VarsB(1)*(Bdxdy.^2) + VarsB(2)*(Bdxda.^2) +
VarsB(3)*(Bdxdb.^2) + VarsB(4)*(Bdxdc.^2) + VarsB(5)*(Bdxdd.^2) +
2*covarB1*Bdxda*Bdxdb + 2*covarB2*Bdxda*Bdxdc + 2*covarB3*Bdxdb*Bdxdc +
2*covarB4*Bdxda*Bdxdd + 2*covarB5*Bdxdb*Bdxdd + 2*covarB6*Bdxdc*Bdxdd;
Berror=real(sqrt(Bvariance));
end



%So have RX, TX, BX, Rerror, Terror, Berror



%*********************************************************************
    %******************    PART FIVE
**********************************

%*********************************************************************

%Part 5 calculates ages from dose in seconds, and writes information to a
%file.
```

```
%Assuming dose error=0 for now.

%Importing in values: dose, aliquot, WK4dr, WK4drerror, RX, TX, BX,
Rerror,
%Terror, Berror Rrecyclingratio, Trecyclingratio, Brecyclingratio, peakT,
%peakB, lengthT, lengthB

%Importing also Rgood, Tgood, Bgood, fitgoodR, fitgoodT, fitgoodB.

%Writing to file:
%disc no.
%aliquot no.
%age (ka)
%age error (ka)
%fit type (1=linear, 2=saturating exponential, 3=saturating exponential
%plus linear)
%recycling ratio (largest always on numerator)
%sum of first two points in TTOSL
%sum of fist two points in BTOSL
%number of data points (each 0.02 seconds) of TTOSL
%number of data points (each 0.02 seconds) of BTOSL


if Rgood==1
    RXGy=RX*dose(aliquot);
    RXGyerror=sqrt(RXGy^2*((Rerror/RX)^2 + 0.08^2));

    ageR=real(abs(RXGy/WK4dr));
    ageRerror=sqrt(ageR^2*((RXGyerror/RXGy)^2+(WK4drerror/WK4dr)^2));

    Rwrite=[disc, aliquot, ageR, ageRerror, fitgoodR, Rrecyclingratio,
peakT, peakB, lengthT, lengthB];
dlmwrite('Rages.txt',Rwrite,'-append','newline','pc');
end

if Tgood==1
    TXGy=TX*dose(aliquot);
    TXGyerror=sqrt(TXGy^2*((Terror/TX)^2 + 0.08^2));

    ageT=(TXGy/WK4dr);
    ageTerror=sqrt(ageT^2*((TXGyerror/TXGy)^2+(WK4drerror/WK4dr)^2));

    Twrite=[disc, aliquot, ageT, ageTerror, fitgoodT, Trecyclingratio,
peakT, peakB, lengthT, lengthB];
dlmwrite('Tages.txt',Twrite,'-append','newline','pc');
end

if Bgood==1
    BXGy=BX*dose(aliquot);
    BXGyerror=sqrt(BXGy^2*((Berror/BX)^2 + 0.08^2));

    ageB=real(abs(BXGy/WK4dr));
    ageBerror=sqrt(ageB^2*((BXGyerror/BXGy)^2+(WK4drerror/WK4dr)^2));
```

```
    Bwrite=[disc, aliquot, ageB, ageBerror, fitgoodB, Brecyclingratio,
peakT, peakB, lengthT, lengthB];
dlmwrite('Bages.txt',Bwrite,'-append','newline','pc');
end

%This is the 'end' for the if good==1
%    end

    alquot=aliquot+1;
    csvwrite('lastaliquot.txt',alquot);
%This is the 'end' for the aliqot statement.
end
%This is the 'end' for the function.
end
```

"NATDOSE"

```
function natdose

%The function of natdose is to calculate the natural equivalent dose of
an
%aliquot of quartz grains from the TT-OSL SAR procedure. The output
%includes the equivalent dose, and its upper and lower error limits.

%Variation 5: includes the ability to use different backgrounds: end of
%OSL, near start TL, and end of TL.
%This variation is more efficient than variation 1. (From variation 2)

%This variation also includes a check of recycling ratio, and prints
%'recycling bad' on the results sheet if the recycling is worse than the
%errors of the first point.

%The check of the recycling ratio was changed on 20120912 to say
'recycling
%bad' on the results sheet if the doubled dose points do not agree with
%each other within errors (each other's 68% confidence limits).

%This variation also reads out the natural signal (unnormalised) of the
%particular aliquot and measurement (TTOSL,BTOSL,REOSL).

%This variation also has a function that allows one to skip over initial
%bins, in order to create an OSL 'plateau test'. Note that OSL plateau
%tests are not as reliable as TL plateau tests, so shouldn't be used as a
%definitive test.

%Earlier variations did not subtract the background from OSL test doses.

%Note that the output reads as: result(Gy), lower bound(Gy), upper
%bound(Gy), normalising type(OSL or TT-OSL), fit type(lin; sat...), which
%background(OSL end; TTOSL end; TTOSL initial), recycling(good or bad),
%unnormalised natural ReOSL count, aliquot number, day, month, year

close all
clear all

%Constants that stay the same throughout all aliquots are defined here.
%Note that some of these constants change for different samples. These
%should not be defined anywhere but here, to avoid accidentally leaving
%these unchanged when going on to different samples. These to-be-changed
%constants will be marked with the sign "**SD**" (sample dependent).

%x' : the column vector defining the doses given to each cycle. **SD**
x=[INSERT DOSES GIVEN EACH CYCLE HERE].*0.092;  %changed from 0.11, then
from 0.091 to (0.092 on 2012-09-03)
x=x';         %**SD**

%natx : the vector facilitating the plotting of the natural dose **SD**
natx=linspace(-1,(max(x)+1),10)';     %**SD**
```

```
%whichn : the integer (1 or 2) that defines which normalising dose is
%used: OSL or TTOSL.
whichn=1;
if whichn==1;
    normsalising='OSL test dose';
elseif whichn==2;
    normalising='TTOSL test dose';
end

%Defines what background is to be used. (1=OSL end; 2=near start TT-OSL;
%3=TT-OSL end.) 20120905
whichbg=1;

%nobins : the integer detailing the number of bins used for a particular
%sample. By default, this is left as one in the original file. **SD**
nobins=1;     %**SD**

%binstart: the bin on which the counting starts.
binstart=1;

%PN : the vector facilitating the plotting of the natural dose (y axis)
PN=ones(1,10);

%F1: the linear fit.
F1=fittype('poly1');

%F2: the saturating exponential fit.
F2=fittype('-a.*exp(-b.*x) + c','coeff',{'a','b','c'});

%F3: the saturating exponential plus linear fit.
F3=fittype('-a.*exp(-b.*x) + c.*x + d','coeff',{'a','b','c','d'});

%Start points and lower and upper bounds for saturating exponential.
RstartptF2(1)=0.5;
RstartptF2(2)=0.001;
RstartptF2(3)=0.5;
RstartptF2=RstartptF2';

RlowF2(1)=RstartptF2(1)-10;
RuppF2(1)=RstartptF2(1)+10;
RlowF2(2)=RstartptF2(2)-25;
RuppF2(2)=RstartptF2(2)+25;
RlowF2(3)=RstartptF2(3)-2;
RuppF2(3)=RstartptF2(3)+2;

%
%
%

%READING OF DATA

%After these aliquots, protocol TTOSLNE4S-02 was used.
file=input('Which aliquot would you like to use (1-8)' );
```

```
if file==1
data=csvread('XX01.txt');
end

if file==2
data=csvread('XX02.txt');
end

if file==3
data=csvread('XX03.txt');
end

if file==4
data=csvread('XXE04.txt');
end

if file==5
data=csvread('XX05.txt');
end

if file==6
data=csvread('XX06.txt');
end

if file==7
data=csvread('XX07.txt');
end

if file==8
data=csvread('XX08.txt');
end


%
%
%

%PREPROCESSING OF DATA
%Getting rid of unwanted columns.

data(:,1)=[];

%
%
%

%PROCESSING OF DATA
%  -Integrating light sums
%  -Finding the error

%Preallocating variables
bgTT=zeros(1,8);
errbgTT=zeros(1,8);
iTTOSL=zeros(1,8);
```

```
erriTTOSL=zeros(1,8);
TTOSL=zeros(1,8);
errTTOSL=zeros(1,8);
tTOSL=zeros(1,8);
errtTOSL=zeros(1,8);
bgtTT=zeros(1,8);
errbgtTT=zeros(1,8);
tiTTOSL=zeros(1,8);
errtiTTOSL=zeros(1,8);
tTTOSL=zeros(1,8);
errtTTOSL=zeros(1,8);
bgBT=zeros(1,8);
errbgBT=zeros(1,8);
iBTOSL=zeros(1,8);
erriBTOSL=zeros(1,8);
BTOSL=zeros(1,8);
errBTOSL=zeros(1,8);
tBOSL=zeros(1,8);
errtBOSL=zeros(1,8);
bgtBT=zeros(1,8);
errbgtBT=zeros(1,8);
tiBTOSL=zeros(1,8);
errtiBTOSL=zeros(1,8);
tBTOSL=zeros(1,8);
errtBTOSL=zeros(1,8);

%Creating variables
for aa=0:7;
    if whichbg==1
%TOSLend
temp=data(aa*8+1,591:600);
bgTT(aa+1)=sum(temp)/10;
errbgTT(aa+1)=sqrt((1/10)^2*(sqrt(sum(temp)) + ((580-563*exp(-
0.2617*10))/sqrt(sum(temp))))^2);
    elseif whichbg==2
%initbgTT (initial background; 20120905)
temp=data(aa*8+2,(nobins-1)+binstart+1:(nobins-1)+binstart+4);
bgTT(aa+1)=sum(temp)/3;
errbgTT(aa+1)=sqrt((1/3)^2*(sqrt(sum(temp)) + ((580-563*exp(-
0.2617*3))/sqrt(sum(temp))))^2);
    elseif whichbg==3
%TendTT
temp=data(aa*8+2,291:300);
bgTT(aa+1)=sum(temp)/10;
errbgTT(aa+1)=sqrt((1/10)^2*(sqrt(sum(temp)) + ((580-563*exp(-
0.2617*10))/sqrt(sum(temp))))^2);
    end

%iTTOSL
iTTOSL(aa+1)=sum(data(aa*8+2,binstart:binstart+(nobins-1)));
erriTTOSL(aa+1)=sqrt(iTTOSL(aa+1)) + ((580-563*exp(-
0.2617*nobins))/sqrt(iTTOSL(aa+1)));

%tTOSL
tTOSL(aa+1)=sum(data(aa*8+3,1));
```

```
errtTOSL(aa+1)=sqrt(tTOSL(aa+1)) + ((580-563*exp(-
0.2617))/sqrt(tTOSL(aa+1)));
tTOSLbg(aa+1)=sum(data(aa*8+3,591:600))/10;
errtTOSLbg(aa+1)=sqrt((1/10)^2*(sqrt(sum(data(aa*8+3,591:600)) + ((580-
563*exp(-0.2617*10))/sqrt(sum(data(aa*8+3,591:600)))))^2));
tTOSL(aa+1)=tTOSL(aa+1)-tTOSLbg(aa+1);
errtTOSL(aa+1)=sqrt(errtTOSL(aa+1)^2+errtTOSLbg(aa+1)^2);

if whichbg==1
%tTOSLend
temp=data(aa*8+3,591:600);
bgtTT(aa+1)=sum(temp)/10;
errbgtTT(aa+1)=sqrt((1/10)^2*(sqrt(sum(temp)) + ((580-563*exp(-
0.2617*10))/sqrt(sum(temp))))^2);
elseif whichbg==2
%initbgtTT
temp=data(aa*8+4,(nobins-1)+binstart+1:binstart+(nobins-1)+4);
bgtTT(aa+1)=sum(temp)/3;
errbgtTT(aa+1)=sqrt((1/3)^2*(sqrt(sum(temp)) + ((580-563*exp(-
0.2617*3))/sqrt(sum(temp))))^2);
elseif whichbg==3
%TendtTT
temp=data(aa*8+4,591:600);
bgtTT(aa+1)=sum(temp)/10;
errbgtTT(aa+1)=sqrt((1/10)^2*(sqrt(sum(temp)) + ((580-563*exp(-
0.2617*10))/sqrt(sum(temp))))^2);
end

%tiTTOSL
tiTTOSL(aa+1)=sum(data(aa*8+4,binstart:binstart+(nobins-1)));
errtiTTOSL(aa+1)=sqrt(tiTTOSL(aa+1)) + ((580-563*exp(-
0.2617*nobins))/sqrt(tiTTOSL(aa+1)));

if whichbg==1
%BOSLend
temp=data(aa*8+5,591:600);
bgBT(aa+1)=sum(temp)/10;
errbgBT(aa+1)=sqrt((1/10)^2*(sqrt(sum(temp)) + ((580-563*exp(-
0.2617*10))/sqrt(sum(temp))))^2);
elseif whichbg==2
%initbgBT
temp=data(aa*8+6,(nobins-1)+binstart+1:(nobins-1)+binstart+4);
bgBT(aa+1)=sum(temp)/3;
errbgBT(aa+1)=sqrt((1/3)^2*(sqrt(sum(temp)) + ((580-563*exp(-
0.2617*3))/sqrt(sum(temp))))^2);
elseif whichbg==3
%TendBT
temp=data(aa*8+6,291:300);
bgBT(aa+1)=sum(temp)/10;
errbgBT(aa+1)=sqrt((1/10)^2*(sqrt(sum(temp)) + ((580-563*exp(-
0.2617*10))/sqrt(sum(temp))))^2);
end

%iBTOSL
iBTOSL(aa+1)=sum(data(aa*8+6,binstart:binstart+(nobins-1)));
```

```
erriBTOSL(aa+1)=sqrt(iBTOSL(aa+1)) + ((580-563*exp(-
0.2617*nobins))/sqrt(iBTOSL(aa+1)));

%tBOSL
tBOSL(aa+1)=data(aa*8+7,1);
errtBOSL(aa+1)=sqrt(tBOSL(aa+1)) + ((580-563*exp(-
0.2617))/sqrt(tBOSL(aa+1)));
tBOSLbg(aa+1)=sum(data(aa*8+7,591:600))/10;
errtBOSLbg(aa+1)=sqrt((1/10)^2*(sqrt(sum(data(aa*8+7,591:600)) + ((580-
563*exp(-0.2617*10))/sqrt(sum(data(aa*8+7,591:600)))))^2));
tBOSL(aa+1)=tBOSL(aa+1)-tBOSLbg(aa+1);
errtBOSL(aa+1)=sqrt(errtBOSL(aa+1)^2+errtBOSLbg(aa+1)^2);

if whichbg==1
%tBOSLend
temp=data(aa*8+7,591:600);
bgtBT(aa+1)=sum(temp)/10;
errbgtBT(aa+1)=sqrt((1/10)^2*(sqrt(sum(temp)) + ((580-563*exp(-
0.2617*10))/sqrt(sum(temp))))^2);
elseif whichbg==2
%initbgtBT
temp=data(aa*8+8,(nobins-1)+binstart+1:(nobins-1)+binstart+4);
bgtBT(aa+1)=sum(temp)/3;
errbgtBT(aa+1)=sqrt((1/3)^2*(sqrt(sum(temp)) + ((580-563*exp(-
0.2617*3))/sqrt(sum(temp))))^2);
elseif whichbg==3
%TendtBT
temp=data(aa*8+8,291:300);
bgtBT(aa+1)=sum(temp)/10;
errbgtBT(aa+1)=sqrt((1/10)^2*(sqrt(sum(temp)) + ((580-563*exp(-
0.2617*10))/sqrt(sum(temp))))^2);
end

%tiBTOSL
tiBTOSL(aa+1)=sum(data(aa*8+8,binstart:binstart+(nobins-1)));
errtiBTOSL(aa+1)=sqrt(tiBTOSL(aa+1)) + ((580-563*exp(-
0.2617*nobins))/sqrt(tiBTOSL(aa+1)));

%TTOSL
TTOSL(aa+1)=iTTOSL(aa+1)-bgTT(aa+1);
errTTOSL(aa+1)=sqrt((erriTTOSL(aa+1)+errbgTT(aa+1))^2);

%tTTOSL
tTTOSL(aa+1)=tiTTOSL(aa+1)-bgtTT(aa+1);
errtTTOSL(aa+1)=sqrt(errtiTTOSL(aa+1)^2+errbgtTT(aa+1)^2);

%BTOSL
BTOSL(aa+1)=iBTOSL(aa+1)-bgBT(aa+1);
errBTOSL(aa+1)=sqrt(erriBTOSL(aa+1)^2+errbgBT(aa+1)^2);

%tBTOSL
tBTOSL(aa+1)=tiBTOSL(aa+1)-bgtBT(aa+1);
errtBTOSL(aa+1)=sqrt(errtiBTOSL(aa+1)^2+errbgtBT(aa+1)^2);

end
```

```
REOSL=TTOSL-BTOSL;

%
%
%

%NORMALISING DATA
%Choosing how to normalise
if whichn==1
    normT=tTOSL;
    errnormT=errtTOSL;
    normB=tBOSL;
    errnormB=errtBOSL;
elseif whichn==2
    normT=tTTOSL;
    errnormT=errtTTOSL;
    normB=tBTOSL;
    errnormB=errtBTOSL;
end

%creating normalised data and their errors.

%nTTOSL
nTTOSL=TTOSL./normT;
%To prevent NaN errors:
nTTOSL2=nTTOSL;
TTOSL2=TTOSL;
normT2=normT;
for ii=1:8;
if nTTOSL2(ii)==0;
   nTTOSL2(ii)=0.0001;
end
if TTOSL2(ii)==0;
   TTOSL2(ii)=1;
end
if normT2(ii)==0;
   normT2(ii)=1;
end
end
errnTTOSL=sqrt((nTTOSL2.^2 .*( (errTTOSL./TTOSL2).^2 +
(errnormT./normT2).^2)));

nrTTOSL=nTTOSL;
nrTTOSL(1)=[];
errnrTTOSL=errnTTOSL;
errnrTTOSL(1)=[];
TW=(1./errnrTTOSL).^2';

natnTTOSL=nTTOSL(1);
errnatnTTOSL=errnTTOSL(1);
PNT=PN.*natnTTOSL;
errPNT=PN.*errnatnTTOSL;

%nBTOSL
```

```
nBTOSL=BTOSL./normB;
%To prevent NaN errors:
nBTOSL2=nBTOSL;
BTOSL2=BTOSL;
normB2=normB;
for ii=1:8;
if nBTOSL2(ii)==0;
   nBTOSL2(ii)=0.0001;
end
if BTOSL2(ii)==0;
   BTOSL2(ii)=1;
end
if normB2(ii)==0;
   normB2(ii)=1;
end
end
errnBTOSL=sqrt((nBTOSL2.^2 .*( (errBTOSL./BTOSL2).^2 +
(errnormB./normB2).^2)));

nrBTOSL=nBTOSL;
nrBTOSL(1)=[];
errnrBTOSL=errnBTOSL;
errnrBTOSL(1)=[];
BW=(1./errnrBTOSL).^2';

natnBTOSL=nBTOSL(1);
errnatnBTOSL=errnBTOSL(1);
PNB=PN.*natnBTOSL;
errPNB=PN.*errnatnBTOSL;

%nREOSL
nREOSL=nTTOSL-nBTOSL;
errnREOSL=sqrt(errnTTOSL.^2 + errnBTOSL.^2);

nrREOSL=nREOSL;
nrREOSL(1)=[];
errnrREOSL=errnREOSL;
errnrREOSL(1)=[];
RW=(1./errnrREOSL).^2';

natnREOSL=nREOSL(1);
errnatnREOSL=errnREOSL(1);
PNR=PN.*natnREOSL;
errPNR=PN.*errnatnREOSL;

%
%
%

%Calculating the recycling ratio (non-order dependent). If the recycling
%ratio is beyond 68% errors, will give a warning.

%changed 20120912

for jj=1:7
```

```
    for ii=1:7
        if (x(ii)==x(jj)) && (ii ~= jj)
            a=ii;
            b=jj;
        end
    end
end


if nrTTOSL(a)>nrTTOSL(b)
    aa=b;
    bb=a;
else
    bb=b;
    aa=a;
end
%TT-OSL
drp=(nrTTOSL(aa)+errnrTTOSL(aa))-(nrTTOSL(bb)-errnrTTOSL(bb));
if drp<0
    Trr='recycling bad';
else
    Trr='recycling good';
end


if nrBTOSL(a)>nrBTOSL(b)
    aa=b;
    bb=a;
else
    bb=b;
    aa=a;
end
%BT-OSL
drp=(nrBTOSL(aa)+errnrBTOSL(aa))-(nrBTOSL(bb)-errnrBTOSL(bb));
if drp<0;
    Brr='recycling bad';
else
    Brr='recycling good';
end



if nrREOSL(a)>nrREOSL(b)
    aa=b;
    bb=a;
else
    bb=b;
    aa=a;
end
%REOSL
drp=(nrREOSL(aa)+errnrREOSL(aa))-(nrREOSL(bb)-errnrREOSL(bb));
if drp<0;
    Rrr='recycling bad';
else
    Rrr='recycling good';
```

```
end


%
%
%

%PLOTTING AND FITTING
%Weighted fits of TTOSL, BTOSL, REOSL
%Fits of linear, saturating exponential, and saturating exponential plus
%linear types.

%Creating start points for saturating exponential plus linear
RstartptF3(1)=TTOSL(3);
RstartptF3(2)=0.01;
RstartptF3(3)=0.001;
RstartptF3(4)=TTOSL(3);
RstartptF3=RstartptF3';

%Plotting and fitting TTOSL
%errorbar(x,nrTTOSL,errnrTTOSL,'bo');
plot(x,nrTTOSL,'bo')
hold on
%errorbar(natx,PNT,errPNT,'k-');
plot(natx,PNT,'k-');

try
      [tf1,goflin]=fit(x,nrTTOSL',F1,'Weights',TW);
      plot(tf1,'r');
      disp('Linear');
      disp(goflin);
catch
    disp('Linear equation cannot be fitted');
end

try
    [tf2,gofsate]=fit(x,nrTTOSL',F2,'StartPoint', RstartptF2,'Lower',
RlowF2, 'Upper', RuppF2,'Weights',TW);
    plot(tf2,'g');
    disp('Saturating exponential');
    disp(gofsate);
catch
    disp('Saturating exponential equation cannot be fitted.');
end

try

[tf3,gofsatelin]=fit(x,nrTTOSL',F3,'StartPoint',RstartptF3);%,'Weights',T
W);
    plot(tf3,'b');
    disp('Saturating exponential plus linear');
    disp(gofsatelin);
catch
        disp('Saturating exponential plus linear equation cannot be
fitted; none=0.');
```

```
end

hold off

legend off
title('TT-OSL');
whichTTOSL=input('Which fit is best? (linear=1; sat exp = 2; sat exp plus
lin = 3.  ');

close figure 1

%

%Plotting and fitting BTOSL
%errorbar(x,nrBTOSL,errnrBTOSL,'bo');
plot(x,nrBTOSL,'bo');
hold on
%errorbar(natx,PNB,errPNB,'k-');
plot(natx,PNB,'k-');

try
      [bf1,goflin]=fit(x,nrBTOSL',F1,'Weights',BW);
      plot(bf1,'r');
      disp('Linear');
      disp(goflin);
catch
    disp('Linear equation cannot be fitted');
end

try
    [bf2,gofsate]=fit(x,nrBTOSL',F2,'StartPoint', RstartptF2,'Lower',
RlowF2, 'Upper', RuppF2,'Weights',BW);
    plot(bf2,'g');
    disp('Saturating exponential');
    disp(gofsate);
catch
    disp('Saturating exponential equation cannot be fitted.');
end

try

[bf3,gofsatelin]=fit(x,nrBTOSL',F3,'StartPoint',RstartptF3);%,'Weights',B
W);
    plot(bf3,'b');
    disp('Saturating exponential plus linear');
    disp(gofsatelin);
catch
        disp('Saturating exponential plus linear equation cannot be
fitted.');
end

hold off

legend off
title('BT-OSL');
```

```
whichBTOSL=input('Which fit is best? (linear=1; sat exp = 2; sat exp plus
lin = 3; none=0.  ');

close figure 1

%

%Plotting and fitting REOSL
%errorbar(x,nrREOSL,errnrREOSL,'bo');
plot(x,nrREOSL,'bo');
hold on
%errorbar(natx,PNR,errPNR,'k-');
plot(natx,PNR,'k-');

try
      [rf1,goflin]=fit(x,nrREOSL',F1,'Weights',RW);
      plot(rf1,'r');
      disp('Linear');
      disp(goflin);
catch
    disp('Linear equation cannot be fitted');
end

try
    [rf2,gofsate]=fit(x,nrREOSL',F2,'StartPoint', RstartptF2,'Lower',
RlowF2, 'Upper', RuppF2,'Weights',RW);
    plot(rf2,'g');
    disp('Saturating exponential');
    disp(gofsate);
catch
    disp('Saturating exponential equation cannot be fitted.');
end

try

[rf3,gofsatelin]=fit(x,nrREOSL',F3,'StartPoint',RstartptF3);%,'Weights',R
W);
    plot(rf3,'b');
    disp('Saturating exponential plus linear');
    disp(gofsatelin);
catch
        disp('Saturating exponential plus linear equation cannot be
fitted.');
end

hold off

legend off
title('RE-OSL');
whichREOSL=input('Which fit is best? (linear=1; sat exp = 2; sat exp plus
lin = 3; none=0.  ');

close figure 1

%
```

```
%
%

%FINDING THE NATURAL DOSE

%For TTOSL:

ifthere=exist('whichTTOSL','var');
if (ifthere==1) && (whichTTOSL ~= 0);

%Finding the natural dose from the fit
if whichTTOSL==1
    TTOSLfit='linear';
    fitT=tf1;
    coeffsT=coeffvalues(tf1);
    Tnatx=(natnTTOSL-coeffsT(2))/coeffsT(1);
    %Error of fit at natx
    errTs=predint(fitT,Tnatx,0.682689,'functional');
    errT=natnTTOSL-errTs(1);
end

if whichTTOSL==2
    TTOSLfit='saturating exponential';
    fitT=tf2;
    coeffsT=coeffvalues(tf2);
    Tnatx=log((coeffsT(3)-natnTTOSL)/coeffsT(1))./(-coeffsT(2));
    %Error of fit at natx
    errTs=predint(fitT,Tnatx,0.682689,'functional');
    errT=natnTTOSL-errTs(1);
end

if whichTTOSL==3
    TTOSLfit='sat exp + lin';
    fitT=tf3;
    coeffsT=coeffvalues(tf3);

    %Note that there are restrictions on the sat exp + lin result:
    %-No extrapolation
    %-Low-res digital type result.
    %-Always rounds up, not down (for positive slope).
    mx=max(x);
    TX3=linspace(0,mx,5000);
    TY3=-coeffsT(1).*exp(-coeffsT(2).*TX3) + coeffsT(3).*TX3 +
coeffsT(4);
    Tnatx=0;
    for ii=1:5000;
        if TY3(5001-ii)>natnTTOSL;
            Tnatx=TX3(5001-ii);
        end
    end

    %Error of fit at natx
    errTs=predint(fitT,Tnatx,0.682689,'functional');
    errT=natnTTOSL-errTs(1);
```

```
end

%Finding the y-axis error

errorTy=sqrt(errT^2+errnatnTTOSL^2);

%Finding the x-axis translation of the y-axis error
if whichTTOSL==1
    errorloT=((natnTTOSL-errorTy)-coeffsT(2))/coeffsT(1);
    errorhiT=((natnTTOSL+errorTy)-coeffsT(2))/coeffsT(1);
end

if whichTTOSL==2
    errorloT=log((coeffsT(3)-(natnTTOSL-errorTy))/coeffsT(1))./(-
coeffsT(2));
    errorhiT=log((coeffsT(3)-(natnTTOSL+errorTy))/coeffsT(1))./(-
coeffsT(2));
end

if whichTTOSL==3
    %Note that there are restrictions on the sat exp + lin result:
    %-No extrapolation
    %-Low-res digital type result.
    %-Always rounds up, not down (for positive slope).
    TX=linspace(0,mx,5000);
    TY=-coeffsT(1).*exp(-coeffsT(2).*TX3) + coeffsT(3).*TX3 + coeffsT(4);

    errorloT=0;
    for ii=1:5000;
        if TY(5001-ii)>(natnTTOSL-errorTy);
            errorloT=TX(5001-ii);
        end
    end

    errorhiT=0;
    for ii=1:5000;
        if TY(5001-ii)>(natnTTOSL+errorTy);
            errorhiT=TX(5001-ii);
        end
    end
end

else
    Tnatx='x';
    TTOSLfit='none';
end

%For BTOSL:

ifthere=exist('whichBTOSL','var');
if (ifthere==1) && (whichBTOSL ~= 0);

%Finding the natural dose from the fit
```

```
if whichBTOSL==1
    BTOSLfit='linear';
    fitB=bf1;
    coeffsB=coeffvalues(bf1);
    Bnatx=(natnBTOSL-coeffsB(2))/coeffsB(1);
    %Error of fit at natx
    errBs=predint(fitB,Bnatx,0.682689,'functional');
    errB=natnBTOSL-errBs(1);
end

if whichBTOSL==2
    BTOSLfit='saturating exponential';
    fitB=bf2;
    coeffsB=coeffvalues(bf2);
    Bnatx=log((coeffsB(3)-natnBTOSL)/coeffsB(1))./(-coeffsB(2));
    %Error of fit at natx
    errBs=predint(fitB,Bnatx,0.682689,'functional');
    errB=natnBTOSL-errBs(1);
end

if whichBTOSL==3
    BTOSLfit='sat exp + lin';
    fitB=bf3;
    coeffsB=coeffvalues(bf3);

    %Note that there are restrictions on the sat exp + lin result:
    %-No extrapolation
    %-Low-res digital type result.
    %-Always rounds up, not down (for positive slope).
    mx=max(x);
    BX3=linspace(0,mx,5000);
    BY3=-coeffsB(1).*exp(-coeffsB(2).*BX3) + coeffsB(3).*BX3 +
coeffsB(4);
    Bnatx=0;
    for ii=1:5000;
        if BY3(5001-ii)>natnBTOSL;
            Bnatx=BX3(5001-ii);
        end
    end

    %Error of fit at natx
    errBs=predint(fitB,Bnatx,0.682689,'functional');
    errB=natnBTOSL-errBs(1);

end

%Finding the y-axis error

errorBy=sqrt(errB^2+errnatnBTOSL^2);

%Finding the x-axis translation of the y-axis error
if whichBTOSL==1
    errorloB=((natnBTOSL-errorBy)-coeffsB(2))/coeffsB(1);
    errorhiB=((natnBTOSL+errorBy)-coeffsB(2))/coeffsB(1);
end
```

```
if whichBTOSL==2
    errorloB=log((coeffsB(3)-(natnBTOSL-errorBy))/coeffsB(1))./(-
coeffsB(2));
    errorhiB=log((coeffsB(3)-(natnBTOSL+errorBy))/coeffsB(1))./(-
coeffsB(2));
end

if whichBTOSL==3
    %Note that there are restrictions on the sat exp + lin result:
    %-No extrapolation
    %-Low-res digital type result.
    %-Always rounds up, not down (for positive slope).
    BX=linspace(0,mx,5000);
    BY=-coeffsB(1).*exp(-coeffsB(2).*BX3) + coeffsB(3).*BX3 + coeffsB(4);

    errorloB=0;
    for ii=1:5000;
        if BY(5001-ii)>(natnBTOSL-errorBy);
            errorloB=BX(5001-ii);
        end
    end

    errorhiB=0;
    for ii=1:5000;
        if BY(5001-ii)>(natnBTOSL+errorBy);
            errorhiB=BX(5001-ii);
        end
    end
end

else
    Bnatx='x';
    BTOSLfit='none';
end

%For REOSL:

ifthere=exist('whichREOSL','var');
if (ifthere==1) && (whichREOSL ~= 0);

%Finding the natural dose from the fit
if whichREOSL==1
    REOSLfit='linear';
    fitR=rf1;
    coeffsR=coeffvalues(rf1);
    Rnatx=(natnREOSL-coeffsR(2))/coeffsR(1);
    %Error of fit at natx
    errRs=predint(fitR,Rnatx,0.682689,'functional');
    errR=natnREOSL-errRs(1);
end

if whichREOSL==2
    REOSLfit='saturating exponential';
    fitR=rf2;
```

```
    coeffsR=coeffvalues(rf2);
    Rnatx=log((coeffsR(3)-natnREOSL)/coeffsR(1))./(-coeffsR(2));
    %Error of fit at natx
    errRs=predint(fitR,Rnatx,0.682689,'functional');
    errR=natnREOSL-errRs(1);
end

if whichREOSL==3
    REOSLfit='sat exp + lin';
    fitR=rf3;
    coeffsR=coeffvalues(rf3);

    %Note that there are restrictions on the sat exp + lin result:
    %-No extrapolation
    %-Low-res digital type result.
    %-Always rounds up, not down (for positive slope).
    mx=max(x);
    RX3=linspace(0,mx,5000);
    RY3=-coeffsR(1).*exp(-coeffsR(2).*RX3) + coeffsR(3).*RX3 +
coeffsR(4);
    Rnatx=0;
    for ii=1:5000;
        if RY3(5001-ii)>natnREOSL;
            Rnatx=RX3(5001-ii);
        end
    end

    %Error of fit at natx
    errRs=predint(fitR,Rnatx,0.682689,'functional');
    errR=natnREOSL-errRs(1);

end

%Finding the y-axis error

errorRy=sqrt(errR^2+errnatnREOSL^2);

%Finding the x-axis translation of the y-axis error
if whichREOSL==1
    errorloR=((natnREOSL-errorRy)-coeffsR(2))/coeffsR(1);
    errorhiR=((natnREOSL+errorRy)-coeffsR(2))/coeffsR(1);
end

if whichREOSL==2
    errorloR=log((coeffsR(3)-(natnREOSL-errorRy))/coeffsR(1))./(-
coeffsR(2));
    errorhiR=log((coeffsR(3)-(natnREOSL+errorRy))/coeffsR(1))./(-
coeffsR(2));
end

if whichREOSL==3
    %Note that there are restrictions on the sat exp + lin result:
    %-No extrapolation
    %-Low-res digital type result.
    %-Always rounds up, not down (for positive slope).
```

```
    RX=linspace(0,mx,5000);
    RY=-coeffsR(1).*exp(-coeffsR(2).*RX3) + coeffsR(3).*RX3 + coeffsR(4);

    errorloR=0;
    for ii=1:5000;
        if RY(5001-ii)>(natnREOSL-errorRy);
            errorloR=RX(5001-ii);
        end
    end

    errorhiR=0;
    for ii=1:5000;
        if RY(5001-ii)>(natnREOSL+errorRy);
            errorhiR=RX(5001-ii);
        end
    end
end

else
    Rnatx='x';
    REOSLfit='none';

end

%
%

%WRITING DATA TO A TEXT FILE
%Includes:

%natural dose
%dose error (upper)
%dose error (lower)
%what test dose used (whichn)
%what fit type used
%number of bins used
%what aliquot used
%date of calculation

doc=datevec(date);
doc(4:6)=[];

%For TTOSL
fid=fopen('natdoseTTOSL.txt','a');
if Tnatx=='x';
    fprintf(fid,'x,x,x,%s,%s,%d
bins,%f,%s,%f,%f,%f,%f,%f\r\n',normalising,TTOSLfit,nobins,whichbg,Trr,TT
OSL(1),file,doc(1),doc(2),doc(3));
else
    fprintf(fid,'%f,%f,%f,%s,%s,%d
bins,%f,%s,%f,%f,%f,%f,%f\r\n',Tnatx,errorloT,errorhiT,normalising,TTOSLf
it,nobins,whichbg,Trr,TTOSL(1),file,doc(1),doc(2),doc(3));
end
fclose(fid);
```

```
%For BTOSL
fid=fopen('natdoseBTOSL.txt','a');
if Bnatx=='x';
    fprintf(fid,'x,x,x,%s,%s,%d
bins,%f,%s,%f,%f,%f,%f,%f\r\n',normalising,BTOSLfit,nobins,whichbg,Brr,BT
OSL(1),file,doc(1),doc(2),doc(3));
else
    fprintf(fid,'%f,%f,%f,%s,%s,%d
bins,%f,%s,%f,%f,%f,%f,%f\r\n',Bnatx,errorloB,errorhiB,normalising,BTOSLf
it,nobins,whichbg,Brr,BTOSL(1),file,doc(1),doc(2),doc(3));
end
fclose(fid);

%For REOSL
fid=fopen('natdoseREOSL.txt','a');
if Rnatx=='x';
    fprintf(fid,'x,x,x,%s,%s,%d
bins,%f,%s,%f,%f,%f,%f,%f\r\n',normalising,REOSLfit,nobins,whichbg,Rrr,RE
OSL(1),file,doc(1),doc(2),doc(3));
else
    fprintf(fid,'%f,%f,%f,%s,%s,%d
bins,%f,%s,%f,%f,%f,%f,%f\r\n',Rnatx,errorloR,errorhiR,normalising,REOSLf
it,nobins,whichbg,Rrr,REOSL(1),file,doc(1),doc(2),doc(3));
end
fclose(fid);


%For TTOSL
%dlmwrite('natdoseTTOSL.txt',Tnatx,'-append','coffset',1);
%dlmwrite('natdoseTTOSL.txt',errorloT,'-append','coffset',1);
%dlmwrite('natdoseTTOSL.txt',errorhiT,'-append','coffset',1);
%dlmwrite('natdoseTTOSL.txt',whichn,'-append','coffset',1);
%dlmwrite('natdoseTTOSL.txt',whichTTOSL,'-append','coffset',1);
%dlmwrite('natdoseTTOSL.txt',file,'-append','coffset',1);
%dlmwrite('natdoseTTOSL.txt',doc,'-append','newline','pc','coffset',1);

%For BTOSL
%dlmwrite('natdoseBTOSL.txt',Bnatx,'-append','coffset',1);
%dlmwrite('natdoseBTOSL.txt',errorloB,'-append','coffset',1);
%dlmwrite('natdoseBTOSL.txt',errorhiB,'-append','coffset',1);
%dlmwrite('natdoseBTOSL.txt',whichn,'-append','coffset',1);
%dlmwrite('natdoseBTOSL.txt',whichBTOSL,'-append','coffset',1);
%dlmwrite('natdoseBTOSL.txt',file,'-append','coffset',1);
%dlmwrite('natdoseBTOSL.txt',doc,'-append','newline','pc','coffset',1);

%For REOSL
%dlmwrite('natdoseREOSL.txt',Rnatx,'-append','coffset',1);
%dlmwrite('natdoseREOSL.txt',errorloR,'-append','coffset',1);
%dlmwrite('natdoseREOSL.txt',errorhiR,'-append','coffset',1);
%dlmwrite('natdoseREOSL.txt',whichn,'-append','coffset',1);
%dlmwrite('natdoseREOSL.txt',whichREOSL,'-append','coffset',1);
%dlmwrite('natdoseREOSL.txt',file,'-append','coffset',1);
%dlmwrite('natdoseREOSL.txt',doc,'-append','newline','pc','coffset',1);

end
```

"VARIATIONS"

```
function variations

% A function to process the different variations in reproducibility
experiments.

close all
clear all

data=csvread('repdNE.txt');

discid=input('What identifier would you like for this disc? (in
charstring mode)');

if isempty(discid)
    discid='NE01_280ph_350wash';
end


%deleting blank columns

data(:,1)=[];

for integral=0:1;
nobins=(integral*4)+1;


for whichbg=1:3;

for whichn=1:2;

if whichbg==1
background='end OSL';
elseif whichbg==2
background='near start TT-OSL';
elseif whichbg==3
background='end TT-OSL';
end

if whichn==1;
    normalising='OSL test dose';
elseif whichn==2;
    normalising='TTOSL test dose';
end

integrated=nobins./10;

%Preallocating variables
bgTT=zeros(1,13);
errbgTT=zeros(1,13);
iTTOSL=zeros(1,13);
erriTTOSL=zeros(1,13);
```

```
TTOSL=zeros(1,13);
errTTOSL=zeros(1,13);
tTOSL=zeros(1,13);
errtTOSL=zeros(1,13);
bgtTT=zeros(1,13);
errbgtTT=zeros(1,13);
tiTTOSL=zeros(1,13);
errtiTTOSL=zeros(1,13);
tTTOSL=zeros(1,13);
errtTTOSL=zeros(1,13);
bgBT=zeros(1,13);
errbgBT=zeros(1,13);
iBTOSL=zeros(1,13);
erriBTOSL=zeros(1,13);
BTOSL=zeros(1,13);
errBTOSL=zeros(1,13);
tBOSL=zeros(1,13);
errtBOSL=zeros(1,13);
bgtBT=zeros(1,13);
errbgtBT=zeros(1,13);
tiBTOSL=zeros(1,13);
errtiBTOSL=zeros(1,13);
tBTOSL=zeros(1,13);
errtBTOSL=zeros(1,13);

%Creating variables
for aa=0:12;
    if whichbg==1
%TOSLend
temp=data(aa*8+1,591:600);
bgTT(aa+1)=sum(temp)/10;
errbgTT(aa+1)=sqrt((1/10)^2*(sqrt(sum(temp)) + ((580-563*exp(-
0.2617*10))/sqrt(sum(temp))))^2);
    elseif whichbg==2
%initbgTT (initial background; 20120905)
temp=data(aa*8+2,nobins+1:nobins+11);
bgTT(aa+1)=sum(temp)/10;
errbgTT(aa+1)=sqrt((1/10)^2*(sqrt(sum(temp)) + ((580-563*exp(-
0.2617*10))/sqrt(sum(temp))))^2);
    elseif whichbg==3
%TendTT
temp=data(aa*8+2,291:300);
bgTT(aa+1)=sum(temp)/10;
errbgTT(aa+1)=sqrt((1/10)^2*(sqrt(sum(temp)) + ((580-563*exp(-
0.2617*10))/sqrt(sum(temp))))^2);
    end

%iTTOSL
iTTOSL(aa+1)=sum(data(aa*8+2,1:nobins));
erriTTOSL(aa+1)=sqrt(iTTOSL(aa+1)) + ((580-563*exp(-
0.2617*nobins))/sqrt(iTTOSL(aa+1)));

%tTOSL
tTOSL(aa+1)=data(aa*8+3,1);
errtTOSL(aa+1)=sqrt(tTOSL(aa+1)) + ((580-563*exp(-
0.2617))/sqrt(tTOSL(aa+1)));
```

```
if whichbg==1
%tTOSLend
temp=data(aa*8+3,591:600);
bgtTT(aa+1)=sum(temp)/10;
errbgtTT(aa+1)=sqrt((1/10)^2*(sqrt(sum(temp)) + ((580-563*exp(-
0.2617*10))/sqrt(sum(temp))))^2);
elseif whichbg==2
%initbgtTT
temp=data(aa*8+4,nobins+1:nobins+11);
bgtTT(aa+1)=sum(temp)/10;
errbgtTT(aa+1)=sqrt((1/10)^2*(sqrt(sum(temp)) + ((580-563*exp(-
0.2617*10))/sqrt(sum(temp))))^2);
elseif whichbg==3
%TendtTT
temp=data(aa*8+4,591:600);
bgtTT(aa+1)=sum(temp)/10;
errbgtTT(aa+1)=sqrt((1/10)^2*(sqrt(sum(temp)) + ((580-563*exp(-
0.2617*10))/sqrt(sum(temp))))^2);
end

%tiTTOSL
tiTTOSL(aa+1)=sum(data(aa*8+4,1:nobins));
errtiTTOSL(aa+1)=sqrt(tiTTOSL(aa+1)) + ((580-563*exp(-
0.2617*nobins))/sqrt(tiTTOSL(aa+1)));

if whichbg==1
%BOSLend
temp=data(aa*8+5,591:600);
bgBT(aa+1)=sum(temp)/10;
errbgBT(aa+1)=sqrt((1/10)^2*(sqrt(sum(temp)) + ((580-563*exp(-
0.2617*10))/sqrt(sum(temp))))^2);
elseif whichbg==2
%initbgBT
temp=data(aa*8+6,nobins+1:nobins+11);
bgBT(aa+1)=sum(temp)/10;
errbgBT(aa+1)=sqrt((1/10)^2*(sqrt(sum(temp)) + ((580-563*exp(-
0.2617*10))/sqrt(sum(temp))))^2);
elseif whichbg==3
%TendBT
temp=data(aa*8+6,291:300);
bgBT(aa+1)=sum(temp)/10;
errbgBT(aa+1)=sqrt((1/10)^2*(sqrt(sum(temp)) + ((580-563*exp(-
0.2617*10))/sqrt(sum(temp))))^2);
end

%iBTOSL
iBTOSL(aa+1)=sum(data(aa*8+6,1:nobins));
erriBTOSL(aa+1)=sqrt(iBTOSL(aa+1)) + ((580-563*exp(-
0.2617*nobins))/sqrt(iBTOSL(aa+1)));

%tBOSL
tBOSL(aa+1)=data(aa*8+7,1);
errtBOSL(aa+1)=sqrt(tBOSL(aa+1)) + ((580-563*exp(-
0.2617))/sqrt(tBOSL(aa+1)));
```

```
if whichbg==1
%tBOSLend
temp=data(aa*8+7,591:600);
bgtBT(aa+1)=sum(temp)/10;
errbgtBT(aa+1)=sqrt((1/10)^2*(sqrt(sum(temp)) + ((580-563*exp(-
0.2617*10))/sqrt(sum(temp))))^2);
elseif whichbg==2
%initbgtBT
temp=data(aa*8+8,nobins+1:nobins+11);
bgtBT(aa+1)=sum(temp)/10;
errbgtBT(aa+1)=sqrt((1/10)^2*(sqrt(sum(temp)) + ((580-563*exp(-
0.2617*10))/sqrt(sum(temp))))^2);
elseif whichbg==3
%TendtBT
temp=data(aa*8+8,291:300);
bgtBT(aa+1)=sum(temp)/10;
errbgtBT(aa+1)=sqrt((1/10)^2*(sqrt(sum(temp)) + ((580-563*exp(-
0.2617*10))/sqrt(sum(temp))))^2);
end

%tiBTOSL
tiBTOSL(aa+1)=sum(data(aa*8+8,1:nobins));
errtiBTOSL(aa+1)=sqrt(tiBTOSL(aa+1)) + ((580-563*exp(-
0.2617*nobins))/sqrt(tiBTOSL(aa+1)));

%TTOSL
TTOSL(aa+1)=iTTOSL(aa+1)-bgTT(aa+1);
errTTOSL(aa+1)=sqrt((erriTTOSL(aa+1)+errbgTT(aa+1))^2);

%tTTOSL
tTTOSL(aa+1)=tiTTOSL(aa+1)-bgtTT(aa+1);
errtTTOSL(aa+1)=sqrt(errtiTTOSL(aa+1)^2+errbgtTT(aa+1)^2);

%BTOSL
BTOSL(aa+1)=iBTOSL(aa+1)-bgBT(aa+1);
errBTOSL(aa+1)=sqrt(erriBTOSL(aa+1)^2+errbgBT(aa+1)^2);

%tBTOSL
tBTOSL(aa+1)=tiBTOSL(aa+1)-bgtBT(aa+1);
errtBTOSL(aa+1)=sqrt(errtiBTOSL(aa+1)^2+errbgtBT(aa+1)^2);

end


%
%
%

%NORMALISING DATA
%Choosing how to normalise
if whichn==1
    normT=tTOSL;
    errnormT=errtTOSL;
    normB=tBOSL;
    errnormB=errtBOSL;
```

```
elseif whichn==2
    normT=tTTOSL;
    errnormT=errtTTOSL;
    normB=tBTOSL;
    errnormB=errtBTOSL;
end

%creating normalised data and their errors.

%nTTOSL
nTTOSL=TTOSL./normT;
%To prevent NaN errors:
nTTOSL2=nTTOSL;
TTOSL2=TTOSL;
normT2=normT;
for ii=1:8;
if nTTOSL2(ii)==0;
   nTTOSL2(ii)=0.0001;
end
if TTOSL2(ii)==0;
   TTOSL2(ii)=1;
end
if normT2(ii)==0;
   normT2(ii)=1;
end
end
errnTTOSL=sqrt((nTTOSL2.^2 .*( (errTTOSL./TTOSL2).^2 +
(errnormT./normT2).^2)));

%nBTOSL
nBTOSL=BTOSL./normB;
%To prevent NaN errors:
nBTOSL2=nBTOSL;
BTOSL2=BTOSL;
normB2=normB;
for ii=1:8;
if nBTOSL2(ii)==0;
   nBTOSL2(ii)=0.0001;
end
if BTOSL2(ii)==0;
   BTOSL2(ii)=1;
end
if normB2(ii)==0;
   normB2(ii)=1;
end
end
errnBTOSL=sqrt((nBTOSL2.^2 .*( (errBTOSL./BTOSL2).^2 +
(errnormB./normB2).^2)));


%nREOSL
nREOSL=nTTOSL-nBTOSL;
errnREOSL=sqrt(errnTTOSL.^2 + errnBTOSL.^2);

fid=fopen('NE01.txt','a');
```

```
fprintf(fid,'%s\r\n%s\r\n background is %s\r\n integral is %f s\r\n DD-
TT-OSL\r\n %f,%f,%f,%f,%f,%f,%f,%f,%f,%f,%f,%f,%f \r\n errors\r\n
%f,%f,%f,%f,%f,%f,%f,%f,%f,%f,%f,%f,%f\r\n DI-TT-OSL\r\n
%f,%f,%f,%f,%f,%f,%f,%f,%f,%f,%f,%f,%f\r\n errors
\r\n%f,%f,%f,%f,%f,%f,%f,%f,%f,%f,%f,%f,%f\r\n TT-OSL\r\n
%f,%f,%f,%f,%f,%f,%f,%f,%f,%f,%f,%f,%f\r\n errors\r\n
%f,%f,%f,%f,%f,%f,%f,%f,%f,%f,%f,%f,%f\r\n',discid,normalising,
background,integrated,nREOSL(1),nREOSL(2),nREOSL(3),nREOSL(4),nREOSL(5),n
REOSL(6),nREOSL(7),nREOSL(8),nREOSL(9),nREOSL(10),nREOSL(11),nREOSL(12),n
REOSL(13),errnREOSL(1),errnREOSL(2),errnREOSL(3),errnREOSL(4),errnREOSL(5
),errnREOSL(6),errnREOSL(7),errnREOSL(8),errnREOSL(9),errnREOSL(10),errnR
EOSL(11),errnREOSL(12),errnREOSL(13),nBTOSL(1),nBTOSL(2),nBTOSL(3),nBTOSL
(4),nBTOSL(5),nBTOSL(6),nBTOSL(7),nBTOSL(8),nBTOSL(9),nBTOSL(10),nBTOSL(1
1),nBTOSL(12),nBTOSL(13),errnBTOSL(1),errnBTOSL(2),errnBTOSL(3),errnBTOSL
(4),errnBTOSL(5),errnBTOSL(6),errnBTOSL(7),errnBTOSL(8),errnBTOSL(9),errn
BTOSL(10),errnBTOSL(11),errnBTOSL(12),errnBTOSL(13),nTTOSL(1),nTTOSL(2),n
TTOSL(3),nTTOSL(4),nTTOSL(5),nTTOSL(6),nTTOSL(7),nTTOSL(8),nTTOSL(9),nTTO
SL(10),nTTOSL(11),nTTOSL(12),nTTOSL(13),errnTTOSL(1),errnTTOSL(2),errnTTO
SL(3),errnTTOSL(4),errnTTOSL(5),errnTTOSL(6),errnTTOSL(7),errnTTOSL(8),er
rnTTOSL(9),errnTTOSL(10),errnTTOSL(11),errnTTOSL(12),errnTTOSL(13));
fclose(fid);


end
end
end
end
```

"SIMDEPOP"

```
function simdepop

%A simulation to show how simple model traps deplete at different
%temperatures. E and s values are variables one can change. The heating
%includes a 5 K/s ramp up to a particular temperature and then a hold at
%that temperature for 10 seconds.

close all

clear all

%constants

k=8.627343*(10^-5); %Boltzmann's constant

%Note for this function to work the temperature iteration must go up by
0.2
%s every time. eg, T=linspace(x,y,(y-x)*5;

min=150;
max=500;
Tlen=(max-min)*5;

T=linspace(min,max,Tlen)+273.25; % Temperature K

x=linspace(min,max,Tlen); % Temperature degC

%Trap variables

s=4.8*10^13; %s^-1

E=1.88; %eV

% Result array
result=zeros(1,Tlen);

%For each temperature:
for ii=1:Tlen;


%Ramp up:

%How many fifth of seconds? Assume starting from 0 deg C/ 273.25 K

temps=linspace(1,x(ii),x(ii));
temps=temps+273.25;

%Calculating the fraction left from the start of each fifth of a second
to
%the end of the fifth of a second.
Fraction=exp(-0.2./(s^-1.*exp(E./(k.*temps))));
```

```
lf=length(Fraction);

ramp=1;
for jj=1:lf;
    ramp=ramp*Fraction(jj);
end

%Hold for 10 s:

Hold=exp(-10./(s^-1.*exp(E./(k.*T(ii)))));

%Result for each temperature

result(ii)=ramp*Hold;

end

plot(x,result);
title('Simulation of emptying trap by heating');
xlabel('Temperature in degrees Celsius');
ylabel('Proportion of population left in trap');

%In case of wanting to write down to file the simulation data, let a = 1.

writing=1;

if writing==1;

    %The date record
simdate=datevec(date);
simdate(4:6)=[];

%Any notes to go with data
note='375 Red by Spooner and Franklin 2002';

fid=fopen('simulation_data.txt','a');
fprintf(fid,'Simulation data for E = %f and s = %f on %f %f %f notes:
%s\r\n',E,s,simdate(1),simdate(2),simdate(3),note);
fclose(fid);

dlmwrite('simulation_data.txt',x,'-append','newline','pc');
dlmwrite('simulation_data.txt',result,'-append','newline','pc');

disp('Wrote to file.');
disp('Thank you. Simulation ends.');

end
```

"SIMDEPOPFIT"

```
function simdepopfit

%A simulation to show how simple model traps deplete at different
%temperatures. E and s values are variables one can change. The heating
%includes a 5 K/s ramp up to a particular temperature and then a hold at
%that temperature for 10 seconds.

close all

clear all

%constants

k=8.627343*(10^-5); %Boltzmann's constant

%Results data and SST

%Experimental results
expresults=[];

l=length(expresults);

mean=sum(expresults)/l;

SSTparts=(expresults-mean).^2;

SST=sum(SSTparts);

%Temperature variables.

%NOTE: This particular function only works if the temperatures given are
%whole numbers in degrees Celsius.

%Experimental value temperatures
exaxis=[];

T=exaxis+273.25;

Tl=length(T);

%result variables

result=zeros(1,Tl);
difres=zeros(1,Tl);

Values=[0,0];
Plotvalues=zeros(1,Tl);
MinNLLSprev=inf;


%Trap variables
```

```
s=[1*10^09 5*10^09 1*10^10 5*10^10 1*10^11 5*10^11 1*10^12 5*10^12
1*10^13 5*10^13 1*10^14 5*10^14 1*10^15 5*10^15]; %s^-1

sl=length(s);

E=[0.5 0.6 0.7 0.8 0.9 1.0 1.1 1.2 1.3 1.4 1.5 1.6 1.7 1.8 1.9 2.0 2.1
2.2 2.3 2.4 2.5 2.6 2.7 2.8 2.9 3.0]; %eV

El=length(E);

%For each E value:
for jj=1:El;

    %For each s value:
    for kk=1:sl;

%For each temperature:
for ii=1:Tl;


%Ramp up:

%How many fifth of seconds? Assume starting from 0 deg C/ 273.25 K

temps=linspace(1,T(ii),5*T(ii));
temps=temps+273.25;

%Calculating the fraction left from the start of each fifth of a second
to
%the end of the fifth of a second.
Fraction=exp(-0.2./(s(kk)^-1.*exp(E(jj)./(k.*temps))));

lf=length(Fraction);

ramp=1;
for ll=1:lf;
    ramp=ramp*Fraction(ll);
end

%Hold for 10 s:

Hold=exp(-10./(s(kk)^-1.*exp(E(jj)./(k.*T(ii)))));

%Result for each temperature

result(ii)=ramp*Hold;

difres(ii)=(result(ii)-expresults(ii)).^2;

end

Rsquared=1-(sum(difres)/SST);
```

```
NLLS=sum(difres);


if NLLS < MinNLLSprev;

    MinNLLSprev=NLLS;
    Values=[E(jj),s(kk)];
    Plotvalues=result;
    Rsq=Rsquared;
end
    end
end

disp('The Least Squares value of the E and s values observed are:');
disp('E = ');
disp(Values(1));
disp('s = ');
disp(Values(2));
disp('NLLS value =');
disp(MinNLLSprev);
disp('Rsquared = ');
disp(Rsq);
plot(exaxis,expresults,'bo');
hold on
plot(exaxis,Plotvalues,'rx');

end
```

B: NATURAL QUARTZ FOURIER TRANSFORM SPECTROMETER MEASUREMENTS

Robe:

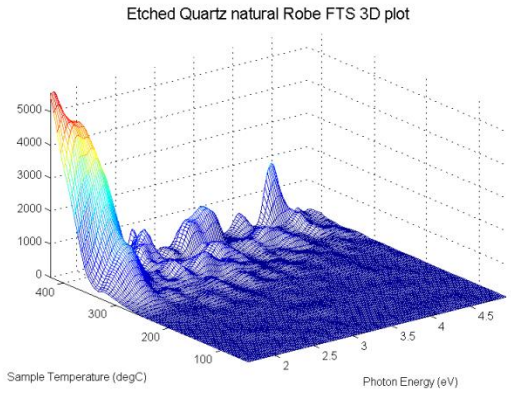

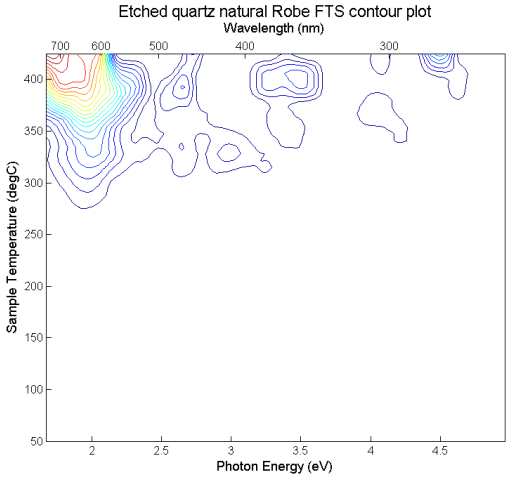

East Dairy:

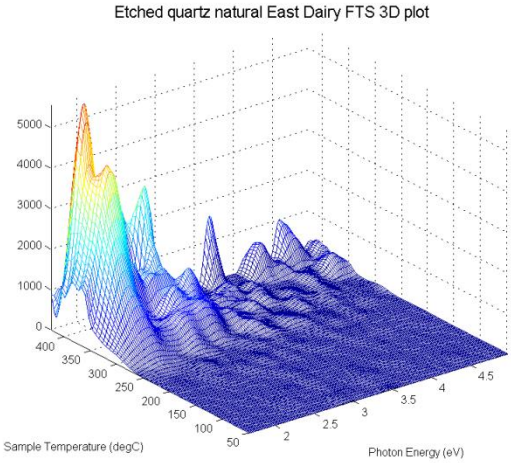

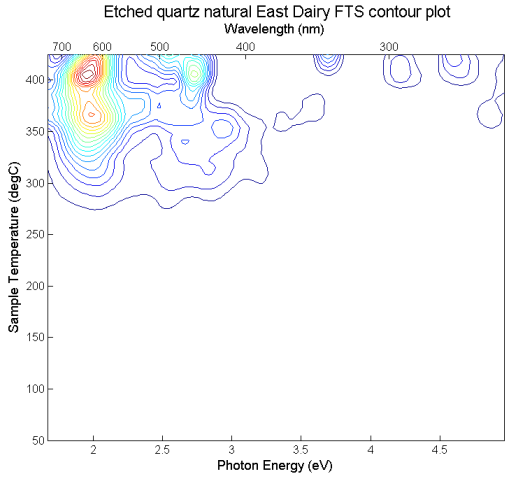

Baker:

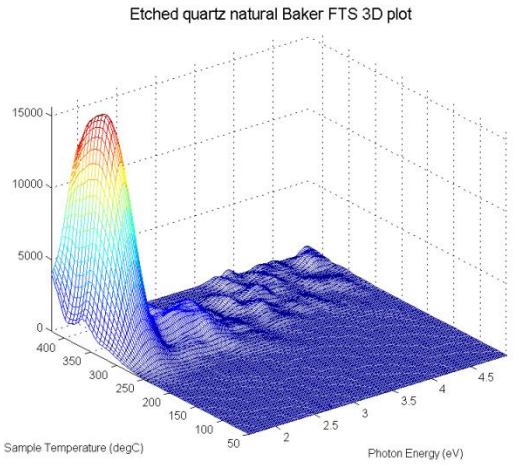

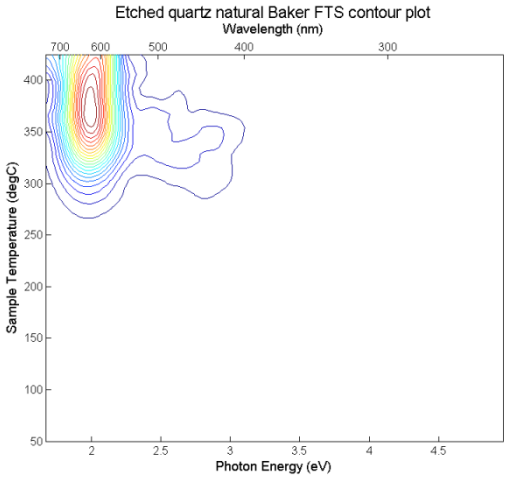

Harper:

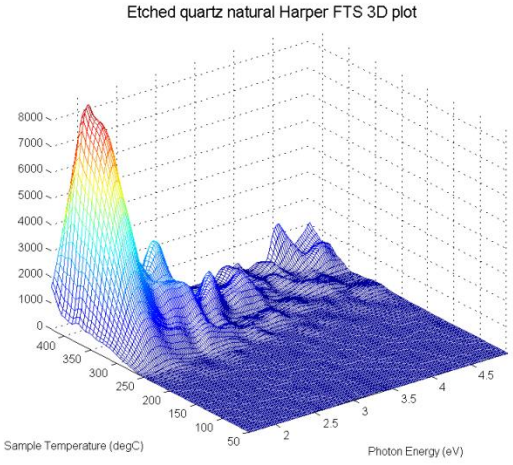

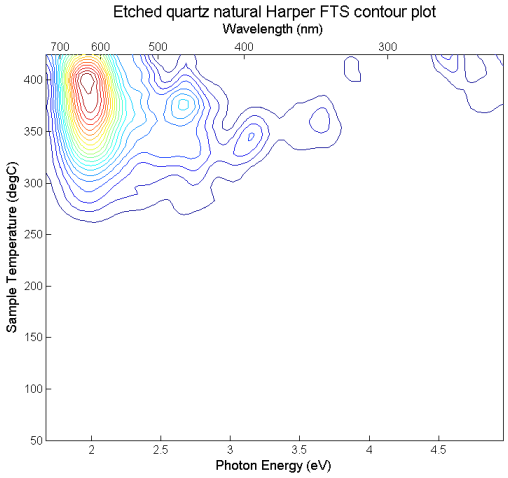

Naracoorte East:

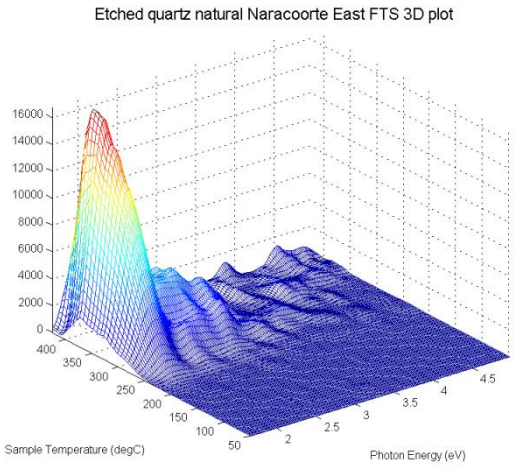

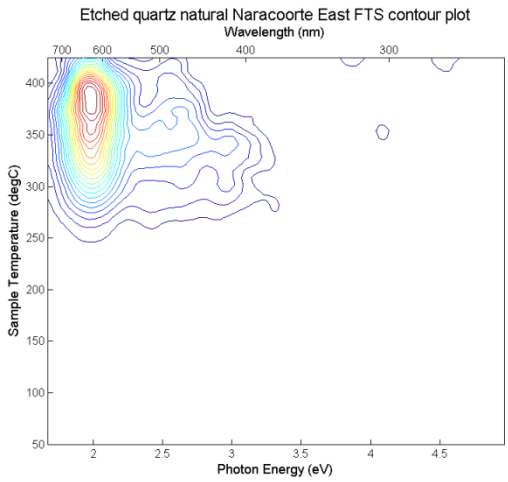

REFERENCES

Adamiec G, Bailey R M, Wang X L, and Wintle A G (2008) The mechanism of thermally transferred optically stimulated luminescence in quartz. Journal of Physics D: Applied Physics vol. 41 pp. 135503-135517

Adamiec G, Duller G A T, Roberts H M, and Wintle A G (2010) Improving the TT-OSL SAR protocol through source trap characterisation. Radiation Measurements, vol. 45, pp. 768-777.

Aitken M J (1985) Thermoluminescence dating. Academic Press, London.

Aitken M J (1998) An introduction to optical dating: The dating of quaternary sediments by the use of photon-stimulated luminescence. Oxford University Press, New York.

Aitken M J, and Smith B W (1988) Optical dating: recuperation after bleaching. Quaternary Science Reviews, vol. 7 pp. 387-393.

Akber R A (1986) Materials and techniques for thermoluminescence dating. Unpublished PhD thesis, Deparment of Physics, University of Adelaide, Australia.

Ankjaergaard C, Jain M, Thomsen K J, and Murray A S (2010) Optimising the separation of quartz and feldspar optically stimulated luminescence using pulsed excitation. Radiation measurements, vol. 45, pp. 778-785.

Arnold L, Demuro, M, Navazo M, Benito-Calvo A, and Pérez-González A (2013) OSL dating of the Middle Palaeolithic Hotel California site, Sierra de Atapureca, north-central Spain. Boreas, vol. 42, pp. 285-305.

Athanassas C, and Zacharias N (2010) Recuperated-OSL dating of quartz from Aegean (South Greece) raised Pleistocene marine sediments: current results. Quaternary Geochronology, vol. 5, pp. 65-75.

Bailey R M (2001) Towards a general kinetic model for optically and thermally stimulated luminescence of quartz. Radiation Measurements, vol. 33, pp. 17-45.

Banerjee D, Hildebrand A N, Murray-Wallace C V, Bourman R P, Brooke B P, and Blair M (2003) New quartz SAR-OSL ages from the stranded beach dune sequence in south-east South Australia. Quaternary Science Reviews vol. 22, pp. 1019-1025.

Belperio A P, and Cann, J H (1990) Quaternary evolution of the Robe-Naracoorte coastal plain: an excursion guide. Department of Mines and Energy, Report no. 90/27, Adelaide, South Australia.

Bevington, Phillip R and Robinson, D Keith (2003) Data reduction and error analysis for the physical sciences (3rd Ed.) McGraw-Hill New York, NY USA.

Blackburn G, Bond R D, and Clarke A R P (1965) Soil development associated with stranded beach ridges in south-east South Australia. Soil Publication No. 22, CSIRO.

Bøtter-Jensen L (1997) Luminescence techniques: Instrumentation and methods. Radiation Measurements, vol. 27, pp. 749-768.

Bøtter-Jensen L, Bulur E, Duller G A T, and Murray A S (2000) Advances in luminescence instrument systems. Radiation Measurements, vol. 32, pp. 523-528.

Bøtter-Jensen L, McKeever S W S, and Wintle A G (2003) Optically stimulated luminescence dosimetry. Elsevier Science B.V., Amsterdam.

Boyle R (1664) A short account of some observations made by Mr. Boyle about a diamond that shines in the dark (Annex to Experiments and considerations touching colours). Henry Herringman, London.

de Brito Farias T M and Watanabe S (2012) A comparative study of the thermoluminescence properties of several varieties of Brazilian natural quartz. Journal of Luminescence, vol. 132, pp 2684-2692.

Brown N D, and Forman S L (2012) Evaluating a SAR TT-OSL protocol for dating fine-grained quartz within Late Pleistocene loess deposits in the Missouri and Mississppi river valleys, United States. Quaternary Geochronology, vol. 12, pp. 87-97.

Bulur E (1996) An alternative technique for optically stimulated luminescence (OSL) experiment. Radiation Measurements, vol. 26, pp. 701-709.

Burbidge C I, Cabo Verde S I, Fernandes A C, Prudencio M I, Botelho M L, Dias M I, and Cardoso G (2009) Dosimetry in the multi Kilo-Gray range using optically stimulated luminescence (OSL) and thermally-transferred OSL from quartz. Radiation Measurements, vol. 46, pp. 860-865.

Buylaert J P, Murray A S, Thomsen K J, Jain M (2009) Testing the potential of an elevated temperature IRSL signal from K-feldspar. Radiation Measurements, vol. 44, pp. 560-565.

Climate Data Online, online. <http://www.bom.gov.au/climate/data> [Accessed 19/09/13]. Bureau of Meteorology, Australia.

Curie D (translated by Garlick G F J) (1963) Luminescence in Crystals, Methuen and Co Ltd, London.

Denby P M, Bøtter-Jensen L, Murray A S, Thomsen K J, and Moska P (2006) Application of pulsed OSL to the separation of the luminescence components from a mixed quartz/feldspar sample. Radiation Measurements, vol. 41, pp. 774-779.

Drexel J P and Preiss W V (Eds) (1995) The geology of South Australia, Volume 2: The Phanerozoic. Bulletin 54. Geological survey of South Australia, South Australia.

Duller G A T, Bøtter-Jensen L, and Murray A S (2000) Optical dating of sand-sized grains of quartz: Sources of variability. Radiation Measurements, vol. 32, pp. 453-457.

Duller G A T, Penkman K E H, and Wintle A G (2009) Assessing the potential for using biogenic calcites as dosemeters for luminescence dating. Radiation Measurements, vol. 44, pp. 429-433.

Duller G A T, and Wintle A G (2012) A review of the thermally transferred optically stimulated luminescence signal from quartz for dating sediments. Quaternary Geochronology, vol. 7, pp. 6-20.

Du Fay (1738) Recherches sur la lumiere des diamants, et de plusieurs autres matieres. Histoire de L'Academie Royale des sciences, vol. 1738, pp. 347-372.

Fleming S J (1972) Thermoluminescence authenticity testing of ancient ceramics using radiation-sensitivity changes in quartz. Die Naturwissenschaften, vol. 54, pp. 145-151.

Fox P J (1990) Optical studies of thermoluminescent materials. Unpublished PhD thesis, Department of Physics and Mathematical Physics, University of Adelaide, Australia.

Franklin A D, Prescott J R, and Scholefield R B (1995) The mechanism of thermoluminescence in an Australian sedimentary quartz. Journal of Luminescence, vol. 63, pp. 317-326.

Furetta C (2008) Questions and answers on thermoluminescence (TL) and optically stimulated luminescence (OSL). World Scientific Publishing Co. Pte. Ltd., Toh Tuck Link, Singapore.

Galbraith R F, and Laslett G M (1993) Statistical models for mixed fission track ages. Nuclear Tracks Radiation Measurements, vol. 4, pp. 459-470.

Galbraith R F, Roberts R G, Laslett G M, Yoshida H, and Olley J M (1999) Optical dating of single grains of quartz from Jinmium rock shelter, northern Australia. Part I: Experimental design and statistical models. Archaeometry, vol. 4, pp. 339-364.

Grün R (2009) The "AGE" program for the calculation of luminescence age estimates. Ancient TL, vol. 27, pp. 45-46.

Grün R, Wells R, Eggins S, Spooner N, Aubert M, Brown L, and Rhodes E (2008) Electron spin resonance dating of South Australian megafaunal sites. Australian Journal of Earth Sciences, vol. 55, pp. 917-935.

Hashimoto T, Yanagawa Y, Yawata T (2007) Blue and red thermoluminescence of natural quartz in the temperature region from -196 to 400 °C. Radiation Measurements, vol. 42, pp. 341-346.

Hu G, Zhang J-F, Qiu W-L, and Zhou L-P (2010) Residual OSL signals in modern fluvial sediments from the Yellow River

(HuangHe) and the implications for dating young sediments. Quaternary Geochronology, vol. 5, pp. 187-193.

Huntley D J, Godfrey-Smith D I, and Thewalt, M L W (1985) Optical dating of sediments. Nature, vol. 313 pp 105-107.

Huntley D J, Hutton J T, and Prescott J R (1985) South Australian sand dunes: A TL sediment test sequence: Preliminary results. Nuclear Tracks, vol. 10, pp. 757-758.

Huntley D J, Hutton J T, and Prescott J R (1993a) The stranded beach-dune sequence of south-east South Australia: A test of thermoluminescence dating, 0-800 ka. Quaternary Science Reviews, vol. 12, pp. 1-20.

Huntley D J, Hutton J T, and Prescott J R (1993b) Optical dating using inclusions within quartz grains. Geology, vol. 21, pp. 1087-1090.

Huntley D J, Hutton J T, and Prescott J R (1994) Further thermoluminescence dates from the dune sequence in the southeast of South Australia. Quaternary Science Reviews, vol. 13, pp. 201-207.

Huntley D J and Kirkey J J (1985) The use of an image intensifier to study the TL intensity variability of individual grains. Ancient TL, vol. 3, pp. 1-4.

Huntley D J, and Prescott J R (2001) Improved methodology and new thermoluminescence ages for the dune sequence in south-east South Australia. Quaternary Science Reviews, vol. 20, pp. 687-699.

Idnurm M, and Cook P J (1980) Palaeomagnetism of beach ridges in South Australia and the Milankovitch theory of ice ages. Nature, vol. 286, pp. 699-702.

Jacobs Z, Roberts R G, Lachlan T J, Karkanas P, Marean C W, and Roberts D L (2011) Development of the SAR TT-OSL procedure for dating Middle Pleistocene dune and shallow marine deposits along the southern Cape coast of South Africa. Quaternary Geochronology, vol. 6, pp. 491-513.

Jain M, Murray A S, and Botter-Jensen L (2003) Characterisation of blue-light stimulated luminescence components in different quartz samples: implications for dose measurement. Radiation Measurements, vol. 37, pp. 441-449.

Jensen H E (1982) Physical measurements associated with thermoluminescence dating. Unpublished PhD thesis, Department of Physics, University of Adelaide, Australia.

Kim J C, Duller G A T, Roberts H M, Wintle A G, Lee Y I, and Yi S B (2009) Dose dependence of thermally transferred optically stimulated luminescence in quartz. Radiation Measurements, vol. 44, pp. 132-143.

Kim J C, Duller G A T, Roberts H M, Wintle A G, Lee Y I, and Yi S B (2010) Re-evaluation of the chronology of the palaeolithic site at Jeongokri, Korea, using OSL and TT-OSL signals from quartz. Quaternary Geochronology, vol. 5, pp. 365-370.

Kiyotaka, N (1987) Thermoluminescence dating of fossil calcite shells. Japanese Journal of Applied Physics, Part 1: Regular Papers and Short Notes, vol. 26, pp. 2127-2133.

Krbetschek M R, Gotze J, Dietrich A, and Trautmann T (1997) Spectral information from minerals relevant for luminescence dating. Radiation Measurements, vol. 27, pp. 695-748.

Li Bo, and Li Sheng-Hua (2006) Studies of thermal stability of charges associated with thermal transfer of OSL from quartz. Journal of Physics D: Applied Physics, vol. 39, pp. 2941-2949.

Li Bo, and Li Sheng-Hua (2011) Luminescence dating of K-feldspar from sediments: A protocol without anomalous fading correction. Quaternary Geochronology, vol. 6, pp. 468-479.

Li S-H, Tso M-Y, Westaway K E, and Chen G (1999) Choice of the most appropriate thermal treatment in optical dating of quartz. Radiation Protection Dosimetry, vol. 84, pp. 495-498.

Liritzis, Y (1980) 110 °C quartz peak: A new normalization factor. Ancient TL, vol. 11, pp. 6-7.

Lucovsky G (1965) On the photoionization of deep impurity centers in semiconductors. Solid State Communications, vol. 3, pp. 299-302.

McKeever S W S (1985) Thermoluminescence of solids. Cambridge University Press, Cambridge.

Murray A S (1999) Incomplete stimulation of luminescence in young quartz sediments and its effect on the regenerated signal. Radiation Measurements, vol. 26, pp. 221-231.

Murray A S, and Roberts R G (1998) Measurement of the equivalent dose in quartz using a regenerative-dose single-aliquot protocol. Radiation Measurements, vol. 29, pp. 503-515.

Murray A S, and Wintle A G (2000) Luminescence dating of quartz using an improved single-aliquot regenerative-dose protocol. Radiation Measurements, vol. 32, pp. 57-73.

Moore, David and McCabe, George (2003) Introduction to the practice of statistics, W.H. Freeman and Company, New York, USA.

Nian X M, Zhou L P, and Qin J T (2009) Comparisons of equivalent dose values obtained with different protocols using a lacustrine sediment sample from Xuchang, China. Radiation Measurements, vol. 44, pp. 512-516.

Pagonis V, Tatsis E, Kitis G, and Drupieski C (2002) Search for common characteristics in the glow curves of quartz of various origins. Radiation Protection Dosimetry, vol. 100 pp 373-376.

Pagonis V, Wintle A G, Chen R, and Wang X L (2009) Simulations of thermally transferred OSL experiments and of the ReSAR dating protocol for quartz. Radiation Measurements, vol. 44, pp. 634-638.

Pickering R, Jacobs Z, Herres A I R, Karkanas P, Bar-Matthews M, Woodhead J D, Kappen P, Fisher E, and Marean C W (2013) Paleoanthropologically significant South African sea caves dated to 1.1—1.0 million years using a combination of U-Pb, TT-OSL, and palaeomagnetism. Quaternary Science Reviews, vol. 65, pp. 39-52.

Porat N, Duller G A T, Roberts H M, and Wintle A G (2009) A simplified SAR protocol for TT-OSL. Radiation Measurements, vol. 44, pp. 538-542.

Prescott J R, and Fox P J (1990) Dating quartz sediments using the 325C TL peak: new spectral data. Ancient TL, vol. 8, pp. 32-34.

Prescott J R, Fox P J, Akber R A, and Jensen H E (1988) Thermoluminescence emission spectrometer. Applied Optics, vol. 27, pp. 3496-3502.

Prescott J R, Huntley D J, Hutton J T (1993) Estimation of equivalent dose in thermoluminescence dating—the Australian slide method. Ancient TL, vol. 11, pp. 1-5.

Prescott J R and Hutton D J (1995) Environmental dose rates and radioactive disequilibrium from some Australian luminescence dating sites. Quaternary Science Reviews, vol. 14, pp. 439-448.

Rhodes E J, and Bailey R M (1997) The effect of thermal transfer on the zeroing of the luminescence of quartz from recent glaciofluvial sediments. Quaternary Science Reviews, vol. 16, pp. 291-298.

Risø DTU National Laboratory for Sustainable Energy, 2011. The Risø TL/OSL reader, online. <http://www.risoe.dtu.dk/Risoe_dk/Home/business_relations/Products_Services/Dosimetri/NUK_instruments/TL_OSL_readers.aspx>. [Accessed 3/5/12].

Rosenberg T M, Preusser F, Blechschmidt I, Fleitmann D, Jagher R, and Matter A (2012) Late Pleistocene palaeolake in the interior of Oman: a potential key area for the dispersal of anatomically modern humans out-of-Africa? Journal of Quaternary Science, vol. 27, pp. 13-16.

Ryb U, Matmon A, Porat N, and Katz O (2013) From mass-wasting to slope stabilization—putting constains on a tectonically induced transition in slope erosion mode: a case study in the Judea Hills, Israel. Earth Surface Processes and Landforms, vol. 38, pp. 551-560.

Scholefield R B (1994a) Luminescence of quartz. Unpublished MSc thesis, Department of Physics and Mathematical Physics, University of Adelaide.

Scholefield R B (1994b) Observations on some thermoluminescence emission centres in geological quartz. Radiation Measurements, vol. 23, pp. 409-412.

Schmidt E D, Frechen M, Murray A S, Tsukamoto S, and Bittmann F (2011) Luminescence chronology of the loess record from the Tönchesberg section: A comparison of using quartz and

feldspar as dosimeter to extend the age range beyond the Eemian. Quaternary International, vol. 234, pp. 10-22.

Schwebel D A (1983) Quaternary Dune systems. In: Tyler M J, Twidale C R, Ling J K, and Holmes, J W (eds). Natural History of the South East, pp. 15-24. Royal Society of South Australia, Inc., Adelaide.

Schwebel D A (1984) Quaternary stratigraphy and sea-level variation in the southeast of South Australia. in Tyler, M J et al (eds) Natural history of the south east. Royal Society of South Australia, Adelaide.

Shen Z X, Mauz B, and Lang A (2011) Source-trap characterization of thermally transferred OSL in quartz. Journal of Physics D: Applied Physics, vol. 44, pp. 295405-295417.

Smith B W (1983) New applications of thermoluminescence dating. Unpublished PhD thesis, Department of Physics, University of Adelaide, Australia.

Smith B W, Aitken M J, Rhodes E J, Robinson P D, and Geldard D M (1986) Optical dating: Methodological aspects. Radiation Protection Dosimetry, vol. 17, pp. 229-233.

Spooner N A (1987) The effect of light on the luminescence of quartz. Unpublished MSc thesis. Department of Physics, University of Adelaide, Australia.

Spooner N A (1994) On the optical dating signal from quartz. Radiation Measurements, vol. 23, pp. 593-600.

Spooner N A, Prescott J R, and Hutton J T (1988) The effect of illumination wavelength on the bleaching of the thermoluminescence (TL) of quartz. Quaternary Science Reviews, vol. 11, pp. 325-329.

Spooner, N A and Questiaux, D G (2000) Kinetics of red, blue and UV thermoluminescence and optically-stimulated luminescence from quartz. Radiation Measurements, vol. 32 pp. 659-666.

Sprigg R C (1979) Stranded and submerged sea-beach systems of southeast South Australia and the aeolian desert cycle. Sedimentary Geology, vol. 22, pp. 53-96.

Stevens T, Buylaert J P, and Murray A S (2009) Towards development of a broadly-applicable SAR TT-OSL dating protocol in quartz. Radiation Measurements, vol. 44, pp. 639-645.

Strickertsson K and Murray A S (1999) Optically stimulated luminescence dates for Late Pleistocene and Holocene sediments from Nørre Lyngby, Northern Jutland, Denmark. Quaternary Science Reviews, vol. 18, pp. 169-178.

Sudebi B, Polymeris G S, Tsirliganis N C, Pagonis V, and Kitis G (2012) Reconstruction of thermally quenched glow curves in quartz. Radiation Measurements, vol. 47, pp. 250-257.

Sun X, Lu H, Wang S, Yi S, Shen C, and Zhang W (2013) TT-OSL dating of Longyadong Middle Paleolithic site and paleoenvironmental implications for hominin occupation in Luonan Basin (central China). Quaternary Research, vol. 79, pp. 168-174.

Sutton S R and Zimmerman D W (1979) The zircon natural method: Initial results and low level thermoluminescence measurement. PACT, vol. 3 p. 465.

Templer R H (1985) The dating of zircons by auto-regenerated TL at low temperatures. Nuclear Tracks, vol. 10 pp. 789-798.

Templer R H (1986) (PhD Thesis) Thermoluminescence techniques for dating zircon inclusions. Balliol College, Oxford.

Thiel C, Buylaert J-P, Murray A S, Elmejdoub N, and Jedoui Y (2012) A comparison of TT-OSL and post-IR IRSL dating of coastal deposits on Cape Bon penninsula, north-eastern Tunisia. Quaternary Geochronology, vol. 10, pp. 209-217.

Thomsen, K J (2004) (PhD Thesis) Optically stimulated luminescence techniques in retrospective dosimetry using single grains of quartz extracted from unheated materials. Risø National Laboratory, Denmark.

Tsukamoto Sumiko, Duller Geoff A T, and Wintle Ann G (2008) Characteristics of thermally transferred optically stimulated luminescence (TT-OSL) in quartz and its potential for dating sediments. Radiation Measurements, vol. 43, pp. 1204-1218.

Twidale C R, and Bourne J A (2010) 21.5: South Australia. In: Bird E (ed). Encyclopedia of the World's Coastal Landforms. pp. 1293-1303. Springer Science+Business Media, Dordrecht.

Valladas, H (1985) Some TL properties of burnt prehistoric flints. Nuclear Tracks and Radiation Measurements, vol. 10, pp. 785-788.

Visocekas R, Ceva T, Marti C, Lefaucheux F, and Robert M C (1976) Tunneling processes in afterglow of calcite. Physica Status Solidi (A), vol. 35, pp. 315-327.

Wang X L, Lu Y C, and Wintle A G (2006a) Recuperated OSL dating of fine-grained quartz in Chinese Loess. Quaternary Geochronology, vol. 1, pp. 89-100.

Wang X L, Wintle A G, and Lu Y C (2006b) Thermally transferred luminescence in fine-grained quartz from Chinese loess: Basic observations. Radiation Measurements, vol. 41, pp. 649-658.

Wang X L, Wintle A G, and Lu Y C (2007) Testing a single-aliquot protocol for recuperated OSL dating. Radiation Measurements, vol. 42, pp. 380-391.

Westaway K E (2009) The red, white and blue of quartz luminescence: A comparison of D_e values derived for sediments from Australia and Indonesia using thermoluminescence and optically stimulated luminescence emissions. Radiation Measurements, vol. 44, pp. 462-466.

Wiedemann E (1888) Ueber Fluorescenz und Phosphorescenz I. Abhandlung. Annalen der Physik, vol. 34, pp. 446-463.

Wintle A G (1973) Anomalous fading of thermoluminescence in mineral samples. Nature, vol. 245, pp. 143-144.

Wintle A G (1975) Thermal quenching of thermoluminescence in quartz. Geophysical Journal of the Royal Astronomical Society, vol. 41, pp. 107-113.

Wintle A G and Murray A S (1997) The relationship between quartz thermoluminescence, photo-transferred thermoluminescence, and optically stimulated luminescence. Radiation Measurements, vol. 27, pp. 611-624.